Institut für Nutzpflanzenwissenschaften und Ressourcenschutz

Genetic and physiological characterization of traits related to salinity tolerance in an advanced backcross population of wheat

Inaugural-Dissertation

zur Erlangung des Grades

Doktor der Agrarwissenschaften

(Dr. agr.)

der landwirtschaftlichen Fakultät

der Rheinischen Friedrich-Wilhelms-Universität Bonn

vorgelegt von

Dipl. Ing agr.

Said Abdul Wali Dadshani

Aus Hagen (Westfalen)

Bonn 2018

Referent: Prof. Dr. Jens Léon

Korreferent: Prof. Dr. Heiner Goldbach

Tag der mündlichen Prüfung: 09.03.2018

Angefertigt mit Genehmigung der Landwirtschaftlichen Fakultät der Universität Bonn

”تا که جوانی و توانی بکوش“

“As long as you are young. As long as you can: Learn!”

- My Mother -

Dedicated to Diba and Ariana

In loving memory of my parents and my brother

I. ZUSAMMENFASSUNG

Die Versalzung der Böden beeinträchtigt in weiten Teilen der Welt die Weizenproduktion. Zum Ausgleich von hohen Ertragseinbußen, bzw. zur Sicherung der Ernährung der Bevölkerung, könnte eine zunehmende genetische Variabilität von aktuell genutzten Weizensorten einen effizienten Lösungsansatz bieten. Synthetischer hexaploider Weizen wird als Quelle von nützlichen exotischen Allelen im Hinblick auf Toleranzen gegenüber biotischen und abiotischen Stressfaktoren, wie etwa Salzstress angesehen. Ziel der vorliegenden Arbeit war die Lokalisation von genomischen Regionen, die zur Salztoleranz von Weizen in verschiedenen Entwicklungsstadien beitragen. Dazu wurden 151 AB-Linien (Advanced Backcross) der Winterweizenpopulation "Z86" ($BC_2F_{3:7}$) untersucht, welche vorteilhafte Gene des synthetischen hexaploiden Weizens Syn86L im Hintergrund der deutschen Eliteweizensorte Zentos beinhaltet. Experimente unter Salzstress wurden sowohl im Keimungs- und Jungpflanzenstadium, als auch unter natürlichen Bedingungen in Usbekistan in drei aufeinanderfolgenden Jahren auf Feldern mit hoher Salinität durchgeführt. Die AB-Linien als auch ihre Eltern waren zu unterschiedlichen Entwicklungsstadien verschieden stark vom Salzstress betroffen. Bei Natriumsulfat (Na_2SO_4) führte die gleiche molare Salzkonzentration zu einer stärkeren Schädigung der Pflanzen als bei Natriumchlorid (NaCl). Bei den meisten untersuchten Parametern schnitt der rekurrente Eliteelter Zentos besser ab als der synthetische Elter Syn86. Nur im Hinblick auf Wurzel- und Sprosslänge übertraf Syn86 den Kulturweizen. Für dieses Projekt kamen verschiedene nicht-invasive Sensortechnologien zum Einsatz, welche ein akkurates und kontinuierliches Beobachten der morphophysiologischen Parameter bei den gestressten Pflanzen erlaubten. Im Rahmen dieser Arbeit wurde ein Dual-Mode Mikrowellensensor präsentiert, der zerstörungsfrei sowohl den Wassergehalt, als auch die Ionenleitfähigkeit von mono- und dikotylen Pflanzen erfasst. Außerdem wurden in dieser Arbeit erstmalig Daten von Weizenpflanzen präsentiert, die einem plötzlichen Salzschock zugeführt wurden. Hierbei konnte festgestellt werden, dass genotypisch signifikante Unterschiede 20 Minuten nach der Initiation von Salzstress feststellbar waren, wobei Zentos höhere Photosyntheseraten aufzuweisen hatte als Syn86.

Um genomische Regionen zu detektieren, die mit den untersuchten Merkmalen unter Salzstress assoziieren, wurde die Z86-Population mit dem iSelect 90K Chip genotypisiert. Die nach der Datenreinigung verbliebenen 11.050 polymorphen Single-Nucleotide Polymorphism (SNP) Marker wurden im Rahmen der Quantitative Trait Loci (QTL) Analyse für die 48 untersuchten

Merkmale verwendet. Durch Verwendung von SAS (Version 9.4) wurde das Multi-Locus-Verfahren in das hierarchische QTL-Model eingebunden, um die Zahl der Falsch-positiven QTL zu reduzieren und dadurch die Aussagekraft der echten QTL zu verstärken. Hierbei wurden insgesamt 116 QTL für Haupteffekte (inklusive QTL mit epistatischen Effekten) und 165 QTL für die Interaktion mit der Behandlung (inklusive QTL mit epistatischen Effekten in Interaktion mit der Behandlung) detektiert. Ein bedeutendes QTL mit pleiotropischen Effekten (u.a. für das Sprosstrockengewicht unter Salzstress) wurde auf dem kurzen Arm des Chromosoms 7D mit der Position 29,87 cM gefunden. *In-silico*-Analyse der QTL-Region des Chromosoms ergab ein Gen, das für *TaGSTu3*, ein Enzym der *tau* Klasse aus der Familie Glutathion-S-Transferasen (GST), kodiert. Die GSTs sind bekannt für ihre Rolle bei der Detoxifikation von reaktiven Sauerstoffspezies (ROS) in Pflanzen, die unter Salzstress vermehrt produziert werden. Die Gen-Expressions-Analysen an drei Zeitpunkten (10, 16 und 30 Tage nach der Applikation von Salzstress) des Jungpflanzenstadiums von Weizenpflanzen zeigte eine höhere Expression von *TaGSTu3* in Zentos im Vergleich zu Syn86, bei der die Expression von *TaGSTu3* unter Stressbedingungen sank. In dieser Arbeit wurde erstmalig der signifikante Beitrag der GST aus der *tau*-Klasse zur Salztoleranz von Weizen nachgewiesen.

Die vorliegende Studie hat erfolgreich QTL identifiziert, wobei die günstigen Allele sowohl von der Eliteweizensorte Zentos als auch von dem synthetischen Weizen Syn86 stammen. Die detektierten nützlichen und exotischen Allele, die in den AB-Linien der Z86-Population vorhanden sind, können direkt in Züchtungsprogrammen über Marker-Assisted Selection eingebunden werden. Dadurch kann zur effizienteren Züchtung von Sorten mit salztoleranten als auch weiteren bevorzugten agromischen Merkmalen beigetragen werden.

II. ABSTRACT

In large areas of the world wheat production is highly affected by soil salinity. Increasing the genetic variability of currently used wheat varieties is an efficient approach to overcome production losses and prevent food insecurity. Synthetic hexaploid wheat is widely regarded as donor of favorable exotic alleles with respect to tolerance against biotic and abiotic stress factors such as salinity stress. The objective of the present study was to identify genomic regions, which contribute to salinity tolerance at various growth stages in wheat. Therefore, the 151 advanced backcross lines (AB-lines) of the winter wheat population "Z86" ($BC_2F_{3:7}$), containing introgressions of the synthetic hexaploid wheat Syn86L in the background of the German elite cultivar Zentos, were employed in this study. Salt stress experiments were conducted at germination and seedling stage as well as under field conditions with natural salinization in Uzbekistan in three consecutive years. At various growth stages, the AB-lines of the Z86 population and their parents were differently affected by salt stress. At the same molar concentration of salts, the impact of sodium sulfate (Na_2SO_4) on plants growth was higher than of sodium chloride (NaCl). Notably, for most studied parameters the recurrent elite parent Zentos was performing better than the synthetic parent Syn86, the donor of exotic alleles. In respect to root and shoot length Syn86 surpassed the elite cultivar.

In this study, several non-destructive sensor technologies were used which allow accurate and continuous monitoring of morpho-physiological parameters of plants exposed to salinity stress. These data present the first report of a dual-mode microwave resonator which was allowing accurate estimation of water content as well as the ionic conductivity in leaves of mono- and dicotyledonous plants. Additionally, measurement of the photosynthetic rate of plants exposed to salt shock revealed highly significant genotype by treatment interaction effect 20 minutes after initiation of salt stress, where Zentos was performing better than Syn86.

In order to detect genomic regions associated with the measured traits under salinity stress the Z86 population was genotyped using the iSelect 90K chip. After data cleaning 11,050 polymorphic SNP marker remained which were applied for quantitative trait loci analysis (QTL) for the 48 studied traits. Using SAS 9.4 the multi-locus approach incorporated in the hierarchical QTL model was able to reduce the number of false-positive putative QTL and hence endorsed the power of detected true QTL. In summary, 116 QTL main effects (including QTL with epistatic effects) and 165 QTL for marker by treatment interaction (including QTL

with epistatic by treatment interaction) were detected. One of the major QTL showing pleiotropic effects, among them on shoot dry weight under salinity stress, was found on the short arm of chromosome 7D at 29.97 cM. *In silico* analysis of the QTL chromosome region revealed a gene coding for *TaGSTu3*, an enzyme belonging to the *tau* class of the glutathione S-transferase family (GST). GSTs are well known for their role in detoxification of reactive oxygen species (ROS) in plants, which is highly increased under salinity stress. Gene expression analysis at three time-points during the seedling stage (10, 16 and 30 days after salt application) revealed higher expression of *TaGSTu3* in Zentos under salinity stress and decreased expression in the comparing parent Syn86. This is the first report of a *tau* class GST found to contribute significantly to salinity tolerance in wheat.

The present study successfully identified QTL from elite cultivar Zentos as well as from the donor germplasm Syn86.The detected favorable alleles introgressed in the AB-lines of the Z86 population can be directly employed in breeding programs via marker-assisted selection for efficiently breeding cultivars with improved salinity tolerance and desired agronomic traits.

III. TABLE OF CONTENT

I. ZUSAMMENFASSUNG I

II. ABSTRACT III

III. TABLE OF CONTENT V

1. INTRODUCTION 1

2. HYPOTHESIS 16

3. MATERIALS AND METHODS 17

3.1. ASSESSMENT OF SALINITY STRESS 17
3.1.1. GERMPLASM 17
3.1.2. ASSESSMENT OF SALINITY RESPONSE AT GERMINATION 19
3.1.3. ASSESSMENT OF SALINITY RESPONSE AT SEEDLING STAGE 20
3.1.4. APPLICATION OF SENSORS FOR NON-DESTRUCTIVE PHENOTYPING 25
3.1.5. EXPERIMENTAL SETUP OF FIELD TRIALS 30
3.2. GENOTYPING 32
3.2.1. MOLECULAR ANALYSIS 32
3.1. STATISTICAL ANALYSIS 35
3.1.1. QTL MAPPING 36
3.1.2. EPISTATIC INTERACTIONS 37
3.1.3. COEFFICIENT OF DETERMINATION (R^2) 38
3.1.4. CALCULATION OF REPEATED MEASURES ANALYSIS OF VARIANCE 38
3.1.5. APPLICATION OF VISUALIZATION SOFTWARE 39

4. RESULTS 40

4.1. PHENOTYPIC CHARACTERIZATION OF THE Z86 POPULATION 40
4.1.1. PHENOTYPING OF THE Z86 POPULATION AT GERMINATION STAGE 41
4.1.2. PHENOTYPING OF THE Z86 POPULATION AT SEEDLING STAGE 48
4.1.3. EVALUATION OF THE Z86 POPULATION UNDER FIELD CONDITION WITH NATURAL SALINIZATION 67
4.1.4. COMBINED ANALYSIS OF PHENOTYPIC PARAMETERS ACROSS ALL ANALYZED GROWTH STAGES 74
4.1.5. APPLICATION OF SENSORS FOR NON-DESTRUCTIVE MEASUREMENT OF WATER-STATUS AND SALINITY STRESS 77
4.2. GENOTYPIC CHARACTERIZATION OF THE Z86 POPULATION 88

4.2.1. Linkage Disequilibrium (LD) Analysis of the Z86 population 90
4.3. Identification of loci for multiple traits under salt stress and control conditions 92
4.4. Sequence and expression analysis of glutathione s-transferase under salinity stress in wheat 101

5. DISCUSSION 105

5.1. Phenotypic characterization of the Z86 population and the parents Zentos and Syn86 106
5.1.1. Germination stage 106
5.1.2. Seedling stage 108
5.1.3. Maturity stage 110
5.1.4. Application of sensors for non-destructive assessment of steady-state conditions 113
5.1.5. Non-destructive measurement of photosynthetic parameters of wheat plants exposed to salinity stress at seedling stage 116
5.2. Genetic characterization of the Z86 population 118
5.3. Detection of QTL for the measured phenotypic traits 121
5.4. Sequence and expression analysis of glutathione S-transferase under salt stress in wheat 126

6. CONCLUSION 131

7. REFERENCES 133

8. LIST OF FIGURES 158

9. LIST OF TABLES 161

10. LIST OF ABBREVIATIONS 163

11. APPENDICES 164

12. LIST OF PUBLICATIONS 215

13. ACKNOWLEDGEMENT 216

1. INTRODUCTION

Salinity is a major threat to agricultural productivity worldwide and presents a tremendous challenge for food security (Ahmad et al. 2013). More than one billion hectares of land, accounting for approximately 25% of the global land area, is affected by salinity. Due to natural salinization or unsuitable irrigation practices, this area is increasing by up to 10 million hectares of land every year (Luo et al. 2017). The global annual yield (economic) losses in agricultural production due to salinization are estimated to exceed US$ 12 billion (Shabala 2013). Beside economic losses, salinity is of major concern as the global food production has to increase between 50-70% in order to meet the demand of the projected global population in 2050 of up to 9.3 billion people (Shabala 2013). Further to this, urbanization and soil degradation are dramatically decreasing the availability of arable land per capita (Godfray et al. 2010).

To overcome the increasing food gap there is a need to increase crop production by cultivating marginal lands and intensification of production on lands that are already under cultivation (Clair and Lynch 2010). Wheat is fundamental to human civilization and it is one of the most important food crops in the world (Shiferaw et al. 2013). Breeding adapted wheat varieties that can cope with salinity stress is widely regarded as one of the most promising options to close the food gap (Colmer et al. 2006, Díaz De León et al. 2010)

Wheat

Accounting for more than 15% of the total cultivated area on earth, wheat covers more of the earth's surface than any other food crop (FAOSTAT 2017). Wheat has been playing an outstanding role in feeding a hungry world and improving global food security. This crop contributes about 20 % of the total dietary calories and proteins worldwide (Shiferaw et al. 2013).

Bread wheat (*Triticum aestivum* L. ssp. *aestivum*) which is a member of the family Poaceae, belonging to the genus *Triticum*, has a hexaploid genome (2n=6x=42) and is a product of two allopolyploidizations events (Figure 1). The first hybridization happened 0.5 million years ago between *Triticum urartu*, as donor of AA genome, and *Aegilops speltoides*-related species, as donor of BB genome, forming the tetraploid wheat *Triticum turgidum* ssp. *dicoccoides* with

AABB genome. The second hybridization happed approximately 8.000 years ago in the southern Caspian basin, between *Triticum turgidum* (AABB genome) and *Aegilops tauschii*, the donor of the DD genome, forming the modern hexaploid wheat with AABBDD genome (Pozzi et al. 2004, Dubcovsky and Dvorak 2007, Vergauwen and De Smet 2017). However, the application of currently available genomic tools on hexaploid wheat is lagging behind their use on other cereals such as maize and rice. This is mainly due to the polyploid nature of wheat, its large genome size of (~17 Gb) and high repeat content of more than 80% (Avni et al. 2017, Uauy 2017).

Due to historically recent hybridization and following less time for accumulation of mutations, the polymorphic loci density and the genetic diversity of the D-genome is rather low (Feldman and Levy 2012). Additionally, according to Marcussen et al. (2014), the persistently limited genetic variability, as well as the limited recombination rate of the D-genome, is due to a single introgression event which resulted in formation of hexaploid wheat. Therefore, in modern bread wheat especially, the D-genome is thought to be a major limiting factor for improvement and adaptation to different environmental conditions, due to its relatively narrow genetic variability (Ogbonnaya et al. 2005, Dubcovsky and Dvorak 2007, Peng et al. 2011, Song et al. 2017). Selection by early farmers and systematic breeding efforts reduced the genetic variability of modern bread wheat furthermore (van Ginkel and Ogbonnaya 2007).

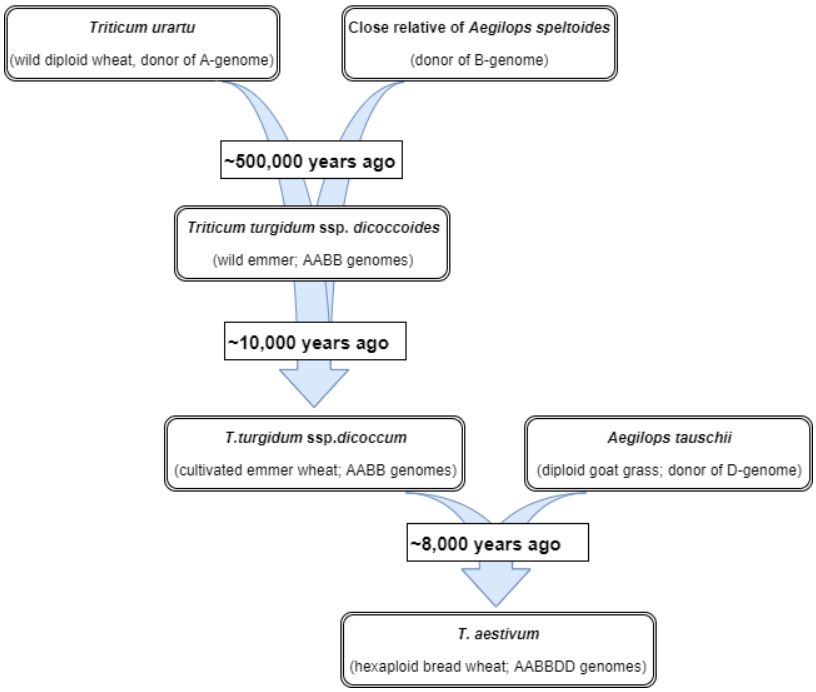

Figure 1. Evolution of wheat (Adopted from Vergauwen and De Smet (2017))

Wild relatives of wheat are regarded as valuable source of genetic diversity harboring potent exotic alleles in respect to withstanding biotic and abiotic stress as well as increasing productivity (Tanksley and McCouch 1997, Colmer et al. 2006, Nevo and Chen 2010). Especially, due to its close evolutionary relationship and extensive genetic diversity, the diploid goat grass is a potent resource for genetic enrichment of bread wheat (Zhang et al. 2008). In order to introduce exotic alleles into modern cultivars across species boundaries, scientists and breeders commonly make use of bride germplasm like synthetic hexaploid wheat (McFadden and Sears 1944, Warburton et al. 2006, Zhang et al. 2008). Synthetic hexaploid wheats (SHW) are neoallopolyploids. They are produced by artificial hybridization between tetraploid wheat (*Triticum turgidum*, 2n=28, AABB) and the diploid goat grass (Aegilops tauschii, 2n=14, DD) followed by chromosome doubling of F_1 hybrids, generally by application of colchicine (Mujeeb-Kazi et al. 1996). SHW are interfertile with bread wheat and as bridge germplasm they not only enable enrichment of genetic diversity of the D-genome but also A-, and B-genome of bread wheat (Colmer et al. 2005, Warburton et al. 2006, van Ginkel and Ogbonnaya 2007, Chapman et al. 2015). Previous reports underline the potential of SHW as donors of favorable alleles with respect to tolerance against abiotic stress (Reynolds et al. 2006, Plamenov and Spetsov 2011), biotic stress (Naz et al. 2008, Ashraf et al. 2015) and agronomic potential (Del Blanco et al. 2001, Yang et al. 2009, Tang et al. 2016). The potential of SHW as donors of favorable genes enhancing salinity tolerance of modern wheat genotypes by discriminating against Na^+, yet preferential uptake of K^+, is widely discussed (Gorham et al. 1990, Pritchard et al. 2002, Lindsay et al. 2004, Colmer et al. 2006).

However, produced SHW show, likewise in other genotypes, high phenotypic variation in respect to diverse traits. According to Dreisigacker et al. (2008) this phenotypic diversity is mainly based on (a) the genetic variation of the utilized *Ae. tauschii* accession that was selected as progenitor, (b) modification of gene expression caused by genomic changes during artificial hybridization and (c) changing epistatic interaction on the background of introduced homeologous chromosomes of A and B genomes.

The use of synthetic backcross-derived lines (SBLs), based on the cross between SHW as donor of exotic alleles and modern wheat cultivars as recurrent parent, are widely used for mapping genomic regions linked to specific traits and for detection of epistatic interactions (Juenger et al. 2005, Ogbonnaya et al. 2013).

Salinity

Soil salinity is one of the most devastating environmental stress factors threating agricultural productivity in many parts of the world. Approximately 25% of the total land area and 50% of cropland in the world is salt-stressed (Munns and Tester 2008, Ahmad et al. 2013, Luo et al. 2017). Soil salinization is defined as the concentration of salts in the surface or near-surface zones of soils. Salinization is a major cause of land degradation, leading to decreased crop yields and the loss of land from production in a range of environments.

Salinity is generally measured in electrical conductivity of the soil saturation extract (ECe). According to the classification by FAO (1988), soil salinity is divided into five categories (Table 1). Soils with ECe above 4 dS m^{-1} at 25°C and pH < 8.5 are recognized as saline, although many crops face yield reduction below this threshold (Jamil et al. 2011, Allbed and Kumar 2013). In many salt affected regions, the ECe is exceeding 8 dS m^{-1}.

Table 1. General classification of saline soils according to FAO (1988)

Soil salinity Class	**ECe (dS m^{-1})**	**Effect on crop plants**
Non- saline	< 2	Salinity effects negligible
Slightly saline	2-4	Yields of sensitive crops may be restricted
Moderately saline	4-8	Yields of many crops are restricted
Highly saline	8-16	Only tolerant crops yield satisfactorily
Extremely saline	> 16	Only a few very tolerant crops yield satisfactorily

Generally, salt-affected soils are classified as saline or sodic soils (Szabolcs and Fink 1974). Sodic soils are characterized mainly by carbonate salts like Na_2CO_3 and $NaHCO_3$, mostly with pH values greater than 8.5 and often EC values less than 2 dS m^{-1} (Ahmad et al. 2013). Unlike sodic soils, saline soils are characterized by the excessive amount of neutral salts like NaCl, Na_2SO_4, and $MgSO_4$, with NaCl and Na_2SO_4 being predominantly present in wide areas of the world (Rogers et al. 1998, Genc et al. 2016). Generally, saline soils are harmful as they exert osmotic stress and ion-induced injury of plants (Munns et al. 2002, Munns 2011). Considering the same molar concentration, many reports underline the greater impairment of Na_2SO_4 over NaCl on plants (Matar et al. 1975, Inal 2002). However, in respect to soil salinity, sodium chloride is considered as most important salt type, especially due to its higher solubility and its prevalence in salt-affected environments. According to Munns (2011) comparing the toxicity

of salt components is difficult as the osmotic effects were overwhelming the salt specific effects.

Soil salinity is classified as primary and secondary salinization. Primary salinization occurs naturally by the accumulation of salts over a long period of time mainly due to natural weathering of rocks , primary minerals, aeolian and marine deposition of salts (Zhu 2016). The secondary salinization or anthropogenic salinity is induced by the clearing of land or improper irrigation management (Allbed and Kumar 2013) which leads to a disrupted hydrologic balance of the soil between applied water and water uptake by plants. Triggered by evapotranspiration, which is induced by heavy vapor pressure deficit (VPD), and capillary forces, salt-contaminated water is rises from deeper soil layers leading to high salt accumulation of the root zone and soil surface (Yadav et al. 2011). Accordingly, in arid and semiarid regions around the world where the annual precipitation is lower than the annual evapotranspiration, salinity is a prevalent environmental hazard (Turki et al. 2012). The extent of secondary salinity, relative to primary salinity, is rather small (Munns 2005). However, the secondary salinity is a dynamic process which triggers huge socioeconomic problems particularly in developing countries, leading to social unrest and migration pressure due to crop failures (Pessarakli 2011). Hence, salinization is regarded as one of the most important contributors to desertification (Thomas and Middleton 1993, Turki et al. 2012, Allbed and Kumar 2013) and global climate change is further leading to the deterioration of soils (Pessarakli 2011).

Leaching and the establishment of drainage systems are methods commonly used to restrict salinization and reclaim salinized soils (Shrivastava and Kumar 2015). Furthermore, the application of appropriate irrigation systems is an effective mechanism to reduce salinization. However, soil reclamation and modern irrigation system are costly and not applicable for all crops (Genc et al. 2016). Effective soil reclamation activities, together with the cultivation of salt-tolerant plants, is generally accepted to be the best option to combat salinity. For sustainable food production under saline conditions, in many parts of the word, the use of adapted crops is regarded as the most promising approach (Munns and Gilliham 2015). In addition, salt-tolerant crops have a much lower leaching requirement than salt-sensitive crops (Munns et al. 2006).

Among the cereals, rice is regarded as most susceptible to salinity stress and barley is regarded as most tolerant. Within this frame, bread wheat is regarded as comparably moderate tolerant

towards salinity stress (Munns and Tester 2008). Moreover, significant genotypic variability with respect to salinity tolerance is widely known for many plant species (Bağci et al. 2003). However, the genetic variability of currently available wheat germplasm is low with respect to salinity tolerance (Ashraf and Akram 2009). Extensive screening approaches of a large number of genotypes led to the detection of only a few landraces like Candeal (Spain), Kharchia (India) and Shorwaki (Pakistan) possessing a certain degree of salinity tolerance (Puntamkar et al. 1970, Sayed 1985, De León et al. 2011, Sharma 2015). Especially, the landrace Kharchia was thereafter employed in multiple breeding programs as the donor of beneficial salinity tolerant alleles by crossing with high yielding and high-quality cultivars. Despite all breeding efforts, little success was achieved in breeding salinity tolerant wheat cultivars as not only the beneficial alleles were introgressed into the elite background but also alleles with adverse effects like lodging, low baking and threshing quality (Colmer et al. 2006, Munns et al. 2006, Genc et al. 2007).

Effect of salinity on plants

Salinity tolerance is a genetically complex trait controlled by a large number of tissue and developmental specific genes (Munns and Tester 2008). Plants undergo characteristic changes by the time of exposure to salinity stress until their maturity. The temporal effect of salinity stress on plants was outlined by Munns et al. (1995) with the concept of "two-phase growth response to salinity" (Figure 2). For most plants, the first phase starts with an ECe value above 4 dS m^{-1} and varies between few days and weeks, depending on the genotype and the osmotic pressure (Munns 2005, Jamil et al. 2011). At this level, the osmotic stress is emerging which is imposed by the low osmotic potential in soil water inhibiting plant roots to uptake water. Consequently, the shoot growth rate is declining. Plants with increased osmotic tolerance withstand the osmotic stress to some degree and maintain growth rates to a certain level (Figure 2A). The ionic phase follows the osmotic phase. Different to the osmotic stress the ionic stress develops not immediately but over time; for most annual plants between few days and weeks (Munns 2005). The accumulation of toxic ions in the cytoplasm leads to cell injury. Along with the transpiration streams toxic ions such as Na^+ accumulate in leaves. Younger leaves dilute the toxic concentration of ions by the expansion of cells. As the cellular expansion of older leaves stops, the concentration of toxic ions is high enough to kill cells, leading untimely to death of older leaves (Munns and Tester 2008). Generally, Na^+ enters plants through ion channels and carrier type transporters (Maathuis et al. 2014). In this regard, non-selective cation channels

(NSCC) play an important role in raising of nutrient imbalances, e.g. Ca^{2+} deficiency as Na^{+} is competing with the uptake of Ca^{2+} (Tester and Davenport 2003, Mian et al. 2011).

The ionic tolerance comprises the ability of plants to withstand higher concentration of adverse ionic compounds, such as Na^{+} and Cl^{-}, within the cytoplasm, especially in mesophyll cells of leaves (Figure 2B). According to Munns and Tester (2008), the osmotic stress not only has an immediate effect on growth but also has a greater effect on growth rates than the ionic stress. Determining the importance of both stresses is strongly genotype specific and a matter of intensive debates (Almansouri et al. 2001). The combined increase in osmotic and ionic tolerance allows plants to resist throughout its life cycle salinity stress and to mitigate the decline of growth rate (Figure 2C).

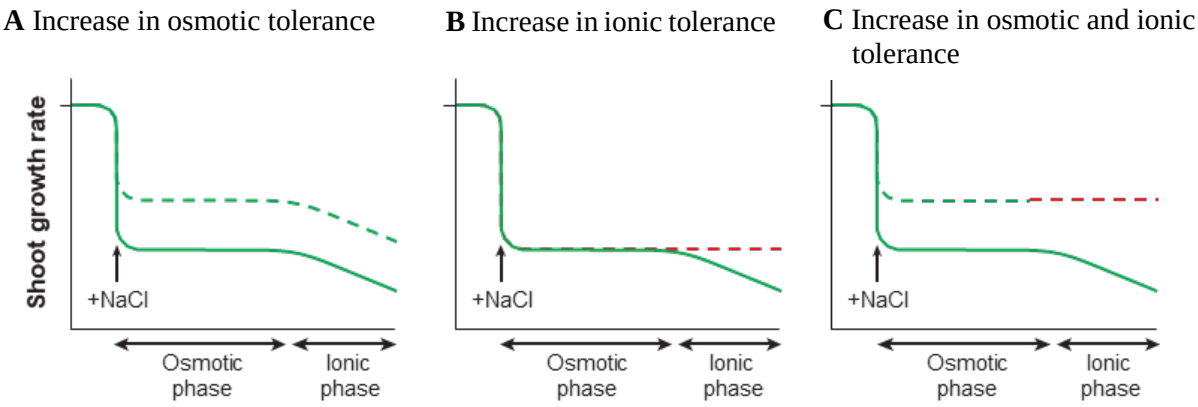

Figure 2. Concept of two-phase growth response to salinity (Munns and Tester 2008)

Note: Solid line indicates the change of shoot growth rate, the dashed green line indicates the hypothetical shoot growth rate with increased osmotic tolerance, the dashed red line indicates the shoot growth rate with increased ionic tolerance.

Plants are categorized as halophytes, that can withstand salinity if 200 mM NaCl or more, and glycophytes that cannot withstand salinity and eventually die without completing the life cycle (Flowers and Colmer 2008). The majority of crop species are glycophytes and hence threated by the high amount of salinity. Additionally, Asch et al. (2000) classified salt tolerant genotypes into two categories, Na^{+} includers and excluders, which are differentiated with respect to the concentration of K^{+} and Na^{+}. Plants with a high concentration of K^{+} and Na^{+} are indicated as Na^{+} includers. Na^{+} excluders are recognized by low Na^{+} and lower K^{+} concentration, in comparison to Na^{+} includers, to maintain high K^{+}/Na^{+} ratio.

Based on plant-specific morphological, physiological and metabolic processes plants developed three major categories of mechanisms to tolerate salinity stress (Flowers et al. 1977, Munns and Tester 2008, Adem et al. 2014, Gupta and Huang 2014), namely

1. Osmotic tolerance,
2. Exclusion of toxic ions and
3. Tissue tolerance.

1. Osmotic tolerance

In most plants, adjustment to osmotic stress is the most critical activity of salinity tolerance. The mechanism of osmotic tolerance includes increasing of osmotic potential in root cells by production and/or allocation of osmoprotectants such as amino acids (e.g. proline) and sugars (Rhodes et al. 2002), selective preferential uptake of K^+ and mechanisms of translocation of K^+ in shoots by diverse K^+ specific channels and transporters.

High-affinity K^+ Transporters (HKT), are meant to be highly important for Na^+/K^+ homeostasis in root and shoot cells. As HKT uniporters are involved in Na^+ exclusion from the cytoplasm, HKT symporters are in involved in Na^+ exclusion and preferential uptake of K^+ (Schachtman and Schroeder 1994, Flowers 2004, Almeida et al. 2017). Additionally, to reduce dehydration plants facilitate uptake of water by the establishment of waters channels like aquaporins (Mansour 2014). Several studies underline the importance of the growth of root cells and rigidity of root cell walls for osmotic tolerance (Neumann et al. 1994).

2. Exclusion of toxic ions

The mechanism of exclusion is mainly to minimize the amount of toxic $Na^{+\,-}$ in the cytoplasm of roots and shoots and maintaining high K^+/Na^+ ratio (Almeida et al. 2017). It is highly accepted that in a wide range of plants, except halophyte, salinity tolerance is correlated with the exclusion of Na^+ from the cytoplasm (Tester and Davenport 2003). However, different from their nature plants of both categories cannot tolerate high salt concentrations in the cytoplasm and maintaining high K^+/Na^+ ratio is regarded as an essential requirement for plants cells (Horie et al. 2012, Gupta and Huang 2014). According to Munns and Rawson (1999), minimizing the uptake of Na^+ by selective discrimination of Na^+ influx into root is accountable major fraction of Na^+ exclusion process. By this means most plants exclude more than 97% of sodium ions from the soil. Energy-dependent Salt-Overlay-Sensitive1 (SOS1) antiporters of Na^+/H^+,

localized in the plasma membrane, are regarded as a key transport system to withdraw Na^+ from the cell into the external media (Cuin et al. 2011, Wu et al. 2015, Almeida et al. 2017). Additionally, reduced Na^+ loading of xylem vessels and retrieval from xylem to prevent Na^+ influx into mesophyll cell of leaves are important requirements of salinity tolerance. Long range translocation of Na^+ from shoot to back to root to further reduced Na^+ concentration was described by Pitman (1977). According to subsequent studies the long-range reabsorption of Na^+ and translocation from shoot tissues back to the root is associated with members of the HKT1 family, preventing the large accumulation of Na^+ in the above-ground tissues (Almeida et al. 2017).

3. Tissue tolerance

If the salt concentration in leaves is high plants with capability of tissue tolerance minimize the concentration of Na^+ in cytoplasm and avoiding detrimental effects on cell metabolism by sequestration of large amount of salts in vacuoles and other cellular compartments (Munns et al. 2006, Adem et al. 2014, Roy et al. 2014). Several energy dependent antiporters like NHX1, NHX2, NHX3, and NHX4 were proposed to be involved in the transport of Na^+/H^+ and K^+/H^+ across the tonoplast in root and shoot cells (Adem et al. 2014, Almeida et al. 2017). Additionally, detoxification of cells by scavenging Reactive Oxygen Species (ROS) and restoration of normal cellular metabolism is a fundamental measurement of tissue tolerance.

However, the importance and extent of the above-mentioned salinity tolerance mechanisms can be different across species and even genotypes (Bağci et al. 2003). In general, plants respond to salinity stress with a combination of the above-mentioned mechanisms including overproduction of different types of low molecular solutes to maintain their osmotic potential. According to Greenway and Munns (1980), salt-loving halophytes sequester high amount of Na^+ and Cl^- in vacuoles and use them as energetically cheap osmolytes to maintain their turgor. Their salt tolerance depends additionally on morphological adaptations such as stronger cell walls and excretion of salt via salt glands (Adem et al. 2014).

Salinity tolerance by detoxification of Reactive Oxygen Species

Apart of exogenous toxins, plants are threatened by endogenous production of reactive oxygen species (ROS), such as superoxide ($O_2^{\bullet -}$), singlet oxygen ($^1O_2$), hydrogen peroxide (H_2O_2) and hydroxyl radical ($OH^{\bullet}$) is increasing (Møller et al. 2007). The specific toxicity of ROS lies in

their highly reactive character, causing substantial oxidative damage to proteins, lipids, carbohydrates and DNA which ultimately results in oxidative stress (Gill and Tuteja 2010).

Plants produce ROS as by-products of normal metabolic processes, particularly in photosynthesis in reaction centers of photosystem I (PSI) and photosystem II (PSII) in chloroplast thylakoids (Moons 2003, Sandermann 2004, Asada 2006). Disturbance of normal cellular metabolism, triggered by biotic and abiotic stress factors, is the main reason for over-excess of ROS (Figure 3). Salinity stress is rapidly inhibiting photosynthetic aperture of plants leading to high increase of ROS production when different pathways like photorespiration, mitochondrial respiration are uncoupled (Ashraf and Akram 2009).

Additionally, several reports indicate the role of ROS in loss of K^+ from the root and shoot cells by activating K^+ efflux channels (Velarde-Buendía et al. 2012, Wu et al. 2015). In plants, ROS have also a protective function as they are also involved in stress and hormone signaling by mediation of Ca^{2+}-signal transduction and activation of Ca^{2+}-permeable channels in plant membranes (Mori and Schroeder 2004, Miller et al. 2010, Suzuki et al. 2012, Kurusu et al. 2015). Therefore, the right balance between ROS scavenging and ROS production, as essential requirement of signaling pathways, is of critical importance for plants (Gill and Tuteja 2010). However, scavenging ROS is highly genotype specific and deficiency of available cellular antioxidants leads to increased accumulation of ROS (Lamb and Dixon 1997).

According to Hossain et al. (2015) ROS in plants is detoxified either by enzymatic or non-enzymatic mechanisms . Among ROS detoxifying enzymes glutathione S-transferases (GSTs) are of outstanding importance and widely studied (Moons 2003, Csiszár et al. 2014, Liu et al. 2015). As part of the superfamily of multifunctional enzymes, glutathione S-transferases are present in all kingdoms of living organisms (Wiktelius and Stenberg 2007). GSTs are participating in cell regulatory functions (Alias 2016) as well as in important biosynthetic or catabolic pathways (Noctor et al. 2012) and are involved in cellular detoxification and excretion of many physiological and xenobiotic and endobiotic substances.

Glutathione (GSH; γ-L-Glutamyl-L-cysteinyl-glycine) is the most important sulfur containing antioxidant in plants with key functions in detoxification of ROS and redox buffering (Edwards et al. 2000, Zechmann 2014, Nahar et al. 2016). As part of phase II detoxification enzymes GSTs are catalyzing the conjugation of electrophilic and hydrophobic compounds of xenobiotic or natural origin to GSH, to form non-toxic derivatives (Wilce and Parker 1994, Frova 2003,

Martínez-Márquez et al. 2017). In respect to detoxification of H_2O_2, GST is catalyzing the conjugation of the reduced GSH to H_2O_2 to produced H_2O (Figure 3).

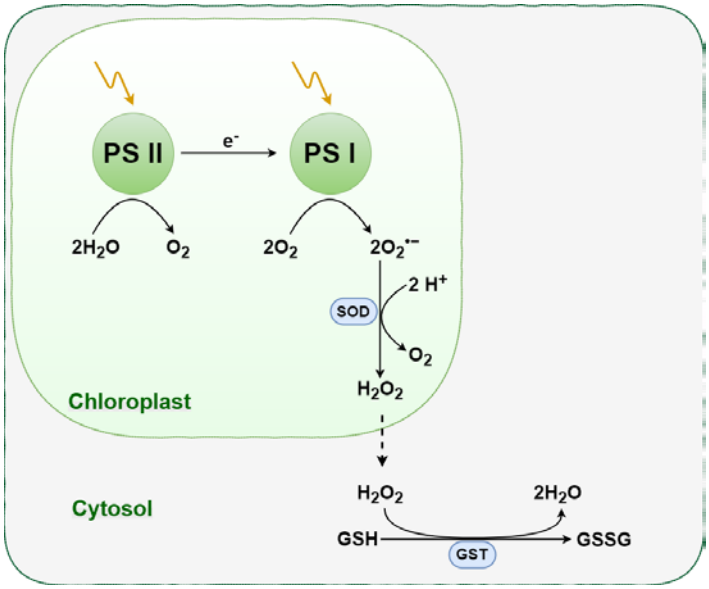

Figure 3. Simplified pathway of ROS generation within chloroplasts

Note: PS I/II Photosystem I and II; $O_2^{\bullet-}$ superoxide; H_2O_2 Hydrogen peroxide; SOD superoxide dismutase; GSH Glutathione; GSSG Oxidized glutathione; GST glutathione S- transferase; Yellow arrows indicate photons of light; As byproducts of photosynthesis activity superoxides are produced continuously. Disruption of photosynthesis increases $O_2^{\bullet-}$ production in chloroplasts, which is quickly catalyzed by SOD to H_2O_2 and O_2. GST is catalyzing the detoxification of the diffused H_2O_2 from chloroplasts with the help of GSH to H_2O and oxidizing GSH to GSSH.

To date, the family of GSTs in plants is classified into 14 classes according to their sequence identity, gene organization, active sites in protein and substrate specificity (Munyampundu et al. 2016). Among all classes the *tau* class (GSTu) is one of the largest group and distinct plant specific. The versatility of GSTu was reported in several studies with respect to plant protection against biotic and abiotic stresses as well as regulator of cell elongation and plant development (Székely et al. 2008, Sharma et al. 2014, Liu et al. 2015). Commonly GSTs from the same class are tandemly-arrayed and gene duplications are clustered on the same chromosomal region. These special characteristics of GSTs have great importance on their multifunctionality and diversification in their enzyme specificity and activity toward different substrates (Dixon et al. 2002, Lan et al. 2009, Liu et al. 2015). Based on this variation scheme, Frova (2003) and recently Nianiou-Obeidat et al. (2017) proposed biotechnical engineering of GSTs of new or enhanced functions based on rational and irrational protein designing approaches. Beyond this

approach, successful introgressions of GST genes from one species to another species improving tolerance towards biotic and abiotic stress factors like salinity were reported for several crops like *Lycopersicon esculentum* Mill. (Xu et al. 2015), *Nicotiana tabacum* L. (Yu et al. 2003) and *Oryza sativa* L. (Zhao and Zhang 2006).

The sensitivity of glycophytes to salinity stress varies with the growth stage. Generally, plants are more sensitive at early growth stages and less at reproduction stage (Flowers and Yeo 1995, Wilson et al. 2000). The importance of germination stage for plants withstanding salinity stress was widely discussed by a large number of publications (Kent and Läuchli 1985, Kaya et al. 2003, Singh et al. 2012). High salinity levels of soil and soil water dramatically induce germination failure of wheat seeds leading to yield losses and reduced grain quality (Francois et al. 1988, Pleijel et al. 1991). According to Ayers (1952) salinity is affecting germination of seeds by decreasing the rate of water entry and the high concentration of toxic ions. The physio-chemical effects also apply to further developmental stages, affecting multiple morphological, physiological and biochemical processes of plants. Among others, production of biomass is the most common traits for evaluation of plants exposed to salinity stress beyond germination stage (Munns and James 2003, Adem et al. 2014). Other frequently measured traits for evaluation of salinity stress in a hydroponic system at the seedling stage are plant height (shoot and root), mineral composition (mainly Na^+ and K^+) of leaves, as well as photosynthetic and gas exchange parameters. With respect to the evaluation of plants under field condition, yield and yield components are considered to have high importance rather than biomass or harvest index (Shannon 1997).

Most studies investigate salinity stress at germination stage or seedling stage in greenhouses or climate chambers as it is feasible to screen a large number of plants under controlled environmental conditions. Implementation of large field experiments on natural saline soils is complex and greatly environmental affected (Agarwal et al. 2013, Genc et al. 2016). Only a few studies were investigating salinity stress of wheat plants at germination stage, seedling stage and furthermore under field conditions. Wheat plants are most susceptible to salt stress at germination and seedling stage. On the other hand, according to Munns and James (2003), at germination stage fields are usually at their least saline at the time of planting due to rainfalls, irrigation or preceding leaching approaches. However, there is a low correlation between the performance of genotypes at germination or seedling stage yield under field conditions (Almansouri et al. 2001, Munns et al. 2006). Ultimately, breeding relies greatly on phenotyping

accuracy of a large number of genotypes under field conditions with natural salinization (Ashraf and Akram 2009, Genc et al. 2016).

Analysis of Quantitative Trait Loci

Generally, statistical models are utilized in order to localization genetic regions coding for quantitative traits such as salinity tolerance (Eshed et al. 1992, Tanksley 1993, Kearsey and Farquhar 1998, Dadshani et al. 2004). However, essential requirements for precise detection of quantitative trait loci (QTL) are detailed phenotypic information on specific traits and highly informative genotypic information.

According to Hawkesford and Lorence (2017) phenotype is the physical manifestation of genotype and interaction of all environmental effects acting on the organism. Precise measurement of phenotypic traits is a fundamental requirement for accurate localization of genes related to the trait, particularly quantitative traits (Poorter et al. 2012, Fiorani and Schurr 2013). However, salinity tolerance is a complex trait and controlled by a large number of genes. A summary of relevant morphological and physiological traits is shown in Munns et al. (2010) and Colmer et al. (2005). Frequently, among common gravimetric measurements, Na^+, K^+ and other salt specific components in diverse parts of plants are analyzed in order to understand genotype specific regulatory mechanism in plants to cope with excess of salts (Cramer et al. 1990, Chhipa and Lal 1995, Asch et al. 2000). However, application of non-invasive sensors is indispensable to observe changes over time and for understating the evolution of salinity stress at various growth stages (Dadshani et al. 2015, Großkinsky et al. 2015)

According to Mackay (2009) detection of QTL in a linkage study needs identification of reliable difference in the average value of the trait between marker genotypes. Hence, besides accurate phenotypic information, the genotypic characterization of genotypes under study is essential. Ideally, the number of markers should be sufficiently large to increase the mapping accuracy (Singh and Singh 2015). Especially with respect to localization of QTL related to a trait with low heritability high marker density is a crucial criterion to narrow down the chromosomal region (Rustgi et al. 2013). The high-density single nucleotide polymorphism (SNP) genotyping array iSelect 90K, comprising almost 90.000 gene-associated markers, provides an invaluable source of genetic information, that can be employed to characterize genetic variation in hexaploid wheat (Wang et al. 2014).

Beside traditional linkage analysis (LA), using segregating populations, e.g. F2-population, Near Isogenic Lines (NILs) or Recombinant Inbred Lines (RILs), genome-wide association study (GWAS), which is based upon the principle of linkage disequilibrium (LD) at the population level, is frequently used to detect marker-trait associations (Tanksley and Nelson 1996, Visscher et al. 2012). For many years, linkage analysis was the preferred approach for identification of Mendelian and quantitative traits in related populations (Ott et al. 2015). In recent years GWAS is gaining more importance and is replacing LA. However, as GWAS is considered as a powerful tool providing a high-resolution evaluation of numerous alleles, it comes along with some substantial drawbacks: One major problematic aspect of GWAS is the existence of population structure in the association population due to evolutionary mechanisms such as natural selection, genetic drift and mutations (Star and Spencer 2013, Kutnjak et al. 2017) as it can lead to an increased number of false-positive results. Ultimately most mapping studies aim to detect functional genetic variants, or the quantitative trait nucleotides, that are responsible for phenotypic variation (Myles et al. 2009). However, as association analysis is highly affected by the extent of LD- Low decay of LD will always make the disentanglement of causative variants difficult (Korte and Farlow 2013) and therefore, in many cases, GWAS is not detecting causal relationship but only associations (Ward and Kellis 2012, Pascual et al. 2016). Consequently, further fine mapping studies are required for determination of causal factors (Ioannidis et al. 2009, Witte 2010). Furthermore, for detection of epistatic interaction especially in complex traits, GWAS is still struggling with computational and statistical difficulties (Korte and Farlow 2013), different than in segregating populations where epistatic analysis is more effective and widely accepted (Juenger et al. 2005). Accordingly, Wilson et al. (2004) proposed the combination of LA and GWAS analysis to circumvent the drawbacks and to exploit the strengths of both approaches. Pyramiding of salinity tolerance genes by application QTL analysis and subsequent marker-assisted selection in breeding approaches has an enormous potential to accelerate the breeding process (Genc et al. 2010).

Identification of salt-responsive genes by application of GWAS and QTL analysis has been widely used in many plants, including *Arabidopsis* (DeRose-Wilson and Gaut 2011), tomato (Foolad et al. 1997), barley (Mano and Takeda 1997, Xue et al. 2017), rice (Gong et al. 1999, Ren et al. 2005, Bernier et al. 2007), maize (Bänziger and Araus 2007, Luo et al. 2017) and wheat (Dubcovsky et al. 1996, Genc et al. 2010).

Forward genetic approaches by application of AM and QTL analysis revealed a vast number of loci that related to salt tolerance. Several loci were detected with relation to Na^+ concentration of leaf tissues, as much of recent works focused more on Na^+ exclusion, among them Nax1 (TaHKT1;4), Nax2 (TaHKT1;5A) which are involved in limiting massive Na^+ transport from xylem to leaves (Munns and James 2003, Genc et al. 2016) and KNa1 (TaHKT1;5D) which is responsible for the maintenance of a high cytosolic K^+/ Na^+ ratio in the leaves of salt-stressed plants (Byrt et al. 2014).

However, recent studies question the importance of the over two decades propagated theory of Na^+ exclusion as the main mechanism of salinity tolerance, as according to Munns (2005) most plants are efficient Na+ excluder (Benderradji et al. 2011, Genc et al. 2016). While some scientists suggest focusing more on tissue tolerance mechanism of plants as a more important component of salinity tolerance (Shavrukov et al. 2011, Genc et al. 2016) other scientists prefer combined investigation of tissue tolerance and osmotic tolerance as both are regarded as inseparable from each other (Munns et al. 2016).

Despite of some success in identification of genes that confer salinity tolerance in model plants, such as *Arabidopsis* and complex plants with polyploid genomes, like hexaploid wheat under controlled environmental conditions, little success has been achieved in transferring this research outcome to the fields (Flowers 2004, Munns et al. 2006, Sanchez et al. 2011, Genc et al. 2016). The reason for this is that most studies were conducted under controlled environmental conditions and not under natural field conditions with multiple environmental effects and that the focus was laid on distinct growth stages and not the entire life cycle of plants (Foolad 1999, Munns 2011).

The new advances in phenotyping plants at different growth stage, under lab and field condition, especially non-destructively by application of sensors, QTL mapping by incorporation of high density genotyping information along with sequencing technologies are expected to improve the precision and speed of detection of favorable alleles in and to pave the way to introgress these genes into elite cultivars by marker-assisted selection (Flowers and Flowers 2005, Mondal et al. 2016).

2. HYPOTHESIS

1. Salinity tolerance in bread wheat is genetically controlled.

2. Crop wild relatives of wheat harbor favorable alleles for salinity tolerance.

3. Various mechanisms are responsible for salinity tolerance in wheat plants in different growth stages.

4. Non-destructive senor technologies allow accurate and continuous monitoring of morpho-physiological parameters of plants exposed to salinity stress.

5. Expression of specific genes modulates tolerance of wheat salinity stress.

3. MATERIALS AND METHODS

Central objective of this thesis was the phenotypic and genotypic assessment of salinity stress on wheat. Additional experiments were conducted in order to detect water status in plant leaves non-destructively by using microwave resonator technique.

3.1. Assessment of salinity stress

Several experiments at different development stages of wheat were conducted in order to characterize the diverse effects of salt stress at specific developmental stages of wheat. The development stages of interest were:

- Germination stage
- Seedling stage
- Maturity stage

The following section outlines the materials and methods that were applied to conduct the experiments at germinations, juvenile and maturity stage of wheat.

3.1.1. Germplasm

The tested plant material consisted out of 151 advanced backcross lines (AB-lines) of the winter wheat population "Z86" ($BC_2F_{3:7}$). The seeds of the Z86 population was provided by Dr. Ram Sharma (Central Asia & Caucasus Regional Program ICARDA). Originally the Z86 population was produced at University of Bonn (Germany) - Institute of Crop Science and Resource Conservation, chair of Plant Breeding by crossing the German elite winter wheat cultivar Zentos (*Triticum aestivum* L.; Syngenta Seeds GmbH, Bad Salzuflen) with the synthetic hexaploid wheat Syn086L (Kunert et al. 2007). The elite cultivar Zentos (Syngenta Seeds GmbH, Bad Salzuflen, Germany) was registered at Bundessortenamt (the Federal Plant Varieties Office of Germany) in 1989 as high performant and high yielding variety (Bundessortenamt 2016).

The synthetic parent, Syn086L, was produced by Lange and Jochemsen (1992) by crossing wild emmer (*Triticum turgidum* spp. *dicoccoides*; accession number G4M-1M) as donor for AABB genome and *Triticum tauschii* (accession number Gat-525) as donor of DD genome. Since the emasculation of *Triticum tauschii* was more complicated than of wild emmer, *Triticum tauschii*

was acting as male parent and wild emmer as female. Syn086L served as the donor of exotic alleles located on the D genome.

For the establishment of the Z86 advanced backcross winter wheat population the initial cross was between the elite cultivar Zentos as female parent and Syn086L as male parent (Figure 4). The resulting F1 plants (maternal) were backcrossed two times with the recurrent elite cultivar Zentos (paternal). After regular selfing the plants achieved BC_2F_3. Without additional selfing, the F_3 lines were bulk propagated under field conditions two more generations deriving the F_3 lines to F_7. denoted as $F_{3:7}$.

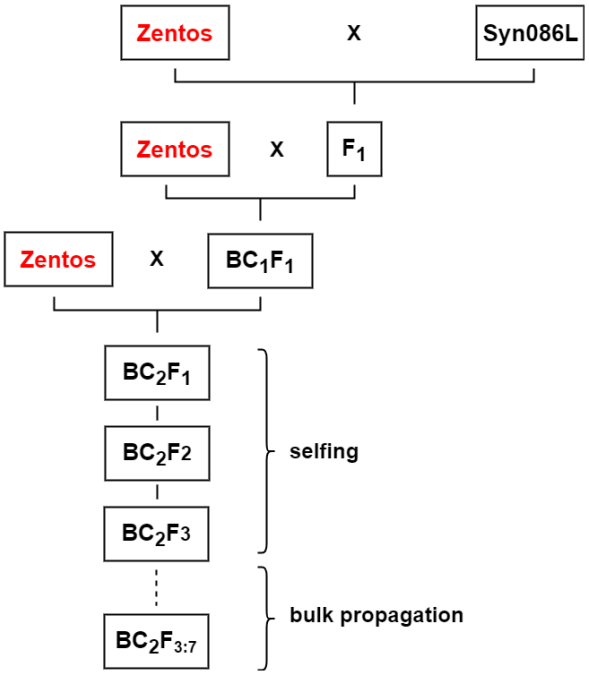

Figure 4. Establishment of the Z86 backcross population

The bulk propagation process was continued by the Central Asian division of ICARDA and collaborating National Agricultural Research Systems (NARS) of Uzbekistan in the years 2010 and 2011 deriving the BC_2F_5 population of F_7; denoted as $BC_2F_{3:7}$. The names and entry numbers of the AB-lines of the Z86 population is presented in Table 29 in Appendix 1. For the sake of simplicity, instead of genotype names the entry numbers will be used in this work.

3.1.2. Assessment of salinity response at germination

Germination tests were carried out, following the method described by Mano and Takeda **(**1998**)**, in order to investigate the performance of the tested genotypes exposed to various concentrations of sodium chloride and sodium sulfate salt treatments (see Table 2).

Within the context of the germination test, the Z86 population including the parents Zentos and Syn86 were subjected to salt stress at germination stage. Seeds of the testing population were surface sterilized with 70% ethanol for one minute followed by three times rinsing with deionized water. Ten seeds of average size were sown on filter paper with 160 g per m² (C 160; Munktell & Filtrak GmbH; Bärenstein, Germany) placed in crystal clear rectangular boxes with the dimensions 288 mm x 224 mm x 30 mm (V3-92; Licefa GmbH & Co. KG, Bad Salzuflen, Germany). The plants in the boxes were grown for 10 days in the climate chamber at 20°C, 12h/12h photo/dark period and with 50% humidity. The light condition in the climate chamber was 200 $\mu mol\ m^{-2}\ s^{-1}$.

The seeds were irrigated every second day with the specific salt concentrations summarized in Table 2. The salt solutions were prepared by dilution of the salts in deionized water. For the control treatment, only deionized water without any salt was used.

Table 2. Summary of used salts and salt concentrations for the germination tests

Treatment	Chemical formula	Water	Salt concentration	CAS number	Supplier
Sodium chloride	NaCl	Deionized water	50 mM, 100 mM, 150 mM, 200 mM, 250 mM	7647-14-5	AppliChem GmbH
Sodium sulfate	Na_2SO_4	Deionized water	50 mM, 100 mM, 150 mM, 200 mM	7757-82-6	AppliChem GmbH
Control	-	Deionized water	-	-	-

After 10 days the genotypes were scored from 0 to 9 according to a modified scheme of Mano and Takeda (1998) specified in Badrize et al. (2009). The applied scoring scheme is outlined in Table 3.

Table 3. Scoring scheme for germination stage in wheat according Mano and Takeda (1998).

Score	Explanation
0	No germination
1	One root elongated or poor root development
2	Two roots elongated or more roots with brown tips
3	Three or more roots elongated, normal root development
4	Shoot less than 10 mm with green color
5	Shoot elongated between 10 and 25 mm
6	First leaf protruded the coleoptile up to 1 cm
7	First leaf developed up to 3 cm from the coleoptile
8	First leaf developed up to 6 cm from the coleoptile
9	First leaf is longer than 6 cm from the coleoptile

3.1.3. Assessment of salinity response at seedling stage

A hydroponic system under greenhouse condition was established in the year 2013-2015 in order to characterize salinity tolerance of the Z86 wheat population at seedling stage. As described under 3.1.2, seeds were pre-germinated in germination boxes for 8 to 9 days. Seedlings of equal size were transferred at the two-leaf stage into the hydroponic system. The utilized hydroponic system followed partly the methods described in Dubcovsky et al. (1996) and Genc et al. (2007, 2010). It consisted out of 12 light-tight polypropylene boxes with 170 L capacity (EG 86/42 HG by Auer Packaging, Amerang, Germany). Each box was aerated by four adjustable air diffusers (Eheim 4002650, Eheim GmbH & Co. KG, Deizisau, Germany) fixed on the bases of each box. The air was supplied by electric air pumps (Eheim 400, Eheim GmbH & Co. KG, Deizisau, Germany) operating continuously. The boxes were covered with light-tight panels (Styrodur 3035 CS, BASF SE, Ludwigshafen, Germany). Each panel was prepared with 54 holes where hydrophobic sponges were inserted to keep the plants above the solution. The boxes were filled with 170 L tap water including nutrient solution according to Asao et al. (2012) summarized in Table 4. According to the monthly report of the Stadtwerke Bonn “Energie und Wasser” (2013) the EC value of the used tab water was 0.08 mS/cm.

With respect to reproducibility and comparability, the hydroponic experiments were carried out with 100 mM NaCl and Na_2SO_4, respectively, as the majority of recent salt stress studies in wheat were conducted with this salt concentration. After nine days of adaptation in the

hydroponic system, the salinity level of the salt treated boxes was increased incrementally in three days by adding NaCl and Na_2SO_4, respectively, until reaching the final concentration of 100 mM.

Table 4. Composition of nutrient solutions for the hydroponic system

Chemical	Chemical formula	CAS number	Concentration	Supplier
Ammonium nitrate	NH_4NO_3	6484-52-2	0.2 mM / L	AppliChem GmbH
Potassium nitrate	KNO_3	7757-79-1	5 mM / L	AppliChem GmbH
Calcium nitrate	CaN_2O_6	10124-37-5	2 mM / L	AppliChem GmbH
Magnesium sulfate	$MgSO_4$	7487-88-9	2 mM / L	AppliChem GmbH
Potassium dihydrogen phosphate	H_2KO_4P	7778-77-0	0.1 mM / L	AppliChem GmbH
Di-Sodium Metasilicate	Na_2SiO_3	6834-92-0	0.5 mM / L	SIGMA-ALDRICH CHEMIE GmbH
Iron (III) monosodium salt	NaFe(III)-EDTA	15708-41-5	100 µM / L	Alfa Aesar GmbH
Boric acid	H_3BO_3	10043-35-3	12.5 µM / L	Pharmacia Biotech
Mangan chloride	$MnCl_2$	7773-01-5	2 µM / L	SIGMA-ALDRICH CHEMIE GmbH
Zinc sulfate	$ZnSO_4$	7733-02-0	3 µM / L	J.T.Baker Chemicals
Copper (II) sulfate	$CuSO_4$	7758-98-7	0.5 µM / L	AppliChem GmbH
Sodium molybdate	Na_2MoO_4	7631-95-0	0.1 µM / L	SIGMA-ALDRICH CHEMIE GmbH
Nickel sulfate	$NiSO_4$	7786-81-4	0.1 µM / L	AppliChem GmbH
Potassium chloride	KCl	7447-40-7	25 µM / L	Merck KGaA

Portable pH-/EC-meter (Mettler Toledo SG2-FK SevenGO, Columbus, Ohio, United States) was used to measure pH- and EC values every second day. The temperature adjusted EC value of the control solution with no additional salt was around 1.8 mS/cm, 12 mS/cm at 100 mM NaCl and 16 mS/cm at 100 mM Na_2SO_4. HCl and NaOH were added to adjust the pH value between 6.2 and 6.5. The solutions were renewed every nine days. The hydroponic boxes were placed during the testing period in the greenhouse with 20°C day and 12°C night temperature and 12h/12h photo/dark period.

Measurement of morphological and physiological parameters

Table 5 summarizes parameters measured during the hydroponic experiments that were conducted under control, 100 mM NaCl and 100 mM Na_2SO_4 condition.

Table 5. Overview of phenotypic parameters collected from hydroponic experiments

Parameter	Treatment		
	Control	100 mM NaCl	100 mM Na_2SO_4
Shoot fresh weight / dry weight	✓	✓	✓
Root fresh weight/ dry weight	✓	✓	✓
Root length at day 0 (DAS 0)	✓		✓
Root length at day 9 (DAS 9)	✓		✓
Root length at day 16 (DAS 16; harvest)	✓	✓	✓
Shoot height at day 0 (DAS 0)	✓		✓
Shoot height at day 9 (DAS 9)	✓		✓
Shoot height at day 16 (DAS 16; harvest)	✓	✓	✓
Leaf Membrane Leakage	✓	✓	
Length of 3rd leaf	✓		✓
Fresh weight / dry weight of 3rd leaf	✓		✓
Chemical components analysis (K, and Na) of 3rd leaf	✓		✓

Note: DAS=days after stress application

The dry weight of plant material was measured after drying for three days in the drier with 65°C.

K and Na concentrations were measured by the Atomic Absorption Spectrometer (AAS) AAnalyst 200 (Perkin Elmer, USA) following the method described by Madejczyk and Baralkiewicz (2008).

Leaf Membrane Leakage

Leaf membrane leakage (LML) or electrolyte leakage is an indication of plant's membrane integrity. Membrane permeability was assessed according to Lutts et al. (1995). A cork cutter of the diameter of 4 mm was used to cut 10 discs of leaf sheath of wheat plants at harvesting (DAS 16). The discs were rinsed briefly with millipore water. Immediately after drying with soft paper tissue the discs were put in 50 ml Falcon tubes containing 30 ml millipore water. The falcon tubes were placed horizontally on an electric shaker and were gently shaken for 4h at room temperature (22°C). After that, the initial electrical conductivity (EC) of the water was measured with portable pH-/EC-meter (Mettler Toledo SG2-FK SevenGO, Columbus, Ohio, United States). Thereafter the samples were kept in a freezer at minus 20°C for one day. After thawing at room temperature, the EC of the samples were measured again (EC_{final}). The percentage of membrane leakage (LML) was calculated as

Eq. 1

$$LML\ [\%]\ = \frac{EC_{innitial}}{EC_{final}} * 100$$

Where $EC_{innitial}$ stands for the EC value of the solution prior freezing and EC_{final} for the EC value after thawing.

The percentage of water content [%] of plant material was calculated by

Eq. 2

$$Water\ content\ [\%] = 100 - \frac{dry\ weight}{fresh\ weight} * 100$$

Fresh weight was measured of immediately after removing plant material from the solution. The dry weight of plant material was measured after drying for 3 days in the drier with 65°C.

The Stress tolerance index (STI) was calculated according to Fernandez et al. (1992) to differentiate genotypes in terms of stress tolerance and performance:

Eq. 3

$$STI = \frac{Parameter_{\ control} * Parameter_{\ treatment}}{(Parameter_{\ av;\ control})^2}$$

Where $Parameter_{control}$ stands for the value of the parameter under controlled condition and $Parameter_{treatment}$ stands for the value of the parameter under treatment. $Parameter_{av;control}$ stands for the population average under control condition.

With respect to parameters measured from field trials, the Stress-weighted performance index (SWP), established by Saade et al. (2016) was calculated following this equation:

Eq. 4

$$SWP = \frac{Parameter_{treatment}}{\sqrt{Parameter_{control}}}$$

Where $Parameter_{control}$ stands for the value of the parameter under controlled condition and $Parameter_{treatment}$ stands for the value of the parameter under treatment.

3.1.4. Application of sensors for non-destructive phenotyping

The sensors that were used to detect salt stress non-destructively are shown in Table 6. All sensors were applied on the third leaf of the plant at seedling stage.

Table 6. Applied sensors for non-destructive phenotyping

Sensor	Treatment		
	Control	100 mM NaCl	100 mM Na_2SO_4
SPAD meter, Chlorophyll meter	✓	✓	
Microwave sensor	✓	✓	✓
LI-COR LI-6400XT, IR photometer	✓		✓

SPAD meter

The Minolta-SPAD-502 Chlorophyll Meter (Minolta Camera Co., Osaka, Japan) was used to measure the greenness of leaves. The SPAD- meter measures the chlorophyll absorbance in the red and near-infrared regions and calculates a numeric SPAD value which is proportional to the amount of chlorophyll in the leaf (Markwell et al. 1995). SPAD values were determined for each plant, using the third fully expanded leaf. The mean of SPAD values was calculated by measuring on five different positions on the same leaf.

Microwave sensor

A prototype of a dual-mode EMISENS's microwave resonator (EMISENS GmbH, Juelich, Germany) was applied to assess non-invasively the water status and ionic conductivity of leaves exposed to salt stress (Figure 5). The properties of the microwave sensor are reported in Dadshani et al. (2015) (see Appendix 5). Briefly, the dual-mode sensor which was employed in this study allows measurements at two distinct and far separated resonant frequencies, one at 150 MHz (denoted as Mode 0) and the second at 2.5 GHz (denoted as Mode 1).

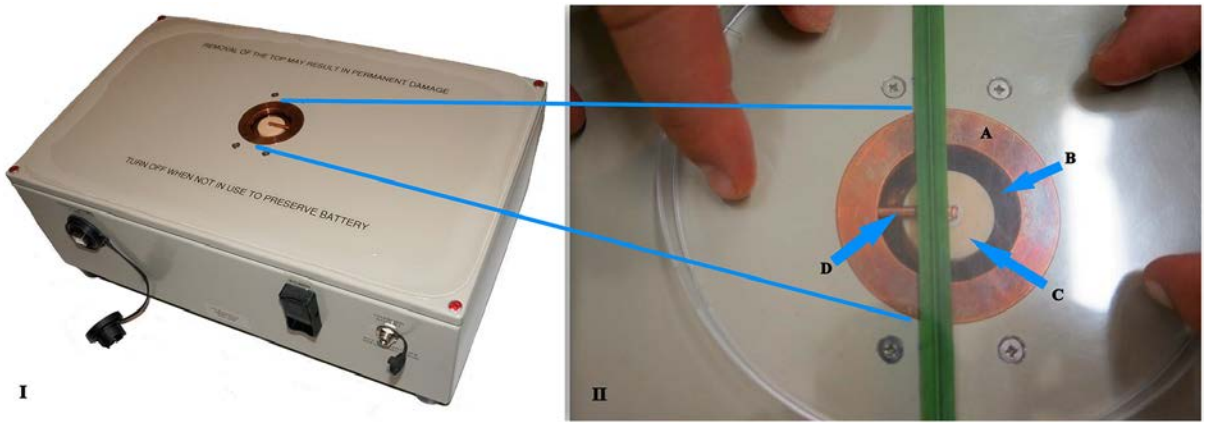

Figure 5. EMISENS dual-mode microwave resonator

Note: (I) – Photograph of the employed sensor system comprising a compact battery - powered circuit board - microwave electronic module, and (II) the zoomed measurement-window: dual mode cavity (copper, A) embedded in a housing with a wheat leaf in measurement position. The aperture in the copper cavity (dark circle, B) allows the evanescent field of the ceramic dielectric resonator (smaller light circle, C) to penetrate into the sample under test. The radial copper rod (D) which is partially covered by the leaf is a requirement for Mode 0 only.

As discussed in Dadshani et al. (2015) Mode 0 is ideally suited for contact-free assessment of the ionic conductivity of bulky plant leaves such potato and sugar beet leaves and Mode 1 is highly correlated with the osmotic potential of leaves.

During the assessment of a leaf under test, by the use of cavity perturbation theory (Pozar 1998) the change of the inverse quality factor (Q) and the resonant frequency (f_r) with respect to the empty resonator is recorded. Both Q and f_r are determined from a fit of a Lorentzian to the measured transmission curve using.

For the analysis, the negative relative frequency shift (*FRS*) due to the sample was calculated accordingly:

Eq. 5

$$FRS \equiv -\frac{f_{r,sample} - f_{r,empty}}{f_{r,empty}}$$

In Eq. 5, $f_{r,sample}$ stands for the resonant frequency (f_r) measured with the sample placed on the resonator and $f_{r,empty}$ stands for the resonant frequency (f_r) with respect to the resonator.

Since the frequency shift due to a dielectric object is usually negative, FRS is defined to be a positive number.
The sample induced change of the losses, i.e. change of the inverse Q factor (*IQS*) was recorded:

Eq. 6

$$IQS \equiv \frac{1}{Q_{sample}} - \frac{1}{Q_{empty}}$$

Where Q_{sample} stands for the Q factor of the sample and Q_{empty} stands for the Q factor of the empty resonator.

Relative change of both parameters, *FRS* and *IQS*, based on values for the specific parameters at initial fresh weight was calculated accordingly:

Eq. 7

$$rel.Parameter\ [\%] = \frac{Parameter_i}{Parameter_{initial}} * 100$$

In Eq. 7 $Parameter$ stands for *FRS* and *IQS*; $Parameter_{initial}$ stands for the *FRS* and *IQS* value, respectively, at initial fresh weight of the tested leaf, whereas $Parameter_i$ stands for the *FRS* and *IQS* value, respectively, with *i* standing for the six time-points from initial fresh weight (100%) up to 50% of the initial weight by consecutive 10% drying in each step.

Plant material

In this study four plant species being analyzed, wheat cultivar Zentos, maize (*Zea mays* L.) cultivar Aurelia, potato (*Solanum tuberosum* L.) cultivar Linda and canola (*Brassica napus* L.), cultivar Expert, were selected considering the size and morphology of their leaves. Wheat and maize leaves have similar shape, both are long, but wheat leaves are thinner. On the other hand, the potato and canola have compound leaves with oval leaflets, the canola leaves are larger and thicker. The plants were grown under greenhouse conditions in pots filled with soil (clay peat mix) and watered regularly.

Measurements of salt content (and ionic conductivity)

For the salt stress experiment, nine wheat genotypes were grown in three replicates in aerated hydroponic system as described in 3.1.3. The tested wheat genotypes were the parents of the Z86 population, Zentos and Syn086, and seven of their progenies which were selected based on their performance under salinity stress, representing salt tolerant and salt sensitive genotypes. The stress was induced by adding to the nutritional solution either NaCl or Na_2SO_4, to end-concentration of 100 mM and 50 mM, respectively. EC at control = 2.5 mS, NaCl = 11.5 mS, Na_2SO_4 = 9.5 mS), pH was checked every day and adjusted at 6.1 to 6.4.

Using the Microwave resonator sensor five measurements were performed in the center of each leaf without changing the position. By calculating the means, the five measurements were considered as technical replicates.

Measurements of water content

In order to follow the kinetics of water content the measurements were performed on detached leaves of the tested plants (wheat - cultivar “Zentos”, maize, potato, canola). Three leaves detached from each plant were chosen from three developmental stages in order to characterize tissues of various ages.

The stepwise reduction of water content in leaves was achieved by incubating them at high temperatures. The gravimetric measurement of water loss in the leaves was done by weighting them before and after drying. Shortly, after removal from the plant the leaves were weighted and measured with the microwave sensor system. This first-time point was considered as reference for a leaf with 100% (w/w) water. After that, the leaves were placed in an incubator at 45°C until 10% of initial water content was lost and the microwave assessment was performed instantaneously. The drying procedure with 10% loss each step and subsequent microwave measurement was repeated 5 times until reduction to 50% of the initial weight was reached. In fact, the time interval between removal and measurement was less than 30 seconds in any case.

The leave was placed on the window such the measured frequency shift is maximized, as shown in Figure 5 for wheat.

LI-COR LI-6400XT Portable Photosynthesis System

The gas exchange system (LI-6400XT; LI-COR Environmental, Lincoln, USA) was applied to measure the photosynthetic parameters of the Z86 population exposed to 100mM Na_2SO_4 salt stress. The infrared flow-through gas analyzer system (LI-6400XT) measures continuously photosynthesis parameters such as photosynthesis rate (*A*), transpiration rate (*E*), stomatal conductance (g_s) and intercellular CO_2 concentration (*Ci*) (Biosciences 2008).

Settings for the LI-COR LI-6400XT were the following: The flow rate was set to 400 µmol s^{-1} because leaves were relatively small at harvest and only with low a flow rate differences in photosynthetic activity could be measured. Because of an elevated level of CO_2 in the greenhouse, the CO_2 reference was set to 500 µmol CO_2 mol air^{-1} at the built-in mixer. To resemble the light conditions inside the greenhouse (lamps+ sunlight), the artificial light inside the leaf chamber was set to 200 µmol m^{-2} *s^{-1}. The relative humidity (RH) inside the leaf chamber was maintained at about 50 % RH with the help of the built-in desiccant.

An additional, a salt shock experiment, following the principal described by Shavrukov (2012) was established, in order to investigate the immediate response of plants exposed suddenly to a high level of salinity. In contrast to the previously described gradual application of salt in three increments until reaching the final concentration of 100 mM NaCl or Na_2SO_4, respectively, for the salt shock experiment the 50 days old plants were transferred suddenly from control solution into solution with 100 mM NaCl. The third fully expanded leaf was placed in the chamber of the LI-6400XT and an automated program was recording the photosynthetic parameters in intervals of 30 seconds, over a period of 60 minutes. Each measurement was regarded as one time-point. After 15 minutes in control solution (water + nutrients) the whole plants were removed and placed immediately into solution with 100 mM NaCl (including nutrients) without detaching from the sensor. Thus, continuous measurement of photosynthetic parameters of the plants exposed to immediate salt stress was possible. The first 15 minutes, after the plants were placed in the control condition, were considered as control values for the entire duration of the test. This experiment was conducted on the parents of the Z86 population, Zentos and Syn86 and on two lines of the Z86 population (genotype 84 and genotype 117) which were selected as extremes in respect to their tolerance towards salinity stress.

3.1.5. Experimental setup of field trials

In order to evaluate the performance of the Z86 population, including the parents Zentos and Syn-86, field experiments were conducted under non-saline and saline soil conditions with natural salinization in three planting seasons, in year 2010/11, 2011/12 and 2012/13, in Karshi (Uzbekistan; 38°52′N 65°48′E). The soil type was silty clay with a mixture of chloride-sulphate salts (sulphate/chloride ration 1.9 to 4.6). Due to the natural soil salinization, the intensity of soil salinity of the experimental site was heterogeneous. For all field trials, the plots were arranged according to Alpha Lattice design with three replications. The incomplete block design (IBD) was 10 plots with two rows per plot and the individual plot size was 1 m² (1.67m*0.6 m). Due to the limited number of available seeds in the year 2010/11 and 2011/12 only field experiments under saline condition were conducted.

Agronomic traits were collected according to the procedure described by Sharma et al. (2004). Briefly, at maturity stage, plant height (PH) in each plot was measured from ground level to the tip of the spikes in cm, days to heading (DHD) and days to maturity (DMD) were calculated starting from January 1st, Days to heading was recorded when spikes of approximately 50% of the plants in a plot fully emerged. Days to maturity were recorded when glumes completely lost their green color, according to Hanft and Wych (1982) and Knott and Gebeyehou (1987). Yield value harvested from 1 m² were converted from kg/m² to tons per hectare by multiplication with 10,000 (Sharma et al. 2011).

To assess the effect of salinity stress on the quality of produced wheat seeds under natural field conditions, seed quality parameters were analyzed by using near infrared reflectance spectroscopy (NIR) with Diode Array 7250 NIR analyzer (Perten Instruments, Inc., USA). According to several reports, NIR sensors are highly usable for assessment of milling quality of wheat seeds (Blažek et al. 2005, Mutlu et al. 2011, Pojić and Mastilović 2013). Grain quality parameters obtained by using the NIR analyzer are listed in Table 7.

Table 7. Grain quality parameter analyzed with NIRS sensor

Parameter	Unit
Starch	%
Protein	%
Fiber	%
Neutral Detergent Fiber (NDF)	%
Ash	%
Hardness of seeds	%
Zeleny sedimentation value	ml
Moisture	%

The summary of the phenotypic parameters collected from field experiments in growing season 2010/11, 2011/12 and 2012/13 are presented in Table 8. The implementation of field trials was limited by the availability of homogenous saline land for the stress treatment and less salt effected land for the control treatment. In addition, due to the limited number of available seeds in the growing season 2010/11 and 2011/12, field experiments were conducted only for stress treatment.

Table 8. Overview of phenotypic traits collected from field experiments in year

Parameters	**2010/11**		**2011/12**		**2012/13**	
	Control	Stress	Control	Stress	Control	Stress
DHD		✓		✓	✓	✓
DMD				✓		
PH [cm]		✓		✓	✓	✓
TLN		✓				
PL [cm]					✓	✓
SL [cm]					✓	✓
SpS [cm]					✓	✓
Yield [t/ha]		✓		✓	✓	✓
TKW [g])					✓	✓
NIRS (Grain quality parameters)					✓	✓

Note: DHD days to heading, DMD days to maturity, PH plant height, TLN number of tillers, PL length of peduncle, SL length of spike, SpS spikelet per spike, TKW 1,000 kernel weight, NIRS Near-Infrared Reflectance Spectroscopy.

3.2. Genotyping

The 151 AB-lines of the Z86 population and their parents Zentos and Syn86 were genotyped by pooling the extracted DNA of ten plants, using the Infinium iSelect 90K single nucleotide polymorphism (SNP) bead array assaying 81,587 gene-associated SNPs (Wang et al. 2014). The genotyping was outsourced to TraitGenetics in Gatersleben, Germany. Monomorphic markers giving no genotypic diversity were discarded additionally to SNPs with MAF (Minor Allele Frequency) less than 2.5% and more than 5% missing data (due to the presence of null alleles or poor genotype call rates). Allelic variants of the parent Zentos and Syn86 were codes with 1 and 3, respectively, whereas 2 was the coding for the heterogeneous variant.
The genetic map developed by Wang et al. (2014) with rescaled centimorgan (cM) distances comprising 40,267 markers with known positions was applied for further statistical and genetic analysis.

3.2.1. Molecular analysis

DNA extraction

DNeasy Plant Mini Kit (Qiagen, Hilden, Germany) was used to extract DNA from frozen plant tissues stored at -20°C following manufacturer´s instructions. The quality of the extracted samples was checked by spectrophotometric analysis using nanodrop 2000 (Thermo Fisher, Rochester, USA) following manufacturer´s instructions. The integrity of DNA was tested by applying on 1% agarose gel electrophoresis at 100V for 30 min. Peqgreen (Peqlab, Fareham, UK) was utilized as dye to visualize the nucleic acids and was added to melted agarose (4 – 6 µl per 100 ml of agarose solution). GeneRuler 1 kb DNA Ladder (Thermo Fisher Scientific) was also loaded in the gel for estimation of DNA size and approximate quantification. An easy visual tracking of DNA migration during electrophoresis was possible by loading the gel with bromophenol blue (Thermo Fisher Scientific). Extracted DNA was stored in -20°C for later use.

RNA isolation and cDNA synthesis

Samples of plant tissues were frozen in liquid nitrogen and stored at -80°C for subsequent processing. RNeasy Plant Mini Kit (Qiagen, Hilden, Germany) was used to extract RNA from frozen plant tissues following manufacturer´s instructions. The quality and quantity of extracted RNA were checked as described above (chapter 0). Afterward, DNase digestion procedure was

used to remove traces of genomic DNA from extracted RNA samples using Removal of Genomic DNA from RNA Preparations of RevertAid RT Reverse Transcription Kit (ThermoScientific). RevertAid H Minus First Strand cDNA Synthesis Kit (Thermo Fisher Scientific) was used to produce cDNA from purified RNA samples following manufacturer´s instructions. Extracted RNA and cDNA samples were stored at -80°C for later use.

Amplification of DNA strands

The standard protocol polymerase chain reaction (PCR) protocol was followed for amplification of DNA and cDNA fragments. Locus-specific sequence primers were generated following the pipeline described in Ma et al. (2015) and the primer characteristics required for LIGHTRUN sequencing at GATC Biotech AG (Konstanz, Germany).

Semi-quantitative RT-PCR

The semi-quantitative RT-PCR method was used to determine the expression of candidate genes in specific genotypes. For normalization and quantification of cDNA samples Cyclophilin A (Tenea et al. 2011) was selected as reference gene (Forward primer 5'-GGTCTCCCTTGCCAGATCAC-3'; Reverse primer 5'-GGGACGGTGCAGATGAAGAA-3'; 60°C annealing temperature; fragment size 500 bp). To normalize the amount of applied cDNA samples for Semi-quantitative RT-PCR foregoing tests were conducted to estimate the intensity applied with 2µl, 4µl and 8µl of PCR products on agarose gel.

Quantitative Real-time PCR (qRT-PCR)

In contrast to the semi-quantitative RT-PCR method, the quantitative real-time PCR (qRT-PCR) enables quantitative measurement of amplicons not at the end of the reaction but during the entire process of amplification. The principal described by Denman and McSweeney (2005) was conducted for microarray analysis by qRT-PCR using 7500 Fast Real-Time PCR System (Applied Biosynthesis, Darmstadt, Germany) with MicroAmp fast optical 96 well reaction plate (Applied Biosynthesis, Darmstadt, Germany). DyNAmo Flash SYBR Green qPCR Kit (Thermo Fisher Scientific) was employed as DNA-binding dye. Elongation factor *TaEf-1α* was selected as reference gene (Forward primer: 5'-CTGGTGTCATCAAGCCTGGT-3'; Reverse

primer: 5'-TCCTTCACGGCAACATTC-3'; 60°C annealing temperature; fragment size 151 bp) (Nicot et al. 2005). The standard $2^{-\Delta\Delta Ct}$ method described by Livak and Schmittgen (2001) was applied to analyze the gene expression relative to the reference gene *TaEf-1α*.

Sequencing for DNA and cDNA fragments

The amplified fragments were purified using QIAquick PCR purification kit. The purified template had a concentration of 20 to 80 ng/µl and of the sequencing primers 5 µM (5 pmol/µl). Sanger sequencing was performed by GATC Biotech AG (Konstanz, Germany).

Computer-assisted sequence analysis

Web-based blast servers such as National Center for Biotechnology Information (NCBI, http://blast.ncbi.nlm.nih.gov/Blast.cgi), ViroBLAST in Unité de Recherche Génomique Info (URGI, https://urgi.versailles.inra.fr/blast/blast.php) and EnsemblPlants genome annotation system (http://plants.ensembl.org/Triticum_aestivum/Tools/Blast?db=core) were used to find regions of similarity between biological sequences of barley, rice, maize, *Arabidopsis* and to detect homoeologous chromosomal location (Deng et al. 2007, Johnson et al. 2008, Kersey et al. 2016). All sequences were analyzed with the DNAStar package version 12.1 (DNAStar Inc., Madison, USA). MAFFT (Multiple Alignment using Fast Fourier Transform, http://mafft.cbrc.jp/alignment/server/) was conducted for additional sequence alignments (Yamada et al. 2016).

In-silico mapping of the conserved Transcription Factor Binding Sites (TFBS) was performed using the multiTF program of MULAN online package (Ovcharenko et al. 2005).

3.1. Statistical analysis

Analysis of variance (ANOVA) of phenotypic parameters

PROC GLM of SAS (2015) was applied to run analysis of variance of the Z86 population considering all replications and treatment levels by application of the following model

Eq. 8.

$$Y_{ij} = \mu + T_i + G_j + T_i * G_j + \varepsilon_{ij}$$

where Y_{ij} is vector of the phenotypic values; μ is general mean; $T_{i\ (i=1,2)}$ is the fixed effect of *i*-th treatment; $G_{j\ (j=1\ldots n)}$ is the random effect of *j*-th genotype, with n= number of genotypes; $T_i * G_j$is the random interaction effect of *i*-th treatment with *j*-th genotype; ε_{ij} is random errors (the residual).

Broad-sense heritability (H^2)

PROC VARCOMP of SAS (2015) was applied to run analysis of variance and to obtain the variance components for estimation of broad-sense heritability (H^2) across all the treatments using Restricted Maximum Likelihood (REML) method described in Holland et al. (2003).

Eq. 9

$$H^2 = \frac{V_G}{V_G + \frac{V_{G*T}}{t} + \frac{V_E}{t * r}}$$

where V_G genetic variance, T treatment, V_E error term, t and r denote the number of treatments and the number of replications, respectively.

Pairwise correlations

Pearson's correlation coefficient (r) assessing the linear relationships of traits measured in the Z86 population were calculated with Proc CORR procedure of SAS (2015) for each treatment.

Linkage disequilibrium

Pair-wise measures of linkage disequilibrium (LD) between two markers was calculated using R package 'genetics' version 1.3.8.1 (Warnes et al. 2012). The curves of LD decay were fitted using LOESS regression (Cleveland 1979). The decay of LD [cM] for each chromosome was estimated at the threshold of R^2=0.1. The genome-wide length of LD decay was obtained by calculating the mean of LD decays of all 21 chromosomes at R^2=0.1. R package 'LDheatmap' version 0.99.1 was applied to visualize genetic linkage groups for each chromosome (Shin et al. 2006).

3.1.1. QTL mapping

The QTL detection was carried out as a multiple QTL model in SAS (2015) using PROC MIXED procedure. Forward selection and backward elimination approach described in Bauer et al. (2009) was applied iteratively to reduce the number of false-positive and hence to endorse the power of detected true QTL. After each completed cycle the most significant markers were recognized as fixed factors in the following round to be tested with the remaining markers with lower F values in the previous round. In general, the P-value for F-tests was set to 0.001 and False Discovery Rate (FDR) < 0.05 as the threshold for the iterative multi-locus approach in the QTL model. The integration of 5-fold cross-validation procedure with 20% leave-out was incorporated to increase the accuracy of localization of informative markers and the estimation of the genetic effect. This procedure was repeated 20 times, and the resulting mean was used as a new p-value to define significant SNPs (QTLs).

Iteratively this procedure was conducted until no new QTL according to the defined threshold was detected. The applied QTL model is shown in the following equation:

Eq. 10

$$Y_{ijk} = \mu + T_k + M_i + L_j(M_i) + M_i * T_k + L_j(M_i * T_k) + \varepsilon_{ijk}$$

where Y_{ijk} is the vector of phenotypic values, μ is general mean, $T_{k\ (k=1,\ 2)}$ is fixed effect of *k*-th treatment, $M_{i\ (i=1\ldots p)}$ is fixed effect of *i*-th marker, p is the number of markers; $L_j(M_i)$ is random effect of each genotype nested in the *j*-th marker, where *j*=1…n and *i*=1….p, with n is the number of genotypes, $M_i * T_k$ is the fixed interaction effect of *i*-th marker with the *k*-th

treatment, $L_j(Mi * Tk)$ is the fixed effect of *j*-th genotype nested in the *i*-th marker interaction with the *k*-th treatment and ε_{ijk} is the residual.

The following equation summarizes the applied hierarchical model including an incorporated multi-locus approach for detection of QTL:

Eq. 11

$$Y_{ijk} = \mu + \Sigma QTL + M_i + L_j(M_i) + \Sigma QTL_{M*T} + M_i * T_k + L_j(M_i * T_k) + \varepsilon_{ijk}$$

where ΣQTL is the $\Sigma QTL_{Main\ effect}$ and ΣQTL_{MxT} from multi-locus analysis.

3.1.2. Epistatic interactions

The epistatic interactions between SNP markers pairs were tested with PROC MIXED of SAS (2015).

Eq. 12

$$Y_{ijkl} = \mu + T_l + M1_i * M2_j + L_k(M1_i * M2_j) + M1_i * M2_j * T_l + L_k(M1_i * M2_j * T_l) + \varepsilon_{ijkl}$$

For this purpose, the hierarchical QTL model (Eq. 11) was extended by terms of marker (1) by marker (2) interaction (digenic markers) using the multi-locus approach resulting in the following hierarchical model:

Eq. 13

$$Y_{ijkl} = \mu + \Sigma QTL + M1_i + M2_j + M1_i * M2_j + L_k(M1_i * M2_j) + \Sigma QTL_{M*T} + M1_i * M2_j * T_l + L_k(M1_i * M2_j * T_l) + \varepsilon_{ijkl}$$

where Y_{ijkl} is phenotypic variable, μ is general mean, Σ*QTL* represents the detected QTL from multi-locus approach, $M1_i$ and $M2_j$ are fixed effects of the *i*-th marker and the *j*-th marker, $M1_i*M2_j$ is the fixed interaction effect of the *i*-th *M1* marker genotype with the *j*-th *M2* marker genotype; $L_k\ (M1_i*M2_j)$ is the random effect of the *k*-th genotype nested in the *i*-th *M1* marker genotype and *j*-th *M2* marker genotype interaction; T_l is the fixed effect of *l*-th treatment, $M1_i*M2_j*T_l$ is the fixed interaction of the *i*-th *M1* marker genotype with the *j*-th *M2* marker

genotype and the *l*-th treatment, $L_k(M1_i*M2_j*T_l)$ is the random effect of the *k*-th genotype nested in the *i*-th *M1* marker genotype, *j*-th *M1* marker genotype and *l*-th treatment interaction and ϵ_{ijkl} is the residual.

3.1.3. Coefficient of determination (R^2)

The Coefficient of determination (R^2), which is estimating the genetic variance explained by a marker ($R^2{}_M$) and by marker*treatment interaction ($R^2{}_{M*T}$), was calculated according von Korff et al. (2006):

Eq. 14

$$R^2{}_M = \frac{SQ_M}{SQ_g}$$

Eq. 15

$$R^2{}_{M*T} = \frac{SQ_{M*T}}{SQ_{g*T}}$$

where in SQ_M is sum of square for marker main effect, SQ_{M*T} is the sum of square for marker*treatment effect, SQ_g stands for Type I sums of square of the the Z86 population in Eq. 1.

3.1.4. Calculation of repeated measures analysis of variance

To analyze the effects and interactions of genotype, treatment and temporal response repeated measures ANOVA using GLM of SAS (2015) by application of orthogonal polynomial transformation option (Eq. 16) . In this model genotype and treatment were set as independent variables. The different time points were regarded as a within-subjects factor, where every time point was regarded as a single measurement. The first 15 minutes of measurement in control condition was regarded as a control for the entire experimental time.

Eq. 16

$$Y_{ijx} = \mu + T_i + G_j + Z_x + T_i * G_j + G_j * Z_x + T_i * Z_x + T_i * G_j * Z_x + \varepsilon_{ijx}$$

where Y_{ijx} is the phenotypic value; μ is general mean; T_i is the fixed effect of *j*-th treatment; G_j is the fixed effect of *j*-th genotype; Z_x (x=1...60) is the time point; $T_i * G_j$ is the fixed interaction effect of *i*-th treatment with *j*-th genotype; $G_j * Z_x$ is the random interaction effect of of *j*-th genotype with of *x*-th time point; $T_i * Z_x$ is the effect of interaction of *i*-th treatment with *x*-th time point; $T_i * G_j * Z_x$ is the fixed interaction effect of *i*-th treatment and with *j*-th genotype and with *x*-th time point; and ε_{ijx} is random errors (the residual).

PROC GLM of SAS (2015) was applied to run analysis of variance of the Z86 population considering all replications and treatment levels by application of the following model:

Eq. 17

$$Y_{ij} = \mu + T_i + G_j + T_i * G_j + \varepsilon_{ij}$$

where Y_{ij} is vector of the phenotypic values; μ is general mean; T_i is the fixed effect of *j*-th treatment; G_j is the random effect of *j*-th genotype; $T_i * G_j$is the random interaction effect of *i*-th treatment with *j*-th genotype; ε_{ij} is random errors (the residual).

3.1.5. Application of visualization software

The software package CIRCOS was applied to create circular plots with chromosomal ideograms **(**Krzywinski et al. 2009**)**.

GGE Biplot graphics, visualizing main effect (G) plus Genotype by Environment (GE) interaction (G+GE) **(**Yan et al. 2000**)**, were produced using R **(**R Core Team 2016**)** by employing the package **(**Bernal and Villardon 2014**)**. The GGE biplot is based on the principal component analysis (PCA) which was based on Singular Value Decomposition SVP (see Yan and Kang (2002) for more details).

The web-based application Venny was used to create Venn diagrams (Oliveros 2007).

4. RESULTS

4.1. Phenotypic characterization of the Z86 population

To assess the phenotypic and genotypic variability of the synthetic backcrossed winter wheat population Z86 towards salinity stress, various experiments were carried out at germination and seedling stage. Additional field experiments were conducted in Central Asia under natural salinization. Subsequently, marker-trait association analysis was performed in order to detect chromosomal regions associated with the traits of interest. Finally, expressional analysis was performed to validate the detected candidate genes.

The following section is divided into five subsections according to the conducted experiments. The first subsection is dedicated to germination stage as salt affects wheat seeds primarily at this early developmental stage. The second section outlines the results of the hydroponic experiment with the results of the phenotypic characterization of wheat seedlings exposed to different salt stress regimes. The third subsection presents the outcome of the field experiments under saline and non-saline soil conditions. The results of the marker-trait association studies with the data obtained from the phenotypic characterization of the Z86 population at germination, seedling and maturity stage will be presented in subsection four. Finally, subsection five outlines the outcome of the gene structure and the gene expression analysis of some candidate genes related to salinity stress.

Overview of subsections of the results of the phenotypic characterization of the Z86 population:

1. Phenotyping of the Z86 population at germination stage
2. Phenotyping of the Z86 population at seedling stage
3. Phenotyping of the Z86 population under field conditions
4. Combined analysis of phenotypic parameters across all analyzed growth stages
5. Application of sensors for non-destructive measurement of water-status and salinity stress

4.1.1. Phenotyping of the Z86 population at germination stage

Germination tests of wheat seeds exposed to different solutions with sodium chloride (50, 100, 15, 200 and 250 mM), sodium sulphate (50, 100 and 150 mM) and control treatment solely with deionized water, were conducted under controlled conditions in climate chambers. After 10 days the scoring scheme described by Mano and Takeda (1998) was applied to score shoot and root development of the seeds (see Figure 6).

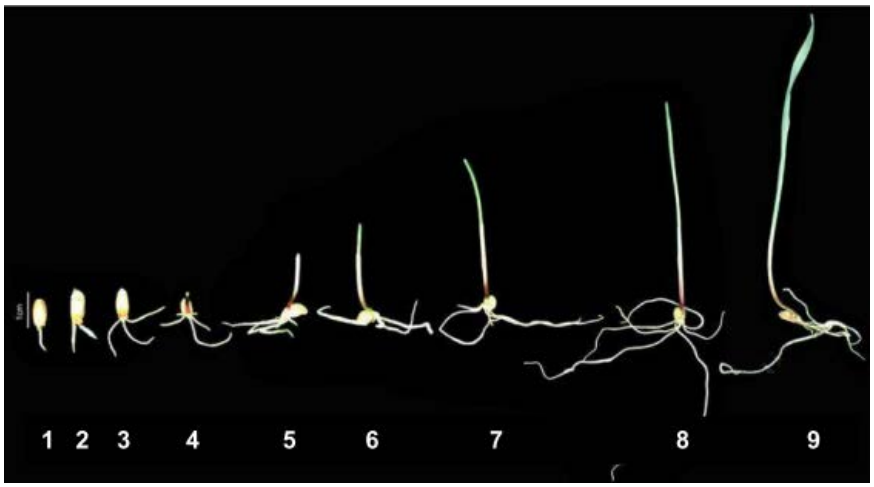

Figure 6. Scoring scheme for scoring salinity stress at seedling stage according to Mano and Takeda (1998); (Image: Dadshani, 2006)

As expected, irrigation with saline water was negatively affecting the germination of the tested genotypes. The degree of inhibition at germination stage was increasingly by higher salt concentrations. Furthermore, the effects of the two tested salt types, NaCl and Na_2SO_4, were different. In comparison to the same sodium chloride concentration, the treatments with sodium sulfate were more adversely affecting germination of the seeds. Table 9 summarizes the analysis of variance and descriptive statistics of germination scorings of the Z86 population at different concentrations of NaCl and Na_2SO_4. Looking at equivalent concentrations the adverse effect of Na_2SO_4 was comparably higher than that of NaCl. Furthermore, increasing the salt concentration, the gap between Na_2SO_4 and NaCl increased in affecting germination of seeds and hence seedling growth, e.g. the mean germination score of the Z86 population at 50 mM Na_2SO_4 was on the same level as 100 mM NaCl with 7.9 and 7.8, respectively. The effect of 100 mM Na_2SO_4 was slightly higher than 200 mM NaCl but dramatically higher than 100 mM NaCl. At 150 mM Na_2SO_4, the average score value of the Z86 population was 1.9 and hence considerably lower than 150 mM NaCl with a score of 5.8. The average germination score for seeds treated with 250 mM NaCl was slightly higher than with the highest Na_2SO_4 concentration

with 2.1 and 1.9, respectively. The F-value of the genotype effect increases by increasing the concentration of the tested salt treatments. The genotype by treatment effects are small for lower salt concentrations and increase slightly for higher salt stress levels.

Table 9. Analysis of variance and descriptive statistics of germination scorings of Z86 population for different salt treatments

	Genotype (G)	Treatment (T)	GxT	Mean	SD	CV [%]	CI 95%		H^2 [%]
Treatment	**(df 150)**	**(df 1)**	**(df 150)**				**Lower**	**upper**	
Control	1.96 ***	-	-	8.9	0.3	3.4	8.85	8.91	32.4
NaCl 50 mM	1.86 ***	51.97 ***	1.02 ns	8.6	0.5	5.8	8.56	8.71	22.3
100 mM	2.36 ***	585.35 ***	1.98 ***	7.8	1.5	19.2	7.70	7.95	31.2
150 mM	3.63 ***	4103.84 ***	3.53 ***	6.0	1.1	18.3	5.81	6.14	46.7
200 mM	6.00 ***	13893.3***	5.67 ***	4.3	1.6	37.2	4.07	4.44	62.5
250 mM	8.24 ***	52010.2 ***	7.82 ***	2.3	1.2	52.2	2.15	2.47	70.7
Na_2SO_4 50 mM	1.71 ***	460.52 ***	1.53 ***	7.9	0.7	8.9	7.75	7.98	19.2
100 mM	3.80 ***	8599.17 ***	3.85 ***	4.9	1.0	20.4	4.75	5.07	48.2
150 mM	8.63 ***	57544.2 ***	8.47 ***	2.0	1.0	50.0	1.84	2.17	71.8

Note: *F*-values are shown; Significance levels: *** $p \leq 0.001$; ns not significant, df degree of freedom, SD standard deviation, CV coefficient of variation, CI 95% confidence interval of 95%, H^2 broad sense heritability, GxT Genotype by treatment interaction.

In contrast to expectation, the parents, Zentos and Syn86, showed weaker performance at the tested salinity levels in in comparison to most of their progenies. Obviously, throughout all tested salt types and concentrations Syn86 was more susceptible than Zentos. Especially higher concentrations of sodium sulfate dramatically affected the germination of Syn86 (Figure 7).

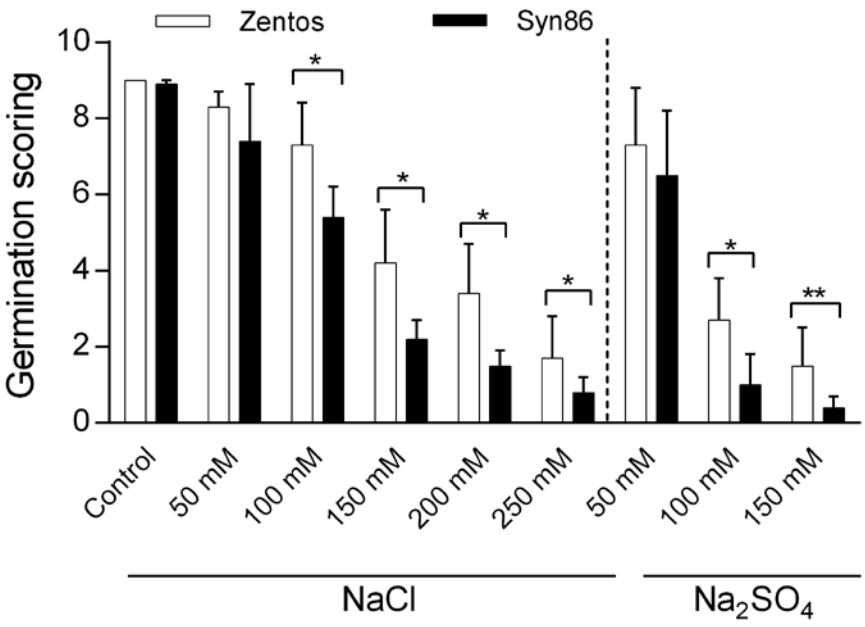

Figure 7. Overview of germination scoring of Zentos and Syn86 exposed to different concentrations of NaCl and Na_2SO_4; significance levels of p: * $p \leq 0.05$; ** p ≤ 0.01

The effects of different salt types and concentration on germination of the Z86 population and of Zentos and Syn86 are illustrated in Figure 8. The sharp drop of lines from control to 50 mM to 100 mM and to 150 mM Na_2SO_4, impressively illustrates the severe inhibition of seed germination relative to the equivalent NaCl concentration of irrigating water

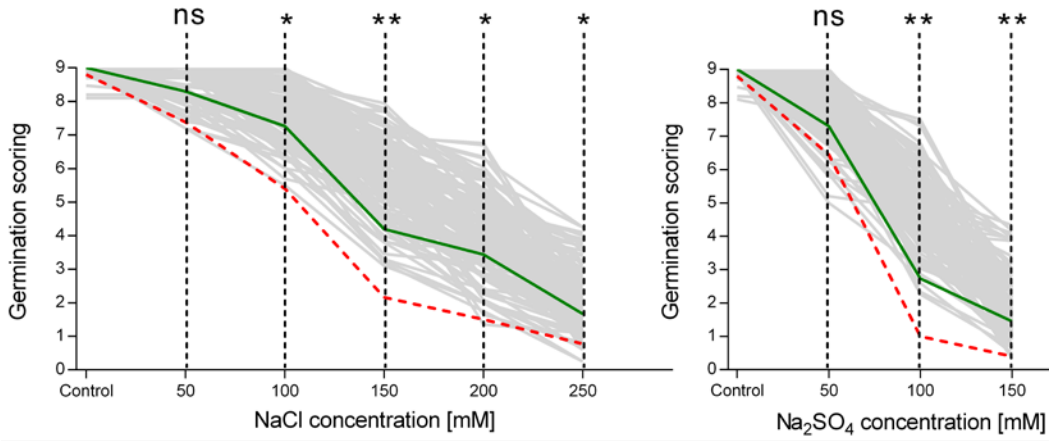

Figure 8. Overview of the germination scoring the Z86 population; the parents are highlighted with green solid line (Zentos) and red dashed line (Syn86); significance levels p: * $p \leq 0.05$; ** p ≤ 0.01; ns not significant.

The germination experiment with different salt stress treatments did not produce an unambiguous result in respect to salinity tolerance of the tested genotypes. For the highest NaCl concentration (250 mM) genotype 64 and 120 are performing best. The highest Na_2SO_4 treatment (150 mM) genotypes 31 and 33 are outperforming other genotypes. At this salinity level genotypes 31 and 33 achieve 4.1 and 4.3 scoring values, respectively. These two genotypes can be classified as most salt tolerant towards 150 mM Na_2SO_4 at germination stage.

In order to investigate the potential of the tested genotypes towards different concentrations of NaCl and Na_2SO_4, the germination scoring values were aggregated. Figure 9 summarizes the outcome of the germination experiment by aggregation of germinations score of the Z86 population treated with different concentrations of sodium chloride (A) and sodium sulfate (B). According to the aggregated scoring values genotype 16, 129, 114, 13 and 64 are regarded as tolerant across all tested salt regimes with 15.9%, 16.1%, 17,6%, 18.7% and 19.3% over the population mean with 34.6 aggregated scoring value.

Looking at Figure 9B with the aggregated scorings of the Z86 population tested with different Na_2SO_4 treatments, genotype 17, 113, 114 and 43 show the highest scores with +22.8, +25.3%, +26.7% and +30.9% higher values than the population mean. Also, the aggregated scoring value of genotype 16 was + 20.7% higher than the population mean.

Interestingly, as well NaCl as Na_2SO_4 are highly affecting the germination of Syn86. In both cases this genotype is showing the lowest aggregated scoring values with -39% under NaCl, and -45.9% under Na_2SO_4 treatment, relative to the population mean. Although slightly better than Syn86, also the elite parent Zentos is highly affected by NaCl and Na_2SO_4 treatment with -12% and -20.1%, respectively.

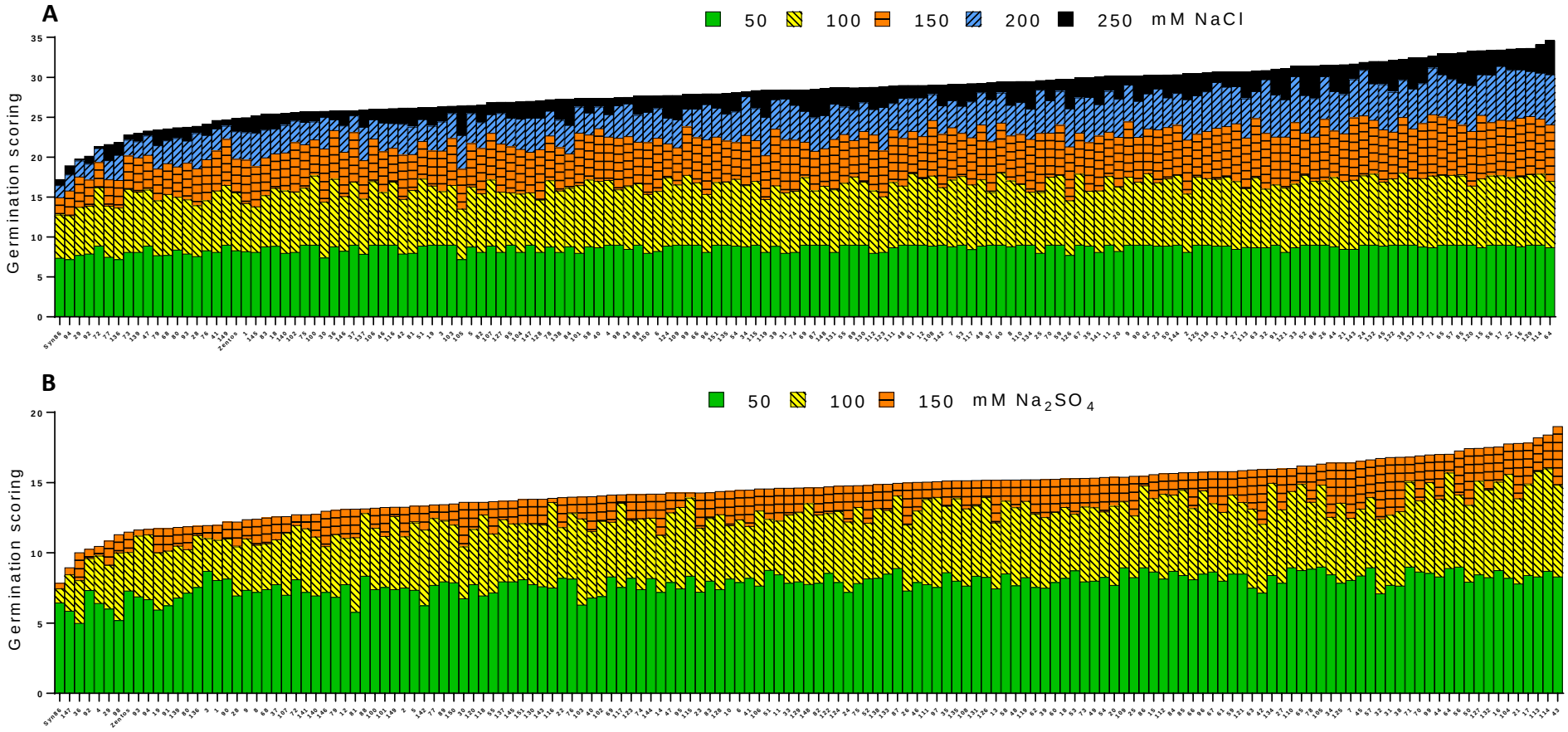

Figure 9. Average germination score values of the genotypes of the Z86 population, including Zentos and Syn86

Note: Colors indicate different salt types and concentration according the legend, **A** 50-250 mM NaCl, **B** 50-150 mM Na_2SO_4, genotypes sorted according to highest aggregating genotypic values of all tested concentrations of the specific salt types

The “Mean vs. Stability” view of GGE biplot in Figure 10 is constructed to facilitate the genotypes comparison across all tested salt treatments or environments. Based on their mean performance across all treatments/environments, the genotypes are ranked along the average-environmental axis (AEA, indicated as red line). The stability of the genotypes across the tested salt treatments is illustrated by the stability axis, which is the ordinate of the biplot (Figure 10 indicated as green line). The either direction away from the stability axis indicates greater genotype by environmental interaction effect (GEI) and reduced stability. As the arrow on the AEA (red line) is indicating higher average performance across all tested environments (salt treatments), the stability of the genotypes is decreasing with the distance of the genotypes from the stability axis (green line) indicating higher genotype by treatment interaction.

According to the biplot analysis, AB-lines 64 and 114 show the highest performance across all salt treatments at germination stage. Although, both genotypes show higher GEI effects and hence reduced stability. Based on the mean performance across all treatments genotype 16 and 17 are showing similar performance. However, the GEI effect of genotype 17 is higher than of genotype 16, which was showing consistent performance across all tested environments. Both parents, Zentos and Syn86, are located on the left side of the stability axes, indicating that both genotypes had a below-average mean performance across the tested salt treatments, with Syn86 showing the weakest performance across all treatments. Consequently, Syn86 can be regarded as most susceptible among the tested genotypes at germination stage.

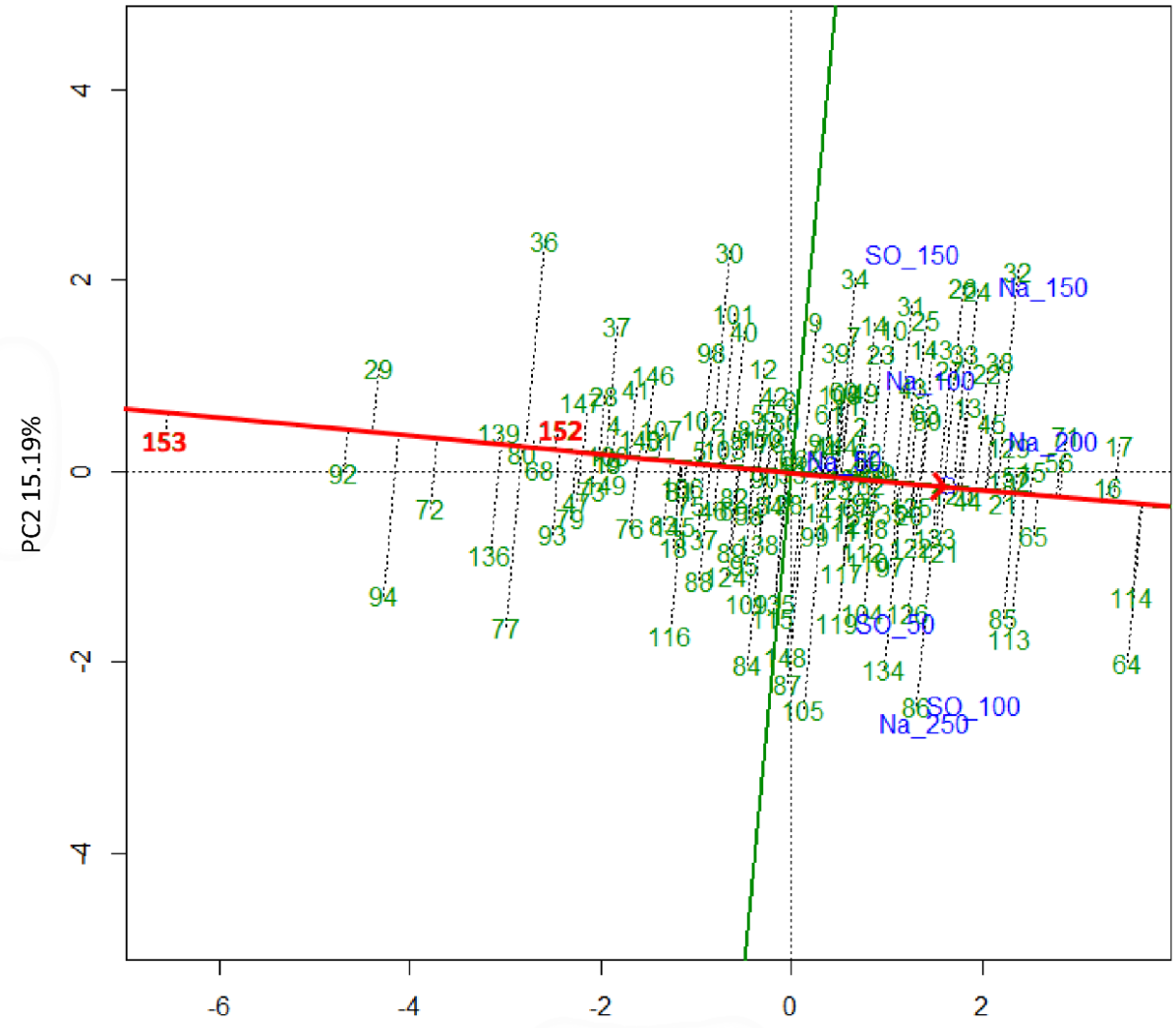

Figure 10. “Mean vs. Stability” plot of Z86 population (including the parents) tested with different concentrations of NaCl and Na_2SO_4 at germination stage

Note: Blue represents the salt types and concentration (Na_50 to Na_250 for 50 mM to 250 mM NaCl; SO_50 to SO_150 for 50 to 150 mM Na_2SO_4), green the genotypes of the Z86 population, 152 and 153 indicate the parents Zentos and Syn86, respectively. The different environments stand for the different salt treatments. Based on their mean performance across all salt treatments, the genotypes are ranked along the average-environmental axis (AEA; red line). The green line, perpendicular to AEA passing through the biplot origin represents the stability axis. It is also separating the genotypes with below average means (left from the green line) from those with above-average mean (right from the green line). The arrow on the AEA (red line) is indicating higher average performance across all tested environments (salt treatments). The stability of the genotypes is decreasing with the distance of the genotypes from the stability axis (green line) indicating higher genotype by treatment interaction.

4.1.2. Phenotyping of the Z86 population at seedling stage

Hydroponic experiments with 100 mM sodium chloride and sodium sulfate salts, respectively, and controlled condition without application of additional salts were carried out under greenhouse conditions in order to assess the phenotypic and genotypic variability of the Z86 population, including the parents Zentos and Syn86, exposed to salt stress at seedling stage. For this purpose, uniform pre-germinated 8 to 9 days old seedlings (2nd leaf stage) were transferred into the hydroponic system.

Figure 11. Setup of the aerated hydroponic system for phenotyping of the Z86 population under control and salinity stress conditions

Firstly, the results of the experiment with 100 mM NaCl will be outlined, followed by the results of the hydroponic experiment with 100 mM Na_2SO_4.

Effect of 100 mM NaCl on seedling stage

The Z86 population, including the parents Zentos and Syn86, were phenotyped in hydroponic experiments with control and 100 mM NaCl under greenhouse conditions in the year 2013 and 2014. The outcome of the hydroponic experiments, including the descriptive statistics is summarized in Table 10. The corresponding analysis of variance, as well as the coefficients of broad-sense heritability (H^2), are shown in Table 11.

Table 10. Phenotypic parameters and traits of Z86 population and the parents measured from hydroponic experiment with control condition and 100 mM NaCl

	Control									100 mM NaCl								
Parameter	**Zentos Mean**	**Syn86 Mean**	**Z86 Mean**	**SD**	**CV**	**ci 95% lower**	**ci 95% upper**	**Max**	**Min**	**Zentos Mean**	**Syn86 Mean**	**Z86 Mean**	**SD**	**CV**	**ci 95% lower**	**ci 95% upper**	**Max**	**Min**
SFW	6.5	4.9	4.29	1.03	23.9	4.12	4.46	7.24	2.07	3.4	2.6	2.70	0.51	18.9	2.62	2.78	3.89	1.25
SDW	0.7	0.5	0.49	0.11	23.3	0.47	0.51	0.73	0.23	0.5	0.4	0.38	0.07	18.4	0.37	0.39	0.57	0.18
SWC	88.4	88.8	89.61	0.65	0.7	89.51	89.72	91.36	85.69	85.5	85.3	88.01	0.93	1.1	87.86	88.16	90.03	81.56
RFW	2.3	1.7	1.74	0.37	21.0	1.68	1.80	2.46	0.49	1.7	1.3	1.45	0.30	21.0	1.40	1.50	2.36	0.59
RDW	0.2	0.1	0.13	0.03	25.2	0.13	0.14	0.41	0.04	0.1	0.1	0.11	0.02	19.5	0.11	0.12	0.17	0.05
SL (DAS 16)	52.5	59.4	47.10	4.62	9.8	46.36	47.85	59.55	29.20	45.0	52.1	42.81	3.33	7.8	42.28	43.35	51.73	33.33
RL (DAS 16)	32.6	50.5	36.78	5.88	16.0	35.83	37.72	52.10	22.83	35.2	46.2	35.31	5.09	14.4	34.49	36.13	52.80	23.33
PFW	9.0	4.9	6.03	1.36	22.5	5.81	6.25	9.42	2.97	5.1	3.9	4.15	0.79	18.9	4.03	4.28	6.03	1.88
PDW	0.9	0.6	0.62	0.14	22.0	0.60	0.64	0.91	0.32	0.6	0.5	0.49	0.09	18.0	0.48	0.51	0.72	0.23
LML	22.7	22.1	24.12	5.09	21.1	23.30	24.94	61.90	16.38	30.8	17.1	26.52	3.55	13.4	25.95	27.09	35.95	18.86
SPAD	44.2	36.9	41.76	3.29	7.9	41.23	42.29	52.37	34.15	45.4	52.4	45.49	3.24	7.1	44.96	46.01	52.68	33.58

Note: SFW shoot fresh weight, SDW shoot dry weight, SWC shoot water content, RFW root fresh weight, RDW root dry weight, PFW plant fresh weight, PDW plant dry weight, RL root length, SL shoot length, LML leaf membrane leakage, SPAD SPAD value, SD standard deviation, CV coefficient of variation, ci confidence interval, Max maximum value, Min minimum value, DAS days after stress application.

Table 11. Analysis of variance of measured parameters of Z86 population from hydroponic experiment with control and 100 mM NaCl treatment

	Genotype (G)	Treatment (T)	GxT	H^2
Parameter	**(df 149)**	**(df 1)**	**(df 148)**	[%]
SFW	1.53 ***	320.70 ***	0.67 ns	38.3
SDW	1.29 ns	95.09 ***	0.57 ns	36.0
SWC	0.85 ns	238.63 ***	0.69 ns	12.4
RFW	1.34 **	53.99 ***	0.59 ns	41.4
RDW	1.07 ns	38.86 ***	0.65 ns	25.6
SL (DAS 16)	1.12 ns	64.88 ***	0.34 ns	68.0
RL (DAS 16)	2.06 ***	7.07 ***	0.50 ns	73.5
PFW	1.63 ***	257.34 ***	0.69 ns	40.9
PDW	1.25 *	87.36 ***	0.57 ns	36.3
LML	1.09 ns	30.78 ***	1.03 ns	9.8
SPAD	1.11 ns	90.29 ***	0.65 ns	36.6

Note: *F*-values are shown; significance levels p: * $p \leq 0.05$; ** $p \leq 0.01$; *** $p \leq 0.001$; ns not significant; df degree of freedom; H^2 broad sense heritability; SFW shoot fresh weight; SDW shoot dry weight; SWC shoot water content; RFW root fresh weight; RDW root dry weight; SL shoot length; RL root length; PFW plant fresh weight; PDW plant dry weight; LML leaf membrane leakage; SPAD SPAD value; DAS days after stress application.

As shown in Table 11, for all collected parameters, the *F*-values of the treatment effect were very high with high significance levels. The *F*-value of the genotypic effect was low, although significant, for SFW, RFW, RL (DAS 16), PFW and PDW. However, there was no significant genotype by treatment interaction detected among the measured parameters. For most measured traits the calculated heritability (H^2) was low. Higher H^2 was detected only for SL and RL (both at DAS 16). Table 12 shows Pearson's correlation coefficients (r) of parameters calculated from LSmeans of collected data from the hydroponic experiment with control and salt treatment (100 mM NaCl). Highly significant correlations are obvious for almost all parameters except correlations with leaf membrane leakage (LML) and SPAD value well for control as well as for stress condition with 100 mM NaCl.

Table 12. Pearson's correlation coefficient (r) for parameters measured from Z86 population tested in hydroponic experiment with 100 mM NaCl; under control (left) and stress (right)

		SFW	SDW	SWC	RFW	RDW	SL	RL	PFW	PDW	LML	SPAD	
Control	**SFW**		0.95**	0.26**	0.85**	0.78**	0.56**	0.53**	0.98**	0.93**	-0.13	0.02	Stress
	SDW	0.97**		-0.06	0.84**	0.82**	0.55**	0.50**	0.94**	0.98**	-0.17*	0.00	
	SWC	0.16*	-0.06		0.12	-0.02	0.09	0.21**	0.22**	-0.06	0.11	0.04	
	RFW	0.85**	0.82**	0.17*		0.89**	0.44**	0.51**	0.94**	0.89**	-0.15*	0.10	
	RDW	0.61**	0.57**	0.18*	0.67**		0.36**	0.43**	0.85**	0.90**	-0.15*	0.05	
	SL	0.75**	0.73**	0.11	0.68**	0.46**		0.44**	0.53**	0.51**	-0.11	-0.01	
	RL	0.45**	0.43**	0.17*	0.56**	0.32**	0.39**		0.54**	0.50**	-0.01	-0.15*	
	PFW	0.96**	0.92**	0.21**	0.93**	0.65**	0.78**	0.52**		0.95**	-0.14*	0.05	
	PDW	0.93**	0.92**	0.10	0.89**	0.75**	0.76**	0.46**	0.96**		-0.17*	0.01	
	LML	-0.05	-0.02	-0.11	-0.08	-0.03	-0.03	0.04	-0.08	-0.07		-0.07	
	SPAD	0.11	0.13	-0.04	0.19*	0.02	0.13	0.29**	0.16*	0.16*	0.09		

Note: Correlations ≥ 0.4 are highlighted with color code: red r 0.8-1.0, orange r 0.6-0-79, yellow r 0.4-0.59; ; significance levels p: * 0.01< p < 0.05; ** 0.001 < p < 0.01; *** 0.0001 <p <0.001; SFW shoot fresh weight; SDW shoot dry weight; SWC shoot water content; RFW root fresh weight; RDW root dry weight; RL root length (DAS 16); SL shoot length (DAS 16); PFW plant fresh weight; PDW plant dry weight; LML leaf membrane leakage; SPAD SPAD value; DAS days after stress

The salt stress tolerance index STI was applied to estimate the effect of salinity stress on measured traits (Bağci et al. 2003). Additionally, the stress-weighted performance index (SWP) proposed by Saade et al. (2016) was applied. SWP facilitates the identification of genotypes showing high yield potential under saline condition.

Table 13 is combining the Pearson's correlation coefficients (r) matrix of the STI (left) and SWP (right) indices calculated from LSmeans of collected data from the hydroponic experiment with control and salt treatment (100 mM NaCl). According to Saade et al. (2016), in comparison to STI, the SWP index is more suitable to differentiate the high performant genotypes from low performant genotypes. Thus, the correlation matrix is elucidating higher correlation coefficients for most correlations calculated with SWP in comparison with STI.

Table 13. Pearson's correlation coefficient (r) for parameters measured from Z86 population tested in hydroponic experiment with 100 mM NaCl; STI values (left) and SWP values (right)

		SFW	SDW	SWC	RFW	RDW	SL	RL	PFW	PDW	LML	SPAD	
STI	SFW		0.95**	-0.13	0.79**	0.77**	0.40**	0.40**	0.88**	0.85**	-0.12	0.08	SWP
	SDW	0.95**		0.05	0.79**	0.79**	0.40**	0.36**	0.85**	0.90**	-0.15*	0.11	
	SWC	-0.07	0.08		-0.18*	0.07	-0.08	-0.11	-0.17*	0.04	0.04	-0.05	
	RFW	0.67**	0.66**	-0.14*		0.85**	0.34**	0.35**	0.90**	0.85**	-0.07	0.06	
	RDW	0.71**	0.71**	0.17*	0.78**		0.27**	0.34**	0.80**	0.86**	-0.04	0.01	
	SL	0.50**	0.47**	-0.09	0.47**	0.34**		0.24**	0.37**	0.36**	-0.06	0.11	
	RL	0.35**	0.32**	-0.05	0.33**	0.29**	0.15*		0.36**	0.36**	0.00	-0.08	
	PFW	0.69**	0.68**	-0.13	0.88**	0.68**	0.54**	0.37**		0.95**	-0.09	0.14*	
	PDW	0.74**	0.77**	0.03	0.81**	0.74**	0.48**	0.35**	0.91**		-0.10	0.14*	
	LML	-0.04	-0.05	0.03	-0.04	0.05	-0.02	0.02	-0.05	-0.02		-0.13	
	SPAD	0.05	0.09	-0.13	0.10	-0.03	0.09	0.16*	0.17*	0.16*	-0.09		

Note: Correlations ≥ 0.4 are highlighted with color code: red r 0.8-1.0, orange r 0.6-0-79, yellow r 0.4-0.59; ; significance levels p: * 0.01< p < 0.05; ** 0.001 < p < 0.01; *** 0.0001 <p <0.001; SFW shoot fresh weight; SDW shoot dry weight; SWC shoot water content; RFW root fresh weight; RDW root dry weight; RL root length (DAS 16); SL shoot length (DAS 16); PFW plant fresh weight; PDW plant dry weight; LML leaf membrane leakage; SPAD SPAD value; DAS days after stress application.

Effect of 100 mM Na_2SO_4 at seedling stage

The Z86 population, including the parents Zentos and Syn86, were tested in hydroponic experiments with 100 mM Na_2SO_4 under greenhouse condition in the years 2014 and 2015. The outcome of the hydroponic experiments, including the descriptive statistics is summarized in Table 14. The corresponding analysis of variance including coefficients of broad-sense heritability (H^2) is shown in Table 15.

Table 14. Phenotypic parameters and traits of Z86 population and the parents Zentos and Syn86 measured from hydroponic experiment with control condition and 100 mM Na_2SO_4

		Control									100 mM Na_2SO_4								
Parameter		**Zentos Mean**	**Syn86 Mean**	**Z86 Mean**	**SD**	**CV [%]**	**ci 95% lower**	**ci 95% upper**	**Max**	**Min**	**Zentos Mean**	**Syn86 Mean**	**Z86 Mean**	**SD**	**CV [%]**	**ci 95% lower**	**ci 95% upper**	**Max**	**Min**
SFW		2.98	2.44	2.70	0.7	25.7	2.6	2.8	5.1	0.7	1.15	0.87	1.18	0.3	21.5	1.1	1.2	1.8	0.6
SDW		0.33	0.27	0.31	0.1	23.6	0.3	0.3	0.6	0.2	0.19	0.15	0.19	0.0	18.5	0.2	0.2	0.3	0.1
SWC		88.6	88.87	88.1	1.4	1.6	87.9	88.4	89.6	72.0	83.44	83.03	83.3	1.4	1.7	83.1	83.5	87.5	73.6
RFW		1.00	0.84	1.03	0.3	26.2	1.0	1.1	2.2	0.4	0.69	0.56	0.74	0.2	25.8	0.7	0.8	1.2	0.3
RDW		0.08	0.07	0.08	0.0	21.2	0.1	0.1	0.2	0.0	0.08	0.06	0.08	0.0	20.8	0.1	0.1	0.1	0.0
3rd LFW		0.34	0.26	0.28	0.1	17.5	0.3	0.3	0.4	0.2	0.16	0.15	0.18	0.0	16.5	0.2	0.2	0.3	0.1
3rd LDW		0.04	0.03	0.04	0.0	16.2	0.0	0.0	0.1	0.0	0.03	0.03	0.005	0.0	15.6	0.0	0.0	0.1	0.0
3rd LL		27.43	26.27	26.2	2.7	10.3	25.8	26.7	35.4	19.0	22.39	23.78	23.8	2.3	9.5	23.5	24.2	28.5	14.0
3rd LW		6.6	na	6.09	0.6	10.3	6.0	6.2	8.0	4.0	82.31	na	4.97	0.5	10.0	4.9	5.1	6.5	4.0
3rd LWC		87.53	87.91	86.9	1.3	1.4	86.7	87.1	89.3	82.7	1.84	82.96	82.4	1.9	2.3	82.1	82.7	87.5	76.9
PFW		3.89	3.28	3.73	1.0	25.5	3.6	3.9	7.3	1.4	0.27	1.43	1.92	0.4	22.6	1.9	2.0	2.9	0.9
PDW		0.41	0.34	0.39	0.1	22.9	0.4	0.4	0.7	0.2	23.04	0.21	0.27	0.1	18.4	0.3	0.3	0.4	0.2
RL (DAS 0)		25.39	28.60	24.9	2.4	9.5	24.6	25.3	34.4	12.6	23.04	28.62	25.2	1.9	7.6	24.9	25.5	31.4	20.3
RL (DAS 9)		32.52	42.70	33.2	3.5	10.6	32.7	33.8	47	18.5	26.44	32.10	27.7	2.4	8.5	27.4	28.1	35.4	22.9
RL (DAS 16)		36.7	50.29	37.2	4	10.8	36.6	37.9	51.3	22.1	27.03	33.25	28.7	2.4	8.5	28.3	29	38.1	19.5
SL (DAS 0)		24.13	25.14	21.8	2.8	12.7	21.4	22.3	27.5	12.6	23.24	26.02	22.5	2.7	12.1	22.1	23	27.6	13.9
SL (DAS 9)		34.61	36.20	32.3	2.6	8	31.9	32.8	37.7	25.5	29.31	31.18	27.8	2.5	9.1	27.4	28.2	33.7	17.8
SL (DAS 16)		40.53	47.20	39.1	3.2	8.2	38.6	39.6	47.4	30.6	32.95	36.85	31.6	2.6	8.2	31.1	32	38.1	19.6
Number of leaves		8.73	2.44	8.75	1.5	16.8	8.5	9.0	13.0	6.0	1.15	0.87	5.77	0.9	16.3	5.6	5.9	9.0	3.5
Photosynthetic parameters	**Photo**	7.3	5.9	9.20	1.7	18.2	8.9	9.5	14.5	5.2	6.6	4.9	8.19	2.0	24.2	7.9	8.5	13.3	2.8
	Cond	0.3	0.4	0.29	0.1	28.0	0.3	0.3	0.7	0.1	0.1	0.1	0.11	0.0	37.4	0.1	0.1	0.3	0.0
	Ci	342.9	356.2	333.6	15.4	4.6	331.1	336.1	366.6	291.8	295.5	328.2	263.4	29.6	11.2	258.7	268.2	351.0	168.8
	Trans	2.6	4.1	3.06	0.9	29.5	2.9	3.2	6.3	1.2	1.4	1.4	1.47	0.5	33.7	1.4	1.6	3.6	0.6

Note: SFW shoot fresh weight; SDW shoot dry weight; SWC shoot water content; RFW root fresh weight; RDW root dry weight 3rd LFW fresh weight of 3rd leaf; 3rd LDW dry weight of 3rd leaf; 3rd LL leaf length of 3rd leaf; 3rd LW width of 3rd leaf; PFW plant fresh weight; PDW plant dry weight; RL root length; SL shoot length; Photo photosynthetic activity; Cond stomatal conductance; Ci stomatal CO_2 concentration; Trans transpiration rate; SD standard deviation; CV coefficient of variation; Ci confidence interval; Max maximum value; Min minimum value; na data not available.

Table 15. Analysis of variance of measured parameters of Z86 populations from experiment with control and 100 mM Na_2SO_4 treatment

Parameter	Genotype (G) (df 150)	Treatment (T) (df 1)	GxT (df 150)	H^2 [%]
SFW	0.628 ^{ns}	329.967 ***	0.33 ^{ns}	33.2
SDW	0.694 ^{ns}	161.539 ***	0.303 ^{ns}	39.3
SWC	1.58 ***	1340.903 ***	1.064 ^{ns}	26.9
RFW	0.736 ^{ns}	64.383 ***	0.287 ^{ns}	44.8
RDW	0.964 ^{ns}	2.7653 ^{ns}	0.335 ^{ns}	32.4
3rd LFW	1.608 ***	589.434 ***	0.868 ^{ns}	29.6
3rd LDW	1.459 **	74.56 ***	1.000 ^{ns}	17.5
3rd LL	1.459 **	79.664 ***	0.643 ^{ns}	47.8
3rd LW	1.264 *	344.073 ***	0.865 ^{ns}	19.9
3rd LWC	1.054 ^{ns}	563.514 ***	0.88 ^{ns}	11.2
PFW	0.660 ^{ns}	246.433 ***	0.301 ^{ns}	38.8
PDW	0.724 ^{ns}	108.026 ***	0.293 ^{ns}	42.3
RL (DAS 0)	1.669 ***	1.611 ^{ns}	0.572 ^{ns}	57.7
SL (DAS 0)	1.8381 ***	6.731 ***	0.731 ^{ns}	48.9
RL (DAS 9)	1.343 *	228.706 ***	0.424 ^{ns}	51.9
SL (DAS 9)	1.777 ***	300.548	0.677 ^{ns}	55.2
RL (DAS 16)	1.445 **	486.076 ***	0.468 ^{ns}	62.3
SL (DAS 16)	1.664 ***	611.024 ***	0.66 ^{ns}	57.4
NoL	1.027 ^{ns}	309.079 ***	0.339 ^{ns}	47.5
Photosynthetic parameter ***A***	1.110 ^{ns}	22.051 ***	0.842 ^{ns}	21.1
gs	1.425 **	551.703 ***	0.96 ^{ns}	13.7
Ci	0.944 ^{ns}	499.116 ***	0.751 ^{ns}	5.9
E	1.092 ^{ns}	307.334 ***	0.721 ^{ns}	16.3

Note: Significance levels p: * $p \leq 0.05$; ** $p \leq 0.01$; *** $p \leq 0.001$; ns not significant; df degree of freedom; H^2 broad sense heritability; SFW shoot fresh weight; SDW shoot dry weight; SWC shoot water content; RFW root fresh weight; RDW root dry weight 3rd LFW fresh weight of 3rd leaf; 3rd LDW dry weight of 3rd leaf; 3rd LL leaf length of 3rd leaf; 3rd LW width of 3rd leaf; PFW plant fresh weight; PDW plant dry weight; RL root length; SL shoot length; NoL number of leaves; *A* photosynthetic activity; g_s stomatal conductance; *Ci* stomatal CO_2 concentration; *E* transpiration rate

The results of the analysis of variance on parameters collected from hydroponic experiment (100 mM Na_2SO_4) with Zentos and Syn86 is presented in Table 18. Most parameters were affected either by treatment or genotype or genotype and treatment. However, only for RL (DAS 16), significant genotype by treatment interaction was detectable.

Table 16. Analysis of variance of parameters measured for Zentos and Syn86 from hydroponic experiment with control and 100 mM Na_2SO_4

	Genotype (G)	**Treatment (T)**	**GxT**
Parameter	(df 1)	(df 1)	(df 1)
SFW	2.6 ^{ns}	52.34 ***	0.14 ^{ns}
SDW	3.49 ^{ns}	25.75 ***	0.03 ^{ns}
SWC	4.99 *	24.83 ***	0.27 ^{ns}
RFW	2.9 ^{ns}	12.64 **	0.03 ^{ns}
RDW	4.72 *	1.25 ^{ns}	0.11 ^{ns}
3rd LFW	2.7 ^{ns}	23.4 ***	1.27 ^{ns}
3rd LDW	3.49	5.36 *	2.23 ^{ns}
3rd LL	0 ^{ns}	3 ^{ns}	0.34 ^{ns}
3rd LW	4.99 *	24.83 ***	0.27 ^{ns}
3rd LWC	0.40 ^{ns}	62.13 ***	1.48 ^{ns}
PFW	2.81 ^{ns}	41.01 ***	0.1 ^{ns}
PDW	3.96 ^{ns}	18.12 ***	0 ^{ns}
SL			
DAS 0	2.65 ^{ns}	0 ^{ns}	0.57 ^{ns}
DAS 9	1.58	14.02 ***	0.01 ^{ns}
DAS 16	11.26 **	32.37 ***	0.78 ^{ns}
RL			
DAS 0	15.98 ***	1.13 ^{ns}	1.16 ^{ns}
DAS 9	25.63 ***	28.41 ***	2.08 ^{ns}
DAS 16	42.26 ***	76.83 ***	5.84 *
NoL	2.92 ^{ns}	45.19 ***	0.24 ^{ns}
Photosynthetic parameter			
A	2.44 ^{ns}	0.65 ^{ns}	0.02 ^{ns}
gs	0.44 ^{ns}	10.28 *	0.57 ^{ns}
Ci	5.29 *	14.19 ***	0.94 ^{ns}
E	1.71 ^{ns}	10.61 **	1.49 ^{ns}

Note: *F*-values are shown; significance levels p: * $p \leq 0.05$; ** $p \leq 0.01$; *** $p \leq 0.001$; ns not significant; df degree of freedom; SFW shoot fresh weight; SDW shoot dry weight; SWC shoot water content; RFW root fresh weight; RDW root dry weight 3rd LFW fresh weight of 3rd leaf; 3rd LDW dry weight of 3rd leaf; 3rd LL leaf length of 3rd leaf; 3rd LW width of 3rd leaf; PFW plant fresh weight; PDW plant dry weight; RL root length; SL shoot length; NoL number of leaves; Photosynthetic parameter: *A* photosynthetic activity; g_s stomatal conductance; *Ci* stomatal CO_2 concentration; *E* transpiration rate; DAS days after stress application.

Table 17 shows Pearson's correlation (r) of measured phenotypic parameters calculated from LSmeans of parameters collected from the hydroponic experiment with 100 mM Na_2SO_4. Strong and highly significant correlations are obvious for almost all parameters except correlations with leaf membrane leakage (LML) and SPAD value.

Table 17. Pearson's correlation coefficient (r) for parameters measured from Z86 population tested in hydroponic experiment with 100 mM Na_2SO_4

		SFW	SDW	SWC	RFW	RDW	3rd LFW	3rd DW	3rd LL	3rd LW	3rd LWC	PFW	PDW	RL (0)	SL (0)	RL (9)	SL (9)	RL (16)	SL (16)	NoL	*A*	g_s	*Ci*	*E*	
Control	**SFW**		**0.95****	**0.58****	**0.90****	**0.87****	**0.70****	0.49**	0.39**	0.43**	0.39**	**0.98****	**0.95****	0.24**	0.42**	0.29**	**0.53****	0.28**	**0.58****	0.48**	0.29**	0.22**	-0.04	0.22**	**Stress**
	SDW	**0.96****		0.29**	**0.86****	**0.87****	**0.66****	**0.51****	0.38**	0.39**	0.29**	**0.93****	**0.98****	0.24**	0.44**	0.30**	**0.52****	0.28**	**0.58****	0.46**	0.31**	0.21**	-0.07	0.24**	
	SWC	0.38**	0.172*		0.50**	0.38**	0.40**	0.14*	0.23**	0.25**	0.44**	**0.56****	0.35**	0.06	0.14*	0.12	0.27**	0.12	0.27**	0.29**	0.12	0.18*	0.09	0.07	
	RFW	**0.93****	**0.92****	0.23**		**0.92****	**0.58****	0.41**	0.29**	0.36**	0.33*	**0.97****	**0.90****	0.17*	0.36**	0.24**	0.42**	0.24**	0.48**	0.47**	0.34**	0.35**	0.10	0.34**	
	RDW	**0.89****	**0.90****	0.19**	**0.95****		**0.68****	**0.54****	0.40**	0.38**	0.31**	**0.91****	**0.93****	0.14*	0.44**	0.17*	**0.50****	0.16*	**0.56****	0.37**	0.37**	0.27**	-0.01	0.32**	
	3rd LFW	0.46**	0.41**	0.31**	0.39**	0.37**		**0.80****	**0.77****	0.48**	0.41**	**0.66****	**0.68****	0.20**	**0.58****	0.15*	**0.74****	0.10	**0.75****	-0.02	0.18*	0.05	-0.11	0.10	
	3rd DW	0.41**	0.39**	0.26**	0.35**	0.36**	**0.84****		**0.72****	0.40**	-0.2**	0.47**	**0.54****	0.17*	**0.50****	0.09	**0.66****	0.02	**0.64****	-0.06	0.167*	0.05	-0.12	0.15*	
	3rd LL	0.01	-0.03	0.16*	-0.02	-0.04	**0.71****	**0.68****		0.18*	0.15*	0.36**	0.40**	0.22**	**0.70****	0.18*	**0.87****	0.09	**0.86****	-0.2**	0.147*	0.00	-0.09	0.07	
	3rd LW	0.37**	0.34**	0.30**	0.30**	0.29**	**0.69****	**0.57****	0.34**		0.14*	0.41**	0.40**	0.11	0.16*	0.03	0.20**	0.01	0.19*	-0.04	-0.01	-0.10	-0.11	-0.10	
	3rd LWC	0.14*	0.07	0.11	0.11	0.06	0.38**	-0.17*	0.13	0.26**		0.37**	0.30**	0.04	0.17*	0.10	0.22**	0.13	0.26**	0.07	0.07	0.03	0.02	-0.03	
	PFW	**0.99****	**0.96****	0.34**	**0.96****	**0.92****	0.45**	0.40**	0.00	0.37**	0.13*		**0.95****	0.21**	0.40**	0.28**	0.49**	0.27**	**0.55****	0.48**	0.32**	0.29**	0.02	0.28**	
	PDW	**0.96****	**0.99****	0.17*	**0.94****	**0.93****	0.41**	0.39**	-0.02	0.34**	0.08	**0.97****		0.22**	0.45**	0.26**	**0.53****	0.25**	**0.59****	0.44**	0.33**	0.23**	-0.06	0.28**	
	RL (DAS 0)	0.20**	0.21**	0.09	0.30**	0.26**	0.09	328.00	0.10	0.07	-0.06	0.23**	0.23*		0.30**	**0.90****	0.25**	**0.87****	0.22**	0.02	-0.04	-0.10	-0.03	-0.06	
	SL (DAS 0)	0.17*	0.20**	-0.05	0.26**	0.28**	0.35**	0.37**	0.43**	0.16*	0.03	0.19**	0.22**	0.43**		0.22**	**0.74****	0.10	**0.62****	-0.12	0.07	-0.02	-0.06	0.04	
	RL (DAS 9)	0.42**	0.43**	0.11	**0.52****	0.48**	0.22**	0.21**	0.18*	0.19**	0.04	0.46**	0.45**	**0.87****	0.42**		0.26**	**0.96****	0.25**	0.14*	-0.01	-0.06	-0.03	-0.04	
	SL (DAS 9)	0.44**	0.44**	0.04	0.44**	0.44**	**0.55****	**0.53****	**0.60****	0.21**	0.09	0.44**	0.45**	0.31**	**0.50****	0.42**		0.17*	**0.89****	-0.05	0.16*	-0.02	-0.15*	0.05	
	RL (DAS 16)	0.39**	0.39**	0.12	0.49**	0.45**	0.18*	0.17*	0.15*	0.18*	0.02	0.43**	0.41**	**0.79****	0.30**	**0.94****	0.38**		0.17*	0.19*	-0.03	-0.04	0.00	-0.04	
	SL (DAS 16)	**0.62****	**0.59****	0.20**	**0.57****	**0.56****	**0.51****	0.46**	0.46**	0.25**	0.14*	**0.61****	**0.60****	0.21**	0.35**	0.38**	**0.78****	0.36**		0.02	0.23**	0.05	-0.12	0.12	
	NoL	**0.74****	**0.76****	0.15*	**0.71****	**0.69****	0.08	0.03	-0.3**	0.18*	0.09	**0.74****	**0.76****	0.07	-0.10	0.22**	0.09	0.22**	0.25**		0.22**	0.38**	0.172*	0.31**	
	A	0.05	0.08	-0.05	0.05	0.06	-0.02	0.01	-0.04	-0.12	-0.04	0.05	0.08	0.13	-0.01	0.07	0.12	0.06	0.18*	0.16*		**0.60****	-0.15*	**0.68****	
	g_s	-0.01	0.01	-0.03	0.03	0.02	-0.14*	-0.03	-0.17	-0.14*	-0.2**	0.01	0.01	0.24**	-0.08	0.13	-0.09	0.12	-0.08	0.06	0.49**		**0.57****	**0.90****	
	Ci	-0.09	-0.09	-0.07	-0.04	-0.05	-0.2**	-0.12	-0.18*	-0.19*	-0.17*	-0.08	-0.08	0.17*	-0.04	0.03	-0.19*	0.01	-0.3**	-0.06	-0.08	**0.73****		0.37**	
	E	0.12	0.15*	-0.03	0.21**	0.19**	-0.12	-0.03	-0.2**	-0.12	-0.17*	0.15*	0.16*	0.27**	-0.05	0.21**	-0.05	0.19**	-0.04	0.19**	0.40**	**0.83****	**0.61****		

Note: correlations ≥ 0.5 are highlighted (bold/red); significance levels p: * $p \leq 0.05$; ** $p \leq 0.01$; *** $p \leq 0.001$; SFW shoot fresh weight; SDW shoot dry weight; SWC shoot water content; RFW root fresh weight; RDW root dry weight 3rd LFW fresh weight of 3rd leaf; 3rd LDW dry weight of 3rd leaf; 3rd LL leaf length of 3rd leaf; 3rd LW width of 3rd leaf; PFW plant fresh weight; PDW plant dry weight; RL root length, SL shoot length, (0)/(9)/(16) 0/ days after stress application; NoL number of leaves; Photosynthetic parameter: *A* photosynthetic activity; g_s stomatal conductance; *Ci* stomatal CO_2 concentration; *E* transpiration rate; DAS days after stress application.

Different salt treatments and higher salt stress levels have an increasing impact on production of biomass and consequently inhibit plant growth. Figure 12 illustrates the effect of the tested treatments on shoot dry weight and root dry weight of the Z86 population. The effect of the tested treatments on shoot and root length of the Z86 population is plotted in Figure 13.

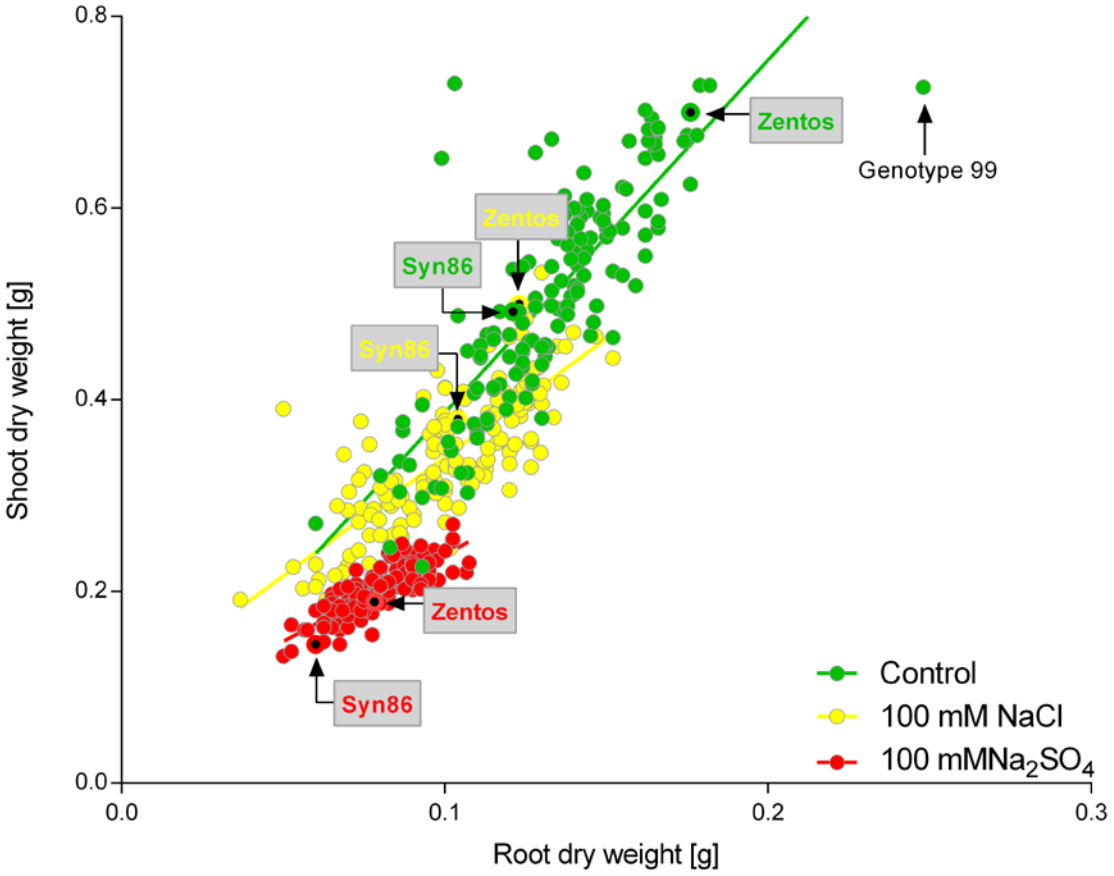

Figure 12. Shoot and root dry weight of the Z86 population grown in hydroponic systems without salt control condition (green), 100 mM NaCl (yellow) and 100 mM Na_2SO_4 (red)

Both figures give an overview about the severity of the tested salt treatments on the specific plant parameters. Obviously, the phenotypic variability of the observed traits declines by increasing the salt stress level. Regarding Figure 12 and Figure 13, affected by highest salt stress treatment of 100 mM Na_2SO_4 all genotypes cluster in a denser cloud than under 100 mM NaCl and under control condition with no additional salt application. Shoot dry weight (SDW), root dry weight (RDW), shoot length (SL) and root length (RL) are the predominantly analyzed parameters in the literature for assessing the effect of salinity stress on plant growth.

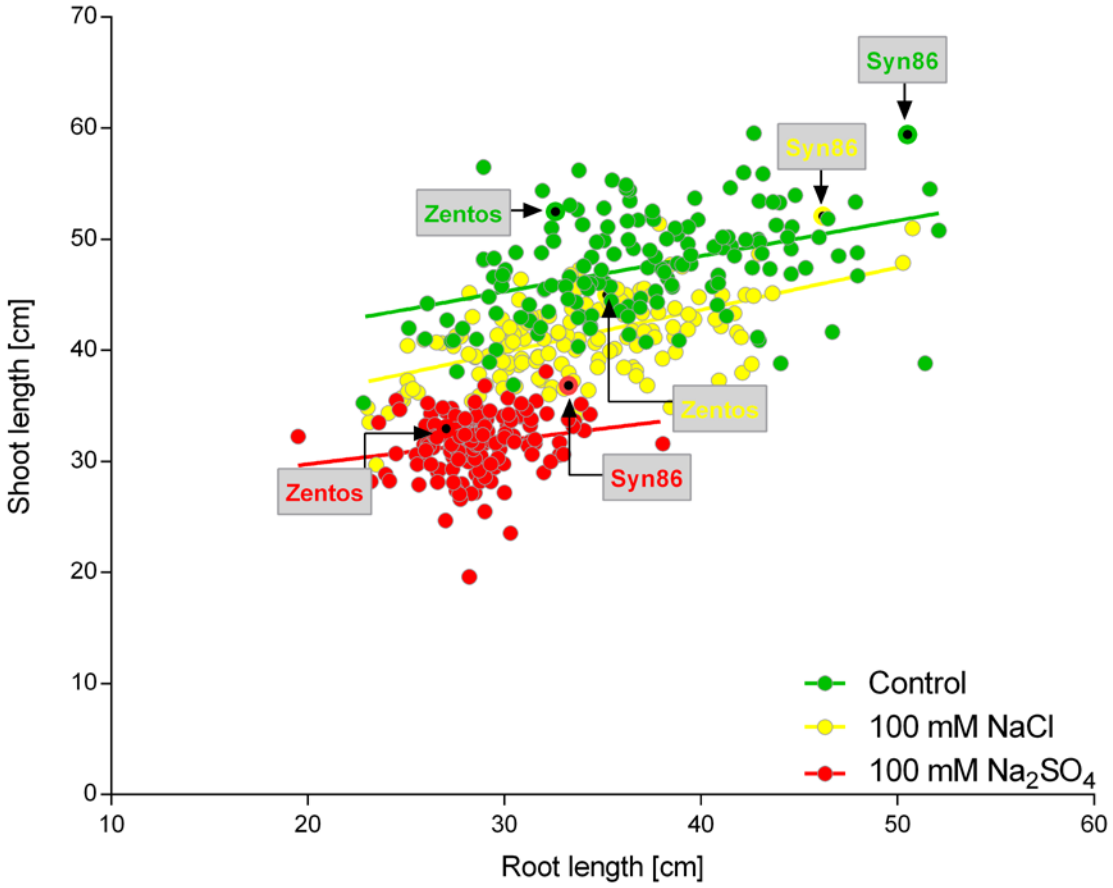

Figure 13. Shoot and root length of the Z86 population grown in hydroponic systems without salt control condition (green), 100 mM NaCl (yellow) and 100 mM Na_2SO_4 (red)

Hence, Figure 14 is summarizing the effect of 100 mM NaCl and Na_2SO_4, respectively, on these parameters relative to control condition, for the Z86 population as well for the parents Zentos and Syn86.

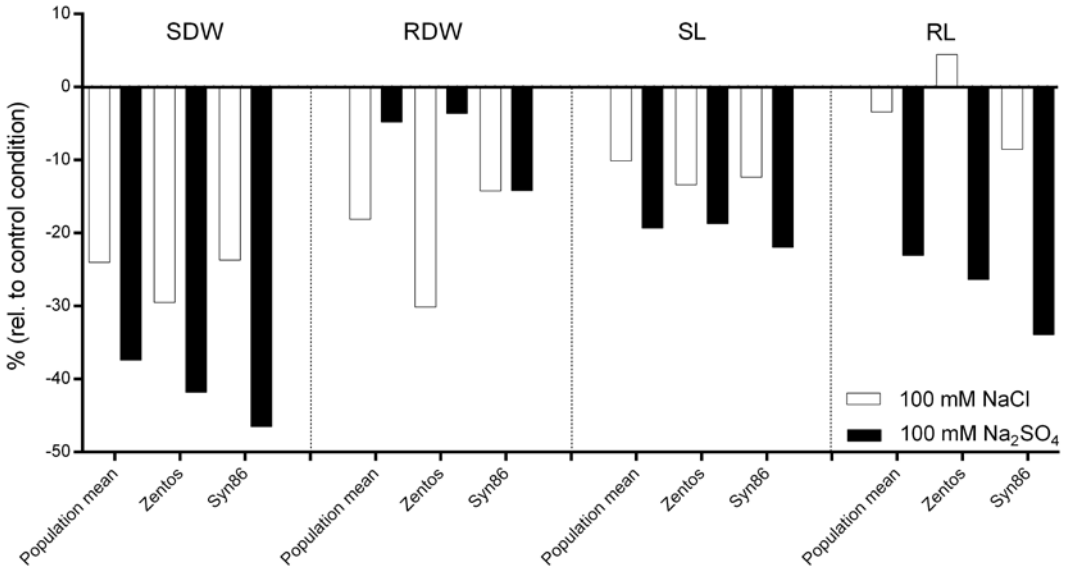

Figure 14. Overview of shoot fresh weight (SDW), root dry weight (RDW), shoot length (SL) and root length (RL) of Zentos, Syn86 and Z86 population mean under 100 mM NaCl and Na_2SO_4 relative to control conditions

For SDW and SL the adverse effect of 100 mM Na_2SO_4 in comparison to 100 mM NaCl was dramatic. Surprisingly, Na_2SO_4 had marginal negative effect in respect to the mean RDW of the Z86 population (-4.8% relative to control condition) and Zentos (-3.6%) but strongly reduced RDW of Syn86. Furthermore, RL of all genotypes was highly decreasing RL at 100 mM Na_2SO_4. Noteworthy, under the two salt types NaCl and Na_2SO_4, RDW and RL of Zentos and Syn86 behaved contrastingly. Surprisingly, the RL of Zentos was slightly increasing under 100 mM NaCl. For all genotypes, including the parents, the adverse effect of Na_2SO_4 on SDW was distinctly higher than at the same concentration of NaCl.

The STI values of SDW, RDW, SL and RL of the Z86 population tested in a hydroponic system with 100 mM NaCl and Na_2SO_4, respectively, are plotted in Figure 15 and Figure 16. Looking at the STI values for SDW, which is the most commonly used parameter in salt stress experiments at the seedling stage, it becomes apparent that the elite cultivar Zentos is outperforming the synthetic parent Syn86. Interestingly, as Zentos is facing a severe reduction of root length under 100 mM Na_2SO_4, Syn86 is showing better performance under stress condition than under control condition with no additional salt application. Generally, most genotypes performing higher under 100 mM NaCl treatment also show higher STI values under the concentration of Na_2SO_4. Genotype number 99 is one of the candidates showing consistently high STI value for SDW with +110% under NaCl and +92% under Na_2SO_4 treatment, comparing to the population average. Another genotype showing high STI values for SDW

under both salt types is genotype 117 with +93.9% and 73.3% under NaCl and Na_2SO_4, respectively, relative to the population mean. On the other side, genotypes with the highest reduction of shoot dry weight under 100 mM sodium chloride also perform weak under sodium sulfate treatment. Genotype 84 is facing under both treatments high losses of shoot dry weight. Expressed in STI value for SDW the reduction was by -58.2% and -53.2% under 100 mM NaCl and 100 mM Na_2SO_4, respectively.

Consequently, with respect to the performance under both salt treatments and to the stability of measured parameters, genotype 117 was selected as one of the best performing genotypes. On the downside, genotype 84 and 57 were selected as the most susceptible genotypes. These genotypes, together with the parents Zentos and Syn86, were selected as candidate genotypes for further deep phenotyping and expressional analysis.

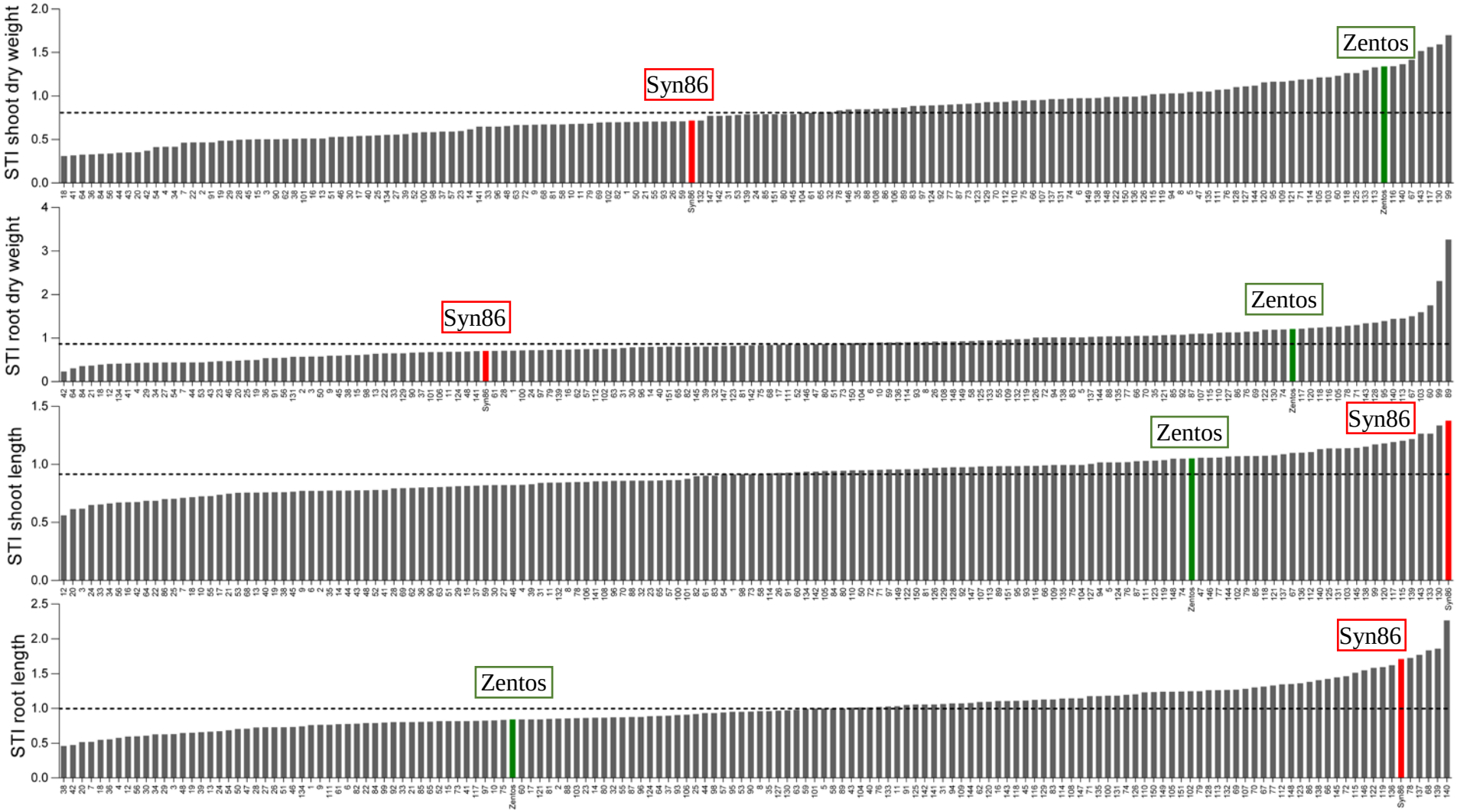

Figure 15. Bar plot of STI values of shoot dry weight (A), root dry weight (B), shoot length (C), root length (D) of the Z86 population tested in hydroponic system with 100 mM NaCl; genotypes are sorted according to the highest value; the parents are highlighted in green (Zentos) and red (Syn86); dashed lines = population means

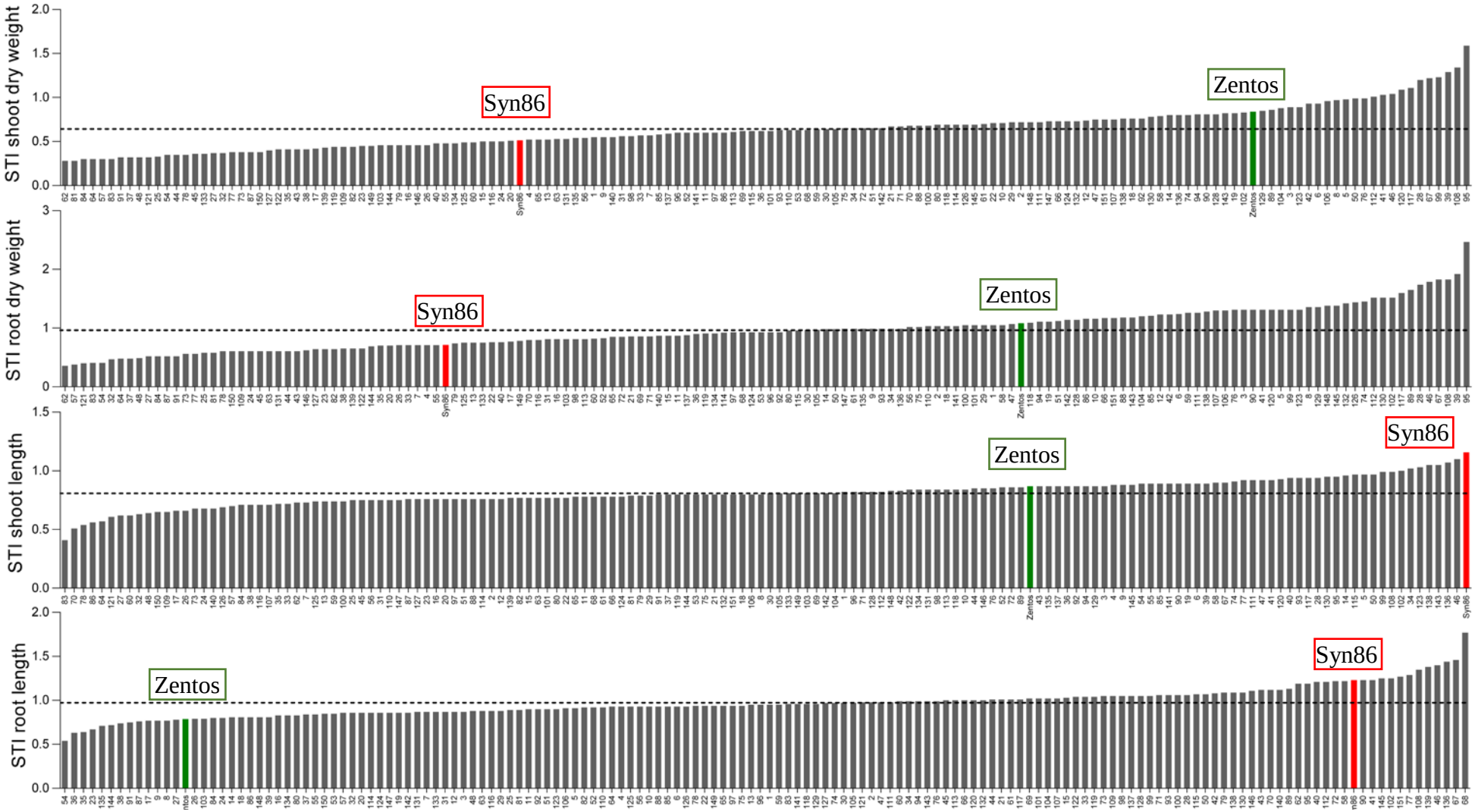

Figure 16. Bar plot of STI values of shoot dry weight (A), root dry weight (B), shoot length (C), root length (D) of the Z86 population tested in hydroponic system with 100 mM Na_2SO_4; genotypes are sorted according the highest value; the parents are highlighted in green (Zentos) and red (Syn86); dashed lines = population means

Assessment of K^+ and Na^+ concentration in leaves under salinity stress and control condition

To assess the sodium and potassium concentration of wheat plants exposed to salinity stress, the third leaf of the plants exposed to100 mM Na_2SO_4 and plants under control condition were analyzed using the Atomic Absorption Spectrometer (AAS).

For most tested genotypes the Na^+ concentration under salt stress condition was increasing while the K^+ concentration was reduced. Nevertheless, as shown in Figure 17A the correlation of sodium and potassium concentration in both treatments was weak.

Figure 17B is showing the relation between SDW and Na^+/K^+ ratio since shoot dry weight (SDW) is the main criteria for assessment of salinity tolerance at seedling stage. There was no correlation detected between both parameters, neither under controlled condition nor stress condition.

Figure 18 is showing the fold change of K^+ and Na^+ under salt stress condition relative to control condition. However, both parameters were showing weak correlation. In this figure ten genotypes with highest and ten genotypes with lowest STI values for SDW are highlighted. Among the highlighted genotypes only genotype 95 is showing increased accumulation of K^+ and high value for SDW. Interestingly, genotype 99 and 117, which also show high SDW values, show reduced K^+ concentration in leaves under stress condition relative to control condition. However, both genotypes accumulate slightly less Na^+ under salt stress condition than under control condition.

The parents of the Z86 population, Syn86 and Zentos, were facing a strong reduction in K^+ concentration and low increase in Na^+ concentration under salt stress condition relative to control condition. The elite cultivar Zentos was not only performing better than the synthetic parent Syn86 with respect to SDW, it was facing a smaller reduction of potassium concentration under salt stress condition than Syn86.

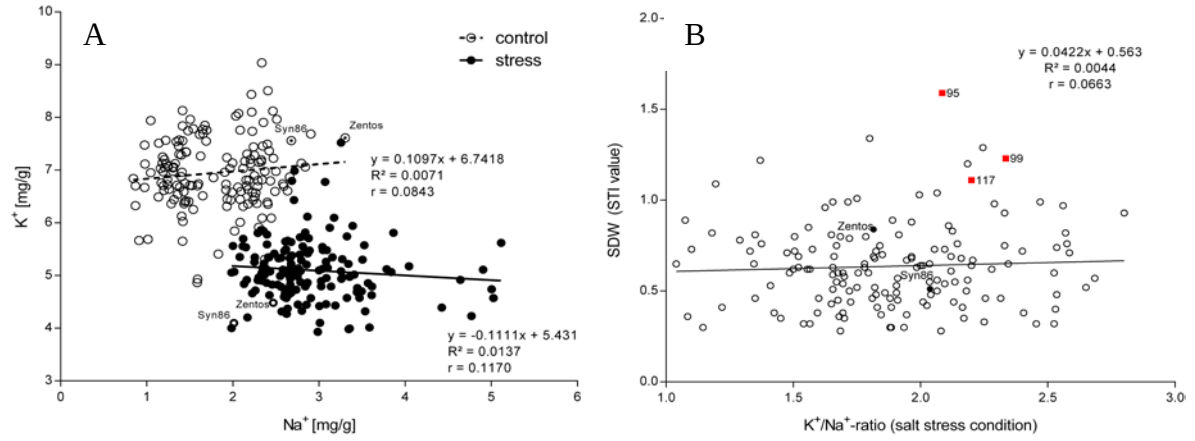

Figure 17. (A) Na^+ and K^+ concentration [mg/g dry weight] and (B) relation between K^+/Na^+-ratio (salt stress condition with 100 mM Na_2SO_4) in leaves of salt stress plants and SDW (STI value)

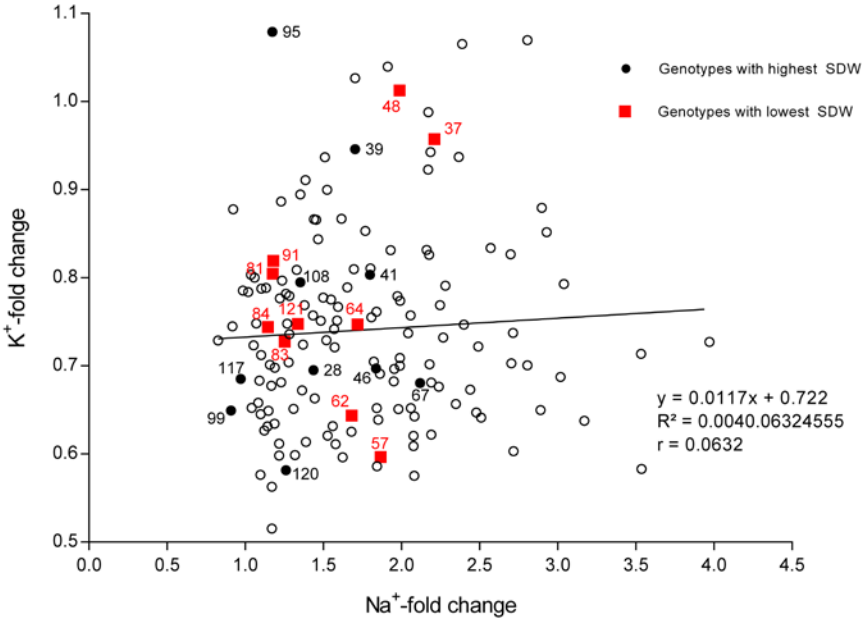

Figure 18. K^+ and Na^+ fold change in leaves of Z86 population under salt stress condition relative to control condition

Note: Black dots stand for 10 genotypes with highest SDW and red boxes indicate 10 genotypes with lowest SDW.

The exceptional performance of the genotypes 95, 99 and 117 are outlined by the "Mean vs. Stability" biplot (Figure 19) which is incorporating STI values of SDW under 100 mM NaCl and Na_2SO_4 and K^+/Na^+ ratio in leaves. These three genotypes show the highest performance

under salinity stress at seedling stage and outperform their parents Zentos and Syn86. Genotype number 8 is among the genotypes with the highest K^+/Na^+ ratio measured under salt stress condition. Nevertheless, as SDW is not correlated with K^+/Na^+ ratio, the biomass production of this genotypes is moderate.

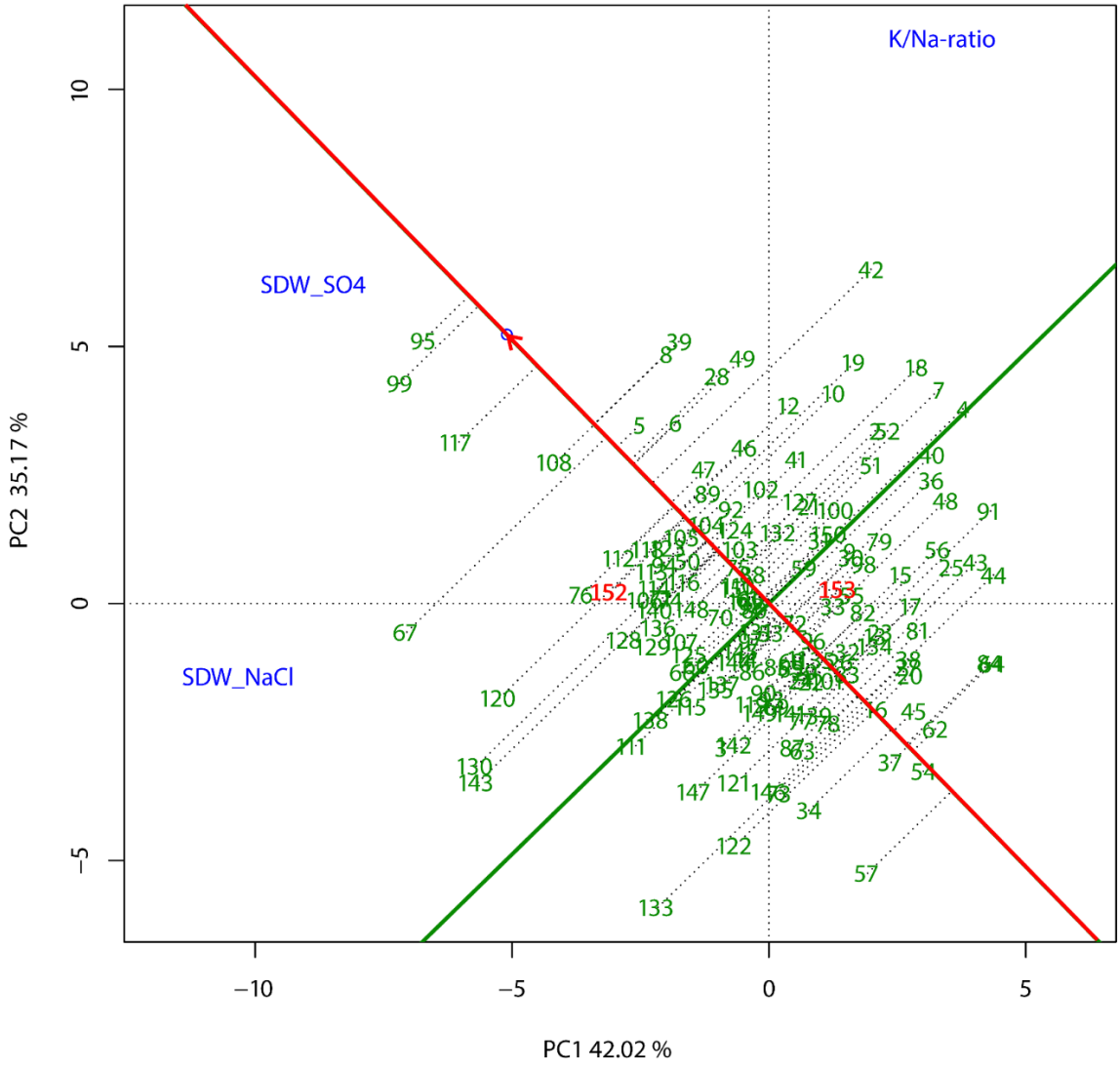

Figure 19. “Mean vs. Stability” plot of STI values for shoot dry weight (SDW) of Z86 tested under 100 mM NaCl and Na_2SO_4, respectively and K^+/Na^+-ratio in leaves.

Note: Based on STI values for shoot dry weight (SDW) with 100 mM NaCl and Na_2SO_4 and K^+/Na^+-ratio. In blue, the different parameters (SDW at 100 mM NaCl and Na_2SO_4 and K^+/Na^+ ratio of in leaves), in green the genotypes of the Z86 population, 152 and 153 indicate the parents Zentos and Syn86, respectively. The data were scaled based on the standard deviation. The red line passing through the biplot origin is referred to as the average-environmental axis (AEA). The arrow on the AEA indicates higher phenotypic performance. The green line, perpendicular to AEA passing through the biplot origin represents the stability axis. Positions distal to the biplot center indicate instability.

4.1.3. Evaluation of the Z86 population under field condition with natural salinization

To assess the performance of the lines of the Z86 population field experiments under natural salinization, in three planting seasons were conducted in Karshi (Uzbekistan) during 2010, 2011 and 2012. Due to the limited number of available seeds in the year 2010 and 2011 only field experiments under saline condition were conducted. Also, the parents of the Z86 population (Zentos and Syn86) were not tested under field conditions due to the limited number of available seeds. In the year 2012 field trials were conducted on both, saline and non-saline soils. Therefore, Table 18 presenting data from descriptive statistics is incomplete due to missing data from control plots. Furthermore, Table 19 includes data from analysis of variance and coefficients of broad-sense heritability only for parameters with available data from control and saline plots. In general, due to the spatial heterogeneity of the experimental site in respect to salinization level and salt type, the outcome of the measured parameters under control and stress condition were not distinct. Consequently, different from expectation, some parameters, e.g. yield, length of the spike (Table 18), were higher under stress condition than under control condition.

Table 18. Phenotypic parameters of the Z86 population collected from field experiments under control and saline soil conditions and grain quality characteristics

		Control							Saline condition						
Parameter		**Z86 Mean**	**SD**	**CV [%]**	**ci 95% lower**	**ci 95% upper**	**Max**	**Min**	**Z86 Mean**	**SD**	**CV [%]**	**ci 95% lower**	**ci 95% upper**	**Max**	**Min**
Germination rate [%]		na	na	na	na	na	na	na	94.4	21.8	23.1	91.4	94.4	100.0	10.0
Days to heading (DHD)		167.0	1.1	0.7	166.9	167.0	169.0	163.0	158.6	12.8	8.1	157.7	158.6	179.0	138.0
Days to maturity (DMD)		na	na	na	na	na	na	na	210.4	5.1	2.4	209.7	210.4	217.0	191.0
Plant height (PH)		115.9	11.5	10.0	114.6	115.9	138.0	80.0	95.4	12.8	13.4	94.5	95.4	133.0	63.0
Number of tillers (TLN)		na	na	na	na	na	na	na	266.5	85.4	32.0	256.6	266.5	472.0	90.0
Length of peduncle (PL)		42.8	5.5	12.8	42.1	42.8	60.0	28.0	42.5	5.6	13.2	41.9	42.5	52.0	28.0
Length of spike (SL)		10.9	2.1	19.6	10.6	10.9	36.0	8.0	11.3	2.3	20.2	11.1	11.3	17.0	5.0
SpS		20.5	2.5	12.0	20.2	20.5	25.0	10.0	20.5	2.5	12.3	20.2	20.5	25.0	15.0
TKW		30.6	3.3	10.8	30.6	30.2	38.6	21.2	24.4	3.7	15.2	24.0	24.4	36.9	15.6
Yield [T/ha]		1.96	0.68	34.85	1.88	1.96	4.43	0.52	1.99	0.94	47.44	1.92	1.99	4.67	0.22
Grain quality	**Ash [%]**	1.71	0.06	3.72	1.70	1.71	1.86	1.55	1.76	0.06	3.29	1.75	1.76	1.88	1.58
	Moisture [%]	10.21	0.85	8.31	10.11	10.21	11.81	9.25	8.89	0.22	2.47	8.87	8.89	9.81	8.50
	Hardness [%]	58.74	3.20	5.45	58.36	58.74	66.20	47.22	56.54	3.13	5.54	56.17	56.54	62.54	48.41
	Protein [%]	18.08	2.33	12.88	17.81	18.08	23.90	13.10	20.62	1.95	9.43	20.39	20.62	25.70	12.80
	Starch [%]	68.00	2.66	3.91	67.68	68.00	73.65	61.31	64.76	2.57	3.98	64.45	64.76	72.95	58.71
	Fiber [%]	2.70	0.21	7.74	2.67	2.70	3.28	2.14	2.63	0.23	8.57	2.61	2.63	3.26	2.16
	NDF [%]	18.60	1.20	6.47	18.46	18.60	24.68	15.00	18.45	1.11	6.01	18.31	18.45	21.18	16.15
	Sedimentation [ml]	58.10	11.44	19.69	56.75	58.10	92.09	28.09	70.22	9.05	12.89	69.14	70.22	89.62	29.00

Note: SpS spikelet per spike; TKW 1,000 kernel weight; NDF neutral detergent fiber; na data not available.

Table 19. Analysis of variance on parameters collected of Z86 populations tested on field experiment

	Genotype (G)	Treatment (T)	GxT	H^2 [%]
Parameter	(df 150)	(df 1)	(df 150)	
Days to heading (DHD)	0.06 ^{ns}	90.90 ***	0.05 ^{ns}	0.10
Plant height (PH)	1.07 ^{ns}	518.99 ***	0.96 ^{ns}	13.7
Length of peduncle (PL)	0.05 ^{ns}	2.69 ***	0.01 ^{ns}	98.6
Length of spike (SL)	1.23 ^{ns}	5.58 *	0.75 ^{ns}	31.2
SpS	0.00 ^{ns}	2.50 ***	0.05 ^{ns}	94.3
TKW	2.72 ***	563.85 ***	0.72 ^{ns}	46.2
Yield [T/ha]	0.14 ^{ns}	1.23 *	0.78 ^{ns}	23.3
Starch	1.31 *	208.43 ***	0.73 ^{ns}	38.2
Protein	1.21 ^{ns}	184.85 ***	0.77 ^{ns}	30.8
Fiber	3.68 ***	14.79 ***	0.89 ^{ns}	59.9
NDF	1.91 ***	2.63 ^{ns}	1.13 ^{ns}	28.4
Sedimentation	2.24 ***	233.36 ***	0.87 ^{ns}	61.6
Ash	1.43 **	105.67 ***	0.80 ^{ns}	27.3
Moisture	0.81 ^{ns}	460.25 ***	0.51 ^{ns}	23.8
Hardness	3.18 ***	98.05 ***	0.69 ^{ns}	64.9

Note: Significance levels p: * $p \leq 0.05$; ** $p \leq 0.01$; *** $p \leq 0.001$; ns not significant; H^2 broad sense heritability; SpS spikelet per spike; TKW 1,000 kernel weight; NDF neutral detergent fiber.

Table 19 summarizes the effect of genotype, treatment and genotype by treatment interaction obtained from analysis of variance for the phenotypic parameters of the Z86 population tested under field conditions. Most parameters were affected either by treatment or genotype or genotype and treatment. However, no significant genotype by treatment interaction was detectable. For most parameters, the estimation of broad-sense heritability (H^2) was moderate to very high. Only the heritability for the parameter 'Days To Heading' was close to 0, indicating that the phenotypic variance was due to the treatment and not genetically determined. Figure 20 is showing the data of important baking quality parameters measured with the NIR sensor. Surprisingly, salt stress positively affected the protein content (+14.2%) and the sedimentation rate (+20.1%) of the tested wheat genotypes, relative to control condition. This implies, that salinity stress is positively affecting baking quality of wheat seed. However, the grain yield production is highly affected by salt stress, since the amount of starch, which is the main component in seed endosperm is negatively affected by salt stress.

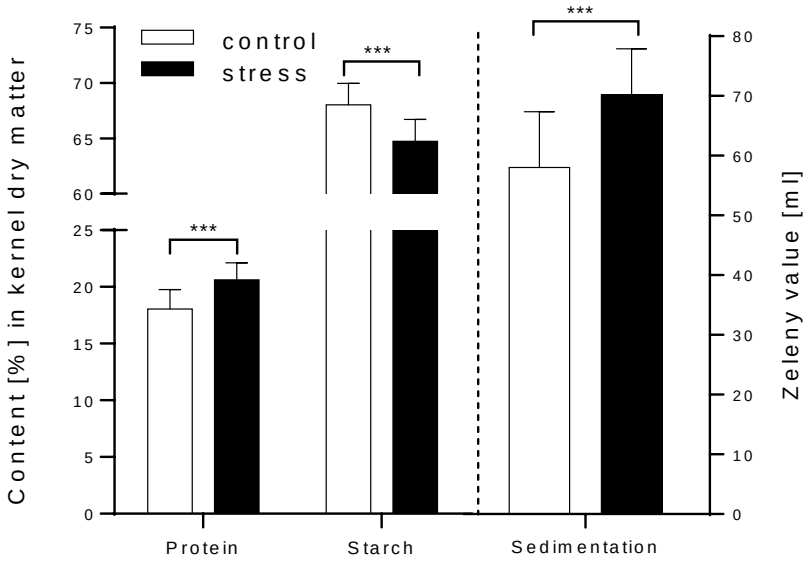

Figure 20. Major baking quality parameters of seeds of Z86 population measured with the NIR sensor; Significance levels p: *** $p < 0.001$

Table 20 is showing the Pearson's correlation (r) of phenotypic parameters measured from field trials under natural salinization and control plots with low salt level. As described earlier, due to the spatial heterogeneity of the experimental site, for some parameters no distinct reduction induced by salt stress was detectable. This was also affecting the calculated correlations factors. However, moderate positive correlation (0.52; $p<0.01$) was detected between grain yield and number of tillers under salinity stress.

Table 20. Pearson's correlation coefficient (r) for parameters measured from Z86 population tested in field trials under natural salinization

		DHD	DMD	PH	TLN	PL	SL	SpS	TKW	Yield	Ash	Moisture	Hard.	NDF	Protein	Starch	Fiber	Sed.	
Control	DHD		0.261**	0.171*	-0.143	0.017	-0.032	-0.106	-0.112	0.108	-0.037	0.038	-0.059	0.101	-0.055	0.046	0.068	-0.112	Stress
	DMD	-		0.042	-0.168*	-0.289**	-0.057	0.071	-0.065	-0.159*	-0.099	0.163	-0.049	0.114	-0.196*	0.134	-0.005	-0.238**	
	PH	-0.0	-		0.001	0.079	0.012	0.041	0.055	0.227**	-0.063	0.181*	0.090	-0.043	-0.035	0.044	0.019	0.002	
	TLN	-	-	-		0.148	0.138	-0.015	0.127**	0.406**	-0.113	0.027	0.042	-0.184*	-0.085	0.107	-0.083	-0.045	
	PL	-0.104	-	0.396**	-		0.138	0.031	0.011	0.142	0.006	-0.095	0.143	-0.175*	0.129	-0.120	-0.017	0.259**	
	SL	0.015	-	0.211*	-	0.085		0.406**	0.089	0.132	-0.115	0.183*	0.056	-0.069	-0.061	0.098	-0.082	-0.007	
	SpS	0.060	-	-0.017	-	0.002	0.031		0.049	-0.125	-0.022	0.087	0.000	0.116	-0.039	0.023	-0.031	-0.024	
	TKW	-0.008	-	0.297**	-	0.170*	0.138	0.029		0.392**	-0.446**	-0.044	0.606**	-0.377**	-0.384**	0.453**	-0.651**	0.010	
	Yield	-0.165*	-	0.270**	-	0.210**	-0.099	0.011	0.308**		-0.393**	0.062	0.312	-0.216	-0.322	0.375**	-0.407**	-0.165	
	Ash	-0.027	-	0.005	-	0.082	-0.079	-0.008	-0.194*	-0.114		-0.362**	-0.642**	0.319**	0.923**	-0.927**	0.686**	0.575**	
	Moisture	-0.019	-	0.076	-	-0.040	0.133	-0.072	0.203*	0.025	-0.094		0.071	-0.017	-0.340	0.406**	-0.003	-0.294	
	Hard.	0.138	-	0.143	-	0.1000	-0.078	-0.016	0.445**	0.197*	-0.385**	0.188*		-0.434**	-0.512**	0.610**	-0.829**	0.110	
	NDF	-0.081	-	-0.352**	-	-0.161	0.003	-0.007	-0.166*	-0.074	0.362**	-0.113	-0.473**		0.156	-0.265**	0.304**	-0.237**	
	Protein	0.002	-	0.028	-	0.167*	-0.060	0.019	-0.193*	-0.143	0.902**	-0.222**	-0.293**	0.256**		-0.951**	0.645	0.770**	
	Starch	-0.007	-	0.028	-	-0.145	0.124	0.004	0.322**	0.205*	-0.903**	0.307**	0.444**	-0.364**	-0.940**		-0.739**	-0.623**	
	Fiber	-0.017	-	-0.016	-	0.003	-0.035	-0.040	-0.360**	-0.164*	0.441**	0.456**	-0.526**	0.160	0.312**	-0.7**		0.151	
	Sed.	0.091	-	0.138	-	0.242**	-0.095	0.042	0.043	-0.059	0.676**	-0.178*	0.233**	-0.042	0.844**	-0.6**	-0.027		

Note: DHD days to heading, DMD days to maturity, PH plant height, PL length of peduncle, SL length of spike, SpS spikelet per spike, TKW 1000 kernel weight, Yield (T/ha), TP1-8 NDVI measurement time points, Hard. seed hardness, NDF Neutral Detergent Fiber, Sed. sedimentation; Significance levels p: * $p \leq 0.05$; ** $p \leq 0.01$.

As for the data collected at germination stage and seedling stage, salt tolerance index STI and stress-weighted performance SWP values were calculated for the parameters obtained from the field experiments (Table 21). Obviously, the correlation matrix is elucidating higher correlation coefficients for most correlations calculated with SWP in comparison with STI. According to Saade et al. (2016), in comparison to STI, the SWP index is more suitable to differentiate the high performant genotypes from low performant genotypes. Such as the correlation between the amount of grain yield and protein content of seeds: STI is showing no significant correction, whereas the SWP value is indicating a highly significant negative correlation of -40% ($p<0.01$).

Table 21. Pearson's correlation coefficient (r) for salinity tolerance index (STI) and stress-weighted performance (SWP) values calculated from parameters obtained from field trials under saline and non-saline conditions

		Yield	Ash	Moisture	Hardness	NDF	Fiber	Protein	Sedimentation	Starch	
STI	Yield		-0.399	-0.018	0.447**	-0.283**	-0.435**	-0.397**	-0.271**	0.390**	SWP
	Ash	-0.199**		-0.083	-0.745**	0.410**	0.799**	0.918**	0.702**	-0.912**	
	Moisture	-0.012	-0.238**		0.155*	-0.125	0.057	-.192**	-0.143*	0.230**	
	Hardness	0.219**	-0.480**	0.096		-0.468**	-0.846**	-0.678**	-0.270**	0.751**	
	NDF	-0.103	0.290**	-0.044	-0.458**		0.405**	0.346**	0.104	-0.394**	
	Fiber	-0.278**	0.507**	0.288**	-0.696**	0.185*		0.742**	0.418**	-0.810**	
	Protein	-0.128	0.930**	-0.285**	-0.309**	0.099	0.396**		0.862**	-0.941**	
	Sedimentation	-0.011	0.543**	-0.232**	0.328**	-0.297**	-0.075	0.769**		-0.724**	
	Starch	0.219**	-0.913**	0.354**	0.475**	-0.240**	-0.555*	-0.924**	-0.575**		

Note: Correlations ≥ 0.4 are highlighted with color code: red r = 0.8-1.0, orange r= 0.6-0-79, yellow r = 0.4-0.59; Significance levels p: * $p \leq 0.05$; ** $p \leq 0.01$; *** $p \leq 0.001$; NDF Neutral Detergent Fiber.

Yield and grain quality are major characteristics for selection of modern wheat varieties. Affected by salt stress the grain quality is increasing but the yield potential is decreasing. However, as the measured raw protein contents of all genotypes fulfill the minimum requirement for category *A* of wheat grain quality of minimum 12.5% protein content (Steinberger et al. 1995), the focus should be laid on grain yield production as the major selection criteria. As described earlier, SWP index for traits measured from field trials under the saline condition is a valuable parameter for identification of salt tolerant genotypes. SWP facilitates the selection of ideal germplasm for cultivation or breeding purpose by identification of salt tolerant genotypes tested in field trials. Figure 21 is showing the SWP values for yield and protein all genotypes of the Z86 population. Among the high yielding genotypes are also individuals with high performance at germination stage (Genotype 17) and SDW at seedling stage (genotype 108 and 117), RL at seedling stage (genotype 108 and 136).

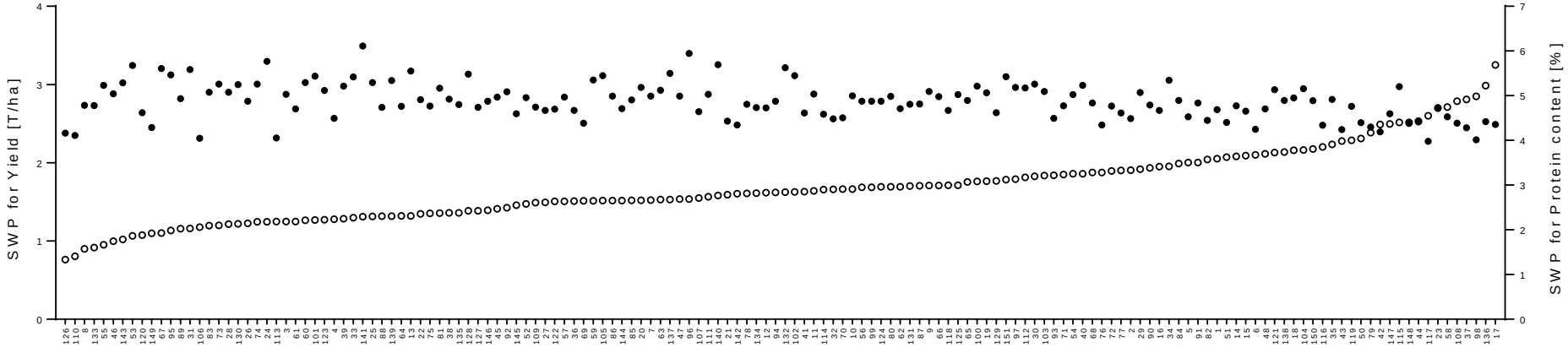

Figure 21. Stress-weighted performance index (SWP) values of yield (circles) and protein content (dots) of the Z86 population tested in field trials under natural salinization; genotypes sorted according to highest yield value

4.1.4. Combined analysis of phenotypic parameters across all analyzed growth stages

As mentioned earlier, yield performance and quality characteristics are essential demands to select appropriate varieties to cultivate under certain environmental conditions. The response of the tested genotypes to salt stress is varying from one development stage to the other. Furthermore, different salt types and concentrations also show diverse views on the impact of salt stress on plant development. To overcome the complexity, biplot analyses were conducted in order to visualize the performance of the tested genotypes across the tested environments and stage. Figure 22 is showing the "Mean vs. Stability" plots for the STI values of three developmental stages, namely germination test (100 mM NaCl and Na_2SO_4), shoot dry weight obtained from hydroponic experiment (100 mM NaCl and Na_2SO_4) and the grain yield obtained from field trials.

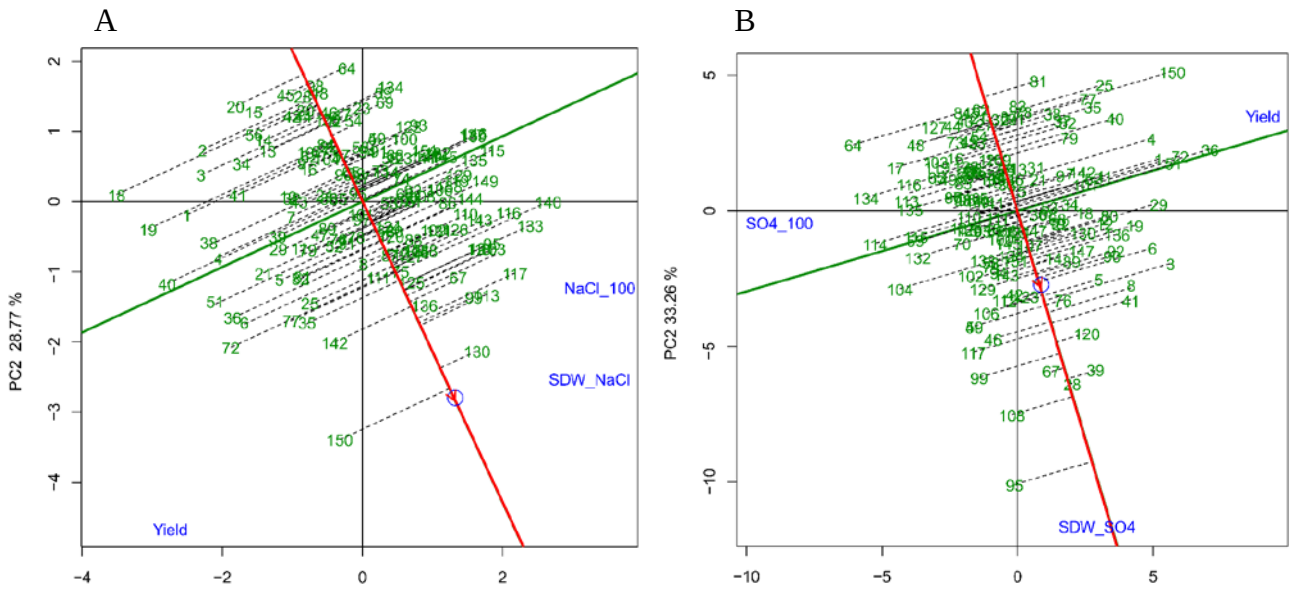

Figure 22. "Mean vs. Stability" plot of salinity tolerance index (STI) values for germination scoring, shoot dry weight (SDW) and grain yield from field trials of Z86 population

Note: **A** based on STI values for germination scoring and SDW with 100 mM NaCl and grain yield data from field trials, **B** based on STI values for germination scoring and SDW with 100 mM Na_2SO_4 and grain yield data from field trials. In blue, the different environments (germination stage, seedling stage and maturity stage), in green the genotypes of the Z86 population; the red line passing through the biplot origin is referred to as the average-environmental axis (AEA). The arrow on the AEA indicates better phenotypic performance. The green line, perpendicular to AEA passing through the biplot origin represents the stability axis. Positions distal to the biplot center indicate instability.

The “Mean vs. Stability” view of the GGE Biplot (Figure 22) incorporates the three developmental stages, germination, seedling and maturity stage to the average-environmental axis (AEA). According to Figure 22A, incorporating data from germination stage and seedling stage tested with NaCl and yield data from field trials under natural salinization, genotype 130 and 150 showed high performance. However, comparing across all tested growth stages, genotype 130 showed higher stability than genotype 150. On the opposite side, genotype 64 was showing weakest performance across all developmental stage. As shown in Figure 22B, incorporating data from germination and seedling stage tested with Na_2SO_4 and yield data from field trials under natural salinization, genotype 28 is regarded as most stable genotype with high performance. This indicates that the rank of this genotype was consistent across all environments with a generalized mega-environment. However, genotype 99 and 108 showed higher phenotypic performance but weaker stability when comparing the three developmental stages. Like under NaCl treatments, the weakest performance was presented by genotype 64, making this genotype most susceptible across all environments.

Obviously, the genotypes were showing differential performance across the tested salt treatments and at the various growth stages. Considering the fact that the correlations of genotypic performance under salinity stress at germination stage and further growth stages are low, a GGE Biplot was constructed incorporating data from SDW at seedling stage and grain yield from field trials. Figure 23 simplified the selection of better performing genotypes and with higher stability at seedling stage and maturity stage. Accordingly, entry number 64 can be regarded as the most susceptible genotype. On the other hand, several genotypes were showing high performance, among them, entry number 67, 95, 99, 108 and 117. These genotypes can be regarded as most tolerant genotypes with entry number 95 showing higher performance and considerably moderate stability across the tested environments.

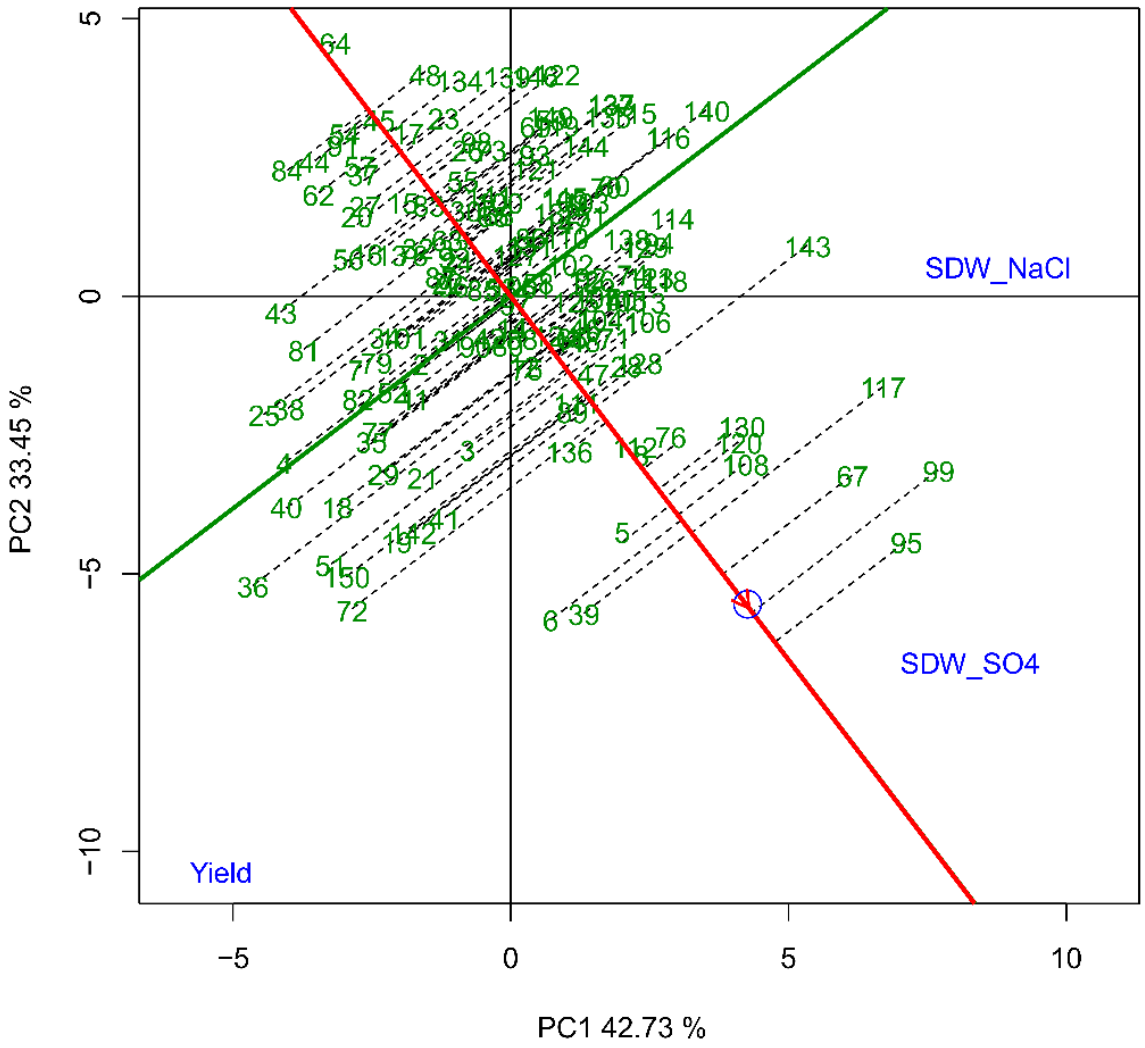

Figure 23. “Mean vs. Stability” plot of salinity tolerance index (STI) values for shoot dry weight (SDW) at seedling stage with 100 mM NaCl and Na_2SO_4 and plot yield of Z86 population

Note: Based on STI values for shoot dry weight (SDW) with 100 mM NaCl (SDW_NaCl), and 100 mM Na_2SO_4 (SDW_ SO_4), and Yield. In blue, the different environments, in green the genotypes of the Z86 population; the red line passing through the biplot origin is referred to as the average-environmental axis (AEA). The arrow on the AEA indicates better phenotypic performance. The green line, perpendicular to AEA passing through the biplot origin represents the stability axis. Positions distal to the biplot center indicate instability.

4.1.5. Application of sensors for non-destructive measurement of water-status and salinity stress

Multiple sensors were utilized within the scope of different experiments for phenotyping plants non-destructively. Salinity stress as well as drought stress to a great extent induce similar physiological processes in plants by implication of osmotic imbalances due to reduced soil water potential (Rao et al. 2006, Pessarakli 2014). Hence, analysis of water content can be a valuable trait for assessment of plants exposed to drought or salinity stress (Uddin et al. 2016).

As the EMISENS dual-mode microwave resonator will be described in detail in the publication presented in Appendix 5, the outcome of the LI-COR LI-6400XT gaze exchange analyzer will be presented within this chapter.

Non-invasive assessment of leaf water status using a dual-mode microwave resonator

The results of the EMISENS dual-mode microwave resonator are presented in detail in the publication attached in Appendix 5. Within the context of this chapter the result of the experiments conducted with the respective sensor will be presented briefly.

A significant change in the resonant frequency shift of Mode 1 (2.4 GHz) between fresh and totally dried wheat leaves was demonstrated, which is far beyond the variation from leaf to leaf for a given plant (Figure 24). It is notable that the frequency shift of the dry leaf is zero within the measurement accuracy limits which indicates that water represents the dominant part of the response.

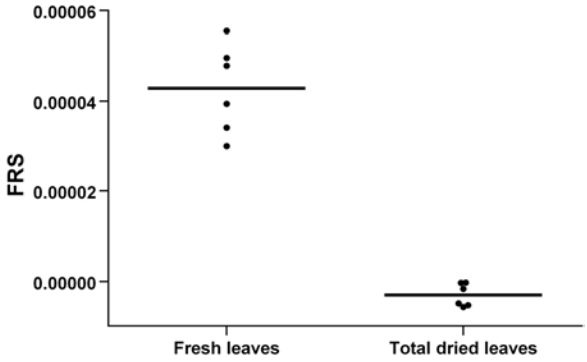

Figure 24. Comparative dielectric conductivity of fresh and totally dried wheat leaves

Note: Six wheat leaves in total were measured fresh and subsequently completely dried. The dots represent the average relative frequency shift values (*FRS*) of five measurements (technical replicates) and the lines the average values of six leaves.

For Mode 1, the measured values of *FRS* and *IQS* as a function of percentage of fresh weight for four different types of plants were normalized to the average value of the corresponding fresh leaves (Figure 25). Although the absolute values of *FRS* and *IQS* differ from leaf to leaf due to a different filling factor κ (Eq. 4 in Appendix 5) the normalized *FRS* and *IQS* values exhibit a systematic decrease with increasing weight loss, which indicates that water provides the most significant contribution to the dielectric permittivity of leaf tissue. The data points of individual leaves show this trend.

The averaged values displayed in Figure 25 as horizontal lines are representative mean values for all leave stages. Based on t-test, significant differences between the mean values were revealed ($p < 0.05$). Measurement of three leaves and calculation of their mean values show stronger correlations to the water content than the single leaves measurement. Assuming that the mass density of the dry leave tissue is small in comparison to that of water, the weight percentage represents the volumetric water concentration – multiplied by factor of about 0.5-0.7 (maximum water volume concentration in a fresh leaf) (Ulaby and Jedlicka 1984). According to our data, the normalized *FRS* values drop to about 0.45-0.55 for wheat and maize, and to slightly higher values of about 0.65-0.75 for potato and canola - as result of weight reduction or water loss from 100% to 50%. It is remarkable, however, that the *FRS* – weight dependences exhibit a recognizable positive curvature and deviate from linearity, in contrast to the slightly negative curvature being observed by broadband dielectric measurements on wheat leaves and stalks (Ulaby and Jedlicka 1984). For potato leaves and in particular for canola leaves, where a considerable portion of water is stored in relatively thick veins, this effect is most pronounced.

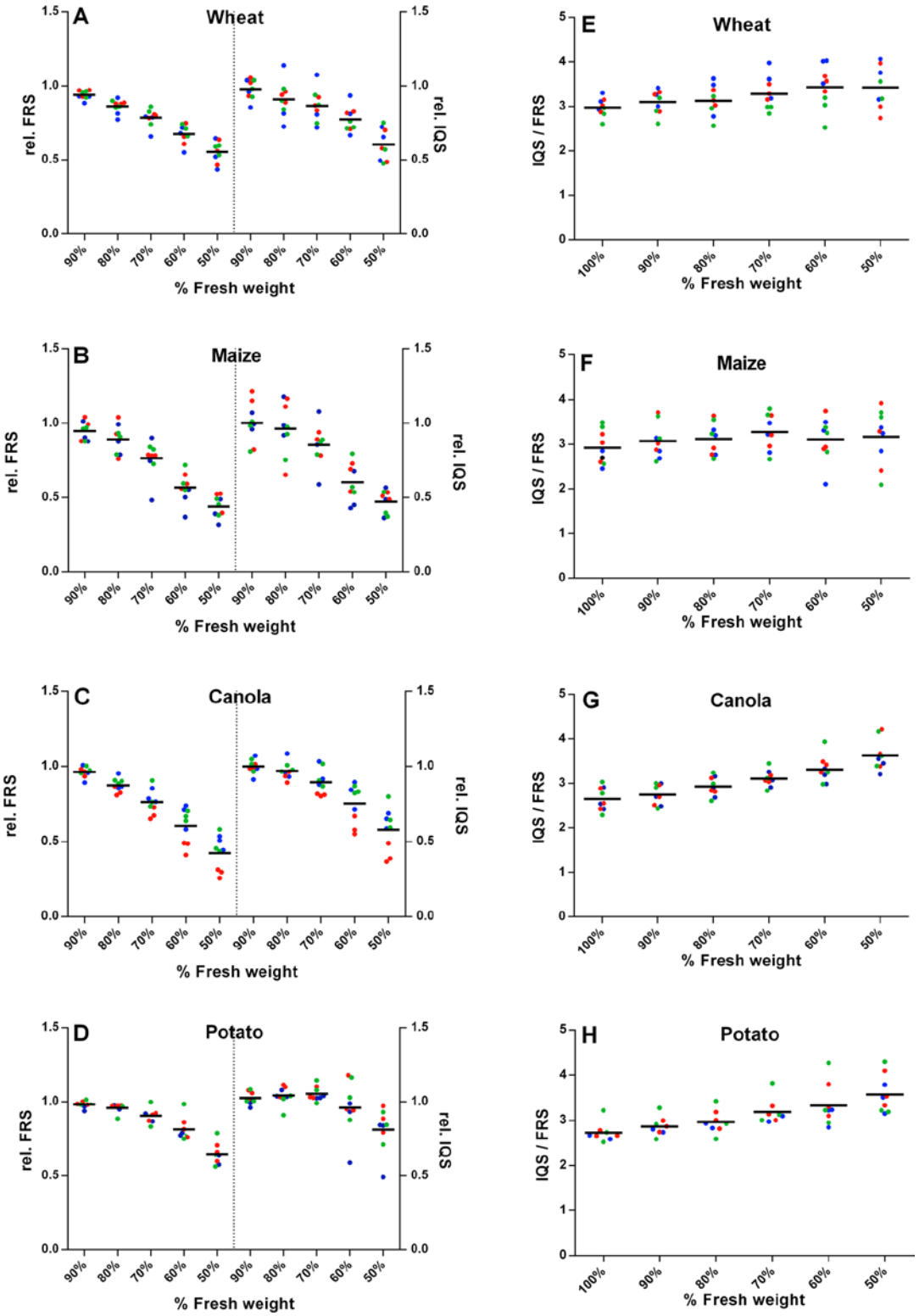

Figure 25. Experimental results of microwave measurements on leaves from four different crops

Note: The analysis was performed at six time-points from initial fresh weight (100%) up to 50% of the initial weight by consecutive 10% drying in each step. (**A**) - Wheat, (**B**)-Maize, (**C**) - Canola, and (**D**) - Potato. Normalized FRS and IQS values based on values at 100% fresh weight for FRS and IQS, respectively are shown. E (Wheat), F (Maize), G (Canola) and H (Potato) display IQS values divided by FRS values for single leaves at different drying stages, and water contents, respectively. Bars indicate arithmetic means over three leaves. The absolute averaged FRS values at 100% fresh weight are $5.5 \cdot 10^{-5}$ for wheat, $1.25 \cdot 10^{-4}$ for maize, $1.41 \cdot 10^{-4}$ for canola and $1.24 \cdot 10^{-4}$ for potato. The colors of the dots indicate the developmental stage of the leaves: blue (first stage, young leaf), green (second stage, intermediate leaf) and red dots (third stage, older leaf).

For the fresh weight data, the average ratio *IQS*/*FRS* varies only slightly between 2.8 and 3 for the three different plants.

Non-invasive assessment of ionic conductivity in leaves using a dual-mode microwave resonator

The loss tangent of distilled water at 2.4 GHz is 0.12 and 0.3 for an assumed ionic conductivity of 14,000 µS/cm. In other words, within the framework of perturbation theory and the assumption that the losses are due to water and ions only, the analysis yields a nearly ten times higher conductivity than reported in the literature. In order to resolve this puzzle, we took a closer look at the *IQS* and *FRS* values of Mode 0, because the separation of ionic conductor losses from water dipole relaxation losses is much more pronounced at this low frequency (Table 22). In order to improve the measurement statistics, we measured *FRS* and *IQS* for 6 fresh leaves from one plant (indicated by the numbers in Table 22). Each of the listed *FRS* and *IQS* values corresponds to the average of five subsequent measurements performed on one leaf, the quoted error represents the standard deviation of these five subsequent measurements.

Table 22. Measured *FRS* and *IQS* (*f*=150MHz, Mode 0) for six different fresh leaves of one wheat plant and calculated ionic conductivity

Leaf number	**FRS (weighted mean)**	**FRS (CV %)**	***IQS* (weighted mean)**	**IQS (CV %)**	**σ[µS/cm] (weighted mean)**	**σ (CV %)**
1	$1.30\cdot10^{-5}$	40	$5.25\cdot10^{-5}$	27	$1.4\cdot10^{4}$	48
2	$1.47\cdot10^{-5}$	26	$6.11\cdot10^{-5}$	15	$1.4\cdot10^{4}$	30
3	$1.27\cdot10^{-5}$	46	$7.78\cdot10^{-5}$	27	$2.0\cdot10^{4}$	53
4	$1.86\cdot10^{-5}$	21	$6.84\cdot10^{-5}$	52	$1.2\cdot10^{4}$	56
5	$1.94\cdot10^{-5}$	7	$8.79\cdot10^{-5}$	20	$1.5\cdot10^{4}$	21
6	$1.96\cdot10^{-5}$	29	$9.52\cdot10^{-5}$	15	$1.6\cdot10^{4}$	14
Average					$1.46\cdot10^{4}$	14

Note: Each data point corresponds to the average of five subsequent measurements; σ ionic conductivity σ, determined from *IQS*/*FRS* by Eq. 6 (Appendix 5); CV coefficient of variation.

Furthermore, in order to demonstrate the practical applicability of the microwave technique, wheat plants being challenged by salt stress were measured (at the moment only by Mode 1). The measured *FRS* values reveal a clear difference between the control leaves and the stressed

ones (Figure 26). The decrease in the *FRS* value is likely to be linked to an increase of osmolarity induced by salt stress which is adversely affecting the uptake of water by the roots.

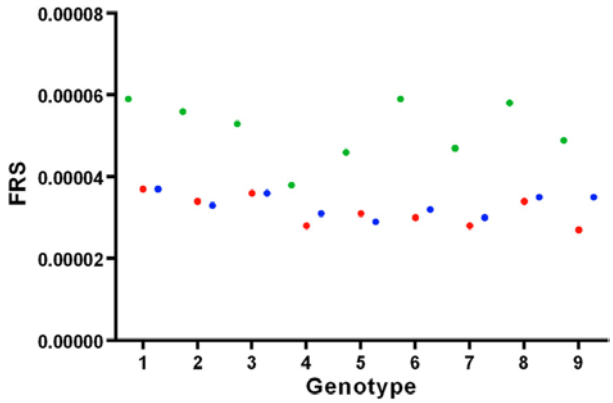

Figure 26. Analysis of wheat leaves from nine genotypes after 15 days of salt stress

Note: Green dots represent control, red and blue dot leaves stressed with 100 mM NaCl and 50 mM Na_2SO_4, respectively. X-axes represent the genotypes analyzed (numbered 1–9) and the y-axes the corresponding *FRS* values.

A reduction of the water content in the plant cell leads to an increase of osmolarity. Therefore, the osmotic potential of canola leaves at 6 time-points was determined. A strong negative correlation (r = -0.97) between *IQS*/*FRS* values and the respective osmotic potential of the leaves at different steps of water reduction was found (Figure 27).

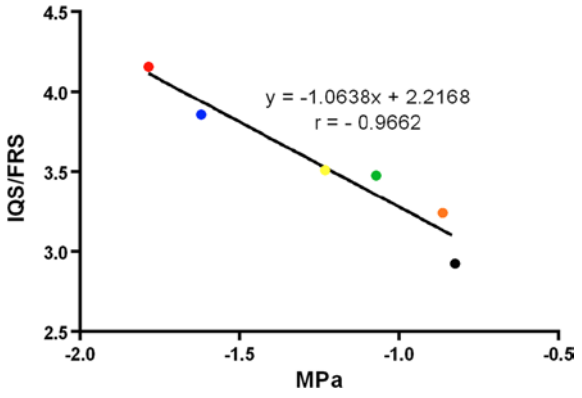

Figure 27. Correlation between osmotic potential and IQS/FRS values for canola leaves

Note: Dot-colors indicate measurement of leaves with water content decreasing stepwise: black -100% (initial fresh weight); brown -90%, green -80%; yellow -70%; blue -60% and red -50% of the initial weight. Each dot represents the mean values from four leaves. For each leave, two measurements were performed to define osmotic potential and five for the *IQS*/*FRS* value.

Fast response of photosynthetic parameters of wheat plants exposed to sudden increase of salt stress

Gaz exchange measurements were conducted in order to investigate the immediate change of photosynthetic parameters that evolve within the first minutes after exposing plants suddenly to high salt concentration. The salt shock experiment was conducted with the parents of the Z86 population, Zentos and Syn86. In contrast to the previously described gradual application of salt in three increments until reaching the final concentration of 100 mM NaCl or Na_2SO_4, respectively, for the salt shock experiment the 50 days old plants were transferred suddenly from control solution into solution with 100 mM NaCl.

The fast and substantial decrease of photosynthetic parameters of wheat seedlings transferred from controlled solution to salt stress solution with 100 mM NaCl was detectable within the first minutes after salt stress initiation, revealing fast reaction of plants exposed to salt shock as the photosynthetic activity of the plants were declining immediately.

Figure 28 is showing the means of the photosynthetic parameters for Syn86 and Zentos 15 minutes before stress initiation until 45 minutes after stress initiation. The gas exchange analyzer LI-COR LI-6400XT (Biosciences 2008) was allowing detection of fast response of photosynthetic parameters of plants exposed to salt shock non-destructively. Both genotypes, exposed to salt shock experienced a drop of measured photosynthetic parameters.

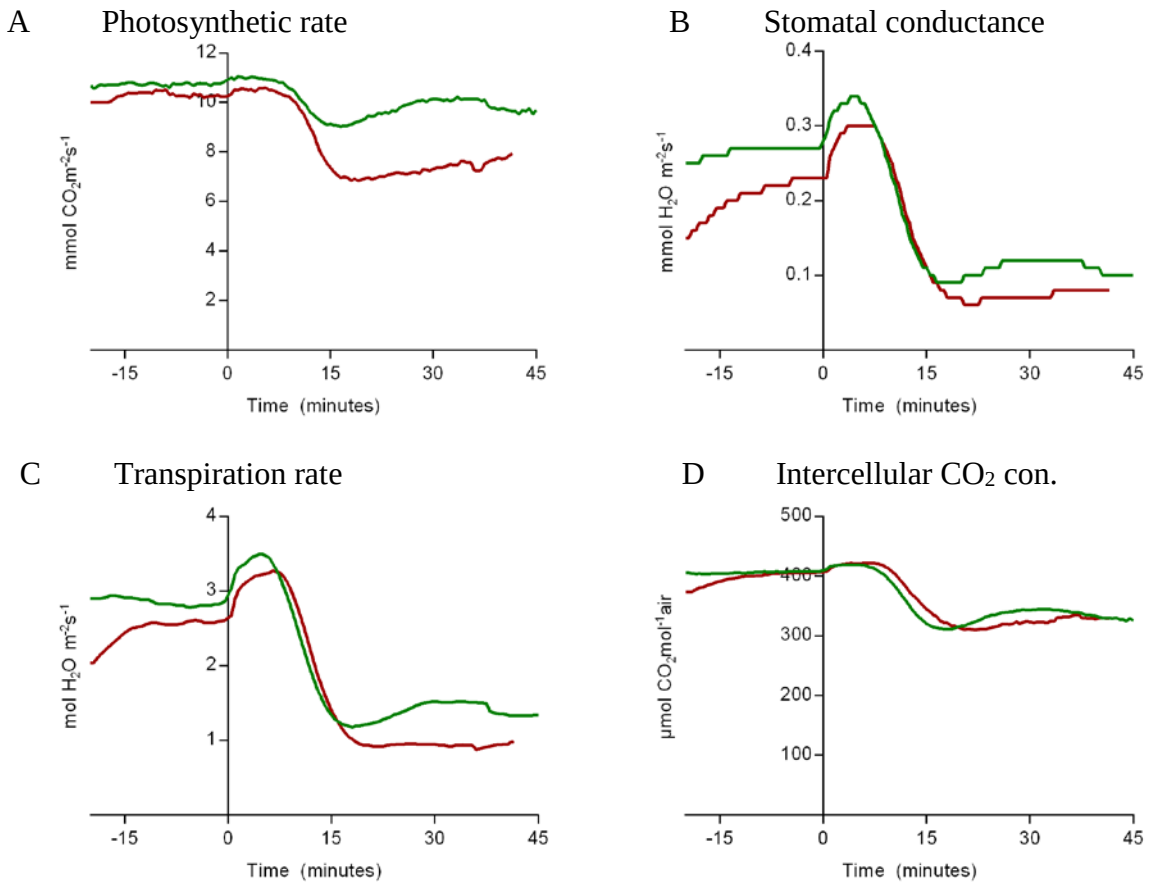

Figure 28. Time course of photosynthetic parameters of Zentos and Syn86 15 minutes before until 45 minutes after exposition to 100 mM NaCl salinity stress

Note: **A** Photosynthetic rate (*A*), **B** stomatal conductance (g_s), **C** transpiration rate (*E*), **D** intercellular CO_2 concentration (C_i); x-axis is showing 15 minutes before initiation of salt stress and 45 after stress initiation; green colored lines indicate the genotype Zentos and red line indicates Syn86.

Immediate response after initiation of salt stress was apparent only for photosynthetic rate indicating genotypic variation (Figure 28A). As the stomatal conductance, intercellular CO_2 concentration and transpiration rate were not showing effects for the genotype, and genotype by treatment interaction, the investigation of fast responses of plants immediately exposed to salinity stress was focused on the photosynthetic rate (*A*), which is assigned for CO_2 fixation by plants.

To examine more closely the differential genotypic response of wheat genotypes exposed to salt shock condition, the experiment was repeated with Syn86, Zentos and two entries of the Z86 population, which were selected based on their performance of SDW production under salinity stress, namely genotype 84 and 117, representing salt sensitive and salt tolerant genotypes, respectively.

Figure 29 illustrates the photosynthetic rate (*A*) of Zentos, Syn86, genotype 84 and genotype 117. With a delay of approximately 8 minutes after stress initiation (SI, 0 minutes) the *A* of Zentos, Syn86 and genotype 84 start declining dramatically. Unlike other genotypes, the *A* of genotype 117 declined with an extended delay of 15 minutes after stress initiation. The photosynthetic rate of Zentos hit the low point of 9 µmol CO_2 m^{-2} s^{-1} after 16.5 minutes (-15.8% rel. to SI). The dramatic drop of *A* of Syn86 reached the bottom of 6.8 µmol CO_2 m^{-2} s^{-1} after 19 minutes of salt stress (-33.1%). After 24.5 minutes *A* of genotype 117 reached the bottom value of 8 µmol CO_2 m^{-2} s-1 (-21.2% rel. to SI).

In contrast to our assumption, the decline of *A* of genotype 84 was less than expected where after 20.5 minutes the bottom value of 9.4 µmol CO_2 m^{-2} s^{-1} was reached. But the extent of decline (-14.3% rel. to SI) was less than of other comparing genotypes.

In summary, genotype 117 was able to maintain the photosynthetic rate for a longer period than all other comparing genotypes. Considering all tested genotypes, Syn86 was more sensitive towards salinity stress showing a severe decline in photosynthetic rate. The extent of variation of other measured photosynthetic parameters (stomatal conductance, transpiration rate, intercellular CO_2 concentration) was less in comparison with photosynthetic rate (see Table 23).

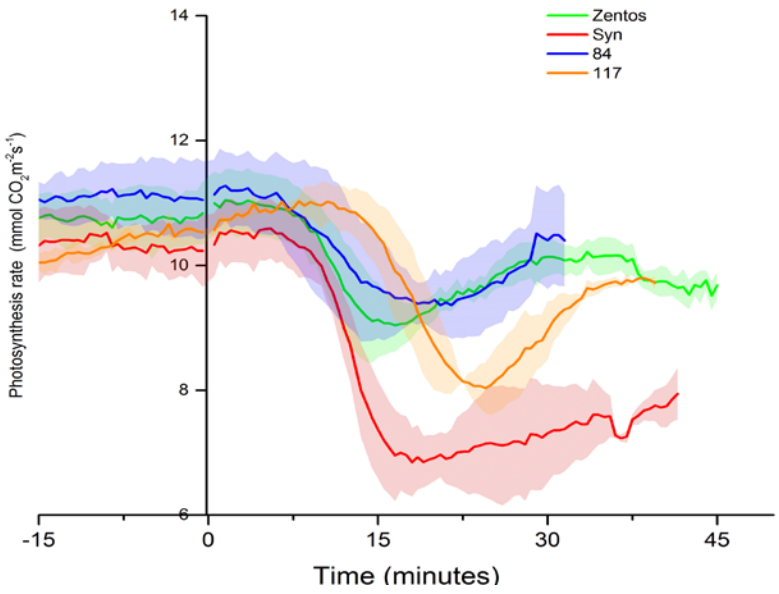

Figure 29. Time course of photosynthetic rate of Zentos, Syn86, genotype number 84 and 117; colored shadows indicate standard deviations

The descriptive statistics of measured photosynthetic parameters are summarized in Table 20. For the sake of comparability and conductance of statistical test only the first 30 minutes after stress application was considered due to the limited available data for genotype 84.

Table 23. Summary of statistics of immediate effect on photosynthetic parameters of Zentos, Syn86, genotype 84 and 117 exposed to salinity stress

Parameter	Zentos	Syn86	Genotype 117	Genotype 84
Photosynthetic rate				
A_0	10.7±0.4	10.2±0.5	10.2±	10.9±0.6
A_{MIN}	9.0	6.8	8.0	9.4
Time to reach A_{MIN}	16.5	18	24.5	20.5
A (rel. to A_0)	-15.8%	-33.1%	-21.2%	-14.3%
Stomatal conductance				
$g_{s\ 0}$	0.27±0.1	0.21±0.0	0.18±0.0	0.24±0.0
$g_{s\ MIN}$	0.09	0.06	0.07	0.09
Time to reach $g_{s\ MIN}$	16.5	20.5	22	17.5
g_s (rel. to $g_{s\ 0}$)	-66.0%	-70.7%	-61.8%	-62.0%
Transpiration rate				
E_0	2.86±0.57	2.48±0.2	1.99±0.1	2.56±0.2
E_{MIN}	1.18	0.92	0.83	1.12
Time to reach E_{MIN}	18	21	24	19.5
E (rel. to E_0)	-58.7%	-62.9%	-58.2%	-56.2%
Intercellular CO_2 conc.				
$C_{i\ 0}$	406.0±13.9	396.4±7.8	386.9±4.9	399.9±11.3
$C_{i\ MIN}$	311.4	310.0	283.6	306.7
Minutes to reach $C_{i\ MIN}$	18.5	22	25.5	20
C_i (rel. to $C_{i\ 0}$)	-23.3%	-21.8%	-26.7%	-23.3%

Note: A Photosynthetic rate, g_s stomatal conductance, E transpiration rate, C_i intercellular CO_2 concentration; 0 time of stress initiation; MIN minimum value.

Repeated measures analysis of variance

Repeated measures analysis was conducted incorporating additionally time (of response) as factor in the ANOVA model to detect genotype by treatment by time interaction effects (genotype*treatment*time). In Table 24Table 24 tests of hypotheses for between-subject effects without integration of time as factor are presented. From this analysis, there is a significant between-genotypes effect (p-value = 0.024) and between-treatment effect (p-value = 0.002). Obviously, without integration of time the genotype by treatment interaction effect is not significant (p-value = 0.29) as the course of the photosynthetic rate of the tested genotypes were showing temporal offsets (Figure 29).

Table 24. The GLM procedure repeated measures analysis of variance tests of hypotheses for between-subjects Effects

Source	DF	Type III SS	Mean Square	*F*-value	*p*-value
Genotype	3	297.53	99.18	4.14	0.024
Treatment	1	326.94	326.94	13.65	0.002
Genotype*Treatment	3	97.99	32.66	1.36	0.290
Error	16	383.36	23.96		

Note: DF degree of freedom, F F-value.

Different to this table, Table 25 is showing the univariate analyses for within-genotype effects and related interactions within the time-dependent course.

Table 25. The GLM procedure repeated measures analysis of variance univariate tests of hypotheses for within-subject effects

Source	DF	Type III SS	Mean square	*F* value	*p* value	Adjusted *p*	
						G - G	H-F-L
Time	56	211.11	3.77	30.87	<.0001	<.0001	<.0001
Time*Genotype	56	37.65	0.67	5.51	<.0001	0.0093	0.0035
Time*Treatment	56	208.29	3.72	30.46	<.0001	<.0001	<.0001
Time*Treatment*Genotype	56	37.00	0.661	5.41	<.0001	0.0100	0.0039
Error(Time)	560	222.42	0.40				

Note: DF degree of freedom, F F-value, G-G Greenhouse-Geisser, H-F-L Huynh-Feldt-Lecoutre.

The p-values were adjusted with the lower-bound estimate Greenhouse-Geisser correction (G-G) and Huynh-Feldt-Lecoutre correction (H-F-L). Both, the Greenhouse-Geisser and Huynh-Feldt-Lecoutre adjusted p-values were significant for all factors and factor interactions, including Time*Treatment*Genotype.

The univariate analysis assumes highly significant effects for all factors and factor interactions (p-value < 0.0001). The repeated measures ANOVA revealed highly significant genotype by treatment interaction effect 20 minutes after initiation of salt stress (F-value=21.25, p-value=0.0058). Beyond the individual low points of the curves, the photosynthetic rate of Zentos was recovering faster and reaching a higher level, although still lower than under control condition, whereas Syn86 was slightly able to recover from the minimum photosynthetic rate values. The salt shock experiment indicates the divergence in the capability of both genotypes, Zentos and Syn86, coping with suddenly salinity stress and the ability to restore prior homeostatic condition.

4.2. Genotypic characterization of the Z86 population

The 151 lines of the Z86 population and their parents Zentos and Syn86 were genotyped using the Infinium iSelect 90K single nucleotide polymorphism (SNP) bead array assaying 81,587 gene-associated SNPs. The number of SNP with known positions according to the rescaled genetic map by Wang et al. (2014) was 37,427 markers. After data cleaning with the removal of markers with more than 5% missing data and minor allele frequency less than 2.5% 11,050 polymorphic SNP markers remained. The remaining Markers including their genetic positions is shown in Figure 30. The density and distribution of SNP markers on the 21 wheat chromosomes are visualized in the table inside the CIRCOS plot (Figure 30).

Apparently, the D-genome is less saturated with SNP markers than the A and B genome. Whereas the marker density of the A and B genome are 3.7 SNP per cM and 4.7 SNP per cM, respectively. The marker density of the D genome was 1.1 markers per cM. Chromosome 4D had the biggest gaps of chromosomal segments with low marker saturation among all chromosomes with 68 markers covering 170 cM of chromosomal length (0.4 markers per cM). In contrast to chromosome 4D, the marker density of chromosome 6B was 6.7 SNP per cM with was 819 SNP covering 123 cM.

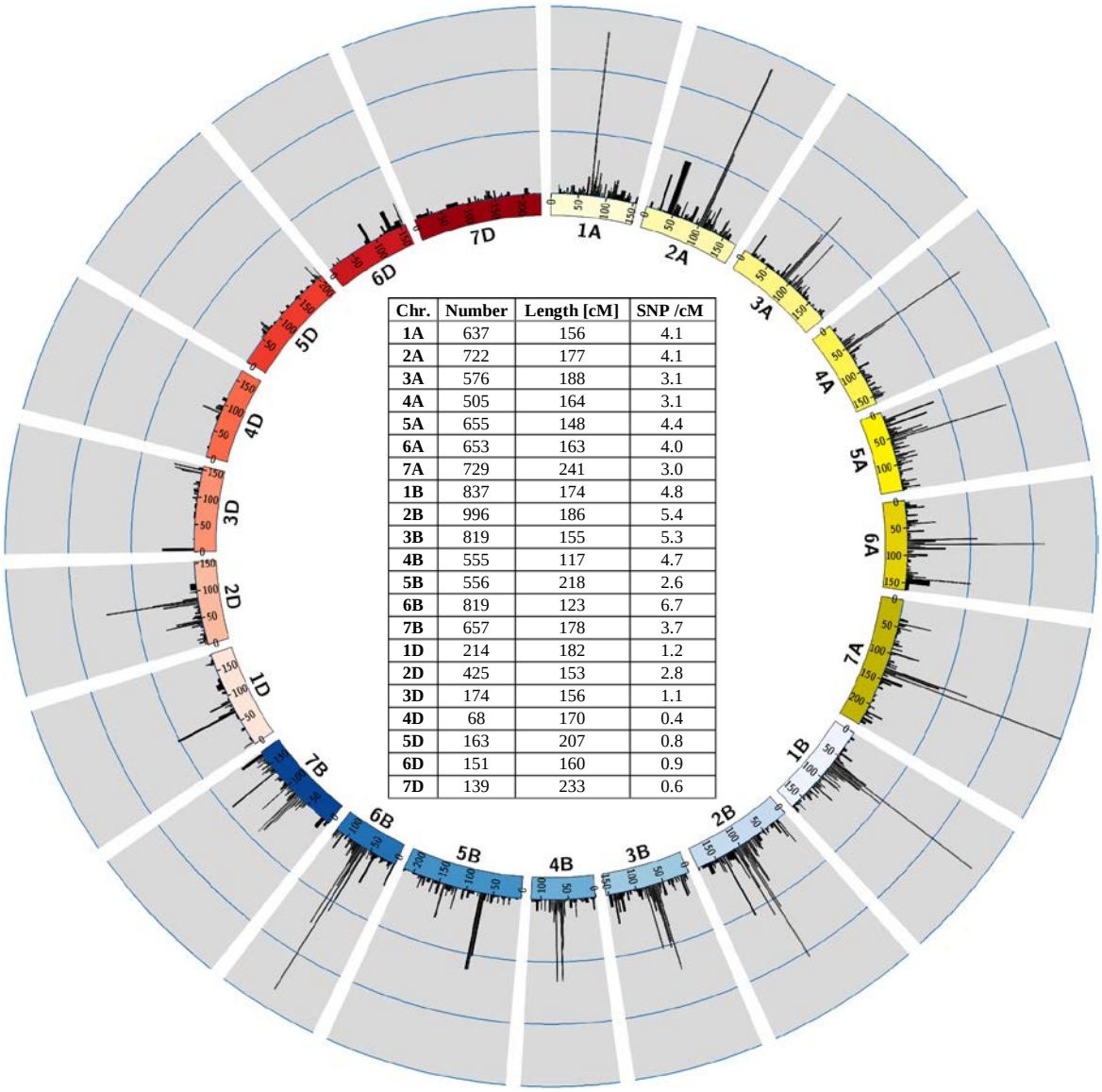

Chr.	Number	Length [cM]	SNP /cM
1A	637	156	4.1
2A	722	177	4.1
3A	576	188	3.1
4A	505	164	3.1
5A	655	148	4.4
6A	653	163	4.0
7A	729	241	3.0
1B	837	174	4.8
2B	996	186	5.4
3B	819	155	5.3
4B	555	117	4.7
5B	556	218	2.6
6B	819	123	6.7
7B	657	178	3.7
1D	214	182	1.2
2D	425	153	2.8
3D	174	156	1.1
4D	68	170	0.4
5D	163	207	0.8
6D	151	160	0.9
7D	139	233	0.6

Figure 30. Overview of marker saturation and marker density on the 21 chromosomes of wheat

Note: The number of markers per cM are plotted in histograms along each chromosome. For better visualization in a histogram plot an interval was constructed aggregating markers in an interval of 1 cM. The scale for the number of markers is plotted as rings on the CIRCOS plot: inner ring = 50 markers, middle ring = 100 markers, outer ring = 150 markers.

Despite preliminary marker cleaning, some particular regions on different chromosomes harbor a large number of markers on the same chromosomal positions. On chromosome 7A position 136 cM, for example, accumulates 150 SNP markers. Furthermore, chromosome 1B (position 65 cM) and chromosome 2A (position 102 cM) were containing 139 and 138 SNP, respectively. However, the largest chromosomal segment without remaining polymorphic and informative marker were on chromosome 4D with a gap of 59 cM (interval: 112 cM – 171 cM) and 46 cM (interval: 19 cM – 65 cM).

4.2.1. Linkage Disequilibrium (LD) Analysis of the Z86 population

The decay of linkage disequilibrium (LD) describes a hypothetical measure of an average genome-wide LD block sizes. Here, the extent of LD for every single chromosome of the three sub-genomes of wheat were calculated separately. Figure 31 shows the LOESS fitted curves of pairwise LD (R^2) value against the genetic distance [cM].

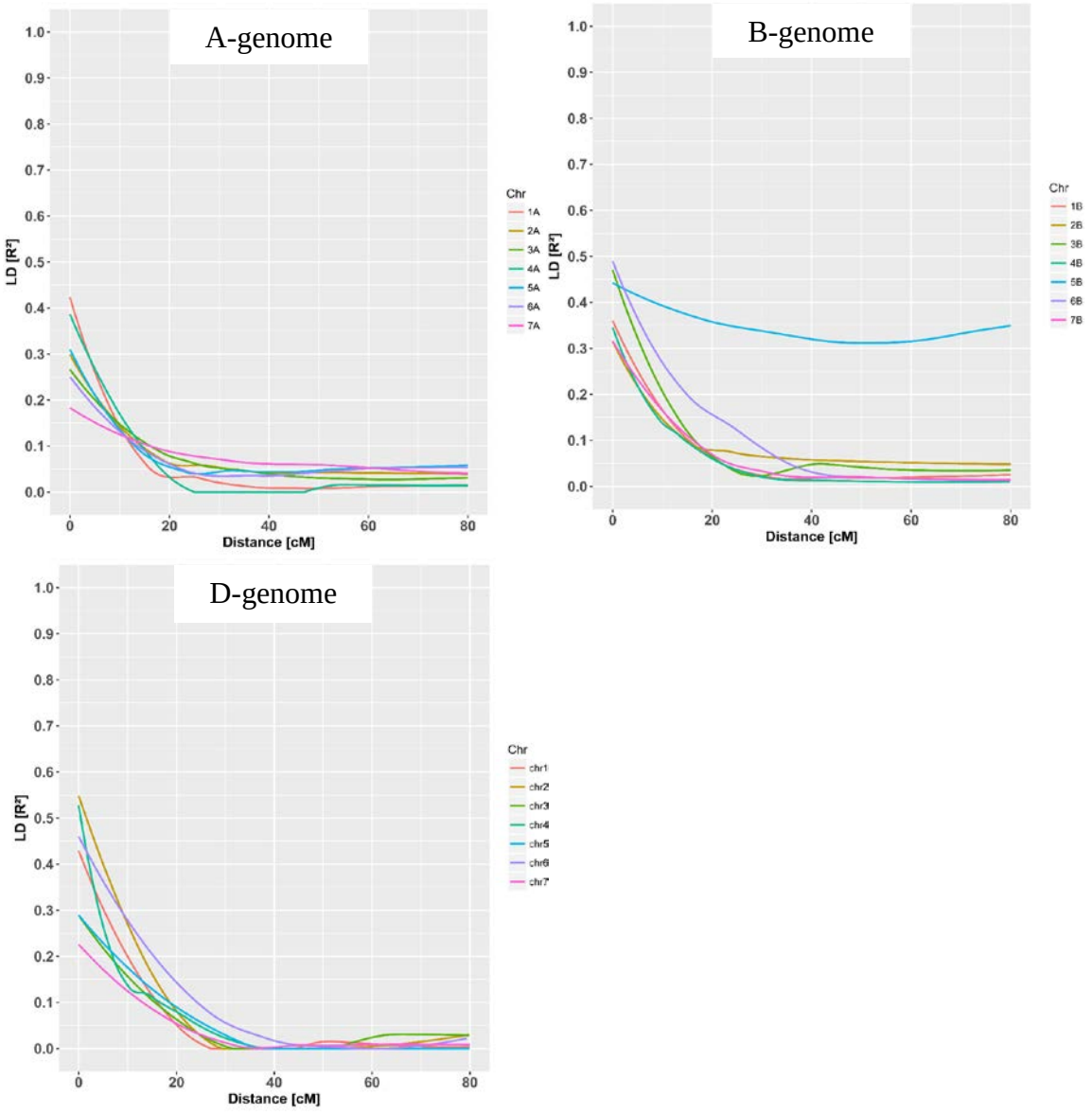

Figure 31. LD decay plots for individual chromosomes of the three sub-genomes of the Z86 population

Note: The LD decay plots show LD value for the distance of up to 80 cM, as for a distance above 50 cM linkage between two markers is generally not assumed. Additionally, it is leading to unreliable estimations of LD. Also, negative LD values were set to zero.

The intersection of the LOESS curve and the threshold line of R^2=0.1 was considered as estimate of LD decay for each chromosome (Breseghello and Sorrells 2006). Table 26 is showing LD decay estimates of all chromosomes, as well as the calculated sub-genome and genome-wide LD decay.

Table 26. Overview of LD decay estimates [cM] at threshold auf R^2=0.1

Chromosome	A-genome	B-genome	D-genome
1	14.1	13.8	16.1
2	11.9	12.9	11.6
3	14.5	14.9	10.4
4	10.1	10.6	11.8
5	11	-	18.1
6	13.4	22.2	14.2
7	11.4	11.3	12
Sub-genome-wide LD	12.3	14.3	13.5
Genome-wide LD		**13.4**	

Note: Errors in the genetic map of markers located on some chromosomes are assumed to be the reason for the disturbance in intra-chromosomal linkage as visible with increasing R^2 values with the higher genetic distance between markers. For the calculation of genome-wide and sub-genome-wide LD the values of chromosome 5B were not considered as the LD decay curve of chromosome 5B didn't touch the threshold of R^2=0.1.

Different than expected the LD decay curve of chromosome 5B didn't follow the expected shape as for the most chromosomes after reaching the minima of LD by increasing the distance between markers LD was increasing too. The LD decay of chromosome 5B reaches the R^2 minima of 0.32 at approximately 50 cM. Beyond the distance of 50 cM, the LD is increasing again.

Frequently LD heatmaps are produced in order to visualize genetic linkage groups of individual chromosomes. Here, only the LD heatmaps of homeologous of chromosome 5 of the Z86 population are shown. The LD heatmaps of all chromosomes of the Z86 population will be presented in Appendix 2. The LD heatmap of chromosome 5B is showing an unexpected manner when compared with the other chromosomes of the Z86 population. Obviously, there is high linkage between almost all markers, indifferent from their distance to each other. This is surprising as by increasing the distance between two markers the linkage between them is reduced because the probability for recombination (crossing over) increases.

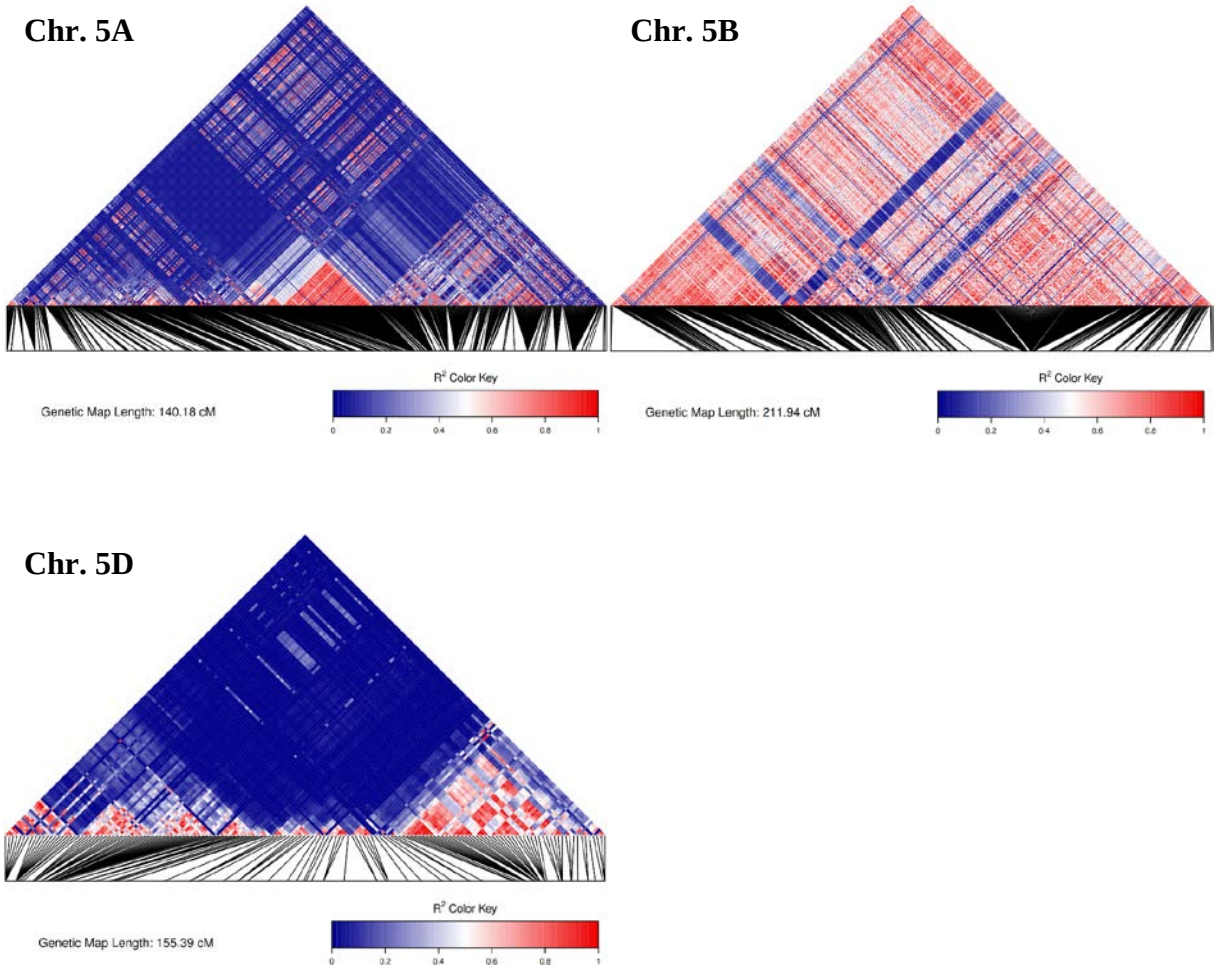

Figure 32. LD Heatmaps of chromosome 5A, 5B and 5B; The "R² key color" is indicating the R² correlation between SNP markers; where 0 stands for no correlation (blue color) and 1 stands to 100% correlation (red color)

4.3. Identification of loci for multiple traits under salt stress and control conditions

This chapter summarizes the results of the QTL analysis conducted for all analyzed trait across all tested environments and development stages (germination, seedling and maturity stage).

The applied multi-locus approach used in the hierarchical QTL model was able to reduce the number of false-positive putative QTL and hence to endorse the power of detected true QTL. However, as shown in Figure 32, this additional procedure reduced the number of detected QTL and highlighting more significant QTL.

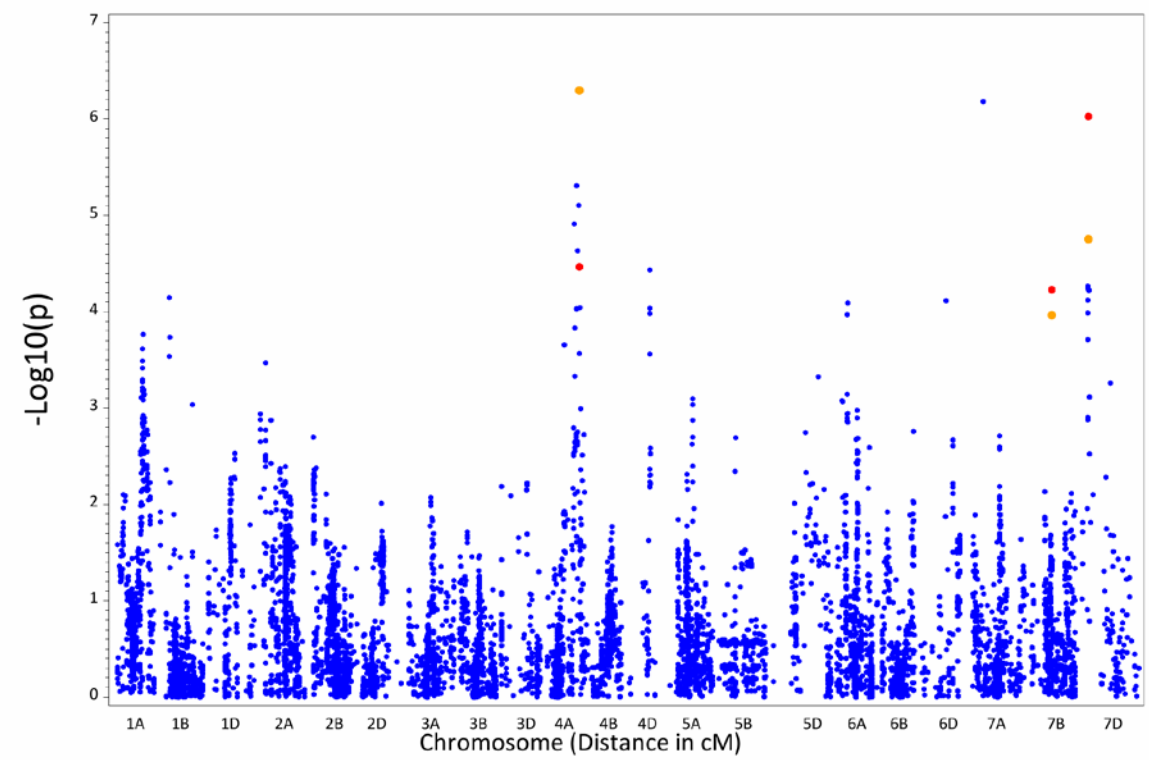

Figure 33. Manhattan plot for germination scoring with 150 mM Na_2SO_4 showing comparison between putative QTL calculated with composite mapping (orange) and multi-locus (red).

The calculated QTL were further employed for detection of associations with informative genes and proteins involved in response to abiotic stress, particularly salinity stress and (important) cell regulatory mechanisms. The *in-silico* analysis was performed by utilization of BLAST tools of NCBI (https://blast.ncbi.nlm.nih.gov) and genome sequence assembly version TGACv1 of *Triticum aestivum* L., which is publicly accessible on EnsemblPlants (http://plants.ensembl.org).

Overall, 116 QTL main effects (including M_1*M_2 interaction) and 165 QTL for marker were detected by treatment interaction (including M_1*M_2*treatment interaction). The full list of all detected QTL will be presented in Table 30 to Table 34 (Appendix 3). A summary of some identified important QTL related to salinity stress is outlined in Table 27.

Table 27. Summary of identified QTL with major effect on salinity tolerance at different growth stages

QTL	Marker	Chr	cM	Annotation	Purpose	Trait	Explained genetic variance [%]	Reference
QTL_2AS_1	BobWhite_c18852_91	2AS	82.23	Concanavalin A-like lectin/glucanase domain containing protein	Involved transcription factor activity for shoot Na^+/K^+ under in salt stress	**NaCl:** RFW **Field (stress):** Sedimentation rate	Epistatic with 2nd QTL: 20.2-24.9	IPR013320
QTL_2AL_1	wsnp_Ra_c4850_8698731	2AL	109.97	Fatty acid desaturase-6 (Fad6)	Na^+/K^+ homeostasis	**NaCl:** RDW	Single QTL: 16.6	AT4G30950
QTL_2AL_2	BS00041707_51	2AL	105.53	FATTY ACID EXPORT 1 (FAX1)	Crucial for biomass production; Fatty acid (wax) transport to pollen cell wall etc.	**Field (stress):** TKW	Single QTL: 12.5	XP_020149029.1
QTL_2DL_1	wsnp_Ra_c22648_32132929	2DL	82.82	P-type ATPase	Ca^{2+} transmembrane domain; ROS scavenging	**Control:** SL, **Na_2SO_4:** K/Na ratio	Single QTL: 12.6-15.0	IPR001757
QTL_3AL_1	Tdurum_contig8674_1236	3AL	188.38	FERONIA; Malectin-like carbohydrate-binding domain	Interacts with RALF (Rapid alkalization factor) for female fertility, growth regulation and ABA signaling	**Field (stress):** Plant height	Epistatic with 2nd QTL: 22.8	IPR024788
QTL_4AS_1	BS00009492_51	4AS	59.99	Zinc finger, RING/FYVE/PHD-type	Regulating Na^+ and K^+ Homeostasis, Reactive Oxygen Species Scavenging and Osmotic Potential	**Na_2SO_4:** SL	Epistatic with 2nd QTL: 20.8	IPR013083
QTL_4BS_1	tplb0050o09_895	3DS	4.46	Aquaporin NIP4-1-like	Non-selective water channel protein; involved in Na^+ uptake	**Na_2SO_4:** SFW, SDW, PFW, PDW,	Single QTL: 11.1-16.3 Epistatic with 2nd QTL: 22.5-29.9	LOC109770355
QTL_5AS_1	BobWhite_c51109_415	5AS	35.38	Cobalamin-Independent Methionine Synthase	Associated with lignification of the cell wall under salt stress	**Na_2SO_4:** Germination	Single QTL: 15.7	cd03312
QTL_5AL_1	Excalibur_c41710_417	5AL	92.87	Myc-type, basic helix-loop-helix (bHLH) domain	Transcription factors in ABA-mediated gene expression under drought and salt stresses	**Na_2SO_4:** Germination	Epistatic with 2nd QTL: 22.3	IPR011598
QTL_5DS_1	BS00000020_51	5DS	102.91	Puroindoline b (PinB-D1)	Grain texture and flour quality	**Field (control):** Sedimentation value **Field (stress):** Fiber content	Single QTL: 7.9-27.7 Epistatic with 2nd QTL: 25.4	KC585018.1
QTL_6AL_1	TA004297_0876	6AL	81.64	S-adenosyl-L-methionine-dependent; methyl-transferase (SAM MTases)	Salt stress response; Glycine betaine regulation	**NaCl:** PFW	Single QTL: 7.6 Epistatic with 2nd QTL: 14.7	IPR029063
QTL_7AL_1	Excalibur_rep_c66918_307	7AL	202.68	Pyrophosphate-energized proton pump	Involved in K^+ transport	**Field (stress):** Protein content, starch content	Single QTL: 21.3 Epistatic with 2nd QTL: 26.9	IPR004131
QTL_7BS_1	Excalibur_rep_c116920_300	7BS	71.66	CLASP N terminal	Regulation and stabilization of cell division	**Control:** RL (0/9/16 DAS) **NaCl:** RL, **Na_2SO_4:** RL	Single QTL: 22.9-47.6 Epistatic with 2nd QTL: 38.1-50.8	Pfam12348
QTL_7BL_1	Tdurum_contig50984_553	7BL	72.74	Zinc finger, RING/FYVE/PHD-type	Regulating Na^+ and K^+ Homeostasis, Reactive Oxygen Species Scavenging and Osmotic Potential	**Field (stress):** Yield	Epistatic with 2nd QTL: 37.5	IPR013083
QTL_7BL_2	Kukri_rep_c101620_1848	7BL	171.10	Zinc finger, FYVE/PHD-type	Regulating Sodium and Potassium Homeostasis, Reactive Oxygen Species Scavenging and Osmotic Potential	**NaCl:** Germination	Single QTL: 10.2	IPR013083
QTL_7DS.1	BobWhite_c8454_782	7DS	29.97	Glutathione S-transferase, N-terminal	Detoxification; scavenging of Reactive Oxygen Species (ROS) regulation of osmotic potential; regulator of cell elongation and plant development	**Control:** Germ, SFW, SDW, RFW, RL, PFW, PDW **NaCl:** SFW, SDW, RFW, RL, PDW **Na_2SO_4:** Germ; K/Na-ratio in 3rd leaves	Single QTL: 7.0-37.1 Epistatic with 2nd QTL: 22.8-53.9	At2g29470

Note: The full list of all detected QTL will be presented in Table 30 to Table 34 (Appendix 3).

The Venn diagram (Figure 33) visualizes the distribution and overlapping of all calculated QTL, including marker main effect, marker by treatment effects and epistatic effects, across all across all environments. Surprisingly, only a small number of common QTL were identified.

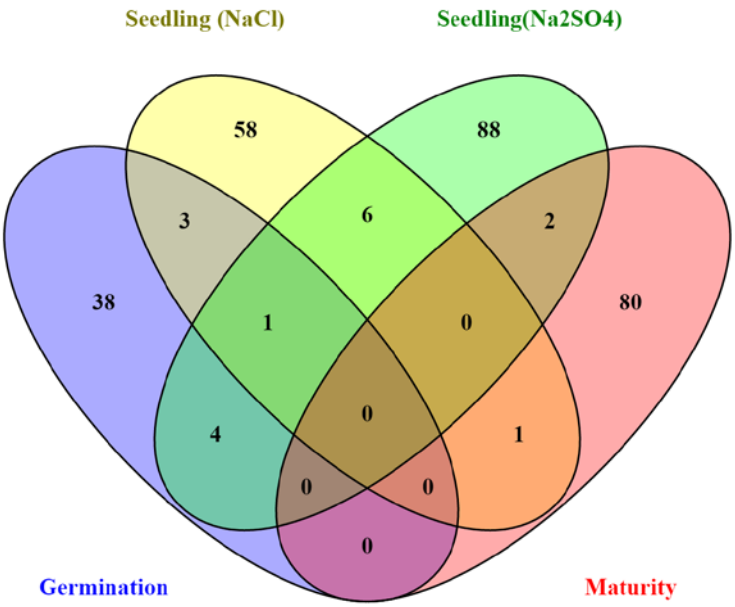

Figure 34. Distribution and overlapping of the marker-trait associations calculated for all traits at germination stage, seedling stage (NaCl, Na_2SO_4) and maturity stage

As shown in Table 28 the marker BobWhite_c8454_782 localized on chromosome 7DS at 29.97cM was the only significant marker that was detected across three developmental stages and environments. There was no marker detected being significant in all tested environments.

Table 28. List of selected QTL detected across the tested environments

Common environments	QTL	Marker	Chr.	cM
Germination stage, seedling stage (NaCl and Na_2SO_4)	QTL_7DS.1	BobWhite_c8454_782	7DS	29.97
Seedling stage (NaCl and Na_2SO_4)	QTL_2DL_1	wsnp_Ra_c22648_32132929	2DL	82.82
	QTL_3BS_1	RAC875_c81076_317	3BS	62.31
	QTL_5AL_2	IAAV1179	5AL	69.34
	QTL_5AL_3	Tdurum_contig17500_876	5AL	70.30
	QTL_7BS_1	Excalibur_rep_c116920_300	7BS	71.66
	QTL_7DS.2	RAC875_c25695_316	7DS	32.16
Germination stage and seedling stage (Na_2SO_4)	QTL_5DL_1	Kukri_c28182_129	5DL	196.08
	QTL_5DL_2	GENE_3006_113	5DL	203.88
	QTL_6BS_1	RAC875_c37871_249	6BS	0.38
	QTL_7DS.3	BS00067140_51	7DS	26.92
Seedling stage (Na_2SO_4) and maturity stage	QTL_4AS_1	Tdurum_contig48049_705	4AS	41.02
	QTL_5DL_3	Kukri_c96249_58	5DL	130.04
Seedling stage (NaCl) and maturity stage	QTL_2AS_1	BobWhite_c18852_91	2AS	82.23

Note: The full list of all detected QTL will be presented in Table 30 to Table 34 (Appendix 3).

For a better overview, the annotations of the detected genes were classified according to five major classes: “Transport and Trafficking”, “Cellular function”, “Repair and Defense”, “Hormone reaction and Signaling” and “Osmotic regulation”. QTL with no detected annotation were grouped in class Unknown.

Figure 34 summarizes the classification of the biological functions of the associated genomic regions for the QTL main effects and QTL by treatment interaction effects. Notable under salt stress condition, the number of detected QTL for the categories “Osmotic regulations”, “Hormone reaction and Signaling” and “Repair and Defense” was more than 2-3 times higher than under control condition. In total, the three GO categories comprise 82% of the detected QTL under stress condition, whereas under control condition merely 36% of all QTL were annotated into these categories. The gene ontology (GO) table (Table 35 in Appendix 4) gives an overview of the calculated QTL and the biological function of the associated genomic regions.

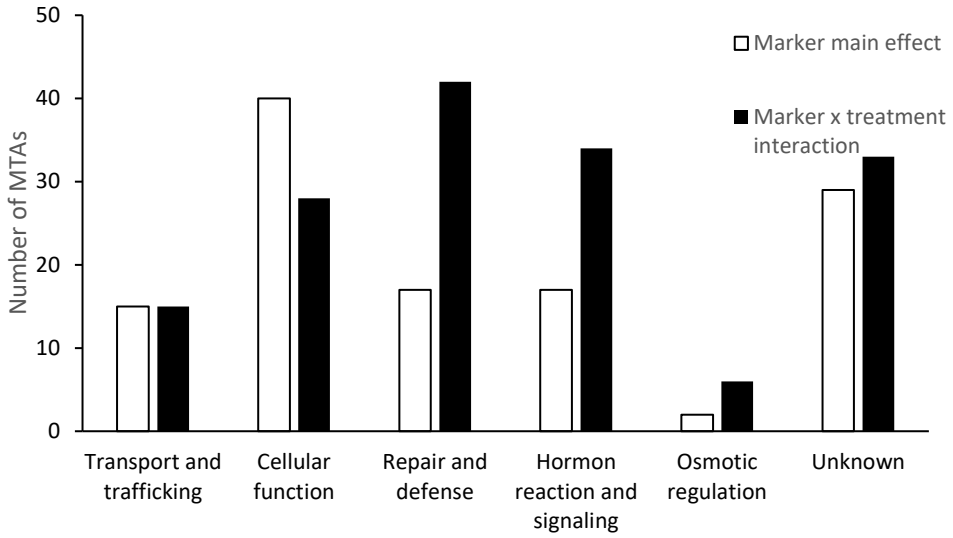

Figure 35. Distribution of marker by trait associations (MTAs) with main effect and treatment interaction according to the ontology classes

The circos plot (Figure 35) gives an overview on the detected QTL and also the digenic epistatic interactions detected at germination stage for control and different salt stress regimes. For all salt stress levels, 26 QTL regions and 11 epistatic interactions were detected. Figure 35 highlights the hotspots for epistatic interactions on chromosome 7A, 7B, 5D and 7D. Furthermore, the SNP marker BobWhite_c8454_782, denoted as QTL_7DS.1, localized on chromosome 7D with 29.97 cM is explaining the highest genetic variation (20.8%) for seed vigor at germination under control condition. Obviously, the chromosomal region between the markers BS00067140_51 (26.92 cM) and BobWhite_c8454_782 (29.97 cM) on chromosome 7D is a hotspot with substantial genetic effect on germination under control and salt stress conditions. Regarding the highest NaCl concentration with 250 mM NaCl the two QTL on chromosome 4A (147.1 cM) and 5A (36.9 cM) were responsible for 10.4% and 13.8% genetic variation, respectively. Whereas for the highest Na_2SO_4 concentration the QTL on chromosome 4A (132.9 cM) and 7A (74.2 cM) explained 13.2% and 13.7% genetic variation, respectively.

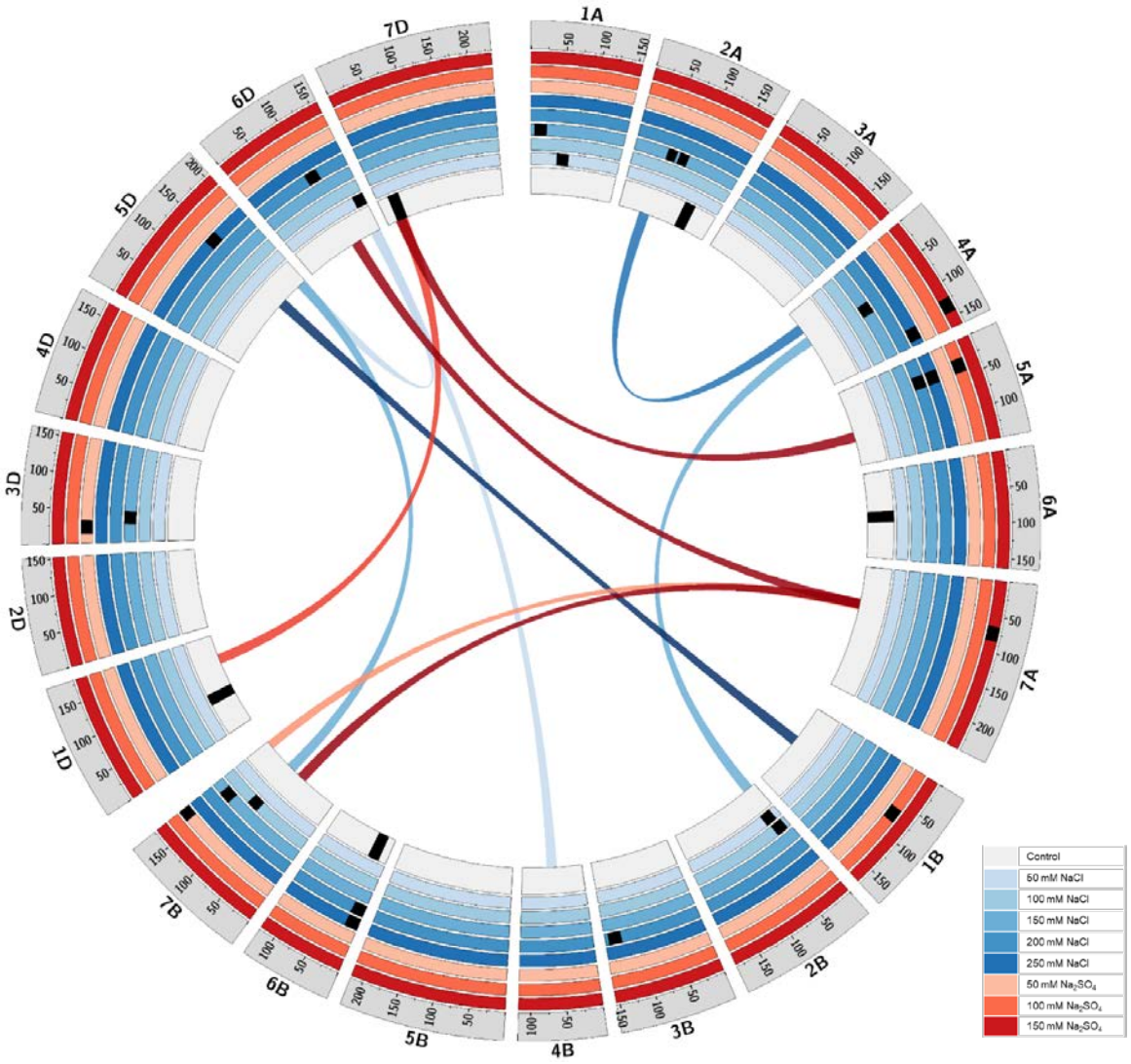

Figure 36. QTL and digenic epistatic interaction detected for control and different salt stress regimes at germination stage.

Note: The rings represent the different tested salt stress levels. First inner ring control, bluish-colored rings represent increasing NaCl concentration (50-250 mM), reddish colored rings represent increasing Na_2SO_4 concentration (50-150 mM). The inner circle links represent M_1xM_2xT epistatic interaction. The colors of the links represent the salt concentration according to the color code. The complete QTL table for detected QTL at germination stage will be presented in Table 30 in Appendix 3.

In respect to the different NaCl concentrations at germination stage 10 QTL with marker main effect, seven marker by treatment interaction effect were detected. In addition, five marker by marker interactions were detected, including SNP marker BS00094095_51 on chromosome 5A position 36.87 cM with epistatic effects with 100 mM and 200 mM NaCl treatments. Eleven epistatic and treatment interactions were found for the NaCl treatments. For both salt types, two hotspots for epistatic by treatment interaction were found on chromosome 7A (36.8 cM and

76.3 cM) and 7B (55-171 cM) affecting germination. Two major QTL BS00094095_51 on chromosome 5A (36.87 cM) and Excalibur_rep_c68955_422 on chromosome 7A (74.19 cM) were highly significant with LOD values higher than 6.3. Both QTL were associated with germination scores at germination tests with 200 mM NaCl and 150 mM Na_2SO_4. For both salt types, mainly three hotspots for epistatic by treatment interaction were found on chromosome 7A (36 cM and 76 cM), 7B (55-171 cM) and 7D (26-30 cM).

Figure 36 is illustrating the locations of the detected QTL for main effects and M*T interaction as well as the digenic epistatic treatment interactions (M_1*M_2*T) for six biomass related traits measured at seedling stage. A large number of the identified QTL are located on chromosome 2A, 6A, 3B, 3D and 7D. Additional investigation of epistatic digenic interaction revealed epistatic interactions on several chromosomes. Noteworthy that multiple loci on chromosome 2A are showing epistatic interactions with loci on other chromosomes. Whereas only a single locus on chromosome 7DS (QTL_7DS.1) is showing epistatic interactions with loci on other chromosomes. Obviously, this locus harbors a gene having pleiotropic effects on multiple quantitative traits.

For the application of QTL analysis in a backcross population, it is a prerequisite that the parents of the segregating population differ genetically for the trait of interest (Tanksley and Nelson 1996). Only with respect to root length and plant height, the synthetic parents Syn86 was outperforming the modern cultivar, whereas both genotypes had extremely contrasting phenotypes for root length under control condition. Accordingly, two major QTL were identified, correlating with root length under control condition. QTL_4BS_1 (SNP marker: TA003708_0300) was located on chromosome 4BS at 61.84 cM explain 43.4% of the genetic variance. QTL_7BS_1 (SNP marker: Excalibur_rep_c116920_300) was located on chromosome 7BS at 71.66 cM, explaining 47.6% of the genetic variance. Progenies of the Z86 population possessing the allelic variation of Syn86 on QTL_4BS_1 and QTL_7BS_1 had in average 16.3% and 13.1% longer roots than genotypes with allelic variation of Zentos. *In-silico* analysis revealed linkage of this QTL_7BS_1 with CLASP N terminal (pfam12348) which has is in *Arabidopsis* a key role in regulation and stabilization of cell division. The second QTL related to root length, QTL_4BS_1 is associated in Arabidopsis with the COPRA protein (XP_020199365.1) which is involved in determining the orientation of cell expansion.

The applied QTL model assigned in the SAS macro was enabling the detection of epistatic by treatment interaction effects (M_1*M_2*T), leading to detection of another pleiotropic QTL

(QTL_3DS_1; SNP marker tplb0050o09_895) on chromosome 3DS at 4.46 cM. Interestingly, this maker was detected for M_1*M_2*T interaction with multiple QTL located on chromosome 2B (109.53 cM), chromosome 2D (49.59cM), and chromosome 3A (173.15 cM) having substantial effect on biomass production (SFW, SDW, PFW and PDW). Further *in-silico* analysis revealed that this QTL_3DS_1 was linked to the gene coding for the aquaporin channel protein (IPR034294). Aquaporins are plasma membrane intrinsic non-selective water exchange proteins involved in uptake of Na^+ by roots.

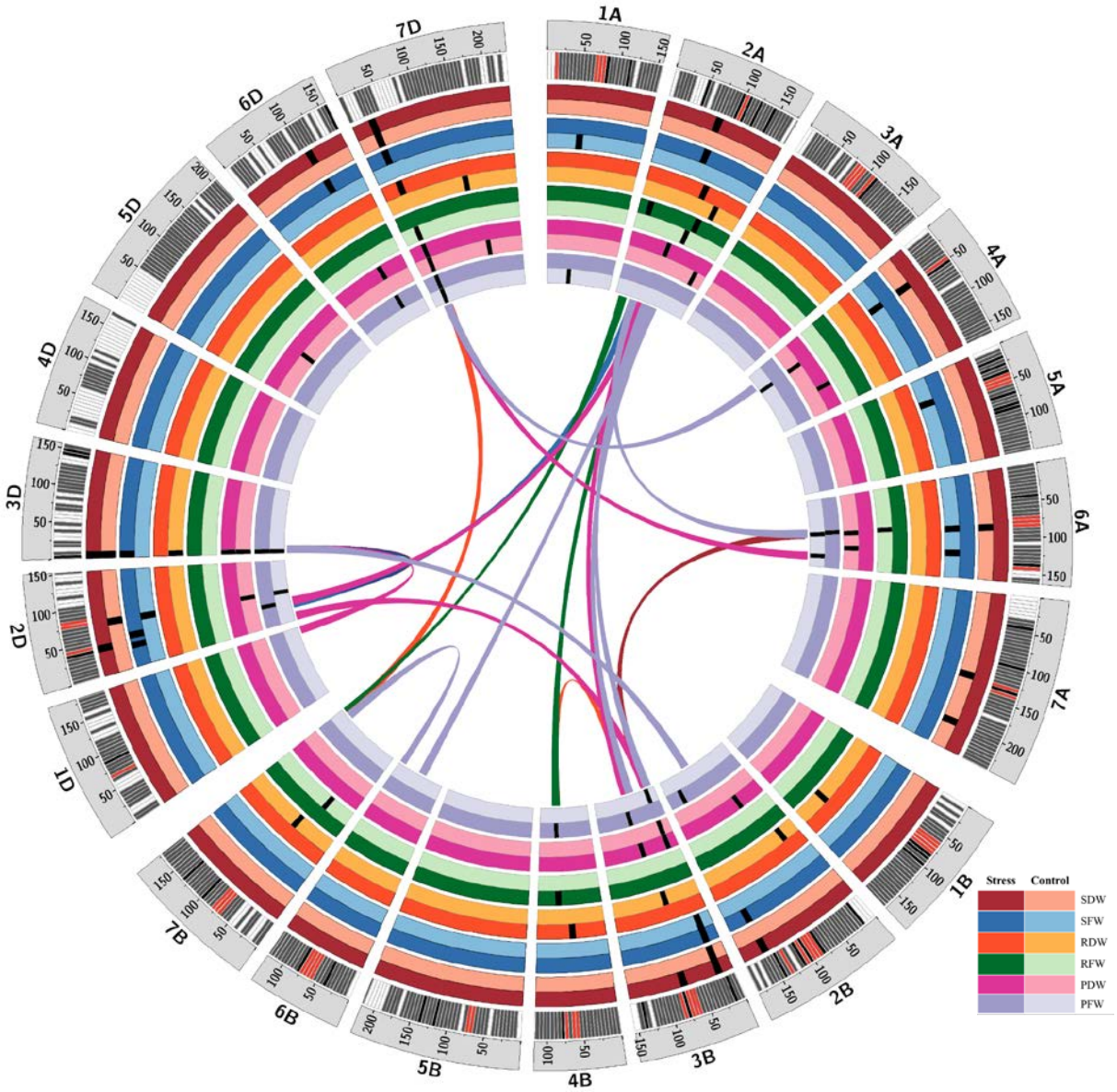

Figure 37. QTL and digenic epistatic interaction detected for control and different salt stress regimes at seedling stage

Note: The colors indicate different traits according the legend (light colors stand for QTL with main effects, dark colors stand for M*T effects under stress conditions). Internal links indicate digenic epistatic treatment interaction (M_1*M_2*T) of the specific traits according the color code shown in the legend. The first outer ring is showing the marker density. The complete QTL table for detected QTL at seedling stage will be presented in Table 30 to Table 34 (Appendix 2).

4.4. Sequence and expression analysis of glutathione s-transferase under salinity stress in wheat

Several highly interesting QTL were detected by the QTL analysis conducted for the three major developmental stages of winter wheat. One of the major QTL with pleiotropic effects on multiple traits including shoot biomass production under salinity stress and control condition was QTL_7DS.1 closely linked to the SNP marker BobWhite_c8454_782 localized on chromosome 7DS at 29.97 cM. The 101 bp of the SNP marker sequence was blasted against the genome sequence assembly version TGACv1 of *Triticum aestivum* L., which is publicly accessible on EnsemblPlants (http://plants.ensembl.org). Hundred percent marker sequence similarity with an expected value (E)-value of 4.1E-49 was detected between 3,573 to 3,673 bp of TGACv1_scaffold_623736_7DS, which is localized on short am of 7DS chromosome of *Triticum aestivum*. Further, *in-silico* investigations revealed the linkage of this marker with the gene glutathione S-transferase *tau* (τ) class, called as *TaGSTu3* (KEGG Enzyme Nomenclature: EC.2.5.1.18), which is known for its involvement in cellular detoxification during biotic and abiotic stress response (Moons 2003, Liu et al. 2015). In general, *TaGSTu3* and *TaGSTu6* genes are tandemly arrayed along the wheat genome and closely linked (Liu et al. 2015). Sequence analysis confirmed the presence of *TaGSTu6* approximately 15K bp downstream of *TaGSTu3*.

Figure 37 shows a schematic overview of *TaGSTu3* and *TaGSTu6* gene structures, including 3 and 5'UTR, exons and introns. The 15K bp distance between both genes was detected by *in-silico* analysis of the genome sequence assembly TGACv1 of *Triticum aestivum* L.

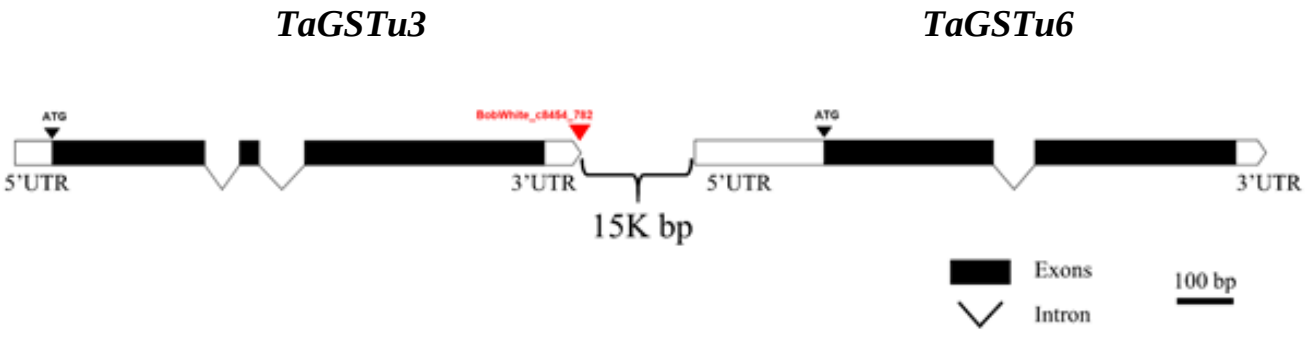

Figure 38. Genetic structure of *TaGSTu3* and *TaGSTu6* on chromosome 7DS; red triangle the corresponding SNP marker BobWhite_c8454_782, black triangles position of start codon ATG; curly bracket indicates the 15K bp gap between *TaGSTu3* and *TaGSTu6*

Both genes, *TaGSTu3* and *TaGSTu6*, were analyzed by Sanger sequencing in order to detect sequence differences between Zentos and Syn86 that might affect protein functions. Since there

was no allelic variation between the analyzed genotypes detectable, focus was laid on gene expression analysis on *TaGSTu3*.

Semi-quantitative PCR (sq-PCR) with RNA samples collected at 10, 16 and 30 days after stress application (DAS) were conducted to examine gene expression kinetics of *TaGSTu3* in Zentos and Syn86. The gel electrophoresis in Figure 38 revealed that the sq-PCR was showing higher expression levels *TaGSTu3* in Zentos under control and stress conditions, relative to Syn86. Except time-point 0, the relative expression of *TaGSTu3* in Zentos was higher than in Syn86. Moreover, the sq-PCR was indicating a slight reduction of expression of *TaGSTu3* in Syn86 under stress condition over time.

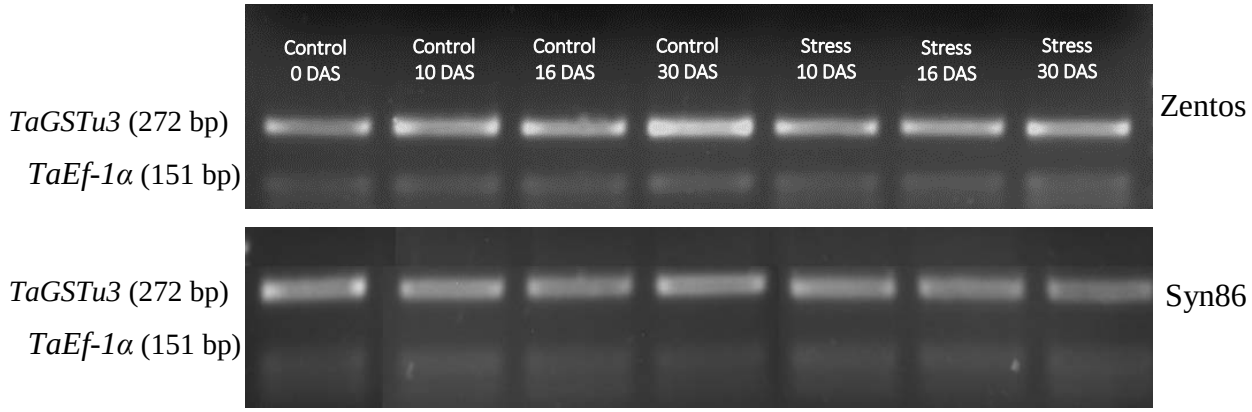

Figure 39. Gel electrophoresis of sq-PCR of *TaGSTu3* gene of Zentos and Syn86 under controlled and salt stress conditions relative to the expression of the reference gene *TaEf-1α* at 0, 10, 16 and 30 days after stress application (DAS)

Subsequently, quantitative Real-Time PCR (qRT-PCR) was conducted to quantify the kinetics of *TaGSTu3* expression in Zentos and Syn86 under control and salt stress conditions. Figure 39 is showing the relative expression of *TaGSTu3* at 10, 16 and 30 DAS for Zentos and Syn86 calculated according to the algorithm described by Livak and Schmittgen (2001).

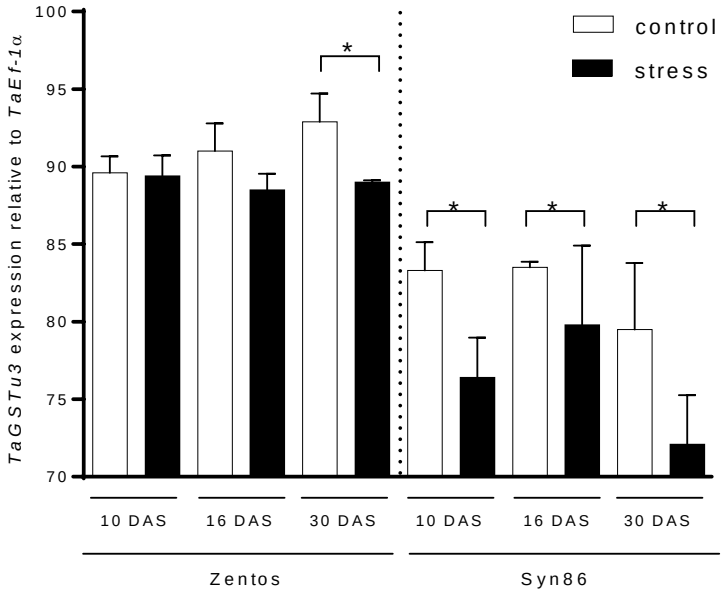

Figure 40. Expression of *TaGSTu3* in Zentos and Syn86 relative to the expression of the reference gene *TaEf-1α* at 10, 16 and 30 DAS under control and salt stress conditions. Significance levels p: * $p \leq 0.05$

As shown in Figure 39 at all three time points the relative expression of *TaGSTu3* in Syn86 was significantly lower under salt stress than under control condition ($p<0.05$). Due to the experimental error, a clear trend during the experimental duration for expression of *TaGSTu3* in Syn86 under salt stress condition was not detectable. Obviously, the expression of *TaGSTu3* in Zentos was higher under both conditions when compared to Syn86. In contrast to Syn86, the expression of *TaGSTu3* in Zentos under stress condition was stable. The *TaGSTu3* expression under control condition was slightly increasing during the experimental period. This leads to a significant difference ($p<0.05$) in the expression of *TaGSTu3* between control and salt stress at 30 DAS.

However, to further understand the reason for the differential expression of *TaGSTu3* in Zentos and Syn86, the promoter regions, ~1.100 bp upstream of the start codon ATG, of both genotypes were analyzed using the multiTF program of MULAN online package (Ovcharenko et al. 2005). This analysis allows effective investigation of *cis*-regulatory elements or Transcription Factor Binding Sites (TFBS). MULAN analysis of the promoter sequence of Zentos and Syn86 revealed differences in number and sequence of specific TFBS which are known for their relationship with salt stress response and involvement of phytohormone activity. The summary of the detected TFBS related to salt stress response is presented in Figure 40.

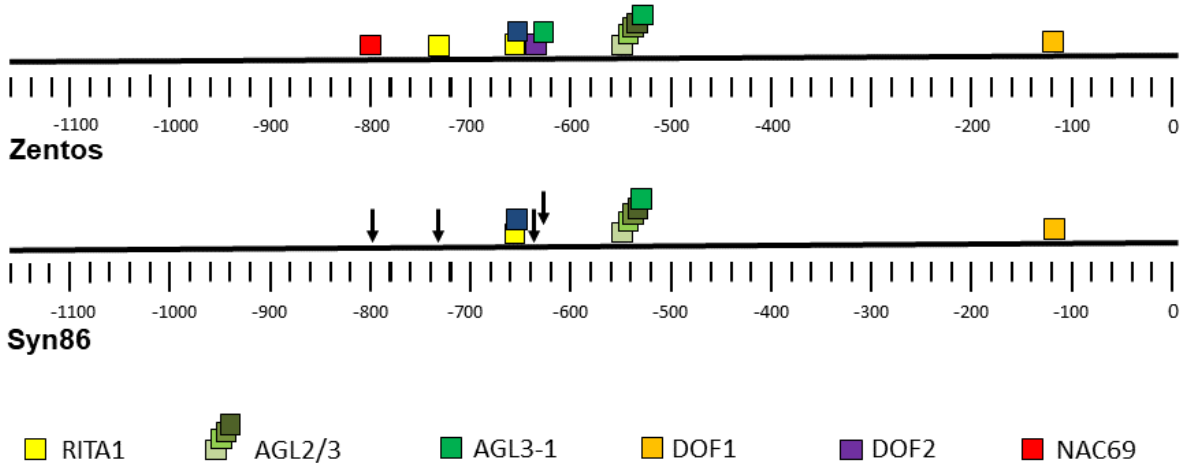

Figure 41. Depiction of transcription binding sites (TFBS) detected by MULAN analysis in the promoter region of Zentos and Syn86; colors indicate specific TFBS; arrows indicate missing TFBS in the promoter region of Syn86

Screening the promoter region of *TaGSTu3* revealed DNA binding motifs in both genotypes which are activating higher expression of genes related to salt stress response. Two of the detected TFBS, namely NAC69, DOF3 were localized in the promoter region of the genotype Zentos, while both motifs were not present in Syn86. Additionally, the promoter region of Zentos had two copies of the motifs AGL3-1 and RITA1 whereas the promoter region of Syn86 had single copies of both TFBS.

Analysis for digenic epistatic interaction (M1*M2) and digenic epistatic treatment interaction (M1*M2*T) revealed epistatic interactions of QTL_7DS.1 with five other QTL. Among them QTL_6AL_2 with the SNP marker RFL_Contig3175_1271 on chromosome 6A at 136.85 cM was explaining 22.8% of the genetic variance of the genotype by treatment interaction effect of the analyzed trait SDW. This QTL was associated with NADH dehydrogenase [ubiquinone] 1 alpha subcomplex subunit 9 (LOC109748854) which is also involved in stress response, ROS detoxification and in electron transport chain. Interestingly, a gene coding for the NAC domain containing protein was localized at a distance of 3.99 cM. This gene was also detected by association with another QTL (QTL_6AL_3; Kukri_rep_c103186_134 on chromosome 6A at 140.87 cM). QTL_6AL_3 was associated with shoot length at 9DAS under 100 mM Na_2SO_4.

5. DISCUSSION

Above all abiotic stress factors, drought and salinity stress have the highest impact on global wheat productivity and pose a major challenge to food security (Chandna et al. 2013, Tardieu et al. 2017). Introgression of exotic alleles, which enhance salinity tolerance in modern elite cultivars is regarded as feasible approach in order to develop adapted high yielding and high-quality cultivars that are tolerant to salinity. Synthetic hexaploid wheat (SHW), descending from hybridization between diploid and tetraploid progenitors of wheat are regarded as a genetic resource of exotic alleles absent in modern cultivars (Mujeeb-Kazi et al. 1996, Colmer et al. 2006).

Previously the synthetic backcrossed wheat population Z86, comprising 151 progenies descending from the synthetic hexaploid wheat Syn86 and the German elite winter wheat cultivar Zentos, was proposed as an ideal population for quantitative trait loci (QTLs) approach enabling the localization of exotic alleles by enhancing baking quality (Kunert et al. 2007) and tolerance towards biotic stress (Naz et al. 2008).

The main aim of the current study was to detect genetic regions in the Z86 population which were associated with salinity tolerance at germination, seedling and at maturity stage under field condition with natural salinization. The assessment of the lines of the Z86 population at different stages and salt treatment levels enables the determination of genomic regions associated with salinity tolerance at specific stress condition at a given developmental stage. The goal was to detect morphological, physiological and genetic differences within the tested genotypes to detect genomic regions which were associated with the respective traits. The following discussion will be divided into five subchapters:

1. Phenotypic characterization of the Z86 population and the parents Zentos and Syn86
2. Genetic characterization of the Z86 population
3. Detection of QTL for the measured phenotypic traits
4. Expression of glutathione s-transferase under salt stress in wheat
5. Non-invasive assessment of leaf water status using a dual-mode microwave resonator (Appendix 5)

5.1. Phenotypic characterization of the Z86 population and the parents Zentos and Syn86

Survival of plants in saline conditions requires multiple adaptations at different developmental stages in respect to adverse effects of salt (Shannon 1997, Munns and Tester 2008). An increasing number of studies focus on specific plant developmental stages for investigation of salinity stress and adaptation mechanisms on multiple crops, such as tomato (Foolad 1999), pepper (Chartzoulakis and Klapaki 2000), spinach (Wilson et al. 2000) and rice (Rad et al. 2011). In the frame of this study, the focus was on the entire life cycle of wheat plants, from germination of seeds to the harvest of produced seeds. For this purpose, the AB-lines of the synthetic advanced backcross winter wheat population Z86 were characterized by their response to different salt treatments at germination, seedling and maturity stage. Whereas the tests at germination and seedling stage were conducted under climate chamber and greenhouse conditions, ultimately the phenotypic characterization of the Z86 at maturity stage was carried out under field conditions with natural salinization in Uzbekistan.

5.1.1. Germination stage

The importance of the germination stage in plants withstanding salinity stress is controversially discussed (Kent and Läuchli 1985, Kaya et al. 2003, Munns and James 2003, Singh et al. 2012). However, the use of germination tests to determine the degree of variation in responses to salt stress levels of a large collection of genotypes helps to identify materials carrying potentially interesting traits for further exploitation in a reasonable timeframe (Mano and Takeda 1997, Chinnusamy et al. 2005, Munns et al. 2006, Charu et al. 2015, Aflaki et al. 2017). As salt tolerance at the germination stage is described as germination rate or germination score value (Mano et al. 1996), the Z86 population was exposed to different concentrations of NaCl and Na_2SO_4 at germination stage. Both, sodium chloride and sodium sulfate are regarded as the most important and widely studied salt types as they predominantly affect soil salinity in many parts of the world (Flowers et al. 1977, Egamberdiyeva et al. 2007, Pessarakli 2011).

With respect to salinity tolerance during seed germination, the response of the genotypes of the Z86 population and their parents Zentos and Syn86 was diverse. In the frame of this research work germination tests with different concentrations of NaCl and Na_2SO_4 confirmed that the deleterious effect of salt on germination of wheat seeds increased by increasing the

concentration of the salt. Furthermore, the effect of the equal concentration of Na_2SO_4 was approximately two-fold higher than the same concentration of NaCl. This was not surprising since at equimolar salt concentration Na_2SO_4 supplied twice the concentration of Na^+ than NaCl. Additionally, the findings in this study are in concordance with several presented observations (Lauter and Munns 1986, Almansouri et al. 2001, Munns 2011). Looking at the parents of the Z86 population, Zentos and Syn86, surprisingly, at germination stage the elite cultivar Zentos was performing better under the tested salt concentrations than the synthetic genotype Syn86 (Figure 7), while many publications endorse synthetic hexaploid wheat as more tolerant than modern elite cultivars, making them ideal donors of exotic alleles contributing to tolerance towards biotic and abiotic stresses like salinity tolerance (Gorham et al. 1990, Pritchard et al. 2002, Dreisigacker et al. 2008, Talbot et al. 2008). As well at highest concentration of sodium chloride and sodium sulfate as the aggregated germination scoring values across all tested salt concentrations, Syn86 is showing the weakest performance. Although the performance of Zentos was better than of Syn86, still the majority of its progenies surpassed their parents, indicating the complex genetic nature of salinity tolerance (Figure 9).

The “Mean vs. Stability” view of the genotype and genotype by environment interaction (GGE) biplot analysis is frequently used for interpretation of multi-environment data structure by scientists and breeders as it is visualizing the relative performance and the variability of performance stability of the tested genotypes at different environments (Yan et al. 2000). With respect to high grain yield and yield stability under salinity stress Sharma et al. (2012) were utilizing GGE analysis to identify superior wheat genotypes by integration of multi-environmental field data from different years. The interpretation of the “Mean vs. Stability” biplot analysis suggests that entry number 16 is performing better than other genotypes with respect to high and stable germination scores across all tested salt treatments. In summary, the performance of Zentos was better and more stable than Syn86 which was can be regarded as most susceptible among the tested genotypes at germination.

5.1.2. Seedling stage

Hydroponic systems are recognized as ideal testing methods for investigating the basic mechanisms plants as they give a high degree of control and reproducibility (Genc et al. 2007, Shavrukov et al. 2012). NaCl and Na_2SO_4 concentrations of 100 mM are prevalently used in hydroponic experiments with wheat (Munns et al. 2006). In the frame of this study, hydroponic experiments with 100 mM NaCl or Na_2SO_4 were used for assessment of salinity stress on the advanced backcross winter wheat population Z86 and their parents Zentos and Syn86. Several morphological parameters including the production of root and shoot biomass were phenotyped as these traits are widely used for phenotyping plants at seedling stage exposed to abiotic stress like drought and salinity stress (Gregorio et al. 1997, Munns and James 2003, Rajendran et al. 2009). Additionally, the aerated hydroponic system designed in this study was enabling quick measurement of root length with little disturbance of the plants.

The adverse effect of 100 mM Na_2SO_4 in comparison to 100 mM NaCl on SDW and SL was dramatically higher. Surprisingly, Na_2SO_4 had marginal negative effects on the mean RDW of the Z86 population (-4.8% relative to control condition) and Zentos (-3.6%) but strongly reduced RDW of Syn86. Furthermore, RL of all genotypes highly decreased at 100 mM Na_2SO_4. Therefore, it is reasonable to conclude that wheat plants exposed to 100 mM Na_2SO_4 concentration at seedling stage tend to compensate the reduction of RL by producing bushy and shorter roots to maintain their root biomass. Obviously, production of root biomass is highly depending on the salt stress concentration and the susceptibility of a specific genotype. Similar observations were described for *Atriplex halimus* subsp. *Schweinfurthii* Nedjimi and Daoud (2006) where the authors describe the halophytic behavior of *Atriplex halimus* subsp. *Schweinfurthii* under different concentrations of Na_2SO_4. The root biomass of *Atriplex halimus* exposed to moderate sodium sulfate concentrations of 50 mM was increasing, where it was reduced exposed to higher concentrations of Na_2SO_4. Noteworthy, under the two salt types NaCl and Na_2SO_4, RDW and RL of Zentos and Syn86 behaved contrastingly. For all genotypes, including the parents, the adverse effect of Na_2SO_4 on SDW was distinctly higher than at the same concentration of NaCl. This is in line with previous studies (Matar et al. 1975, Inal 2002).

The salinity tolerance index (STI), applied for the parameters measured at the seedling stage, showing higher tolerance of Zentos than Syn86. Only a few genotypes, among them genotype 67, 95, 99, 117, surpassed the production of shoot dry weight (SDW) of the elite cultivar under 100 mM NaCl and Na_2SO_4, respectively. These genotypes showed high stability of SDW under

salinity stress at seedling stage. On the opposite side, genotype 57 and 84 was also showing stable but low STI values for SDW.

It is widely accepted that discrimination of Na^+ and preferential uptake of K^+ are important mechanisms of plants to cope with salinity (Greenway and Munns 1980, Flowers and Yeo 1995, Munns et al. 2002, Tester and Davenport 2003, De Leon et al. 2017). Furthermore, maintaining higher K^+/Na^+ ratio is one of the major strategies of non-halophytic plants to overcome excessive concentrations of Na^+ (Greenway and Munns 1980, Munns et al. 2006, Amtmann and Beilby 2010).

Mineral component analysis, assessing Na^+, K^+ and the K^+/Na^+ ratio of third leaves of wheat seedlings exposed to 100 mM Na_2SO_4 and under control condition, was not giving a clear correlation with the shoot dry weight (SDW) at seedling stage. Overall, the results of the hydroponic experiment with 100 mM Na_2SO_4 did not support the widely described observation of Na^+ discrimination and preferential uptake of K^+ in genotypes with salt tolerant genotypes relative to susceptible genotypes (Munns et al. 2006). A similar observation was described by Genc et al. (2007) assessing the salinity tolerance of a diverse collection of 21 bread wheat genotypes. The authors assumed that salinity tolerance might be achieved through a combination of Na^+ exclusion and tissue tolerance. Recently Li et al. (2017) reported the differential response of two genotypes of rice (*Oryza sativa* L. ssp. *Japonica*) to moderate salt stress treatment. Despite the differential performance of the tested genotypes with respect to the production of biomass and other physiological traits, they did not show differences for K^+, Na^+ and K^+/Na^+ ratio in shoots. They assumed that effective osmoregulation is achieved by the accumulation of soluble sugars and proline to maintain water potential and that the up-regulation of ROS detoxifying systems underlie the greater salt tolerance of the tolerant genotype. Interestingly only one genotype (genotype 95), with the highest SDW among the whole population, was able to maintain K^+/Na^+ ratio greater than 1, which is according to Jones et al. (1979) necessary for non-halophytes like wheat to withstand salinity stress. According to the classification of Asch et al. (2000), this genotype is regarded as Na^+-includer since it takes up more potassium under salt stress condition to maintain the K^+/Na^+ ratio. On the other side genotype 99 and 117, which are also regarded as salt tolerant with respect to STI value of SDW, can be classified as Na^+-excluder, since their K^+ concentration was reduced by 35% and 32%, respectively, while both genotypes maintained their sodium concentration under salt stress on the same level as under control condition.

5.1.3. Maturity stage

With respect to the evaluation of plants under field condition, yield and yield components are considered to have higher importance than biomass or harvest index (Shannon 1997). Hence, salinity tolerance for field crops is usually expressed as yield production under salt stress condition relative to control condition. For this purpose, field trials were conducted in the year 2010, 2011 and 2013 under natural salinization in Karshi (Uzbekistan). Due to the spatial heterogeneity of the experimental site with respect to salinization level and salt type, the outcome of the measured parameters under control and stress condition were not distinct. According to the analysis of variance for the parameters measured from field trials, significant treatment effects were measured for almost all traits but none of the traits showed genotype by treatment interaction effects. This is obvious looking at the yield [T/ha], which is the main trait for field trials. The population mean for grain yield was slightly increased under salt stress condition (+1.5%) relative to non-saline condition. This result might due to the heterogeneities for soil salinity condition at the experimental site, which is obvious when looking at the coefficient of variation [CV] for yield. Under the controlled condition, the CV was 34.8% and under salt stress condition 47.4% (Table 18). Consequently, different from expectation, some parameters, e.g. yield, length of the spike (Table 18), were higher than under control under stress conditions. Number of productive tillers (TLN) is one of the most important yield components. Despite a high CV (32%) for number of tillers under stress condition, our observation was in agreement with several authors who also detected a stronger reduction of tillering of salt sensitive wheat genotypes under stress in comparison with more tolerant wheat genotypes (Francois et al. 1986, Akram et al. 2002, Katerji et al. 2005, Läuchli and Grattan 2007, Munns et al. 2016).

Grain protein content and sedimentation values are the most important parameters for nutritional quality and baking properties. Both parameters were positively affected by salinity stress. But there were weak negative correlations between protein content and yield ($r=-0.33$; $p<0.01$) as well as between sedimentation value and grain yield ($r=-0.17$; $p<0.05$). In comparison to control, under salinity conditions, the sedimentation value and protein content increased by 20.9% and 14.2%, respectively. Similar results were obtained for other crops like durum wheat (*Triticum turgidum* L. spp. *durum*) (Francois et al. 1986), barley (*Hordeum vulgare* L.) (Katerji et al. 2006) and faba bean *Vicia faba* L. (Qados 2011). It is widely accepted that salinity stress inhibits starch biosynthesis by reducing photosynthetic activity and consequently decreases the storage of starch in endosperm of kernels (Kashem et al. 2000,

Almansouri et al. 2001, He et al. 2013). Additionally, according to Turki et al. (2012) the nitrogen metabolism, which is contributing to higher protein content, is relatively stable and less effect by salt stress rather than starch metabolism. Furthermore, Rani et al. (2012) assume that salt stress proteins prevent denaturation or natural damage of proteins, which are essential for survival and recovery from salt stress. The protein quality, comprising baking quality protein glutenin and gliadin, were not tested in this study. Nevertheless, reports indicate that as salinity positively affects protein concentration, by increasing the protein/starch ratio in grain, on the other side it reduces protein quality (Francois et al. 1986, Katerji et al. 2005, Naserian et al. 2014).

In the present thesis two indices, particularly the stress tolerance index (STI) and the stress-weighted performance (SWP), were used to investigate the salinity tolerance of the tested genotypes. The stress tolerance index or salinity tolerance index (STI) is frequently used in order to investigate the stress/salinity tolerance of various plants (Clavel et al. 2006, Porch 2006, Rocha et al. 2014, Negrão et al. 2016) as it takes into account the average performance of the specific trait of the population under control condition as well as the performance of the specific genotype under control and stress condition. However, the stress-weighted performance (SWP), established by Saade et al. (2016), is more appropriate for evaluation of genotypes and genotype by treatment interaction effects for traits measured in the field as the SWP index is more suitable to differentiate the high performing genotypes from low performant ones. Different to SWP which selects for lines that have above-average stress/control scores and have high phenotypic values under control conditions, STI is also underlining genotypes with above-average stress/control scores even though some lines do not perform well under control condition (Saade et al. 2016).

The correlation matrix (Table 21) for the grain quality parameters calculated with the ST index and the SWP index elucidates higher correlation coefficients for most correlations calculated with SWP in comparison with STI. Interestingly, the correlation calculated with the STI values shows no significant correction between grain yield and protein content of grains, whereas the SWP value indicates a highly significant negative correlation of -40% ($p<0.01$).

Looking at the combined analysis of the performance of the Z86 population at germination, seedling stage and maturity stage, none of the genotypes selected as tolerant or susceptible at germination stage were showing high performance at seedling stage. This finding was

consistent with several reports, indicating that little or no correlation has been detected between germination and later growth stages for species as diverse as bread wheat (Francois et al. 1986, Mano et al. 1996, Munns and James 2003). Several reports confirm that plants show differential sensitivity to salinity at different growth stages. In general, plants tend to increase their salt tolerance as they progressively develop during the growing season (Maas and Poss 1989, Francois 1994, Wilson et al. 2000). Hence, looking at the seedling and the maturity stages (Figure 23) entry number 64 can be regarded as the most susceptible genotype, a weak performance showing across all tested environments. Interestingly, entry number 64 showing the highest performance at germination stage while at seedling and maturity stage this entry can be regarded as the weakest genotype for salinity tolerance. On the other hand, supported by previous figure (Figure 22), entry number 6, 99, 130 and 150 can be regarded as most tolerant genotypes with entry number 6 showing higher performance stability across the tested environments.

Several authors express their concerns for the robustness of field experiments. They assume that especially grain yield of foreign or not adapted genotypes will be highly influenced by the environmental and exogenic stress factors. Therefore the genotype effect or the genotype by treatment interaction effect might not be significant (Richards et al. 1987, Jafari-Shabestari et al. 1995, Munns et al. 2006). Additionally, evaluation of a large number of genotypes under saline conditions is difficult because of the variability of salinity within fields (Richards 1983, Daniells et al. 2001). Moreover, screening a large number of genotypes for salinity tolerance is difficult due to the complexity and polygenic nature of salinity tolerance, which involves responses to cellular osmotic, ionic and oxidative stresses (Platten et al. 2013, Adem et al. 2014, Hoang et al. 2016). This argumentation may also apply to the field experiments that were conducted under continental climate zone conditions in Karshi, with high annual variation in temperature between summer and winter season (Gintzburger et al. 2005). Whereas the Z86 population was descending from the cross between the German elite cultivar Zentos, which was adapted to temperate European climate and the resynthesized wheat genotype (Syn86).

5.1.4. Application of sensors for non-destructive assessment of steady-state conditions

Multiple sensors were utilized within the scope of different experiments for phenotyping plants non-destructively. Salinity and drought stress induce in part the same physiological processes in plants (Rao et al. 2006, Pessarakli 2014). Both stressors cause osmotic imbalances due to strongly negative soil water potential. Hence, analysis of the water content can be a valuable trait for the assessment of plants exposed to drought or salinity stress (Uddin et al. 2016).

The results of the non-invasive assessment of water content and electrical conductivity in leaves of different crops with the dual-mode microwave sensor are discussed in detail in the publication (See Appendix 5). In this chapter the usage of the microwave sensor will be briefly discussed. Also, the outcome of the LI-COR LI-6400XT gaze exchange analyzer for wheat plants exposed to salinity stress will be presented in this chapter.

Non-invasive assessment of leaf water status using a dual-mode microwave resonator

The definition of the water status in plant tissue is of importance for the plant researcher to better understand the physiological processes and molecular mechanisms leading to tolerance with respect to drought stress on the one hand (Munns et al. 2000, Pessarakli 2014). Systematic phenotyping of plants needs standardized and non-invasive methods to define and assess physiological parameters like the water of single plants or group of plants to environmental (Munns et al. 2010).

Currently water content in plants is measured by destructive methods such as comparing the fresh and dry weight of plant tissues (Jordens et al. 2009). Nevertheless, these methods do not allow the instantaneous and continuous monitoring of the water content in living tissue. Therefore, non-destructive techniques that require very weak interaction with the plant tissue in order to avoid altering its physiological activities are highly desired.

Non-destructive analysis by radiation in the microwave to terahertz range is most promising for the development of non-invasive methods to determine the water content because of the strong water absorption in this frequency range (Ferrazzoli et al. 1992, Menzel et al. 2009, Castro-Camus et al. 2013).

Different to microwave moisture sensors based on planar microwave transmission lines like the one reported by Rezaei et al. (2012) and planar antennae approaches by Sancho-Knapik, et al. (2011) our method allows the determination of the real and imaginary components of the complex dielectric permittivity at two well separated frequencies.

The sensor used in this study (Dadshani et al. 2015), enables simultaneous dielectric measurements at two distinct and far separated frequencies. Due to the combination of a microwave (f = 2.5 GHz) and a sub-microwave frequency (f = 150 MHz) in one sensor device the method has a strong potential for simultaneous non-invasive assessment of water and salt status in a single leaf.

Accordingly, two parameters, relative frequency shift (*FRS*) and inverse Q factor (*IQS*), which were affected by the dielectric properties of the tested plant material, were calculated (See Eq. 5 and Eq. 6). Consequently, the calculated ratio *IQS*/*FRS* measured at 2.4 GHz (Mode 1) was showing a high negative correlation ($r = -0.97$; $p<0.01$) with the osmotic potential of the tested leaves (Figure 27).

The sub-microwave frequency Mode 0 (f = 150 MHz) allows the determination of the ionic conductivity of the leaf juice non-invasively. And a strong correlation between the measured ratio of loss and frequency shift data to the osmotic potential was found, which indicates that the microwave method can be used for contact-free assessment of the osmolytes status of in a leaf.

Previous reports were showing the applicability of a sub-microwave frequency for determination of electrical conductivity of shock compressed fluids (Hawke et al. 1969) and foods (Jha et al. 2011). However, to the best of our knowledge, this is the first report of non-invasive determination of the electrical conductivity of the fluid inside a plant leaf.

For potato leaves and in particular for canola leaves, where a considerable portion of water is stored in relatively thick veins, this effect is most pronounced. We presume that the drying process by evaporation works slower for large veins. As a result, the measured weight may not be representative for the real water concentration in the largest veins: if the largest veins are located close to a field maximum of the resonant field, the measured FRS values may

overestimate the average water concentration in the leaf, which explains the observed curvature qualitatively.

However, our approach has proven to be highly reproducible and applicable for leaves of various size, shape and thickness. The frequency shift versus water content curves are slightly sub linear for the larger leaves, which may result from the inhomogeneous water distribution in the veins. For canola leaves, a strong correlation between the measured ratio of loss and frequency shift data to the osmotic potential was found, which indicates that the microwave method can be used for contact-free assessment of the osmolytes status of a plant.

Due to the combination of a microwave (f = 2.5 GHz) and a sub-microwave frequency (f = 150 MHz) in one sensor device the method has a strong potential for simultaneous non-invasive assessment of water status and electrical conductivity (salt status) in a single leaf under test. Moreover, our evanescent field approach overcomes the wavelength limitation and enables the use of much lower frequencies at 150 MHz and 2.4 GHz, with the advantage of cheap electronic components as being used in wireless communication. The potential commercial availability of an evanescent field dual-mode microwave sensor system at moderate cost enables the implementation of non-invasive water and conductivity assessment in biological research laboratories.

5.1.5. Non-destructive measurement of photosynthetic parameters of wheat plants exposed to salinity stress at seedling stage

Continuous gaze exchange measurements were conducted in order to investigate the immediate change of photosynthetic parameters that evolve within the first minutes after exposing plants suddenly to high salt concentration. The salt shock experiment was conducted with the parents of the Z86 population, Zentos and Syn86 and on two lines of the Z86 population (genotype 84 and genotype 117) which were selected as extremes in respect to their tolerance towards salinity stress. All plants experienced, although different in magnitude, shortly after exposure to salinity stress a drop and subsequent recovery of photosynthetic parameters (see Figure 29). Application of repeated measures analysis of variance by using an orthogonal polynomial transformation option and including time as within-subject factors, revealed highly significant genotype by treatment interaction effect 20 minutes after initiation of salt stress (F-value=21.25, p-value=0.0058).

To the best of our knowledge, this is the first study of continuous measurement of photosynthetic parameters of wheat plants exposed to sudden salinity stress.

Similarly shaped curves of photosynthetic rates were described by Kawasaki et al. (2001), exploring initial phase of salt stress in two contrasting rice genotypes. Measuring gaze exchange parameters in faba beans (*Vicia faba* L.) exposed to 50 mM NaCl, Geilfus et al. (2015) observed no significant difference in photosynthesis rates of stressed plants and plants under controlled conditions within 25 minutes after onset of the treatments. After 25 minutes, the photosynthetic rates declined gradually but even after 60 minutes, no recovery of photosynthesis rate was detectable. As the authors were linking the early metabolite response of plants exposed to salinity, they measured an increase of spermidine production in leaf samples, which is associated with inhibited photosynthetic activity triggering high amount of reactive oxygen species (ROS). However, the deviation in respect to the time point of impairment of photosynthetic activity presented in this study and the study presented in Geilfus et al. (2015) and Kawasaki et al. (2001) might be caused due to differences in tested species and the intensity of the applied salt stress. Exposing maize and barley seedlings to salinity shock Passioura and Munns (2000) observed similarly shaped curves for leaf elongation rates as described for the photosynthetic parameters in this study. Furthermore, Munns et al. (2000) investigated elongation rates of leaves of barley and maize plants exposed to salinity shock with and without excised roots. They experienced a brief decline and quick recovery of elongation rate in plants

with excised roots in contrast to plants with intact roots. Obviously, looking at Syn86 under control condition having 82% longer roots than Zentos (see Table 10), root length has a high impact on the level of impairment induced by salinity stress. Plants with shorter roots and less root surface might have an advantage in comparison with plants with longer roots and greater root surface since they have a comparably smaller root area which is in contact with the deleterious solution. Especially, plants with inefficient exclusion mechanisms are facing an unhampered accumulation of Na^+ in root cytosol (Flowers et al. 1997).

As described earlier, reduction of root length under salinity stress might be a long-term response of plants to cope with salinity in the hydroponic system by avoiding overload of Na^+. In summary, the outcome of this study is supporting the hypothesis established by Neumann (1995), hypothesizing that root reduction might be an adaptive biophysical response of plants to cope with salinity stress. Vice versa, salt-tolerant plants with the efficient regulation of K^+/Na^+ homeostasis might be able to maintain longer roots, which is of importance for uptake of water and nutrients. However, this observation might be in contrast to observation from natural soil conditions since hydroponic systems are artificial systems where plants roots are continuously surrounded by the hydroponic solution.

Hydroponic systems are effective and reliable techniques for evaluation of a large number of plants under controlled environmental conditions. However, along with the practical advantages, hydroponics are artificial systems that come along with some fundamental characteristics. These include the absence of natural substrates like soil that permits plant to develop roots with defined spatial characteristics (architectural and morphological) which might affect the research questions. As under salt stress condition plants tend to reduce root length in order to avoid over-excess of Na^+ intrusion from lower soil levels. However, in hydroponic system this reaction is disturbed as the salinity level in the whole system has the same concentration.

5.2. Genetic characterization of the Z86 population

The 151 AB-lines of the Z86 winter wheat population and their parents Zentos and Syn86 were genetically characterized in order to employ the genetic information for detection favorable alleles for various traits related to salinity tolerance. Due to the biparental character of the population, only 11,050 informative SNP markers remained for application in QTL analysis. As the average marker density on chromosomes of A and B subgenome were 2.6 and 6.7 SNP per cM, respectively, the marker density on chromosomes of subgenome D was comparably low with on average 1.1 SNP per cM. Chromosome 4D showed the lowest marker density with 0.4 markers per cM, generating marker gaps of up to 59 cM. This was not surprising as only 15% of the markers on the 90K array were mapped to the D genome (Wang et al. 2014).

LD decay analysis is commonly used for genome-wide association mapping (GWAS) (Terwilliger and Weiss 1998, Klein et al. 2005, Manolio 2010). Typically, LD is an essential criterion for linkage and association mapping. However, linkage mapping depends usually on linkage as single cause of LD, while association mapping depends on all causes which effect LD, namely breeding system, migration, selection, mutation and drift. For QTL localization it is not trivial to separate the linkage effects on LD from the other ones. One method to detect the linkage effect on LD would be to estimate the LD decay in respect to the distance between the markers on the chromosome. Usually the estimate of the LD decay at threshold of $R^2=0.1$ is taken as a critical value to define a confidence interval for the nonparametric bootstrap approach to increase the accuracy of QTL localization (Visscher et al. 1996, Bennewitz et al. 2002).

In association panels, the highest extent of significant LD is expected to be in the D-genome of polyploid wheat and lower LD in the A- and B-genomes (Chao et al. 2010, Peng et al. 2011). The LD of linkage populations have generally higher values than in natural populations due to the low number of genotypes involved in the construction of the segregating populations and on the other hand numerous historical recombinations among the natural populations (Mackay and Powell 2007, Sakiroglu et al. 2012). Considering the bi-parental crossing scheme and few recombination events, the LD of the Z86 populations was moderate with 12.3, 12.7 and 13.5 for the A-, B and D-genome, respectively. Noteworthy that unlike association panels, LD of the D-genome is not significantly higher than the A- and B-genome.

Figure 31 is showing the LOESS fitted LD curves of the Z86 population. Other than expected the recombination fraction (R^2) of some chromosomes showed increasing values after reaching the bottom line. This phenomenon might be explained by the LOESS function, established by Cleveland (1979) which is a polynomial fit method assigned for smoothing locally weighted regression.

Surprisingly, the LD decay curve of chromosome 5B showed an offset behavior and therefore an unconventional shape. Even at the lowest point (50 cM) R^2 is not lower than 30% and increasing by the enhanced distance between the markers. This might be affected by chromosomal rearrangements on the chromosome 5B induced by the artificial allopolyploidizations of wild emmer (*T. turgidum* spp. *dicoccoides*) with T. tauschii producing the neoallohexaploid wheat. Numerous and structural aberrations of chromosomes of neoalloploids, denoted as 'genomic shock', have been described previously especially in synthetic hexaploid wheat (Gill et al. 1991, Nelson et al. 1995, Frizon et al. 2017, Yu et al. 2017). However, the pairing homeologues gene (*Ph1*), which is usually ensuring the correct homologue pairing and recombination, and hence enabling the bivalent manner of hexaploid wheat chromosomes during meiosis, is also located on chromosome 5BL of hexaploid wheat (Okamoto 1957, Riley and Chapman 1958). The malfunction of homologue pairing in some synthetic hexaploid wheat genotypes was also observed by Yang et al. (2011) who concluded that the cytological instability of synthesized wheat genotypes was due to the absence of *Ph1* gene. However, this might not explain the unusual structural anomaly of the chromosome 5B whereas at this high extent no structural anomaly was detected for other chromosomes.

It has been extensively discussed by several authors (Dvořák et al. 1993, Feldman and Levy 2005, Peng et al. 2011), that the second spontaneous alloploidization process, producing the allohexaploid wheat, was 0.5 million years after the first alloploidization step between two diploid grasses to produce the wild emmer (*T. turgidum spp. dicoccoides*). Additionally, Marcussen et al. (2014) assumed that only a single introgression event for the formation of the hexaploid wheat and hence a reduced genetic variability of the D-genome was the reason for the persistently limited recombination rate. Hence, Dvorak et al. (2011) conclude that gene flow from tetraploid wheat to *T. aestivum* was the main source of genetic variability of modern hexaploid wheat. According to Chao et al. (2010), the high extent of significant LD on the D-genome in natural populations is reflecting the episodes of recent occasions of hybridization

event and subsequent limited number of recombination events affecting the D-genome of the allohexaploid wheat.

Ultimately, it is generally accepted that based on the historical hybridization events the D-genome genetically constitutes a bottleneck with reduced genetic variability (Ogbonnaya et al. 2005, Dubcovsky and Dvorak 2007, Peng et al. 2011). On the other side, increasing the genetic variability of the D-genome of modern wheat by introgression of exotic alleles descending from *Aegilops tauschii* is discussed to be an alternative that could contribute to tolerance against multiple biotic and abiotic stresses (Colmer et al. 2005, van Ginkel and Ogbonnaya 2007).

5.3. Detection of QTL for the measured phenotypic traits

Soil salinity is one of the major abiotic stress factors in many parts of the world threating wheat production, leading to yield reduction and quality losses. Breeding new cultivars with adaptation to harsh environmental conditions by introgression of exotic alleles into modern cultivars is widely accepted are a mean to overcome the genetic bottleneck imposed by domestication and modern breeding process (Tanksley and McCouch 1997, Nevo and Chen 2010). Especially in modern bread wheat, the D genome is thought to be a major limiting factor for improvement and adaptation to different environmental conditions, due to its relatively narrow genetic variability (Song et al. 2017). Many articles underline the potential of synthetic hexaploid wheat (SHW) as bridge germplasm to introduce the genetic diversity of close relatives of wheat into modern breeding programs. The potential of SHW as donor of favorable genes enhancing salinity tolerance of modern wheat genotypes by discriminating Na^+ and preferentially uptake of K^+ are widely discussed (Gorham et al. 1990, Lindsay et al. 2004). The use of synthetic backcross-derived lines (SBLs), based on the cross between SHW as donor of exotic alleles and modern wheat cultivars as recurrent parent, are widely used for application in QTL analysis for multiple traits and for detection of epistatic interactions (Juenger et al. 2005, Ogbonnaya et al. 2013).

In this study, the advanced backcross winter wheat population Z86 was evaluated at different salt treatment regimens during the entire growing cycle, from germination to final maturity stage. Subsequently, QTL analysis was conducted for 48 traits revealing 116 marker-trait associations, including digenic epistatic effects (M_1*M_2) and 165 QTL with marker by treatment interactions, including digenic epistatic treatment interaction effects (M_1*M_{2*}T).

For complex traits such as salinity tolerance, there is a need to estimate the effect of epistatic QTL effects and epistatic by treatment interaction (M_1*M_{2*}T) effects (Ravi et al. 2011) in addition to detection of simple QTL for main effect or M*T interaction effects. Several studies were conducted to calculate M_1*M_{2*}T interaction by application of composite interval mapping (Yang et al. 2007, Xu et al. 2013). However, to the best of our knowledge, the applied hierarchical model established at our institute is the first systematic approach for the detection of QTL main effects, marker by treatment interaction effects as well as for epistatic by treatment interaction effects by application of multi-locus approach.

The detected QTL indicate a shift from more housekeeping and plant development associated genes under control condition to more signaling and stress-responsive genes under salt stress condition. Overall, according to the gene ontology classification, 82% of the identified QTL were denoted as involved in “Osmotic regulations”, “Hormone reaction and Signaling” and “Repair and Defense” under stress condition, whereas under control only 36% of all MTAs were from these categories. The same three gene ontology (GO) categories regulating salinity tolerance were also reported in Munns et al. (2005) and elsewhere. It is also widely accepted that a wide range of physiological and biochemical plant responses to complex stress factors like drought and salinity stress are regulated by constitutive and adaptive genes, with spatial and temporal diversity in their expression pattern (Witcombe et al. 2008, Agarwal et al. 2013, Thoen et al. 2017).

As the correlation between traits measured at the different developmental stages (germination stage, seedling stage, and maturity stage in field trails) was low, only a few overlapping QTL with treatment interaction effects were detected. Plants are differently affected by salt stress at various growth stages. Therefore, it was not surprising that the QTL analysis for germination, seedling and maturity stage showed only a few overlapping QTL. Similar findings were reported for tomato (Foolad 1999), pea (Okçu et al. 2005), rice (Das et al. 2015), barley (Mano and Takeda 1998) and durum wheat (Almansouri et al. 2001).

Other than expected, the German elite cultivar Zentos outperformed the synthetic genotype Syn86 in most of the measured traits. The lower performance of some SHW lines in comparison to elite cultivars, especially in respect to end-use quality and threshing, was reported previously. Moreover, it is widely accepted that the genotypic variability among SHW genotypes is huge and some SHW are more susceptible to different abiotic and biotic stress factors than modern elite cultivars (Dreisigacker et al. 2008). Therefore, according to the QTL analysis conducted for most traits, the majority of the favorable alleles were derived from the elite parent and not from the synthetic parent.

The synthetic parents Syn86 was outperforming the modern cultivar only for root length and plant height under control as well as under salt stress conditions. This was not surprising as decades of breeding efforts focused on the reduction of plant height to reduce lodging risk and on the other hand neglected the root system (Rickman et al. 1985, Waines and Ehdaie 2007). Accordingly, two major QTL, QTL_4BS_1 (4BS, 61.84 cM) and QTL_7BS_1 (7BS, 71.66

cM) correlating with root length under control condition were explaining 43.4% and 46.6% of the genetic variation, respectively. Progenies of the Z86 population possessing the allelic variation of Syn86 on QTL_4BS_1 and QTL_7BS_1 had in average 16.3% and 13.1% longer roots than genotypes with an allelic variation of Zentos. *In-silico* analysis of QTL_4BS_1 and QTL_7BS_1 revealed associations with the COPRA protein (XP_020199365.1) and with CLASP N terminal (pfam12348), respectively. Both genes were involved in cell expansion and cell division. Several studies detected a significant correlation of drought tolerance with root parameters like root length in synthetic wheat (Atta et al. 2013, Becker et al. 2016). The authors suggested the integration of synthetic wheat in breeding programs in order to produce drought-tolerant varieties.

Another interesting QTL (QTL_3DS_1) with the marker tplb0050o09_895 on chromosome 3DS at 4.46 cM was found to have a stress effect on several biomass-related traits (SFW, SDW, PFW and PDW) at seedling stage under control and salinity conditions. The exotic allele was outperforming the elite cultivar and a single QTL (QTL_3DS_1) was adjudicated to explain 11.1-16.3% of the genetic variation by M*T interaction (Table 33 in Appendix 3). In digenic interaction with other QTL (QTL_2BL_1 with Excalibur_rep_c77221_93 on chromosome 2BL at 109.5 cM, QTL_3AL_2 with wsnp_Ku_c46762_53407442 on chromosome 3AL at 173.2 cM and QTL_2DS_1 with Kukri_rep_c72254_186 on chromosome 2DS at 49.6 cM) QTL_3DS_1 was associated with 22.5-29.9% of the genetic variation by M*M*T interaction (Table 27 and Table 33 in Appendix 3). This QTL was linked to the gene coding for the aquaporin transporter protein (IPR034294). Aquaporins are playing a crucial role in the uptake of water by plant roots and they are also involved in the non-selective exchange of cations like Ca^{2+} and Na^{+}, CO_2, urea etc. (Byrt et al. 2017). Several reports indicate that aquaporins are implicated in Na^{+} uptake, whether selective or non-selective and hence a potential source of toxic Na^{+} influx in the plants (Mansour 2014, Assaha et al. 2017). The importance of aquaporins in adaptation to salinity stress was demonstrated in Arabidopsis by overexpression of aquaporin genes from banana, wheat and rice (Mansour 2014, Xu et al. 2014). However, aquaporins seem to play a crucial role in the combined network of transporters and channels mediating Na^{+} transport in plants. The identified aquaporin gene could be a valuable candidate in respect to the approach of mining beneficial alleles for making wheat more tolerant towards salinity stress.

Data from field trials led to the detection of some interesting QTL in respect to salinity tolerance and grain quality. QTL_3AL_1 linked with the marker Tdurum_contig8674_1236 on

chromosome 3AL at 188.38 cM linked with FERONIA, which is a Receptor-like kinase containing a Malectin-like carbohydrate-binding domain (IPR024788). Several studies indicate the pleiotropic property of this gene which seems to play a major role by interacting with RALF (rapid alkalinization factor) in female fertility (Haruta et al. 2014, Li et al. 2016) and involvement in ABA signaling pathways by interacting with ABA Insensitive 1 and 2 (ABI1/2) in cross-talk with RALF which is also involved in downregulation of ABA and upregulation of auxin (Yu et al. 2012). Recent studies underline the importance of FERONIA for salt stress response in Arabidopsis (Chen et al. 2016) and rice (Landi et al. 2017).

In general, QTL mapping has proven to be a powerful tool for identification of genomic regions in a bi-parental population either in F2 population, advanced backcross population (AB), Recombinant Inbred Lines (RILs), Near-isogenic lines (NILs), Double haploid lines (DH) etc. However, QTL analysis is highly depended on the genotypic and phenotypic diversity of the population under study. Low mapping resolution due to limited number of recombination events are leading to large linkage groups, hampering the detection of associated genes. For this purpose, fine mapping by application of sub-ILs, carrying small introgressions of the exotic genotype in the background of the modern cultivar is desirable for detection of favorable alleles.

However, different to GWAS, QTL mapping is an efficient method to detect rare alleles and is widely utilized to discover exotic alleles from wild species if applied for an appropriate population. Uga et al. (Uga et al. 2013) were able to localize the DEEPER ROOTING 1 (DRO1) allele which controls root growth angle descending from a wild rice genotype by application of QTL analysis with a NIL population. By introducing of DRO1 into a shallow-rooting rice cultivar by backcrossing, the authors were able to confirm the contribution of DRO1 in controlling root architecture in rice. By application of a sub-ILs population of barley, carrying small introgression of wild barley (ISR42-8) in the background of the recurrent elite cultivar (Scarlett), Schmalenbach et al. (Schmalenbach et al. 2008) were able to produce a high-resolution fine-mapping population that was applied for detection of agronomic traits (Schmalenbach et al. 2009) as well as for malting quality (Schmalenbach and Pillen 2009).

Advanced backcross QTL populations developed from crosses between wheat cultivars and synthetic genotypes were used for mapping of QTL for several traits including quality traits (Narasimhamoorthy et al. 2006, Kunert et al. 2007). Furthermore, several studies using synthetic backcross populations were able to detect QTL related to salinity tolerance, including

K^+/Na^+ controlling locus *Kna1* (Dubcovsky et al. 1996, Shavrukov et al. 2011). Several authors conclude that synthetic hexaploid wheat could be deployed to mitigate the impact of salinity by application in QTL mapping (De León et al. 2011, Ogbonnaya et al. 2013).

However, besides the requirements of high mapping resolution for the application of QTL analysis, it is a prerequisite that the parents of the used population differ highly in the phenotype of the trait of interest and the respective QTL population is segregating for the target phenotype (Tanksley and Nelson 1996). Within this study the SHW Syn86 was not showing higher salinity tolerance than the modern winter wheat cultivar Zentos. The German elite cultivar was outperforming the synthetic genotype in respect to several traits, under control condition as well as under salinity stress condition. However, Syn86 offers an ideal source of exotic alleles, such as for root length. Application of AB-lines carrying exotic introgressions of Syn86 in breeding programs might help producing varieties with increased and deeper root growth which is essential for drought resistance and exploitation of deeper soil level for essential nutrients.

5.4. Sequence and expression analysis of glutathione S-transferase under salt stress in wheat

Several highly significant QTL were detected by the QTL analysis conducted for the three major developmental stages of winter wheat. One of the major QTL with pleiotropic and digenic epistatic effects on multiple traits, including shoot biomass production under salinity stress and control condition, was QTL_7DS.1 closely linked to the SNP marker BobWhite_c8454_782 localized on the short arm of chromosome 7DS at 29.97 cM. Further *in-silico* investigations revealed the linkage of this marker with the enzymes of glutathione S-transferase *tau* class (*TaGSTu3*). As part of a superfamily of multifunctional enzymes, glutathione S-transferases (GST; KEGG Enzyme Nomenclature EC.2.5.1.18) are present in all kingdoms of living organisms (Wiktelius and Stenberg 2007). GSTs are well known for their role in detoxification of exogenous xenobiotics such as herbicides (Dixon et al. 1998, Moons 2003).

Apart of exogenous toxins, plants are threatened by endogenous production of reactive oxygen species (ROS). Plants produce ROS particularly as by-products of photosynthesis in reaction centers of photosystem I (PSI) and photosystem II (PSII) in chloroplast thylakoids (Sandermann 2004, Asada 2006). ROS accumulation in plants is known to cause substantial oxidative damage to proteins, lipids, carbohydrates and DNA which ultimately results in oxidative stress (Ahmad et al. 2008, Gill and Tuteja 2010). As salinity stress is rapidly inhibiting photosynthetic aperture of plants leading to high increase of ROS production such as H_2O_2. Under salinity stress GST is playing a key role in detoxification of H_2O_2 by catalyzing the conjunction with glutathione (GSH) to produce H_2O (see Figure 3) (Wilce and Parker 1994, Frova 2003, Martínez-Márquez et al. 2017).

In plants, ROS are also involved in stress and hormone signaling by mediation of Ca^{2+}-signal transduction and activation of Ca^{2+}-permeable channels in plant membranes (Mori and Schroeder 2004). However, the right balance between ROS scavenging and ROS production as essential requirement of signaling pathways is of critical importance for plants (Ahmad et al. 2008).

Among the high number of GST classes the *tau* class (τ), denoted as GSTu, are meant to be the only distinct plant-specific GSTs (Munyampundu et al. 2016). Several reports indicate the importance of GSTu enzymes for the alleviation of salinity stress in rice (Moons 2003), tomato

(Csiszár et al. 2014) and sorghum (Chi et al. 2010). Whereas some reports point out GFTs, mainly GSTfs belonging to *phi* class of GSTs, improve salinity tolerance of wheat (Cummins et al. 2003, Niazi et al. 2014, Bacu et al. 2017), till now there is no such report concerning the ameliorating effect of *tau* class GSTs on salinity tolerance of wheat.

Generally, GSTs of the same class are arranged as adjacent as tandem duplications and are grouped cluster-wise (Edwards et al. 2000, Labrou et al. 2015). These special characteristics of GSTs have great importance on their multifunctionality and diversification in their enzyme specificity and activity toward different substrates (Dixon et al. 2002, Lan et al. 2009, Liu et al. 2015). Sequencing the genomic region, we were able to localize *TaGSTu6* approximately 15K bp downstream of *TaGSTu3*. Interestingly, analyzing the divergence in enzymatic activities of GSTu genes in soybean (*Glycine max* L. (Merr.)) Lui et al. (2015) found out that *GSTu3* and *GSTu6* are also tandemly clustered. The authors assumed both genes to be paralogous, arised by gene duplication during polyploidization events in the evolutionary history of soybean. Liu et al. (2015) additionally classified GSTu3/6 tandem genes in soybean sharing affinity to the same substrate spectrum. The genetic structure of *TaGSTu3* with two introns and *TaGSTu6* with one intron confirmed the typical gene structure model of tau class *GTSs* described by Labrou et al. (2015). Since no allelic variation between the sequences of Zentos and Syn86 were detected, either for *TaGSTu3* neither for *TaGSTu6*, gene expressional analysis under control and salt stress condition were conducted. Preceding Semi-quantitative PCR (sq-PCR) and finally, Quantitative Real-Time PCR (qRT-PCR) with RNA, extracted from the third leaf, revealed higher expression of *TaGSTu3* in Zentos in comparison to Syn86. Investigation of *TaGSTu3* kinetics in Zentos and Syn86 at three-time points (10, 16 and 30 days after salt stress application (DAS)) was showing minor but steady increase of *TaGSTu3* expression in Zentos under control condition whereas under salt stress condition the expression of Zentos remained nearly unchanged. Nevertheless, only after 30 DAS the expression of *TaGSTu3* in Zentos was significantly higher than under salt stress conditions. In respect to *TaGSTu3* expression in Syn86, as well under control as under stress condition, the expression was lower than in Zentos. Furthermore, at all time points the expression of *TaGSTu3* in Syn86 leaves under salt stress condition was significantly lower than under control condition.

The evidence from expression analysis, especially the incremental increase in expression of *TaGSTu3* under salt stress condition, may indicate causal mutations in the promoter region of *TaGSTu3* being responsible the differential expression pattern of the gene in both genotypes.

Subsequent analysis of the promoter region 1.1K bp upstream of *TaGSTu3* of Zentos and Syn86 revealed differences in number and sequence of specific TFBS and DNA binding domains which are known for their relationship with salt stress response and involvement of phytohormone activity. The DNA binding domains DOF2 and NAC691/NAM were detected in the promoter region of Zentos but not in Syn86. DOF2 (DNA-binding with one finger) belongs together with DOF1 to the class of zinc finger domains playing critical roles as transcriptional regulators in plant growth and development (Yanagisawa 2004, Hernando-Amado et al. 2012). The DOF2 transcription factor might be a key regulator of *TaGSTu3* inducing, in interplay with other beneficial genes, higher vigor and biomass production of Zentos under controlled conditions as well as under salt stress condition. The involvement of DOF family members in response to biotic stress factor are known for many plants (Kang et al. 2016, Wen et al. 2016). Their involvement in reaction to abiotic stress was discovered recently, including osmotic stress in poplar (*Populus trichocarpa* Torr. & A.Gray ex. Hook.) (Hernando-Amado et al. 2012), salinity, drought, heat and freezing stress in tea plant (*Camellia sinensis* L.) (Li et al. 2016) and against salt stress in Chinese cabbage (Ma et al. 2015).

The members of NAC transcription factor family belong to the large group of transcription factors such as WRKY, bZIP, MYB, AP2/EREBP comprising ~7% of the genome code for putative TFs (Shao et al. 2015). Their role in response to biotic, abiotic and particularly salinity stress in many plants are widely investigated in *Arabidopsis thaliana* (Jiang and Deyholos 2006) rice (Ohnishi et al. 2005) and wheat (Xia et al. 2010). Mao et al. (2012) and Huang et al. (2015) demonstrated an increase in salinity tolerance by transferring the transcription factor *TaNAC2* and *TaNAC29*, from wheat to Arabidopsis. According to Fujita et al. (2004), NAC proteins are involved in ABA-dependent stress-signaling pathway. The phytohormone ABA plays a critical role in linking the stress-responsive signaling cascades under a large number of abiotic and biotic stress factors (Lee and Luan 2012, Lindemose et al. 2013). The positive role of ABA in the response to salinity stress in wheat is widely accepted (Kasuga et al. 1999, Afzal et al. 2006, Niazi et al. 2014). Furthermore, several studies confirmed the higher expression of *GSTs* induced by the phytohormone ABA. Moons et al. (2003) found out that salt stress and ABA rapidly induced expression of *OsGSTu3* in rice roots. Studying wheat gene expression responses to abiotic stresses including drought and salt stress Xue et al. (2006, 2011) revealed that the expression of *TaNAC69* was upregulated in roots of wheat seedlings. Besides this, the authors found out that *TaNAC69* genes were highly expressed in roots under controlled condition. They assumed that *TaNAC69* gene are not only involved in stress response and they

might also be required for normal cellular activity in roots. This assumption is in agreement with our observations. Analysis of digenic epistatic interactions revealed significant M_1*M_2*treatment interaction of QTL_7DS.1 with another QTL (QTL_6AL.2) on chromosome 6AL at 136.85 cM, explaining 22.8% of the genetic variance for SDW under salinity stress. Interestingly, we found at a distance of 3.99 cM a candidate gene coding for a 'NAC domain containing protein' which is assumed to regulate the expression of *TaGSTu3*.

Hence, by analysis of epistatic by treatment interaction not only the gene coding for *TaGSTu3* was detected but also the corresponding gene coding for the NAC-domain, which is assumed to regulate the expression of *TaGSTu3*.

Additionally, the promoter region of *TaGSTu3* in Zentos had two copies of the motifs AGL3-1 and RITA1, whereas the promoter region of Syn86 was containing single copies of both TFBS. As AGL3-1 is known for its involvement in abiotic stress response (Zeng et al. 2015), RITA1 is associated with gene expression in developing seeds (Izawa et al. 1994).

The higher number of TFBS present in the promoter region of Zentos than Syn86 were accountable for the higher expression of *TaGSTu3* in Zentos. This is in line with Shen et al. (1996) and Riley et al. (2008) reporting that ABA-responsive genes were not activated by a single copy of the transcription factor ABRE. And hence, multiple TFBS were needed (required) for efficient activation of the ABA pathway.

In summary, the complex regulation of *TaGSTu3* gene expression, embedded in the network of stress response is regulated by substrate specificity of GSTu genes, tandem arrangement and gene duplication, as well as number and specificity of transcription binding sites in the promoter region of the gene. Additionally, the detection of numerous TFBS associated with multiple effects may indicate the versatility of *TaGSTu3*. As GSTs are involved in manifold cellular functions, induced by a wide variety of phytohormones, they play a vital role in plant development and growth as well (Jiang et al. 2010).

It is also widely accepted that a wide range of physiological and biochemical plant responses to complex stress factors like drought and salinity stress are regulated by constitutive and adaptive genes, with spatial and temporal diversity in their expression pattern (Witcombe et al. 2008, Agarwal et al. 2013, Thoen et al. 2017).

However, for a broad understanding of *TaGSTu3* interacting with its tandem duplicate gene *TaGSTu6* in respect to their effect on salinity tolerance and mechanisms involved, it might be of interest to further analyze the expression of *TaGSTu6* gene, too. Additionally, as Moons (2003) suggested, investigation of *GSTu* expression in root tissue and early after stress application might enlighten involvement of *GSTu* in wheat plants under salinity stress.

Successful introgressions of GST genes from one species to another species improving tolerance towards biotic and abiotic stress factors like salinity were reported for several crops like *Nicotiana tabacum* L. (Yu et al. 2003) and *Oryza sativa* L. (Zhao and Zhang 2006). By producing transgenic *Arabidopsis* plants carrying the *LeGSTu2* gene of tomato (*Lycopersicon esculentum* Mill.) Xu et al. (2015) were able to study the functional analysis of the gene and to enhance the salinity and drought tolerance of *Arabidopsis* plants. Therefore, introgression of *TaGSTu3* and the regulating elements from Zentos to the model plant *Arabidopsis* may contribute to understanding gene regulation pathways of *TaGSTu3* and its role in detoxification process under salinity stress.

Finally, as proposed by Frova (2003) and Nianiou-Obeidat et al. (2017), GST pyramiding might be an effective biotechnical approach to produce improved wheat varieties with enhanced capabilities to withstand various stress conditions, such as salinity stress.

6. CONCLUSION

- In the frame of this study the advanced backcross (AB) winter wheat population "Z86", containing introgressions of the synthetic hexaploid wheat Syn86L in the background of the German elite winter wheat cultivar Zentos, was evaluated under salinity stress. The AB-lines of the Z86 population and their parents were diversely affected by different salt treatments at various growth stages. Notably, the elite cultivar Zentos performed better under salinity stress for most of the studied traits than the donor parent synthetic Syn86.

- Application of the dual-mode microwave resonator tested it this study allowed non-destructive, instantaneous and continuous monitoring of the water content and ionic conductivity in leaves of several mono- and dicotyledonous plants. Furthermore, non-invasive measurement of photosynthetic parameters of wheat plants exposed to sudden salinity stress (salinity shock) revealed genotype specific decrease and subsequent recovery of photosynthetic parameters, where Zentos was performing better than Syn86. Significant genotype by treatment interaction effect was detected 20 minutes after initiation of salt stress.

- Phenotypic data were subjected to QTL analysis using genome data based on iSelect 90K SNP array. QTL analysis revealed for 48 traits 116 marker-trait associations and 165 QTL with marker by treatment interactions. One of the major QTL (QTL_7DS.1) was identified on chromosome 7D having a major effect on shoot dry weight under salt stress. Interestingly, this QTL appeared to have pleiotropic effects on other traits, such as root length, root fresh weight, and K^+/Na^+ ratio in leaves. In this QTL region, I identified a gene which is coding for an enzyme belonging to the *tau* class of the glutathione S-transferase family (GST), denoted as *TaGSTu3*. This was the first report of a *tau* class GST found to be involved in salt stress response in wheat. Expression analysis at three time-points (10, 16 and 30 days after salt application) at seedling stage revealed higher expression of *TaGSTu3* in Zentos under salinity stress whereas in the comparing parent Syn86 the expression of *TaGSTu3* was decreased significantly. In addition, this QTL revealed a digenic epistatic interaction with a transcription factor gene, localized on chromosome 6AL at 136.85 cM, regulating the expression of *TaGSTu3* under salinity stress.

- Finally, the detected favorable alleles introgressed in the AB-lines of the Z86 population can be directly employed in breeding programs via marker-assisted selection. Pyramiding of diverse advantageous alleles might be an effective biotechnological approach to produce improved wheat varieties with enhanced capabilities to withstand various stress conditions, such as salinity stress. Additionally, the integration of the tested sensor technologies in phenotyping procedures allows instantaneous and continuous non-destructive monitoring of plants exposed to various stress conditions.

7. REFERENCES

Abrol, I., J. Yadav and F. Massoud (1988). "Salt-affected soils and their management. Food and Agriculture Organization of the United Nations." FAO soils bulletin **39**.

Adem, G. D., S. J. Roy, M. Zhou, J. P. Bowman and S. Shabala (2014). "Evaluating contribution of ionic, osmotic and oxidative stress components towards salinity tolerance in barley." BMC Plant Biology **14**(1): 113.

Aflaki, F., M. Sedghi, A. Pazuki and M. Pessarakli (2017). "Investigation of seed germination indices for early selection of salinity tolerant genotypes: A case study in wheat." Emirates Journal of Food and Agriculture **29**(3): 222.

Afzal, I., S. M. Basra, M. Farooq and A. Nawaz (2006). "Alleviation of salinity stress in spring wheat by hormonal priming with ABA, salicylic acid and ascorbic acid." Int. J. Agric. Biol **8**(1): 23-28.

Agarwal, P. K., P. S. Shukla, K. Gupta and B. Jha (2013). "Bioengineering for salinity tolerance in plants: state of the art." Molecular biotechnology **54**(1): 102-123.

Ahmad, P., M. Azooz and M. N. V. Prasad (2013). Salt stress in plants: signalling, omics and adaptations, Springer Science & Business Media.

Ahmad, P., M. Sarwat and S. Sharma (2008). "Reactive oxygen species, antioxidants and signaling in plants." Journal of Plant Biology **51**(3): 167-173.

Akram, M., M. Hussain, S. Akhtar and E. Rasul (2002). "Impact of NaCl salinity on yield components of some wheat accessions/varieties." Int J Agric Biol **1**: 156-158.

Alias, Z. (2016). The Role of Glutathione Transferases in the Development of Insecticide Resistance. Insecticides Resistance, InTech.

Allbed, A. and L. Kumar (2013). "Soil salinity mapping and monitoring in arid and semi-arid regions using remote sensing technology: a review." Advances in remote sensing **2**(04): 373.

Almansouri, M., J.-M. Kinet and S. Lutts (2001). "Effect of salt and osmotic stresses on germination in durum wheat (Triticum durum Desf.)." Plant and soil **231**(2): 243-254.

Almeida, D. M., M. M. Oliveira and N. J. Saibo (2017). "Regulation of Na+ and K+ homeostasis in plants: towards improved salt stress tolerance in crop plants." Genetics and molecular biology(AHEAD): 0-0.

Amtmann, A. and M. J. Beilby (2010). The role of ion channels in plant salt tolerance. Ion Channels and Plant Stress Responses, Springer**:** 23-46.

Asada, K. (2006). "Production and scavenging of reactive oxygen species in chloroplasts and their functions." Plant physiology **141**(2): 391-396.

Asao, T. (2012). "Hydroponics – A Standard Methodology for Plant Biological Researches."

Asch, F., M. Dingkuhn, K. Dörffling and K. Miezan (2000). "Leaf K/Na ratio predicts salinity induced yield loss in irrigated rice." Euphytica **113**(2): 109-118.

Ashraf, M. and N. A. Akram (2009). "Improving salinity tolerance of plants through conventional breeding and genetic engineering: an analytical comparison." Biotechnology advances **27**(6): 744-752.

Ashraf, S., A. Shahzad, F. Karamat, M. Iqbal and G. Ali (2015). "Quantitative trait loci (QTLs) analysis of drought tolerance at germination stage in a wheat population derived from synthetic hexaploid and Opata." Journal of Animal and Plant Sciences **25**(2): 539-545.

Assaha, D. V., A. Ueda, H. Saneoka, R. Al-Yahyai and M. W. Yaish (2017). "The Role of Na+ and K+ Transporters in Salt Stress Adaptation in Glycophytes." Frontiers in physiology **8**.

Atta, B. M., T. Mahmood and T. M. Trethowan (2013). "Relationship between root morphology and grain yield of wheat in north-western NSW, Australia." Australian Journal of Crop Science **7**(13): 2108.

Avni, R., M. Nave, O. Barad, K. Baruch, S. O. Twardziok, H. Gundlach, I. Hale, M. Mascher, M. Spannagl and K. Wiebe (2017). "Wild emmer genome architecture and diversity elucidate wheat evolution and domestication." Science **357**(6346): 93-97.

Ayers, A. (1952). "Seed germination as affected by soil moisture and salinity." Agronomy Journal **44**(2): 82-84.

Bacu, A., K. Comashi, M. Hoxhaj and V. Ibro (2017). "GSTF1 gene expression at local Albanian wheat cultivar Dajti under salinity and heat conditions."

Badridze, G., A. Weidner, F. Asch and A. Börner (2009). "Variation in salt tolerance within a Georgian wheat germplasm collection." Genetic resources and crop evolution **56**(8): 1125-1130.

Bağci, S. A., H. Ekiz and A. Yilmaz (2003). "Determination of the salt tolerance of some barley genotypes and the characteristics affecting tolerance." Turkish Journal of Agriculture and Forestry **27**(5): 253-260.

Bänziger, M. and J.-L. Araus (2007). "Recent advances in breeding maize for drought and salinity stress tolerance." Advances in molecular breeding toward drought and salt tolerant crops: 587-601.

Bauer, A. M., F. Hoti, M. von Korff, K. Pillen, J. Leon and M. J. Sillanpaa (2009). "Advanced backcross-QTL analysis in spring barley (H. vulgare ssp spontaneum) comparing a REML versus a Bayesian model in multi-environmental field trials." Theoretical and Applied Genetics **119**(1): 105-123.

Becker, S. R., P. F. Byrne, S. D. Reid, W. L. Bauerle, J. K. McKay and S. D. Haley (2016). "Root traits contributing to drought tolerance of synthetic hexaploid wheat in a greenhouse study." Euphytica **207**(1): 213-224.

Benderradji, L., F. Brini, S. B. Amar, K. Kellou, J. Azaza, K. Masmoudi, H. Bouzerzour and M. Hanin (2011). "Sodium Transport in the Seedlings of Two Bread Wheat ('Triticum aestivum'L.) Genotypes Showing Contrasting Salt Stress Tolerance." Australian Journal of Crop Science **5**(3): 233.

Bennewitz, J., N. Reinsch and E. Kalm (2002). "Improved confidence intervals in quantitative trait loci mapping by permutation bootstrapping." Genetics **160**(4): 1673-1686.

Bernal, E. and P. Villardon (2014). "GGEBiplotGUI: interactive GGE biplots in R. 2014." Disponível em: https://cran.r-project.org/web/packages/GGEBiplotGUI/index.html Acesso em 10 (2014). **10**.

Bernier, J., A. Kumar, V. Ramaiah, D. Spaner and G. Atlin (2007). "A large-effect QTL for grain yield under reproductive-stage drought stress in upland rice." Crop Science **47**(2): 507-516.

Biosciences, L.-C. (2008). Using the LI-6400/LI-6400XT Portable Photosynthesis System, LI-COR Biosciences, Inc., Lincoln, NE.

Blažek, J., O. Jirsa and M. Hrušková (2005). "Prediction of wheat milling characteristics by near-infrared reflectance spectroscopy." Czech journal of food sciences **23**: 145-151.

Breseghello, F. and M. E. Sorrells (2006). "Association mapping of kernel size and milling quality in wheat (Triticum aestivum L.) cultivars." Genetics **172**(2): 1165-1177.

Bundessortenamt (2016). "Blatt für Sortenwesen." Amtsblatt des Bundessortenamtes.

Byrt, C. S., B. Xu, M. Krishnan, D. J. Lightfoot, A. Athman, A. K. Jacobs, N. S. Watson-Haigh, D. Plett, R. Munns and M. Tester (2014). "The Na+ transporter, TaHKT1; 5-D, limits shoot Na+ accumulation in bread wheat." The Plant Journal **80**(3): 516-526.

Byrt, C. S., M. Zhao, M. Kourghi, J. Bose, S. W. Henderson, J. Qiu, M. Gilliham, C. Schultz, M. Schwarz and S. A. Ramesh (2017). "Non-selective cation channel activity of aquaporin AtPIP2; 1 regulated by Ca2+ and pH." Plant, cell & environment **40**(6): 802-815.

Castro-Camus, E., M. Palomar and A. Covarrubias (2013). "Leaf water dynamics of Arabidopsis thaliana monitored in-vivo using terahertz time-domain spectroscopy." Scientific reports **3**.

Chandna, R., M. Azooz and P. Ahmad (2013). Recent Advances of Metabolomics to Reveal Plant Response During Salt Stress. Salt Stress in Plants, Springer**:** 1-14.

Chao, S., J. Dubcovsky, J. Dvorak, M.-C. Luo, S. P. Baenziger, R. Matnyazov, D. R. Clark, L. E. Talbert, J. A. Anderson and S. Dreisigacker (2010). "Population-and genome-specific patterns of linkage disequilibrium and SNP variation in spring and winter wheat (Triticum aestivum L.)." BMC genomics **11**(1): 727.

Chapman, J. A., M. Mascher, A. Buluç, K. Barry, E. Georganas, A. Session, V. Strnadova, J. Jenkins, S. Sehgal and L. Oliker (2015). "A whole-genome shotgun approach for assembling and anchoring the hexaploid bread wheat genome." Genome biology **16**(1): 26.

Chartzoulakis, K. and G. Klapaki (2000). "Response of two greenhouse pepper hybrids to NaCl salinity during different growth stages." Scientia Horticulturae **86**(3): 247-260.

Charu, S., Vibhut, B. Kiran and s. Bargali (2015). "Influence of seed size and salt stress on seed germination and seedling growth of wheat (Triticum aestivum)." Indian Journal of Agricultural Sciences **85**(9): 1134-1137.

Chen, J., F. Yu, Y. Liu, C. Du, X. Li, S. Zhu, X. Wang, W. Lan, P. L. Rodriguez and X. Liu (2016). "FERONIA interacts with ABI2-type phosphatases to facilitate signaling cross-talk

between abscisic acid and RALF peptide in Arabidopsis." Proceedings of the National Academy of Sciences: 201608449.

Chhipa, B. R. and P. Lal (1995). "Na/K Ratios as the Basis of Salt Tolerance in Wheat." Australian Journal of Agricultural Research **46**(3): 533-539.

Chi, Y., Y. Cheng, J. Vanitha, N. Kumar, R. Ramamoorthy, S. Ramachandran and S.-Y. Jiang (2010). "Expansion mechanisms and functional divergence of the glutathione S-transferase family in sorghum and other higher plants." DNA research **18**(1): 1-16.

Chinnusamy, V., A. Jagendorf and J. K. Zhu (2005). "Understanding and improving salt tolerance in plants." Crop Science **45**(2): 437-448.

Clair, S. B. S. and J. P. Lynch (2010). "The opening of Pandora's Box: climate change impacts on soil fertility and crop nutrition in developing countries." Plant and soil **335**(1-2): 101-115.

Clavel, D., O. Diouf, J. L. Khalfaoui and S. Braconnier (2006). "Genotypes variations in fluorescence parameters among closely related groundnut (Arachis hypogaea L.) lines and their potential for drought screening programs." Field crops research **96**(2): 296-306.

Cleveland, W. S. (1979). "Robust locally weighted regression and smoothing scatterplots." Journal of the American Statistical Association **74**(368): 829-836.

Colmer, T. D., T. J. Flowers and R. Munns (2006). "Use of wild relatives to improve salt tolerance in wheat." Journal of experimental botany **57**(5): 1059-1078.

Colmer, T. D., R. Munns and T. J. Flowers (2005). "Improving salt tolerance of wheat and barley: future prospects." Australian Journal of Experimental Agriculture **45**(11): 1425-1443.

Cramer, G. R., E. Epstein and A. Läuchli (1990). "Effects of sodium, potassium and calcium on salt-stressed barley. I. Growth analysis." Physiologia Plantarum **80**(1): 83-88.

Csiszár, J., E. Horváth, Z. Váry, Á. Gallé, K. Bela, S. Brunner and I. Tari (2014). "Glutathione transferase supergene family in tomato: salt stress-regulated expression of representative genes from distinct GST classes in plants primed with salicylic acid." Plant Physiology and Biochemistry **78**: 15-26.

Cuin, T. A., J. Bose, G. Stefano, D. Jha, M. Tester, S. Mancuso and S. Shabala (2011). "Assessing the role of root plasma membrane and tonoplast Na+/H+ exchangers in salinity tolerance in wheat: in planta quantification methods." Plant, cell & environment **34**(6): 947-961.

Cummins, I., D. O'hagan, I. Jablonkai, D. J. Cole, A. Hehn, D. Werck-Reichhart and R. Edwards (2003). "Cloning, characterization and regulation of a family of phi class glutathione transferases from wheat." Plant molecular biology **52**(3): 591-603.

Dadshani, S., A. Kurakin, S. Amanov, B. Hein, H. Rongen, S. Cranstone, U. Blievernicht, E. Menzel, J. Léon and N. Klein (2015). "Non-invasive assessment of leaf water status using a dual-mode microwave resonator." Plant methods **11**(1): 8.

Dadshani, S. A. W., A. Weidner, G. H. Buck-Sorlin, A. Börner and F. Asch (2004). "QTL Analysis for Salt Tolerance in Barley." Deutscher Tropentag 2004 - Book of Abstracts **2004**: 424.

Daniells, I., J. Holland, R. Young, C. Alston and A. Bernardi (2001). "Relationship between yield of grain sorghum (Sorghum bicolor) and soil salinity under field conditions." Australian Journal of Experimental Agriculture **41**(2): 211-217.

Das, P., K. K. Nutan, S. L. Singla-Pareek and A. Pareek (2015). "Understanding salinity responses and adopting 'omics-based'approaches to generate salinity tolerant cultivars of rice." Frontiers in plant science **6**.

De León, J. L. D., R. Escoppinichi, N. Geraldo, T. Castellanos, A. Mujeeb-Kazi and M. S. Röder (2011). "Quantitative trait loci associated with salinity tolerance in field grown bread wheat." Euphytica **181**(3): 371-383.

De Leon, T. B., S. Linscombe and P. K. Subudhi (2017). "Identification and validation of QTLs for seedling salinity tolerance in introgression lines of a salt tolerant rice landrace 'Pokkali'." PLoS One **12**(4): e0175361.

Del Blanco, I., S. Rajaram and W. Kronstad (2001). "Agronomic potential of synthetic hexaploid wheat-derived populations." Crop Science **41**(3): 670-676.

Deng, W., D. C. Nickle, G. H. Learn, B. Maust and J. I. Mullins (2007). "ViroBLAST: a stand-alone BLAST web server for flexible queries of multiple databases and user's datasets." Bioinformatics **23**(17): 2334-2336.

Denman, S. E. and C. S. McSweeney (2005). Quantitative (real-time) PCR. Methods in gut microbial ecology for ruminants, Springer**:** 105-115.

DeRose-Wilson, L. and B. S. Gaut (2011). "Mapping salinity tolerance during Arabidopsis thaliana germination and seedling growth." PLoS One **6**(8): e22832.

Díaz De León, J., R. Escoppinichi, R. Zavala-Fonseca, T. Castellanos, M. Röder and A. Mujeeb-Kazi (2010). "Phenotypic and genotypic characterization of salt-tolerant wheat genotypes." Cereal Research Communications **38**(1): 15-22.

Dixon, D. P., I. Cummins, D. J. Cole and R. Edwards (1998). "Glutathione-mediated detoxification systems in plants." Current Opinion in Plant Biology **1**(3): 258-266.

Dixon, D. P., A. Lapthorn and R. Edwards (2002). "Plant glutathione transferases." Genome biology **3**(3): reviews3004. 3001.

Dreisigacker, S., M. Kishii, J. Lage and M. Warburton (2008). "Use of synthetic hexaploid wheat to increase diversity for CIMMYT bread wheat improvement." Crop and Pasture Science **59**(5): 413-420.

Dreisigacker, S., M. Kishii, J. Lage and M. Warburton (2008). "Use of synthetic hexaploid wheat to increase diversity for CIMMYT bread wheat improvement." Australian Journal of Agricultural Research **59**(5): 413-420.

Dubcovsky, J. and J. Dvorak (2007). "Genome plasticity a key factor in the success of polyploid wheat under domestication." Science **316**(5833): 1862-1866.

Dubcovsky, J., G. Santa Maria, E. Epstein, M.-C. Luo and J. Dvořák (1996). "Mapping of the K+/Na+ discrimination locus Kna1 in wheat." Theoretical and Applied Genetics **92**(3-4): 448-454.

Dvorak, J., M.-C. Luo and E. Akhunov (2011). "NI Vavilov's theory of centres of diversity in the light of current understanding of wheat diversity, domestication and evolution." Czech Journal of Genetics and Plant Breeding **47**(Special Issue).

Dvořák, J., P. d. Terlizzi, H.-B. Zhang and P. Resta (1993). "The evolution of polyploid wheats: identification of the A genome donor species." Genome **36**(1): 21-31.

Edwards, R., D. P. Dixon and V. Walbot (2000). "Plant glutathione S-transferases: enzymes with multiple functions in sickness and in health." Trends in plant science **5**(5): 193-198.

Egamberdiyeva, D., I. Garfurova and K. ISLAM (2007). "Salinity effects on irrigated soil chemical and biological properties in the Aral Sea basin of Uzbekistan." Climate Change and Terrestrial Carbon Sequestration in Central Asia: 147.

Eshed, Y., M. Abu-Abied, Y. Saranga and D. Zamir (1992). "Lycopersicon esculentum lines containing small overlapping introgressions from L. pennellii." TAG Theoretical and Applied Genetics **83**(8): 1027-1034.

FAOSTAT (2017). FAO, Food and Agriculture Organization of the United Nations; http://www.fao.org/faostat/; (Last accessed 1 October 2017).

Feldman, M. and A. Levy (2005). "Allopolyploidy–a shaping force in the evolution of wheat genomes." Cytogenetic and genome research **109**(1-3): 250-258.

Feldman, M. and A. A. Levy (2012). "Genome evolution due to allopolyploidization in wheat." Genetics **192**(3): 763-774.

Fernandez, G. C. (1992). Effective selection criteria for assessing plant stress tolerance. Proceedings of the international symposium on adaptation of vegetables and other food crops in temperature and water stress.

Ferrazzoli, P., S. Paloscia, P. Pampaloni, G. Schiavon, D. Solimini and P. Coppo (1992). "Sensitivity of microwave measurements to vegetation biomass and soil moisture content: A case study." Geoscience and Remote Sensing, IEEE Transactions on **30**(4): 750-756.

Fiorani, F. and U. Schurr (2013). "Future scenarios for plant phenotyping." Annual review of plant biology **64**: 267-291.

Flowers, T., P. Troke and A. Yeo (1977). "The mechanism of salt tolerance in halophytes." Annual review of plant physiology **28**(1): 89-121.

Flowers, T. J. (2004). "Improving crop salt tolerance." Journal of experimental botany **55**(396): 307-319.

Flowers, T. J. and T. D. Colmer (2008). "Salinity tolerance in halophytes." New Phytologist **179**(4): 945-963.

Flowers, T. J. and S. A. Flowers (2005). "Why does salinity pose such a difficult problem for plant breeders?" Agricultural Water Management **78**(1-2): 15-24.

Flowers, T. J., A. Garcia, M. Koyama and A. R. Yeo (1997). "Breeding for salt tolerance in crop plants—the role of molecular biology." Acta Physiologiae Plantarum **19**(4): 427-433.

Flowers, T. J. and A. R. Yeo (1995). "Breeding for salinity resistance in crop plants: Where next?" Australian Journal of Plant Physiology **22**(6): 875-884.

Foolad, M. R. (1999). "Comparison of salt tolerance during seed germination and vegetative growth in tomato by QTL mapping." Genome **42**(4): 727-734.

Foolad, M. R., T. Stoltz, C. Dervinis, R. L. Rodriguez and R. A. Jones (1997). "Mapping QTLs conferring salt tolerance during germination in tomato by selective genotyping." Molecular Breeding **3**(4): 269-277.

Francois, L., T. Donovan, E. Maas and G. Rubenthaler (1988). "Effect of salinity on grain yield and quality, vegetative growth, and germination of triticale." Agronomy journal **80**(4): 642-647.

Francois, L., E. Maas, T. Donovan and V. Youngs (1986). "Effect of salinity on grain yield and quality, vegetative growth, and germination of semi-dwarf and durum wheat." Agronomy Journal **78**(6): 1053-1058.

Francois, L. E. (1994). "Growth, seed yield, and oil content of canola grown under saline conditions." Agronomy Journal **86**(2): 233-237.

Frizon, P., S. P. Brammer, M. I. P. M. Lima, R. L. d. Castro and C. C. Deuner (2017). "Genetic stability in synthetic wheat accessions: cytogenetic evaluation as a support in breeding programs." Ciência Rural **47**(4).

Frova, C. (2003). "The plant glutathione transferase gene family: genomic structure, functions, expression and evolution." Physiologia Plantarum **119**(4): 469-479.

Fujita, M., Y. Fujita, K. Maruyama, M. Seki, K. Hiratsu, M. Ohme-Takagi, L. S. P. Tran, K. Yamaguchi-Shinozaki and K. Shinozaki (2004). "A dehydration-induced NAC protein, RD26, is involved in a novel ABA-dependent stress-signaling pathway." The Plant Journal **39**(6): 863-876.

Geilfus, C.-M., K. Niehaus, V. Gödde, M. Hasler, C. Zörb, K. Gorzolka, M. Jezek, M. Senbayram, J. Ludwig-Müller and K. H. Mühling (2015). "Fast responses of metabolites in Vicia faba L. to moderate NaCl stress." Plant Physiology and Biochemistry **92**: 19-29.

Genc, Y., G. K. Mcdonald and M. Tester (2007). "Reassessment of tissue Na+ concentration as a criterion for salinity tolerance in bread wheat." Plant, cell & environment **30**(11): 1486-1498.

Genc, Y., K. Oldach, J. Taylor and G. H. Lyons (2016). "Uncoupling of sodium and chloride to assist breeding for salinity tolerance in crops." New Phytologist **210**(1): 145-156.

Genc, Y., K. Oldach, A. Verbyla, G. Lott, M. Hassan, M. Tester, H. Wallwork and G. McDonald (2010). "Sodium exclusion QTL associated with improved seedling growth in bread wheat under salinity stress." Theoretical and Applied Genetics **121**(5): 877-894.

Gill, B., B. Friebe and T. Endo (1991). "Standard karyotype and nomenclature system for description of chromosome bands and structural aberrations in wheat (Triticum aestivum)." Genome **34**(5): 830-839.

Gill, S. S. and N. Tuteja (2010). "Reactive oxygen species and antioxidant machinery in abiotic stress tolerance in crop plants." Plant Physiology and Biochemistry **48**(12): 909-930.

Gintzburger, G., H. Le Houerou and K. Toderich (2005). "The steppes of Middle Asia: post-1991 agricultural and rangeland adjustment." Arid Land Research and Management **19**(3): 215-239.

Godfray, H. C. J., J. R. Beddington, I. R. Crute, L. Haddad, D. Lawrence, J. F. Muir, J. Pretty, S. Robinson, S. M. Thomas and C. Toulmin (2010). "Food security: the challenge of feeding 9 billion people." Science **327**(5967): 812-818.

Gong, J. M., P. He, Q. A. Qian, L. S. Shen, L. H. Zhu and S. Y. Chen (1999). "Identification of salt-tolerance QTL in rice (Oryza sativa L.)." Chinese Science Bulletin **44**(1): 68-71.

Gorham, J., A. Bristol, E. M. Young, R. G. W. Jones and G. Kashour (1990). "Salt Tolerance in the Triticeae - K/Na Discrimination in Barley." Journal of experimental botany **41**(230): 1095-1101.

Gorham, J., R. W. Jones and A. Bristol (1990). "Partial characterization of the trait for enhanced K+− Na+ discrimination in the D genome of wheat." Planta **180**(4): 590-597.

Greenway, H. and R. Munns (1980). "Mechanisms of Salt Tolerance in Non-Halophytes." Annual Review of Plant Physiology and Plant Molecular Biology **31**: 149-190.

Gregorio, G. B., D. Senadhira and R. D. Mendoza (1997). Screening rice for salinity tolerance, IRRI discussion paper series.

Großkinsky, D. K., R. Pieruschka, J. Svensgaard, U. Rascher, S. Christensen, U. Schurr and T. Roitsch (2015). "Phenotyping in the fields: dissecting the genetics of quantitative traits and digital farming." New Phytologist **207**(4): 950-952.

Gupta, B. and B. Huang (2014). "Mechanism of salinity tolerance in plants: physiological, biochemical, and molecular characterization." International journal of genomics **2014**.

Haruta, M., G. Sabat, K. Stecker, B. B. Minkoff and M. R. Sussman (2014). "A peptide hormone and its receptor protein kinase regulate plant cell expansion." Science **343**(6169): 408-411.

Hawke, R., A. Mitchell and R. Keeler (1969). "Microwave Measurement of Permittivity and Electrical Conductivity in Shock Compressed Liquids." Review of Scientific Instruments **40**(5): 632-636.

Hawkesford, M. J. and A. Lorence (2017). "Plant phenotyping: increasing throughput and precision at multiple scales." Functional Plant Biology **44**(1): v-vii.

He, J.-F., R. Goyal, A. Laroche, M.-L. Zhao and Z.-X. Lu (2013). "Effects of salinity stress on starch morphology, composition and thermal properties during grain development in triticale." Canadian Journal of Plant Science **93**(5): 765-771.

Hernando-Amado, S., V. González-Calle, P. Carbonero and C. Barrero-Sicilia (2012). "The family of DOF transcription factors in Brachypodium distachyon: phylogenetic comparison with rice and barley DOFs and expression profiling." BMC plant biology **12**(1): 202.

Hoang, T. M. L., T. N. Tran, T. K. T. Nguyen, B. Williams, P. Wurm, S. Bellairs and S. Mundree (2016). "Improvement of salinity stress tolerance in rice: challenges and opportunities." Agronomy **6**(4): 54.

Holland, J. B., W. E. Nyquist and C. T. Cervantes-Martínez (2003). "Estimating and interpreting heritability for plant breeding: an update." Plant breeding reviews **22**: 9-112.

Horie, T., I. Karahara and M. Katsuhara (2012). "Salinity tolerance mechanisms in glycophytes: an overview with the central focus on rice plants." Rice **5**(1): 11.

Hossain, M. A., S. Bhattacharjee, S.-M. Armin, P. Qian, W. Xin, H.-Y. Li, D. J. Burritt, M. Fujita and L.-S. P. Tran (2015). "Hydrogen peroxide priming modulates abiotic oxidative stress tolerance: insights from ROS detoxification and scavenging." Frontiers in plant science **6**.

Huang, Q., Y. Wang, B. Li, J. Chang, M. Chen, K. Li, G. Yang and G. He (2015). "TaNAC29, a NAC transcription factor from wheat, enhances salt and drought tolerance in transgenic Arabidopsis." BMC Plant Biology **15**(1): 268.

Inal, A. (2002). "Growth, Proline Accumulation and Ionic Relations of Tomato (Lycopersicon esculentum L.) as Influenced by NaCl and Na_2SO_4 Salinity." Turkish Journal of Botany **26**(5): 285-290.

Ioannidis, J. P., G. Thomas and M. J. Daly (2009). "Validating, augmenting and refining genome-wide association signals." Nature reviews. Genetics **10**(5): 318.

Izawa, T., R. Foster, M. Nakajima, K. Shimamoto and N.-H. Chua (1994). "The rice bZIP transcriptional activator RITA-1 is highly expressed during seed development." The Plant Cell **6**(9): 1277-1287.

Jafari-Shabestari, J., H. Corke and C. O. Qualset (1995). "Field evaluation of tolerance to salinity stress in Iranian hexaploid wheat landrace accessions." Genetic Resources and Crop Evolution **42**(2): 147-156.

Jamil, A., S. Riaz, M. Ashraf and M. Foolad (2011). "Gene expression profiling of plants under salt stress." Critical Reviews in Plant Sciences **30**(5): 435-458.

Jha, S. N., K. Narsaiah, A. Basediya, R. Sharma, P. Jaiswal, R. Kumar and R. Bhardwaj (2011). "Measurement techniques and application of electrical properties for nondestructive quality evaluation of foods—a review." Journal of food science and technology **48**(4): 387-411.

Jiang, H.-W., M.-J. Liu, C. Chen, C.-H. Huang, L.-Y. Chao and H.-L. Hsieh (2010). "A glutathione S-transferase regulated by light and hormones participates in the modulation of Arabidopsis seedling development." Plant Physiology **154**(4): 1646-1658.

Jiang, Y. and M. K. Deyholos (2006). "Comprehensive transcriptional profiling of NaCl-stressed Arabidopsis roots reveals novel classes of responsive genes." BMC Plant Biology **6**(1): 25.

Johnson, M., I. Zaretskaya, Y. Raytselis, Y. Merezhuk, S. McGinnis and T. L. Madden (2008). "NCBI BLAST: a better web interface." Nucleic acids research **36**(suppl 2): W5-W9.

Jones, R. G. W., C. J. Brady and J. Speirs (1979). Ionic and Osmotic Relations in Plant Cells, R.G., Wyn Jones.

Jordens, C., M. Scheller, B. Breitenstein, D. Selmar and M. Koch (2009). "Evaluation of leaf water status by means of permittivity at terahertz frequencies." J Biol Phys **35**(3): 255-264.

Juenger, T. E., J. K. Mckay, N. Hausmann, J. J. Keurentjes, S. Sen, K. A. Stowe, T. E. Dawson, E. L. Simms and J. H. Richards (2005). "Identification and characterization of QTL underlying whole-plant physiology in Arabidopsis thaliana: δ13C, stomatal conductance and transpiration efficiency." Plant, cell & environment **28**(6): 697-708.

Kang, W.-H., S. Kim, H.-A. Lee, D. Choi and S.-I. Yeom (2016). "Genome-wide analysis of Dof transcription factors reveals functional characteristics during development and response to biotic stresses in pepper." Scientific reports **6**.

Kashem, M. A., N. Sultana, T. Ikeda, H. Hori, T. Loboda and T. Mitsui (2000). "Alteration of starch-sucrose transition in germinating wheat seed under sodium chloride salinity." Journal of Plant Biology **43**(3): 121-127.

Kasuga, M., Q. Liu, S. Miura, K. Yamaguchi-Shinozaki and K. Shinozaki (1999). "Improving plant drought, salt, and freezing tolerance by gene transfer of a single stress-inducible transcription factor." Nature biotechnology **17**(3).

Katerji, N., J. Van Hoorn, C. Fares, A. Hamdy, M. Mastrorilli and T. Oweis (2005). "Salinity effect on grain quality of two durum wheat varieties differing in salt tolerance." Agricultural Water Management **75**(2): 85-91.

Katerji, N., J. Van Hoorn, A. Hamdy, M. Mastrorilli, C. Fares, S. Ceccarelli, S. Grando and T. Oweis (2006). "Classification and salt tolerance analysis of barley varieties." Agricultural water management **85**(1): 184-192.

Kawasaki, S., C. Borchert, M. Deyholos, H. Wang, S. Brazille, K. Kawai, D. Galbraith and H. J. Bohnert (2001). "Gene expression profiles during the initial phase of salt stress in rice." The Plant Cell **13**(4): 889-905.

Kaya, M. D., A. Ipek and A. ÖZTÜRK (2003). "Effects of different soil salinity levels on germination and seedling growth of safflower (Carthamus tinctorius L.)." Turkish Journal of Agriculture and Forestry **27**(4): 221-227.

Kearsey, M. and A. Farquhar (1998). "QTL analysis in plants; where are we now?" Heredity **80**(2): 137-142.

Kent, L. and A. Läuchli (1985). "Germination and seedling growth of cotton: Salinity-calcium interactions." Plant, cell & environment **8**(2): 155-159.

Kersey, P. J., J. E. Allen, I. Armean, S. Boddu, B. J. Bolt, D. Carvalho-Silva, M. Christensen, P. Davis, L. J. Falin and C. Grabmueller (2016). "Ensembl Genomes 2016: more genomes, more complexity." Nucleic acids research **44**(D1): D574-D580.

Klein, R. J., C. Zeiss, E. Y. Chew, J.-Y. Tsai, R. S. Sackler, C. Haynes, A. K. Henning, J. P. SanGiovanni, S. M. Mane and S. T. Mayne (2005). "Complement factor H polymorphism in age-related macular degeneration." Science **308**(5720): 385-389.

Korte, A. and A. Farlow (2013). "The advantages and limitations of trait analysis with GWAS: a review." Plant methods **9**(1): 29.

Krzywinski, M., J. Schein, I. Birol, J. Connors, R. Gascoyne, D. Horsman, S. J. Jones and M. A. Marra (2009). "Circos: an information aesthetic for comparative genomics." Genome research **19**(9): 1639-1645.

Kunert, A., A. A. Naz, O. Dedeck, K. Pillen and J. Léon (2007). "AB-QTL analysis in winter wheat: I. Synthetic hexaploid wheat (T. turgidum ssp. dicoccoides× T. tauschii) as a source of favourable alleles for milling and baking quality traits." Theoretical and Applied Genetics **115**(5): 683-695.

Kurusu, T., K. Kuchitsu and Y. Tada (2015). "Plant signaling networks involving Ca2+ and Rboh/Nox-mediated ROS production under salinity stress." Frontiers in plant science **6**.

Kutnjak, D., S. F. Elena and M. Ravnikar (2017). "Time-sampled population sequencing reveals the interplay of selection and genetic drift in experimental evolution of Potato virus Y." Journal of Virology: JVI. 00690-00617.

Labrou, N. E., A. C. Papageorgiou, O. Pavli and E. Flemetakis (2015). "Plant GSTome: structure and functional role in xenome network and plant stress response." Current Opinion in Biotechnology **32**: 186-194.

Lamb, C. and R. A. Dixon (1997). "The oxidative burst in plant disease resistance." Annual review of plant biology **48**(1): 251-275.

Lan, T., Z.-L. Yang, X. Yang, Y.-J. Liu, X.-R. Wang and Q.-Y. Zeng (2009). "Extensive functional diversification of the Populus glutathione S-transferase supergene family." The Plant Cell **21**(12): 3749-3766.

Landi, S., J.-F. Hausman, G. Guerriero and S. Esposito (2017). "Poaceae vs. Abiotic Stress: Focus on Drought and Salt Stress, Recent Insights and Perspectives." Frontiers in plant science **8**.

Lange, W. and G. Jochemsen (1992). "Use of the Gene Pools of Triticum-Turgidum Ssp Dicoccoides and Aegilops-Squarrosa for the Breeding of Common Wheat (Triticum-Aestivum), through Chromosome-Doubled Hybrids . 2. Morphology and Meiosis of the Amphiploids." Euphytica **59**(2-3): 213-220.

Läuchli, A. and S. Grattan (2007). Plant growth and development under salinity stress. Advances in molecular breeding toward drought and salt tolerant crops, Springer**:** 1-32.

Lauter, D. and D. Munns (1986). "Salt resistance of chickpea genotypes in solutions salinized with NaCl or Na 2 SO 4." Plant and soil **95**(2): 271-279.

Lee, S. C. and S. Luan (2012). "ABA signal transduction at the crossroad of biotic and abiotic stress responses." Plant, cell & environment **35**(1): 53-60.

Li, C., H.-M. Wu and A. Y. Cheung (2016). "FERONIA and her pals: functions and mechanisms." Plant physiology **171**(4): 2379-2392.

Li, H., W. Huang, Z.-W. Liu, Y.-X. Wang and J. Zhuang (2016). "Transcriptome-Based Analysis of Dof Family Transcription Factors and Their Responses to Abiotic Stress in Tea Plant (Camellia sinensis)." International journal of genomics **2016**.

Li, Q., A. Yang and W.-H. Zhang (2017). "Comparative studies on tolerance of rice genotypes differing in their tolerance to moderate salt stress." BMC Plant Biology **17**(1): 141.

Lindemose, S., C. O'Shea, M. K. Jensen and K. Skriver (2013). "Structure, function and networks of transcription factors involved in abiotic stress responses." International journal of molecular sciences **14**(3): 5842-5878.

Lindsay, M. P., E. S. Lagudah, R. A. Hare and R. Munns (2004). "A locus for sodium exclusion (Nax1), a trait for salt tolerance, mapped in durum wheat." Functional Plant Biology **31**(11): 1105-1114.

Liu, H.-J., Z.-X. Tang, X.-M. Han, Z.-L. Yang, F.-M. Zhang, H.-L. Yang, Y.-J. Liu and Q.-Y. Zeng (2015). "Divergence in enzymatic activities in the soybean GST supergene family provides new insight into the evolutionary dynamics of whole-genome duplicates." Molecular biology and evolution **32**(11): 2844-2859.

Livak, K. J. and T. D. Schmittgen (2001). "Analysis of relative gene expression data using real-time quantitative PCR and the 2− ΔΔCT method." methods **25**(4): 402-408.

Luo, J.-Y., S. Zhang, J. Peng, X.-Z. Zhu, L.-M. Lv, C.-Y. Wang, C.-H. Li, Z.-G. Zhou and J.-J. Cui (2017). "Effects of soil salinity on the expression of Bt toxin (Cry1Ac) and the control efficiency of Helicoverpa armigera in field-grown transgenic Bt cotton." PLoS One **12**(1): e0170379.

Luo, M., Y. Zhao, R. Zhang, J. Xing, M. Duan, J. Li, N. Wang, W. Wang, S. Zhang and Z. Chen (2017). "Mapping of a major QTL for salt tolerance of mature field-grown maize plants based on SNP markers." BMC Plant Biology **17**(1): 140.

Ma, J., M.-Y. Li, F. Wang, J. Tang and A.-S. Xiong (2015). "Genome-wide analysis of Dof family transcription factors and their responses to abiotic stresses in Chinese cabbage." Bmc Genomics **16**(1): 33.

Ma, J., J. Stiller, Z. Zheng, Y.-X. Liu, Y. Wei, Y.-L. Zheng and C. Liu (2015). "A high-throughput pipeline for detecting locus-specific polymorphism in hexaploid wheat (Triticum aestivum L.)." Plant methods **11**(1): 1.

Maas, E. and J. Poss (1989). "Salt sensitivity of cowpea at various growth stages." Irrigation Science **10**(4): 313-320.

Maathuis, F. J., I. Ahmad and J. Patishtan (2014). "Regulation of Na+ fluxes in plants." Frontiers in plant science **5**.

Mackay, I. and W. Powell (2007). "Methods for linkage disequilibrium mapping in crops." Trends in plant science **12**(2): 57-63.

Mackay, T. F. (2009). "Q&A: Genetic analysis of quantitative traits." Journal of Biology **8**(3): 23.

Madejczyk, M. and D. Baralkiewicz (2008). "Characterization of Polish rape and honeydew honey according to their mineral contents using ICP-MS and F-AAS/AES." Analytica Chimica Acta **617**(1): 11-17.

Mano, Y., H. Takahashi, K. Sato and K. Takeda (1996). "Mapping genes for callus growth and shoot regeneration in barley (Hordeum vulgare L)." Breeding Science **46**(2): 137-142.

Mano, Y. and K. Takeda (1997). "Mapping quantitative trait loci for salt tolerance at germination and the seedling stage in barley (Hordeum vulgare L)." Euphytica **94**(3): 263-272.

Mano, Y. and K. Takeda (1998). "Genetic resources of salt tolerance in wild Hordeum species." Euphytica **103**(1): 137-141.

Manolio, T. A. (2010). "Genomewide association studies and assessment of the risk of disease." New England Journal of Medicine **363**(2): 166-176.

Mansour, M. M. F. (2014). "The plasma membrane transport systems and adaptation to salinity." Journal of plant physiology **171**(18): 1787-1800.

Mao, X., H. Zhang, X. Qian, A. Li, G. Zhao and R. Jing (2012). "TaNAC2, a NAC-type wheat transcription factor conferring enhanced multiple abiotic stress tolerances in Arabidopsis." Journal of experimental botany **63**(8): 2933-2946.

Marcussen, T., S. R. Sandve, L. Heier, M. Spannagl, M. Pfeifer, K. S. Jakobsen, B. B. Wulff, B. Steuernagel, K. F. Mayer and O.-A. Olsen (2014). "Ancient hybridizations among the ancestral genomes of bread wheat." Science **345**(6194): 1250092.

Markwell, J., J. C. Osterman and J. L. Mitchell (1995). "Calibration of the Minolta SPAD-502 leaf chlorophyll meter." Photosynthesis Research **46**(3): 467-472.

Martínez-Márquez, A., M. J. Martínez-Esteso, M. T. Vilella-Antón, S. Sellés-Marchart, J. A. Morante-Carriel, E. Hurtado, J. Palazon and R. Bru-Martínez (2017). "A Tau Class Glutathione-S-Transferase is Involved in Trans-Resveratrol Transport Out of Grapevine Cells." Frontiers in plant science **8**(1457).

Matar, Y., H. W. Döring and H. Marschner (1975). "Auswirkungen von NaCl und Na2 SO4 auf Substanzbildung, Mineralstoffgehalt und Inhaltsstoffe bei Spinat und Salat." Journal of Plant Nutrition and Soil Science **138**(3): 295-307.

McFadden, E. and E. Sears (1944). The artificial synthesis of Triticum spelta.

Menzel, M. I., S. Tittmann, J. Buehler, S. Preis, N. Wolters, S. Jahnke, A. Walter, A. Chlubek, A. Leon and N. Hermes (2009). "Non-invasive determination of plant biomass with microwave resonators." Plant, cell & environment **32**(4): 368-379.

Mian, A. A., P. Senadheera and F. J. Maathuis (2011). "Improving crop salt tolerance: anion and cation transporters as genetic engineering targets." Plant Stress **5**: 64-72.

Miller, G., N. Suzuki, S. CIFTCI-YILMAZ and R. Mittler (2010). "Reactive oxygen species homeostasis and signalling during drought and salinity stresses." Plant, cell & environment **33**(4): 453-467.

Møller, I. M., P. E. Jensen and A. Hansson (2007). "Oxidative modifications to cellular components in plants." Annu. Rev. Plant Biol. **58**: 459-481.

Mondal, S., J. E. Rutkoski, G. Velu, P. K. Singh, L. A. Crespo-Herrera, C. Guzmán, S. Bhavani, C. Lan, X. He and R. P. Singh (2016). "Harnessing Diversity in Wheat to Enhance Grain Yield, Climate Resilience, Disease and Insect Pest Resistance and Nutrition Through Conventional and Modern Breeding Approaches." Frontiers in plant science **7**(991).

Moons, A. (2003). "Osgstu3 and osgtu4, encoding tau class glutathione S-transferases, are heavy metal-and hypoxic stress-induced and differentially salt stress-responsive in rice roots." FEBS letters **553**(3): 427-432.

Mori, I. C. and J. I. Schroeder (2004). "Reactive oxygen species activation of plant Ca2+ channels. A signaling mechanism in polar growth, hormone transduction, stress signaling, and hypothetically mechanotransduction." Plant physiology **135**(2): 702-708.

Mujeeb-Kazi, A., V. Rosas and S. Roldan (1996). "Conservation of the genetic variation of Triticum tauschii (Coss.) Schmalh.(Aegilops squarrosa auct. non L.) in synthetic hexaploid wheats (T. turgidum L. s. lat. x T. tauschii; 2n= 6x= 42, AABBDD) and its potential utilization for wheat improvement." Genetic Resources and Crop Evolution **43**(2): 129-134.

Munns, R. (2005). "Genes and salt tolerance: bringing them together." New Phytologist **167**(3): 645-663.

Munns, R. (2011). "Plant adaptations to salt and water stress: differences and commonalities." Advances in botanical research **57**: 1-32.

Munns, R. and M. Gilliham (2015). "Salinity tolerance of crops–what is the cost?" New Phytologist **208**(3): 668-673.

Munns, R., J. M. Guo, J. B. Passioura and G. R. Cramer (2000). "Leaf water status controls day-time but not daily rates of leaf expansion in salt-treated barley." Australian Journal of Plant Physiology **27**(10): 949-957.

Munns, R., S. Husain, A. R. Rivelli, R. A. James, A. G. Condon, M. P. Lindsay, E. S. Lagudah, D. P. Schachtman and R. A. Hare (2002). "Avenues for increasing salt tolerance of crops, and the role of physiologically based selection traits." Plant and soil **247**(1): 93-105.

Munns, R. and R. A. James (2003). "Screening methods for salinity tolerance: a case study with tetraploid wheat." Plant and soil **253**(1): 201-218.

Munns, R., R. A. James, M. Gilliham, T. J. Flowers and T. D. Colmer (2016). "Tissue tolerance: an essential but elusive trait for salt-tolerant crops." Functional Plant Biology **43**(12): 1103-1113.

Munns, R., R. A. James and A. Läuchli (2006). "Approaches to increasing the salt tolerance of wheat and other cereals." Journal of experimental botany **57**(5): 1025-1043.

Munns, R., R. A. James, X. R. Sirault, R. T. Furbank and H. G. Jones (2010). "New phenotyping methods for screening wheat and barley for beneficial responses to water deficit." Journal of experimental botany **61**(13): 3499-3507.

Munns, R. and H. M. Rawson (1999). "Effect of salinity on salt accumulation and reproductive development in the apical meristem of wheat and barley." Australian Journal of Plant Physiology **26**(5): 459-464.

Munns, R., D. Schachtman and A. Condon (1995). "The significance of a two-phase growth response to salinity in wheat and barley." Functional Plant Biology **22**(4): 561-569.

Munns, R. and M. Tester (2008). "Mechanisms of salinity tolerance." Annu. Rev. Plant Biol. **59**: 651-681.

Munyampundu, J.-P., Y.-P. Xu and X.-Z. Cai (2016). "Phi class of glutathione S-transferase gene superfamily widely exists in nonplant taxonomic groups." Evolutionary bioinformatics online **12**: 59.

Mutlu, A. C., I. H. Boyaci, H. E. Genis, R. Ozturk, N. Basaran-Akgul, T. Sanal and A. K. Evlice (2011). "Prediction of wheat quality parameters using near-infrared spectroscopy and artificial neural networks." European food research and technology **233**(2): 267-274.

Myles, S., J. Peiffer, P. J. Brown, E. S. Ersoz, Z. Zhang, D. E. Costich and E. S. Buckler (2009). "Association mapping: critical considerations shift from genotyping to experimental design." The Plant Cell **21**(8): 2194-2202.

Nahar, K., M. Hasanuzzaman and M. Fujita (2016). "Physiological Roles of Glutathione in Conferring Abiotic Stress Tolerance to Plants." Abiotic Stress Response in Plants.

Narasimhamoorthy, B., B. Gill, A. Fritz, J. Nelson and G. Brown-Guedira (2006). "Advanced backcross QTL analysis of a hard winter wheat× synthetic wheat population." Theoretical and Applied Genetics **112**(5): 787-796.

Naserian, B., M. Zamani and C. Vedadi (2014). "Effects of Drought and Salinity as Abiotic Stresses on Some Qualitative Traits of Iranian Wheat Genotypes." Romanian Biotechnological Letters **19**(2): 9212.

Naz, A. A., A. Kunert, V. Lind, K. Pillen and J. Léon (2008). "AB-QTL analysis in winter wheat: II. Genetic analysis of seedling and field resistance against leaf rust in a wheat advanced backcross population." Theoretical and Applied Genetics **116**(8): 1095-1104.

Nedjimi, B. and Y. Daoud (2006). Effect of Na 2 SO 4 on the growth, water relations, proline, total soluble sugars and ion content of Atriplex halimus subsp. schweinfurthii through in vitro culture. Anales de Biología.

Negrão, S., S. Schmöckel and M. Tester (2016). "Evaluating physiological responses of plants to salinity stress." Annals of Botany: mcw191.

Nelson, J. C., M. E. Sorrells, A. Van Deynze, Y. H. Lu, M. Atkinson, M. Bernard, P. Leroy, J. D. Faris and J. A. Anderson (1995). "Molecular mapping of wheat: major genes and rearrangements in homoeologous groups 4, 5, and 7." Genetics **141**(2): 721-731.

Neumann, P., H. Azaizeh and D. Leon (1994). "Hardening of root cell walls: a growth inhibitory response to salinity stress." Plant, cell & environment **17**(3): 303-309.

Neumann, P. M. (1995). "Inhibition of root growth by salinity stress: Toxicity or an adaptive biophysical response?" DEVELOPMENTS IN PLANT AND SOIL SCIENCES **58**: 299-299.

Nevo, E. and G. Chen (2010). "Drought and salt tolerances in wild relatives for wheat and barley improvement." Plant, cell & environment **33**(4): 670-685.

Nianiou-Obeidat, I., P. Madesis, C. Kissoudis, G. Voulgari, E. Chronopoulou, A. Tsaftaris and N. E. Labrou (2017). "Plant glutathione transferase-mediated stress tolerance: functions and biotechnological applications." Plant Cell Reports: 1-15.

Niazi, A., A. Ramezani and A. Dinari (2014). "GSTF1 Gene Expression Analysis in Cultivated Wheat Plants under Salinity and ABA Treatments." Molecular biology research communications **3**(1): 9.

Nicot, N., J.-F. Hausman, L. Hoffmann and D. Evers (2005). "Housekeeping gene selection for real-time RT-PCR normalization in potato during biotic and abiotic stress." Journal of experimental botany **56**(421): 2907-2914.

Noctor, G., A. Mhamdi, S. Chaouch, Y. Han, J. Neukermans, B. MARQUEZ-GARCIA, G. Queval and C. H. Foyer (2012). "Glutathione in plants: an integrated overview." Plant, cell & environment **35**(2): 454-484.

Ogbonnaya, F., G. Halloran and E. Lagudah (2005). "D genome of wheat—60 years on from Kihara, Sears and McFadden." Frontiers of wheat bioscience (Wheat Information Service No. 100)'.(Ed. K Tsunewaki) pp: 205-220.

Ogbonnaya, F. C., O. Abdalla, A. Mujeeb-Kazi, A. G. Kazi, S. S. Xu, N. Gosman, E. S. Lagudah, D. Bonnett, M. E. Sorrells and H. Tsujimoto (2013). "Synthetic hexaploids: harnessing species of the primary gene pool for wheat improvement." Plant Breeding Reviews, Volume 37: 35-122.

Ohnishi, T., S. Sugahara, T. Yamada, K. Kikuchi, Y. Yoshiba, H.-Y. Hirano and N. Tsutsumi (2005). "OsNAC6, a member of the NAC gene family, is induced by various stresses in rice." Genes & genetic systems **80**(2): 135-139.

Okamoto, M. (1957). "Asynaptic effect of chromosome V." Wheat Inf. Serv. **5**: 6.

Okçu, G., M. D. Kaya and M. Atak (2005). "Effects of salt and drought stresses on germination and seedling growth of pea (Pisum sativum L.)." Turkish journal of agriculture and forestry **29**(4): 237-242.

Oliveros, J. C. (2007). "VENNY. An interactive tool for comparing lists with Venn Diagrams; http://bioinfogp.cnb.csic.es/tools/venny/index.html."

Ott, J., J. Wang and S. M. Leal (2015). "Genetic linkage analysis in the age of whole-genome sequencing." Nature Reviews Genetics **16**(5): 275-284.

Ovcharenko, I., G. G. Loots, B. M. Giardine, M. Hou, J. Ma, R. C. Hardison, L. Stubbs and W. Miller (2005). "Mulan: multiple-sequence local alignment and visualization for studying function and evolution." Genome research **15**(1): 184-194.

Pascual, L., E. Albert, C. Sauvage, J. Duangjit, J.-P. Bouchet, F. Bitton, N. Desplat, D. Brunel, M.-C. Le Paslier and N. Ranc (2016). "Dissecting quantitative trait variation in the resequencing era: complementarity of bi-parental, multi-parental and association panels." Plant Science **242**: 120-130.

Passioura, J. B. and R. Munns (2000). "Rapid environmental changes that affect leaf water status induce transient surges or pauses in leaf expansion rate." Functional Plant Biology **27**(10): 941-948.

Peng, J. H., D. Sun and E. Nevo (2011). "Domestication evolution, genetics and genomics in wheat." Molecular Breeding **28**(3): 281.

Pessarakli, M. (2011). Handbook of plant and crop stress. Boca Raton, CRC Press.

Pessarakli, M. (2014). Handbook of plant and crop physiology, CRC press.

Pitman, M. (1977). "Ion transport into the xylem." Annual Review of Plant Physiology **28**(1): 71-88.

Plamenov, D. and P. Spetsov (2011). "Synthetic hexaploid lines are valuable resources for biotic stress resistance in wheat improvement." Journal of Plant Pathology: 251-262.

Platten, J. D., J. A. Egdane and A. M. Ismail (2013). "Salinity tolerance, Na+ exclusion and allele mining of HKT1; 5 in Oryza sativa and O. glaberrima: many sources, many genes, one mechanism?" BMC plant biology **13**(1): 32.

Pleijel, H., L. Skärby, G. Wallin and G. Sellden (1991). "Yield and grain quality of spring wheat (Triticum aestivum L., cv. Drabant) exposed to different concentrations of ozone in open-top chambers." Environmental Pollution **69**(2-3): 151-168.

Pojić, M. M. and J. S. Mastilović (2013). "Near infrared spectroscopy - advanced analytical tool in wheat breeding, trade, and processing." Food and Bioprocess Technology **6**(2): 330-352.

Poorter, H., F. Fiorani, M. Stitt, U. Schurr, A. Finck, Y. Gibon, B. Usadel, R. Munns, O. K. Atkin, F. Tardieu and T. L. Pons (2012). "The art of growing plants for experimental purposes: a practical guide for the plant biologist." Functional Plant Biology **39**(11): 821-838.

Porch, T. G. (2006). "Application of stress indices for heat tolerance screening of common bean." Journal of agronomy and crop science **192**(5): 390-394.

Pozar, D. M. (1998). Microwave Engineering, Ch. 8, Wiley, New York.

Pozzi, C., L. Rossini, A. Vecchietti and F. Salamini (2004). Gene and genome changes during domestication of cereals. Cereal genomics, Springer**:** 165-198.

Pritchard, D., P. Hollington, W. Davies, J. Gorham, J. D. de Leon and A. Mujeeb-Kazi (2002). "K+/Na+ discrimination in synthetic hexaploid wheat lines: Transfer of the trait for K+/Na+ discrimination from Aegilops tauschii into a Triticum turgidum background." Cereal Research Communications: 261-267.

Pritchard, D. J., P. A. Hollington, W. P. Davies, J. Gorham, J. L. D. de Leon and A. Mujeeb-Kazi (2002). "K+/Na+ discrimination in synthetic hexaploid wheat lines: Transfer of the trait for K+/Na+ discrimination from Aegilops tauschii into a Triticum turgidum background." Cereal Research Communications **30**(3-4): 261-267.

Puntamkar, S., D. Sharma, O. Sharma and S. Seth (1970). "Effect of common salts of sodium and calcium on the germination of different wheat varieties (Triticum aestivum L.)." Indian Journal of Plant Physiology **13**: 233-239.

Qados, A. M. A. (2011). "Effect of salt stress on plant growth and metabolism of bean plant Vicia faba (L.)." Journal of the Saudi Society of Agricultural Sciences **10**(1): 7-15.

R Core Team (2016). "R: A language and environment for statistical computing. R Foundation for Statistical Computing, Vienna, Austria. 2015. URL h ttp." www. R-project. org.

Rad, H. E., F. Aref, M. Khaledian, M. Rezaei, E. Amiri and O. Y. Falakdehy (2011). "The effects of salinity at different growth stage on rice yield. Effets de la salinite de l'eau sur le rendement du riz aux differents stades de croissance."

Rajendran, K., M. Tester and S. J. Roy (2009). "Quantifying the three main components of salinity tolerance in cereals." Plant, cell & environment **32**(3): 237-249.

Rani, R. J. and C. M. Rose (2012). "Salt Stress Tolerance and Stress Proteins in Wheat." International Research Journal of Pharmacy **3**(3).

Rao, K., A. Raghavendra and K. Reddy (2006). Physiology and molecular biology of stress tolerance, Springer.

Ravi, K., V. Vadez, S. Isobe, R. Mir, Y. Guo, S. Nigam, M. Gowda, T. Radhakrishnan, D. Bertioli and S. Knapp (2011). "Identification of several small main-effect QTLs and a large number of epistatic QTLs for drought tolerance related traits in groundnut (Arachishypogaea L.)." Theoretical and Applied Genetics **122**(6): 1119-1132.

Ren, Z. H., J. P. Gao, L. G. Li, X. L. Cai, W. Huang, D. Y. Chao, M. Z. Zhu, Z. Y. Wang, S. Luan and H. X. Lin (2005). "A rice quantitative trait locus for salt tolerance encodes a sodium transporter." Nature genetics **37**(10): 1141-1146.

Reynolds, M., F. Dreccer and R. Trethowan (2006). "Drought-adaptive traits derived from wheat wild relatives and landraces." Journal of experimental botany **58**(2): 177-186.

Rezaei, M., E. Ebrahimi, S. Naseh and M. Mohajerpour (2012). "A new 1.4-GHz soil moisture sensor." Measurement **45**(7): 1723-1728.

Rhodes, D., A. Nadolska-Orczyk and P. Rich (2002). Salinity, osmolytes and compatible solutes. Salinity: Environment-plants-molecules, Springer**:** 181-204.

Richards, R. (1983). "Should selection for yield in saline regions be made on saline or non-saline soils?" Euphytica **32**(2): 431-438.

Richards, R., C. Dennett, C. Qualset, E. Epstein, J. Norlyn and M. Winslow (1987). "Variation in yield of grain and biomass in wheat, barley, and triticale in a salt-affected field." Field crops research **15**(3-4): 277-287.

Rickman, R., B. Klepper and R. Belford (1985). Developmental relationships among roots, leaves and tillers in winter wheat. Wheat Growth and Modelling, Springer**:** 83-98.

Riley, R. and V. Chapman (1958). "Genetic control of the cytologically diploid behaviour of hexaploid wheat." Nature **182**(4637): 713-715.

Riley, T., E. Sontag, P. Chen and A. Levine (2008). "Transcriptional control of human p53-regulated genes." Nature reviews. Molecular cell biology **9**(5): 402.

Rocha, F. d., F. Bermudez, M. C. Ferreira, K. C. d. Oliveira and J. B. Pinheiro (2014). "Effective selection criteria for assessing the resistance of stink bugs complex in soybean." Crop Breeding and Applied Biotechnology **14**(3): 174-179.

Rogers, M., C. Grieve and M. Shannon (1998). "The response of lucerne (Medicago sativa L.) to sodium sulphate and chloride salinity." Plant and Soil **202**(2): 271-280.

Roy, S. J., S. Negrão and M. Tester (2014). "Salt resistant crop plants." Current Opinion in Biotechnology **26**: 115-124.

Rustgi, S., M. N. Shafqat, N. Kumar, P. S. Baenziger, M. L. Ali, I. Dweikat, B. T. Campbell and K. S. Gill (2013). "Genetic dissection of yield and its component traits using high-density composite map of wheat chromosome 3A: bridging gaps between QTLs and underlying genes." PLoS One **8**(7): e70526.

Saade, S., A. Maurer, M. Shahid, H. Oakey, S. M. Schmöckel, S. Negrão, K. Pillen and M. Tester (2016). "Yield-related salinity tolerance traits identified in a nested association mapping (NAM) population of wild barley." Scientific Reports **6**.

Sakiroglu, M., S. Sherman-Broyles, A. Story, K. J. Moore, J. J. Doyle and E. C. Brummer (2012). "Patterns of linkage disequilibrium and association mapping in diploid alfalfa (M. sativa L.)." Theoretical and Applied Genetics **125**(3): 577-590.

Sanchez, D. H., F. L. Pieckenstain, J. Szymanski, A. Erban, M. Bromke, M. A. Hannah, U. Kraemer, J. Kopka and M. K. Udvardi (2011). "Comparative functional genomics of salt stress in related model and cultivated plants identifies and overcomes limitations to translational genomics." PLoS One **6**(2): e17094.

Sancho-Knapik, D., J. Gismero, A. Asensio, J. J. Peguero-Pina, V. Fernández, T. G. Álvarez-Arenas and E. Gil-Pelegrín (2011). "Microwave l-band (1730MHz) accurately estimates the relative water content in poplar leaves. A comparison with a near infrared water index (R 1300 /R 1450)." Agricultural and Forest Meteorology **151**(7): 827-832.

Sandermann, H. (2004). "Molecular ecotoxicology of plants." Trends in plant science **9**(8): 406-413.

SAS Institute, C., NC, USA (2015). "The SAS system for Windows, release 9.4. TS Level 1M3."

Sayed, H. I. (1985). "Diversity of salt tolerance in a germplasm collection of wheat (Triticum spp.)." TAG Theoretical and Applied Genetics **69**(5): 651-657.

Schachtman, D. P. and J. I. Schroeder (1994). "Structure and transport mechanism of a high-affinity potassium uptake transporter from higher plants." Nature **370**(6491): 655-658.

Schmalenbach, I., N. Korber and K. Pillen (2008). "Selecting a set of wild barley introgression lines and verification of QTL effects for resistance to powdery mildew and leaf rust." Theoretical and Applied Genetics **117**(7): 1093-1106.

Schmalenbach, I., J. Léon and K. Pillen (2009). "Identification and verification of QTLs for agronomic traits using wild barley introgression lines." Theoretical and Applied Genetics **118**(3): 483-497.

Schmalenbach, I. and K. Pillen (2009). "Detection and verification of malting quality QTLs using wild barley introgression lines." Theoretical and Applied Genetics **118**(8): 1411-1427.

Shabala, S. (2013). "Learning from halophytes: physiological basis and strategies to improve abiotic stress tolerance in crops." Annals of Botany **112**(7): 1209-1221.

Shannon, M. C. (1997). "Adaptation of plants to salinity." Advances in agronomy **60**: 75-120.

Shao, H., H. Wang and X. Tang (2015). "NAC transcription factors in plant multiple abiotic stress responses: progress and prospects." Frontiers in plant science **6**.

Sharma, R. (2015). "Genotypic Response to Salt Stress: I–Relative Tolerance of Certain Wheat Cultivars to Salinity." Advances in Crop Science and Technology.

Sharma, R., E. Duveiller, S. Gyawali, S. Shrestha, N. Chaudhary and M. Bhatta (2004). "Resistance to Helminthosporium leaf blight and agronomic performance of spring wheat genotypes of diverse origins." Euphytica **139**(1): 33-44.

Sharma, R., A. Sahoo, R. Devendran and M. Jain (2014). "Over-expression of a rice tau class glutathione s-transferase gene improves tolerance to salinity and oxidative stresses in Arabidopsis." PLoS One **9**(3): e92900.

Sharma, R. C., S. Islomov, T. Yulshadev, Z. Khalikulov and Z. Ziyadullaev (2011). "Diversity among winter wheat germplasm for NDVI (normalized difference vegetation index) under terminal heat stress in central asia." Diversity, characterization and utilization of plant genetic resources for enhanced resilience to climate change: 40.

Sharma, R. C., A. I. Morgounov, H. J. Braun, B. Akin, M. Keser, Y. Kaya, Z. Khalikulov, M. V. Ginkel, A. Yahyaoui and S. Rajaram (2012). "Yield stability analysis of winter wheat genotypes targeted to semi-arid environments in the international winter wheat improvement program."

Shavrukov, Y. (2012). "Salt stress or salt shock: which genes are we studying?" Journal of experimental botany **64**(1): 119-127.

Shavrukov, Y., Y. Genc and J. Hayes (2012). The use of hydroponics in abiotic stress tolerance research. Hydroponics-A Standard Methodology for Plant Biological Researches, InTech.

Shavrukov, Y., N. Shamaya, M. Baho, J. Edwards, C. Ramsey, E. Nevo, P. Langridge and M. Tester (2011). "Salinity tolerance and Na+ exclusion in wheat: variability, genetics, mapping populations and QTL analysis." Czech Journal of Genetics and Plant Breeding **47**(Special Issue).

Shen, Q., P. Zhang and T. Ho (1996). "Modular nature of abscisic acid (ABA) response complexes: composite promoter units that are necessary and sufficient for ABA induction of gene expression in barley." The Plant Cell **8**(7): 1107-1119.

Shiferaw, B., M. Smale, H.-J. Braun, E. Duveiller, M. Reynolds and G. Muricho (2013). "Crops that feed the world 10. Past successes and future challenges to the role played by wheat in global food security." Food Security **5**(3): 291-317.

Shin, J.-H., S. Blay, B. McNeney and J. Graham (2006). "LDheatmap: an R function for graphical display of pairwise linkage disequilibria between single nucleotide polymorphisms." Journal of Statistical Software **16**(3): 1-10.

Shrivastava, P. and R. Kumar (2015). "Soil salinity: a serious environmental issue and plant growth promoting bacteria as one of the tools for its alleviation." Saudi journal of biological sciences **22**(2): 123-131.

Singh, B. and A. K. Singh (2015). Marker-assisted plant breeding: principles and practices, Springer.

Singh, J., E. V. D. Sastry and V. Singh (2012). "Effect of salinity on tomato (Lycopersicon esculentum Mill.) during seed germination stage." Physiology and Molecular Biology of Plants **18**(1): 45-50.

Song, Q., C. Liu, D. G. Bachir, L. Chen and Y.-G. Hu (2017). "Drought resistance of new synthetic hexaploid wheat accessions evaluated by multiple traits and antioxidant enzyme activity." Field crops research **210**: 91-103.

Stadtwere-Bonn (2013). Wasseranalyse

Star, B. and H. G. Spencer (2013). "Effects of genetic drift and gene flow on the selective maintenance of genetic variation." Genetics **194**(1): 235-244.

Steinberger, J., D. Meyer, G. Zimmermann and F. Zeller (1995). "New quality classes of German wheat cultivars." Getreide Mehl und Brot (Germany).

Suzuki, N., S. Koussevitzky, R. Mittler and G. Miller (2012). "ROS and redox signalling in the response of plants to abiotic stress." Plant, cell & environment **35**(2): 259-270.

Szabolcs, I. and J. Fink (1974). Salt affected soils in Europe, Martinus Nijhoff The Hague.

Székely, G., E. Ábrahám, Á. Cséplő, G. Rigó, L. Zsigmond, J. Csiszár, F. Ayaydin, N. Strizhov, J. Jásik and E. Schmelzer (2008). "Duplicated P5CS genes of Arabidopsis play distinct roles in stress regulation and developmental control of proline biosynthesis." The Plant Journal **53**(1): 11-28.

Talbot, S., F. Ogbonnaya, K. Chalmers and D. Mather (2008). Is synthetic hexaploid wheat a useful germplasm source for increasing grain size and yield in bread wheat breeding? 11th International Wheat Genetics Symposium 2008 Proceedings, Sydney University Press.

Tang, Y., C. Li, W. Yang, Y. Wu, X. Wu, C. Wu, X. Ma, S. Li and G. Rosewarne (2016). "Quality potential of synthetic-derived commercial wheat cultivars in south-western China." Crop and Pasture Science **67**(6): 583-593.

Tanksley, S. and J. Nelson (1996). "Advanced backcross QTL analysis: a method for the simultaneous discovery and transfer of valuable QTLs from unadapted germplasm into elite breeding lines." Theoretical and Applied Genetics **92**(2): 191-203.

Tanksley, S. D. (1993). "Mapping polygenes." Annual review of genetics **27**(1): 205-233.

Tanksley, S. D. and S. R. McCouch (1997). "Seed banks and molecular maps: unlocking genetic potential from the wild." Science **277**(5329): 1063-1066.

Tardieu, F., R. K. Varshney and R. Tuberosa (2017). "Improving crop performance under drought–cross-fertilization of disciplines." Journal of experimental botany **68**(7): 1393-1398.

Tenea, G. N., A. P. Bota, F. C. Raposo and A. Maquet (2011). "Reference genes for gene expression studies in wheat flag leaves grown under different farming conditions." BMC research notes **4**(1): 373.

Terwilliger, J. D. and K. M. Weiss (1998). "Linkage disequilibrium mapping of complex disease: fantasy or reality?" Current Opinion in Biotechnology **9**(6): 578-594.

Tester, M. and R. Davenport (2003). "Na+ tolerance and Na+ transport in higher plants." Annals of Botany **91**(5): 503-527.

Thoen, M. P., N. H. Davila Olivas, K. J. Kloth, S. Coolen, P. P. Huang, M. G. Aarts, J. A. Bac-Molenaar, J. Bakker, H. J. Bouwmeester and C. Broekgaarden (2017). "Genetic architecture of plant stress resistance: multi-trait genome-wide association mapping." New Phytologist **213**(3): 1346-1362.

Thomas, D. and N. Middleton (1993). "Salinization: new perspectives on a major desertification issue." Journal of Arid Environments **24**(1): 95-105.

Turki, N., M. Harrabi and K. Okuno (2012). "Effect of salinity on grain yield and quality of wheat and genetic relationships among durum and common wheat." J. Arid Land Studies **22**(1): 311-314.

Uauy, C. (2017). "Wheat genomics comes of age." Current Opinion in Plant Biology **36**: 142-148.

Uddin, M. N., M. A. Hossain and D. J. Burritt (2016). "Salinity and drought stress." Water Stress and Crop Plants: A Sustainable Approach: 86-101.

Uga, Y., K. Sugimoto, S. Ogawa, J. Rane, M. Ishitani, N. Hara, Y. Kitomi, Y. Inukai, K. Ono and N. Kanno (2013). "Control of root system architecture by DEEPER ROOTING 1 increases rice yield under drought conditions." Nature genetics **45**(9): 1097-1102.

Ulaby, F. T. and R. Jedlicka (1984). "Microwave dielectric properties of plant materials." Geoscience and Remote Sensing, IEEE Transactions on **22**(4): 406-415.

van Ginkel, M. and F. Ogbonnaya (2007). "Novel genetic diversity from synthetic wheats in breeding cultivars for changing production conditions." Field crops research **104**(1): 86-94.

van Ginkel, M. and F. Ogbonnaya (2007). "Using synthetic wheats to breed cultivars better adapted to changing production conditions." Field Crops Research **104**: 86-94.

Velarde-Buendía, A. M., S. Shabala, M. Cvikrova, O. Dobrovinskaya and I. Pottosin (2012). "Salt-sensitive and salt-tolerant barley varieties differ in the extent of potentiation of the ROS-induced K+ efflux by polyamines." Plant Physiology and Biochemistry **61**: 18-23.

Vergauwen, D. and I. De Smet (2017). "From early farmers to Norman Borlaug—the making of modern wheat." Current Biology **27**(17): R858-R862.

Visscher, P. M., M. A. Brown, M. I. McCarthy and J. Yang (2012). "Five years of GWAS discovery." The American Journal of Human Genetics **90**(1): 7-24.

Visscher, P. M., R. Thompson and C. S. Haley (1996). "Confidence intervals in QTL mapping by bootstrapping." Genetics **143**(2): 1013-1020.

von Korff, M., H. Wang, J. Leon and K. Pillen (2006). "AB-QTL analysis in spring barley: II. Detection of favourable exotic alleles for agronomic traits introgressed from wild barley (H-vulgare ssp spontaneum)." Theoretical and Applied Genetics **112**(7): 1221-1231.

Waines, J. G. and B. Ehdaie (2007). "Domestication and crop physiology: roots of green-revolution wheat." Annals of Botany **100**(5): 991-998.

Wang, S., D. Wong, K. Forrest, A. Allen, S. Chao, B. E. Huang, M. Maccaferri, S. Salvi, S. G. Milner and L. Cattivelli (2014). "Characterization of polyploid wheat genomic diversity using a high-density 90 000 single nucleotide polymorphism array." Plant Biotechnology Journal **12**(6): 787-796.

Warburton, M., J. Crossa, J. Franco, M. Kazi, R. Trethowan, S. Rajaram, W. Pfeiffer, P. Zhang, S. Dreisigacker and M. Van Ginkel (2006). "Bringing wild relatives back into the family: recovering genetic diversity in CIMMYT improved wheat germplasm." Euphytica **149**(3): 289-301.

Ward, L. D. and M. Kellis (2012). "Interpreting noncoding genetic variation in complex traits and human disease." Nature biotechnology **30**(11): 1095-1106.

Warnes, G., F. Leisch, M. Man and M. G. Warnes (2012). "Package 'genetics'."

Wen, C.-l., Q. Cheng, L. Zhao, A. Mao, J. Yang, S. Yu, Y. Weng and Y. Xu (2016). "Identification and characterisation of Dof transcription factors in the cucumber genome." Scientific reports **6**.

Wiktelius, E. and G. Stenberg (2007). "Novel class of glutathione transferases from cyanobacteria exhibit high catalytic activities towards naturally occurring isothiocyanates." Biochemical Journal **406**(1): 115-123.

Wilce, M. C. and M. W. Parker (1994). "Structure and function of glutathione S-transferases." Biochimica et Biophysica Acta (BBA)-Protein Structure and Molecular Enzymology **1205**(1): 1-18.

Wilson, C., S. M. Lesch and C. M. Grieve (2000). "Growth stage modulates salinity tolerance of New Zealand spinach (Tetragonia tetragonioides, Pall.) and red orach (Atriplex hortensis L.)." Annals of Botany **85**(4): 501-509.

Wilson, L. M., S. R. Whitt, A. M. Ibáñez, T. R. Rocheford, M. M. Goodman and E. S. Buckler (2004). "Dissection of maize kernel composition and starch production by candidate gene association." The Plant Cell **16**(10): 2719-2733.

Witcombe, J., P. Hollington, C. Howarth, S. Reader and K. Steele (2008). "Breeding for abiotic stresses for sustainable agriculture." Philosophical Transactions of the Royal Society of London B: Biological Sciences **363**(1492): 703-716.

Witte, J. S. (2010). "Genome-wide association studies and beyond." Annual review of public health **31**: 9-20.

Wu, H., L. Shabala, X. Liu, E. Azzarello, M. Zhou, C. Pandolfi, Z.-H. Chen, J. Bose, S. Mancuso and S. Shabala (2015). "Linking salinity stress tolerance with tissue-specific Na+ sequestration in wheat roots." Frontiers in plant science **6**.

Wu, H., L. Shabala, M. Zhou and S. Shabala (2015). "Chloroplast-generated ROS dominate NaCl-induced K+ efflux in wheat leaf mesophyll." Plant signaling & behavior **10**(5): e1013793.

Xia, N., G. Zhang, X.-Y. Liu, L. Deng, G.-L. Cai, Y. Zhang, X.-J. Wang, J. Zhao, L.-L. Huang and Z.-S. Kang (2010). "Characterization of a novel wheat NAC transcription factor gene involved in defense response against stripe rust pathogen infection and abiotic stresses." Molecular biology reports **37**(8): 3703-3712.

Xu, J., X.-J. Xing, Y.-S. Tian, R.-H. Peng, Y. Xue, W. Zhao and Q.-H. Yao (2015). "Transgenic Arabidopsis plants expressing tomato glutathione S-transferase showed enhanced resistance to salt and drought stress." PLoS One **10**(9): e0136960.

Xu, Y., W. Hu, J. Liu, J. Zhang, C. Jia, H. Miao, B. Xu and Z. Jin (2014). "A banana aquaporin gene, MaPIP1; 1, is involved in tolerance to drought and salt stresses." BMC Plant Biology **14**(1): 59.

Xu, Y., S. Li, L. Li, X. Zhang, H. Xu and D. An (2013). "Mapping QTLs for salt tolerance with additive, epistatic and QTL× treatment interaction effects at seedling stage in wheat." Plant Breeding **132**(3): 276-283.

Xue, G.-P., N. I. Bower, C. L. McIntyre, G. A. Riding, K. Kazan and R. Shorter (2006). "TaNAC69 from the NAC superfamily of transcription factors is up-regulated by abiotic stresses in wheat and recognises two consensus DNA-binding sequences." Functional Plant Biology **33**(1): 43-57.

Xue, G.-P., H. M. Way, T. Richardson, J. Drenth, P. A. Joyce and C. L. McIntyre (2011). "Overexpression of TaNAC69 leads to enhanced transcript levels of stress up-regulated genes and dehydration tolerance in bread wheat." Molecular Plant **4**(4): 697-712.

Xue, W., J. Yan, G. Zhao, Y. Jiang, J. Cheng, L. Cattivelli and A. Tondelli (2017). "A major QTL on chromosome 7HS controls the response of barley seedling to salt stress in the Nure× Tremois population." BMC genetics **18**(1): 79.

Yadav, S., M. Irfan, A. Ahmad and S. Hayat (2011). "Causes of salinity and plant manifestations to salt stress: a review." Journal of Environmental Biology **32**(5): 667.

Yamada, K. D., K. Tomii and K. Katoh (2016). "Application of the MAFFT sequence alignment program to large data–reexamination of the usefulness of chained guide trees." Bioinformatics: btw412.

Yan, W., L. Hunt, Q. Sheng and Z. Szlavnics (2000). "Cultivar evaluation and mega-environment investigation based on the GGE biplot." Crop Science **40**(3): 597-605.

Yan, W. and M. S. Kang (2002). GGE biplot analysis: A graphical tool for breeders, geneticists, and agronomists, CRC press.

Yanagisawa, S. (2004). "Dof domain proteins: plant-specific transcription factors associated with diverse phenomena unique to plants." Plant and Cell Physiology **45**(4): 386-391.

Yang, D.-L., R.-L. Jing, X.-P. Chang and W. Li (2007). "Identification of quantitative trait loci and environmental interactions for accumulation and remobilization of water-soluble carbohydrates in wheat (Triticum aestivum L.) stems." Genetics **176**(1): 571-584.

Yang, W., D. Liu, J. Li, L. Zhang, H. Wei, X. Hu, Y. Zheng, Z. He and Y. Zou (2009). "Synthetic hexaploid wheat and its utilization for wheat genetic improvement in China." Journal of Genetics and Genomics **36**(9): 539-546.

Yang, Y., L. Zhang, Z. Yan, Y. Zheng and D. Liu (2011). "The cytological instability of neoallopolyploids suggesting a potent way for DNA introgression: The case of synthetic hexaploid wheat Aegilops peregrina." African Journal of Agricultural Research **6**(7): 1692-1697.

Yu, F., L. Qian, C. Nibau, Q. Duan, D. Kita, K. Levasseur, X. Li, C. Lu, H. Li and C. Hou (2012). "FERONIA receptor kinase pathway suppresses abscisic acid signaling in Arabidopsis by activating ABI2 phosphatase." Proceedings of the National Academy of Sciences **109**(36): 14693-14698.

Yu, M., L.-L. Guan, G.-Y. Chen, Z.-E. Pu and D.-B. Hou (2017). "Allopolyploidy-induced rapid genomic changes in newly generated synthetic hexaploid wheat." Biotechnology & Biotechnological Equipment **31**(2): 236-242.

Yu, T., Y. S. Li, X. F. Chen, J. Hu, X. Chang and Y. G. Zhu (2003). "Transgenic tobacco plants overexpressing cotton glutathione S-transferase (GST) show enhanced resistance to methyl viologen." Journal of plant physiology **160**(11): 1305-1311.

Zechmann, B. (2014). "Compartment-specific importance of glutathione during abiotic and biotic stress." Frontiers in plant science **5**.

Zeng, H., L. Xu, A. Singh, H. Wang, L. Du and B. Poovaiah (2015). "Involvement of calmodulin and calmodulin-like proteins in plant responses to abiotic stresses." Frontiers in plant science **6**.

Zhang, L., D. Liu, X. Lan, Y. Zheng and Z. Yan (2008). "A synthetic wheat with 56 chromosomes derived fromTriticum turgidum andAegilops tauschii." Journal of applied genetics **49**(1): 41-44.

Zhao, F. and H. Zhang (2006). "Expression of Suaeda salsa glutathione S-transferase in transgenic rice resulted in a different level of abiotic stress resistance." The Journal of Agricultural Science **144**(6): 547-554.

Zhu, B.-Q. (2016). "Hydrological indications of aeolian salts in mid-latitude deserts of northwestern China." Journal of Earth System Science **125**(4): 809-820.

8. LIST OF FIGURES

FIGURE 1. EVOLUTION OF WHEAT (ADOPTED FROM VERGAUWEN AND DE SMET (2017)) 2
FIGURE 2. CONCEPT OF TWO-PHASE GROWTH RESPONSE TO SALINITY (MUNNS AND TESTER 2008) 7
FIGURE 3. SIMPLIFIED PATHWAY OF ROS GENERATION WITHIN CHLOROPLASTS 11
FIGURE 4. ESTABLISHMENT OF THE Z86 BACKCROSS POPULATION 18
FIGURE 5. EMISENS DUAL-MODE MICROWAVE RESONATOR 26
FIGURE 6. SCORING SCHEME FOR SCORING SALINITY STRESS AT SEEDLING STAGE ACCORDING TO MANO AND TAKEDA (1998); (IMAGE: DADSHANI, 2006) 41
FIGURE 7. OVERVIEW OF GERMINATION SCORING OF ZENTOS AND SYN86 EXPOSED TO DIFFERENT CONCENTRATIONS OF NACL AND Na_2SO_4; SIGNIFICANCE LEVELS OF P: * $P \leq 0.05$; ** P ≤ 0.01 43
FIGURE 8. OVERVIEW OF THE GERMINATION SCORING THE Z86 POPULATION; THE PARENTS ARE HIGHLIGHTED WITH GREEN SOLID LINE (ZENTOS) AND RED DASHED LINE (SYN86); SIGNIFICANCE LEVELS P: * $P \leq 0.05$; ** P ≤ 0.01; NS NOT SIGNIFICANT. 43
FIGURE 9. AVERAGE GERMINATION SCORE VALUES OF THE GENOTYPES OF THE Z86 POPULATION, INCLUDING ZENTOS AND SYN86 45
FIGURE 10. "MEAN VS. STABILITY" PLOT OF Z86 POPULATION (INCLUDING THE PARENTS) TESTED WITH DIFFERENT CONCENTRATIONS OF NACL AND Na_2SO_4 AT GERMINATION STAGE 47
FIGURE 11. SETUP OF THE AERATED HYDROPONIC SYSTEM FOR PHENOTYPING OF THE Z86 POPULATION UNDER CONTROL AND SALINITY STRESS CONDITIONS 48
FIGURE 12. SHOOT AND ROOT DRY WEIGHT OF THE Z86 POPULATION GROWN IN HYDROPONIC SYSTEMS WITHOUT SALT CONTROL CONDITION (GREEN), 100 MM NACL (YELLOW) AND 100 MM Na_2SO_4 (RED) 58
FIGURE 13. SHOOT AND ROOT LENGTH OF THE Z86 POPULATION GROWN IN HYDROPONIC SYSTEMS WITHOUT SALT CONTROL CONDITION (GREEN), 100 MM NACL (YELLOW) AND 100 MM Na_2SO_4 (RED) 59
FIGURE 14. OVERVIEW OF SHOOT FRESH WEIGHT (SDW), ROOT DRY WEIGHT (RDW), SHOOT LENGTH (SL) AND ROOT LENGTH (RL) OF ZENTOS, SYN86 AND Z86 POPULATION MEAN UNDER 100 MM NACL AND Na_2SO_4 RELATIVE TO CONTROL CONDITIONS 60
FIGURE 15. BAR PLOT OF STI VALUES OF SHOOT DRY WEIGHT (A), ROOT DRY WEIGHT (B), SHOOT LENGTH (C), ROOT LENGTH (D) OF THE Z86 POPULATION TESTED IN HYDROPONIC SYSTEM WITH 100 MM NACL; GENOTYPES ARE SORTED ACCORDING TO THE HIGHEST VALUE; THE PARENTS ARE HIGHLIGHTED IN GREEN (ZENTOS) AND RED (SYN86); DASHED LINES = POPULATION MEANS 62
FIGURE 16. BAR PLOT OF STI VALUES OF SHOOT DRY WEIGHT (A), ROOT DRY WEIGHT (B), SHOOT LENGTH (C), ROOT LENGTH (D) OF THE Z86 POPULATION TESTED IN HYDROPONIC SYSTEM WITH 100 MM Na_2SO_4; GENOTYPES ARE SORTED ACCORDING THE HIGHEST VALUE; THE PARENTS ARE HIGHLIGHTED IN GREEN (ZENTOS) AND RED (SYN86); DASHED LINES = POPULATION MEANS 63
FIGURE 17. (A) Na^+ AND K^+ CONCENTRATION [MG/G DRY WEIGHT] AND (B) RELATION BETWEEN K^+/Na^+-RATIO (SALT STRESS CONDITION WITH 100 MM Na_2SO_4) IN LEAVES OF SALT STRESS PLANTS AND SDW (STI VALUE) 65
FIGURE 18. K^+ AND Na^+ FOLD CHANGE IN LEAVES OF Z86 POPULATION UNDER SALT STRESS CONDITION RELATIVE TO CONTROL CONDITION 65

FIGURE 19. "MEAN VS. STABILITY" PLOT OF STI VALUES FOR SHOOT DRY WEIGHT (SDW) OF Z86 TESTED UNDER 100 MM NACL AND Na_2SO_4, RESPECTIVELY AND K^+/Na^+-RATIO IN LEAVES. 66
FIGURE 20. MAJOR BAKING QUALITY PARAMETERS OF SEEDS OF Z86 POPULATION MEASURED WITH THE NIR SENSOR; SIGNIFICANCE LEVELS P: *** P < 0.001 70
FIGURE 21. STRESS-WEIGHTED PERFORMANCE INDEX (SWP) VALUES OF YIELD (CIRCLES) AND PROTEIN CONTENT (DOTS) OF THE Z86 POPULATION TESTED IN FIELD TRIALS UNDER NATURAL SALINIZATION; GENOTYPES SORTED ACCORDING TO HIGHEST YIELD VALUE 73
FIGURE 22. "MEAN VS. STABILITY" PLOT OF SALINITY TOLERANCE INDEX (STI) VALUES FOR GERMINATION SCORING, SHOOT DRY WEIGHT (SDW) AND GRAIN YIELD FROM FIELD TRIALS OF Z86 POPULATION 74
FIGURE 23. "MEAN VS. STABILITY" PLOT OF SALINITY TOLERANCE INDEX (STI) VALUES FOR SHOOT DRY WEIGHT (SDW) AT SEEDLING STAGE WITH 100 MM NACL AND Na_2SO_4 AND PLOT YIELD OF Z86 POPULATION 76
FIGURE 24. COMPARATIVE DIELECTRIC CONDUCTIVITY OF FRESH AND TOTALLY DRIED WHEAT LEAVES 78
FIGURE 25. EXPERIMENTAL RESULTS OF MICROWAVE MEASUREMENTS ON LEAVES FROM FOUR DIFFERENT CROPS 79
FIGURE 26. ANALYSIS OF WHEAT LEAVES FROM NINE GENOTYPES AFTER 15 DAYS OF SALT STRESS 81
FIGURE 27. CORRELATION BETWEEN OSMOTIC POTENTIAL AND IQS/FRS VALUES FOR CANOLA LEAVES 81
FIGURE 28. TIME COURSE OF PHOTOSYNTHETIC PARAMETERS OF ZENTOS AND SYN86 15 MINUTES BEFORE UNTIL 45 MINUTES AFTER EXPOSITION TO 100 MM NACL SALINITY STRESS 83
FIGURE 29. TIME COURSE OF PHOTOSYNTHETIC RATE OF ZENTOS, SYN86, GENOTYPE NUMBER 84 AND 117; COLORED SHADOWS INDICATE STANDARD DEVIATIONS 85
FIGURE 30. OVERVIEW OF MARKER SATURATION AND MARKER DENSITY ON THE 21 CHROMOSOMES OF WHEAT .. 89
FIGURE 31. LD DECAY PLOTS FOR INDIVIDUAL CHROMOSOMES OF THE THREE SUB-GENOMES OF THE Z86 POPULATION 90
FIGURE 32. MANHATTAN PLOT FOR GERMINATION SCORING WITH 150 MM Na_2SO_4 SHOWING COMPARISON BETWEEN PUTATIVE QTL CALCULATED WITH COMPOSITE MAPPING (ORANGE) AND MULTI-LOCUS (RED). .. 93
FIGURE 33. DISTRIBUTION AND OVERLAPPING OF THE MARKER-TRAIT ASSOCIATIONS CALCULATED FOR ALL TRAITS AT GERMINATION STAGE, SEEDLING STAGE (NACL, Na_2SO_4) AND MATURITY STAGE 95
FIGURE 34. DISTRIBUTION OF MARKER BY TRAIT ASSOCIATIONS (MTAS) WITH MAIN EFFECT AND TREATMENT INTERACTION ACCORDING TO THE ONTOLOGY CLASSES 97
FIGURE 35. QTL AND DIGENIC EPISTATIC INTERACTION DETECTED FOR CONTROL AND DIFFERENT SALT STRESS REGIMES AT GERMINATION STAGE. 98
FIGURE 36. QTL AND DIGENIC EPISTATIC INTERACTION DETECTED FOR CONTROL AND DIFFERENT SALT STRESS REGIMES AT SEEDLING STAGE 100
FIGURE 37. GENETIC STRUCTURE OF *TAGSTU3* AND *TAGSTU6* ON CHROMOSOME 7DS; RED TRIANGLE THE CORRESPONDING SNP MARKER BOBWHITE_C8454_782, BLACK TRIANGLES POSITION OF START CODON ATG; CURLY BRACKET INDICATES THE 15K BP GAP BETWEEN *TAGSTU3* AND *TAGSTU6* 101
FIGURE 38. GEL ELECTROPHORESIS OF SQ-PCR OF *TAGSTU3* GENE OF ZENTOS AND SYN86 UNDER CONTROLLED AND SALT STRESS CONDITIONS RELATIVE TO THE EXPRESSION OF THE REFERENCE GENE *TAEF-1A* AT 0, 10, 16 AND 30 DAYS AFTER STRESS APPLICATION (DAS) 102

FIGURE 39. EXPRESSION OF *TAGSTU3* IN ZENTOS AND SYN86 RELATIVE TO THE EXPRESSION OF THE REFERENCE GENE *TAEF-1A* AT 10, 16 AND 30 DAS UNDER CONTROL AND SALT STRESS CONDITIONS. SIGNIFICANCE LEVELS P: * $P \leq 0.05$ 103

FIGURE 40. DEPICTION OF TRANSCRIPTION BINDING SITES (TFBS) DETECTED BY MULAN ANALYSIS IN THE PROMOTER REGION OF ZENTOS AND SYN86; COLORS INDICATE SPECIFIC TFBS; ARROWS INDICATE MISSING TFBS IN THE PROMOTER REGION OF SYN86 104

9. LIST OF TABLES

TABLE 1. GENERAL CLASSIFICATION OF SALINE SOILS ACCORDING TO FAO (1988) 4
TABLE 2. SUMMARY OF USED SALTS AND SALT CONCENTRATIONS FOR THE GERMINATION TESTS 19
TABLE 3. SCORING SCHEME FOR GERMINATION STAGE IN WHEAT ACCORDING MANO AND TAKEDA (1998). 20
TABLE 4. COMPOSITION OF NUTRIENT SOLUTIONS FOR THE HYDROPONIC SYSTEM 21
TABLE 5. OVERVIEW OF PHENOTYPIC PARAMETERS COLLECTED FROM HYDROPONIC EXPERIMENTS 22
TABLE 6. APPLIED SENSORS FOR NON-DESTRUCTIVE PHENOTYPING 25
TABLE 7. GRAIN QUALITY PARAMETER ANALYZED WITH NIRS SENSOR 31
TABLE 8. OVERVIEW OF PHENOTYPIC TRAITS COLLECTED FROM FIELD EXPERIMENTS IN YEAR 31
TABLE 9. ANALYSIS OF VARIANCE AND DESCRIPTIVE STATISTICS OF GERMINATION SCORINGS OF Z86 POPULATION FOR DIFFERENT SALT TREATMENTS 42
TABLE 10. PHENOTYPIC PARAMETERS AND TRAITS OF Z86 POPULATION AND THE PARENTS MEASURED FROM HYDROPONIC EXPERIMENT WITH CONTROL CONDITION AND 100 MM NACL 49
TABLE 11. ANALYSIS OF VARIANCE OF MEASURED PARAMETERS OF Z86 POPULATION FROM HYDROPONIC EXPERIMENT WITH CONTROL AND 100 MM NACL TREATMENT 50
TABLE 12. PEARSON'S CORRELATION COEFFICIENT (R) FOR PARAMETERS MEASURED FROM Z86 POPULATION TESTED IN HYDROPONIC EXPERIMENT WITH 100 MM NACL; UNDER CONTROL (LEFT) AND STRESS (RIGHT) 51
TABLE 13. PEARSON'S CORRELATION COEFFICIENT (R) FOR PARAMETERS MEASURED FROM Z86 POPULATION TESTED IN HYDROPONIC EXPERIMENT WITH 100 MM NACL; STI VALUES (LEFT) AND SWP VALUES (RIGHT) 53
TABLE 14. PHENOTYPIC PARAMETERS AND TRAITS OF Z86 POPULATION AND THE PARENTS ZENTOS AND SYN86 MEASURED FROM HYDROPONIC EXPERIMENT WITH CONTROL CONDITION AND 100 MM Na_2SO_4 54
TABLE 15. ANALYSIS OF VARIANCE OF MEASURED PARAMETERS OF Z86 POPULATIONS FROM EXPERIMENT WITH CONTROL AND 100 MM Na_2SO_4 TREATMENT 55
TABLE 16. ANALYSIS OF VARIANCE OF PARAMETERS MEASURED FOR ZENTOS AND SYN86 FROM HYDROPONIC EXPERIMENT WITH CONTROL AND 100 MM Na_2SO_4 56
TABLE 17. PEARSON'S CORRELATION COEFFICIENT (R) FOR PARAMETERS MEASURED FROM Z86 POPULATION TESTED IN HYDROPONIC EXPERIMENT WITH 100 MM Na_2SO_4 57
TABLE 18. PHENOTYPIC PARAMETERS OF THE Z86 POPULATION COLLECTED FROM FIELD EXPERIMENTS UNDER CONTROL AND SALINE SOIL CONDITIONS AND GRAIN QUALITY CHARACTERISTICS 68
TABLE 19. ANALYSIS OF VARIANCE ON PARAMETERS COLLECTED OF Z86 POPULATIONS TESTED ON FIELD EXPERIMENT 69
TABLE 20. PEARSON'S CORRELATION COEFFICIENT (R) FOR PARAMETERS MEASURED FROM Z86 POPULATION TESTED IN FIELD TRIALS UNDER NATURAL SALINIZATION 71
TABLE 21. PEARSON'S CORRELATION COEFFICIENT (R) FOR SALINITY TOLERANCE INDEX (STI) AND STRESS-WEIGHTED PERFORMANCE (SWP) VALUES CALCULATED FROM PARAMETERS OBTAINED FROM FIELD TRIALS UNDER SALINE AND NON-SALINE CONDITIONS 72
TABLE 22. MEASURED *FRS* AND *IQS* (*F*=150MHZ, MODE 0) FOR SIX DIFFERENT FRESH LEAVES OF ONE WHEAT PLANT AND CALCULATED IONIC CONDUCTIVITY 80
TABLE 23. SUMMARY OF STATISTICS OF IMMEDIATE EFFECT ON PHOTOSYNTHETIC PARAMETERS OF ZENTOS, SYN86, GENOTYPE 84 AND 117 EXPOSED TO SALINITY STRESS 86

TABLE 24. THE GLM PROCEDURE REPEATED MEASURES ANALYSIS OF VARIANCE TESTS OF HYPOTHESES FOR BETWEEN-SUBJECTS EFFECTS 87
TABLE 25. THE GLM PROCEDURE REPEATED MEASURES ANALYSIS OF VARIANCE UNIVARIATE TESTS OF HYPOTHESES FOR WITHIN-SUBJECT EFFECTS 87
TABLE 26. OVERVIEW OF LD DECAY ESTIMATES [CM] AT THRESHOLD AUF R^2=0.1 91
TABLE 27. SUMMARY OF IDENTIFIED QTL WITH MAJOR EFFECT ON SALINITY TOLERANCE AT DIFFERENT GROWTH STAGES 94
TABLE 28. LIST OF SELECTED QTL DETECTED ACROSS THE TESTED ENVIRONMENTS 96
TABLE 29. GENOTYPES OF THE Z86 ADVANCED BACKCROSS WINTER WHEAT POPULATION 164
TABLE 30. SUMMARY OF QTL FOR GERMINATION TEST WITH 50-250 MM NACL 170
TABLE 31. SUMMARY OF QTL FOR GERMINATION TEST WITH 50-150 MM Na_2SO_4 171
TABLE 32. SUMMARY OF QTL DETECTED FOR TRAITS MEASURED AT SEEDLING STAGE WITH 100 MM NACL 172
TABLE 33. SUMMARY OF QTL DETECTED FOR TRAITS MEASURED AT SEEDLING STAGE WITH 100 MM Na_2SO_4 .. 177
TABLE 34. SUMMARY OF QTL DETECTED FOR TRAITS MEASURED FROM FIELD TRIALS 182
TABLE 35. ONTOLOGY OF THE DETECTED MARKER TRAIT ASSOCIATIONS AND THE PROPOSED FUNCTIONS 186

10. LIST OF ABBREVIATIONS

A	Photosynthesis rate
AAS	Atomic Absorption Spectrometer
AB-lines	Advanced backcrossed lines
AEA	Average-environmental axis
Ci	intercellular CO_2 concentration
cM	centimorgan
DAS	Days after stress application
DF	Degree of freedom
DMD	Days to maturity
dS/m	Deci Siements per meter
E	Transpiration rate
EC	Electric conductivity
ECe	Electrical conductivity of the soil saturation extract
FDR	False Discovery Rate
FRS	relative frequency shift
Gb	Giba base pairs
GEI	Genotype by environmental interaction
g_s	Stomatal conductance
GSH	Glutathione
GST	Glutathione S-transferase
H^2	broad sense heritability
HKT	High-affinity K+ transporter
IQS	the inverse quality factor
LD	Linkage disequilibrium
LL	leaf length
LML	Leaf membrane leakage
LW	Leaf width
LWC	Leaf water content
MAF	Minnor Allele Frequency
mM	Milli mol
MTA	Marker by trait association
Na_2SO_4	Sodium sulfate
NaCl	Sodium chloride
NDF	Neutral Detergent Fiber
NIR	Near infrared reflectance spectroscopy
NoL	Number of leaves
NSCC	non-selective cation channels
PCR	Polymerase chain reaction
PDW	Plant dry weight
PFW	Plant fresh weight
PH	Plant height
PL	Length of peduncle
PSI/II	Photosystem I/II
QTL	Quantitative trait loci
RDW	Root dry weight
RFW	Root fresh weight
RH	Relative humidity
RL	Root length
ROS	Reactive oxygen species
SBL	Synthetic backcross-derived lines
SDW	Shoot dry weight
SFW	Shoot fresh weight
SHW	Synthetic hexaploid wheat
SI	Stress initiation
SL	Shoot length
SNP	Single Nucleotide polymorphism
SOS1	Salt-Overlay-Sensitive1
SpS	Spikelet per spike
STI	Stress tolerance index
SWC	Shoot water content
SWP	Stress-weighted performance index
TFBS	Transcription Factor Binding Sites
TKW	1,000 kernel weight
TLN	Number of tillers
VPD	Vapor pressure deficit
µmol	Micromole

11. APPENDICES

Appendix 1

Table 29. Genotypes of the Z86 advanced backcross winter wheat population

EN	Genotype	EN	Genotype	EN	Genotype	EN	Genotype	EN	Genotype
1	WW33-07	34	WW34-51	67	WW35-92	100	WW40-51	133	WW43-17
2	WW33-09	35	WW34-56	68	WW35-93	101	WW40-52	134	WW43-18
3	WW33-10	36	WW34-62	69	WW35-95	102	WW40-59	135	WW43-27
4	WW33-17	37	WW34-63	70	WW36-13	103	WW40-60	136	WW43-30
5	WW33-18	38	WW34-65	71	WW36-28	104	WW40-62	137	WW43-37
6	WW33-19	39	WW34-67	72	WW36-70	105	WW40-63	138	WW43-39
7	WW33-20	40	WW34-71	73	WW36-86	106	WW40-66	139	WW43-45
8	WW33-22	41	WW34-75	74	WW36-91	107	WW40-70	140	WW43-49
9	WW33-32	42	WW34-79	75	WW36-94	108	WW40-72	141	WW43-73
10	WW33-33	43	WW34-80	76	WW36-96	109	WW40-75	142	WW43-74
11	WW33-36	44	WW34-86	77	WW37-15	110	WW41-20	143	WW43-81
12	WW33-44	45	WW34-92	78	WW37-17	111	WW41-22	144	WW43-89
13	WW33-53	46	WW35-04	79	WW37-18	112	WW41-25	145	WW43-91
14	WW33-55	47	WW35-07	80	WW37-22	113	WW41-27	146	WW43-93
15	WW33-67	48	WW35-15	81	WW37-50	114	WW41-68	147	WW44-21
16	WW33-78	49	WW35-21-1	82	WW37-54	115	WW41-92	148	WW44-31
17	WW33-82	50	WW35-21-2	83	WW37-56	116	WW42-31	149	WW44-35
18	WW33-96	51	WW35-25	84	WW37-58	117	WW42-32	150	WW44-78
19	WW34-03	52	WW35-26	85	WW37-69	118	WW42-33	151	WW44-92
20	WW34-16	53	WW35-30	86	WW38-02	119	WW42-35		
21	WW34-25	54	WW35-32	87	WW38-09	120	WW42-42		
22	WW34-27	55	WW35-33	88	WW38-14	121	WW42-48		
23	WW34-28	56	WW35-36	89	WW38-20	122	WW42-56		
24	WW34-30	57	WW35-48	90	WW38-57	123	WW42-58		
25	WW34-31	58	WW35-51	91	WW38-62	124	WW42-59		
26	WW34-33	59	WW35-55	92	WW38-78	125	WW42-77		
27	WW34-36	60	WW35-56	93	WW39-07	126	WW42-80		
28	WW34-37	61	WW35-60	94	WW39-62	127	WW42-81		
29	WW34-38	62	WW35-70	95	WW40-15	128	WW42-83		
30	WW34-41	63	WW35-75	96	WW40-20	129	WW42-84		
31	WW34-45	64	WW35-78	97	WW40-22	130	WW42-94		
32	WW34-48	65	WW35-84	98	WW40-23	131	WW43-04		
33	WW34-49	66	WW35-91	99	WW40-40	132	WW43-15		

Note: EN entry number

Appendix 2

LD Heatmaps

The heat maps shown below are graphically displaying for each chromosome the measure of pairwise linkage disequilibria between SNP markers. The "R^2 key color" is indicating the R^2 correlation between SNP markers; where 0 stands for no correlation (blue color) and 1 stands to 100% correlation (red color).

A-Genome

1A

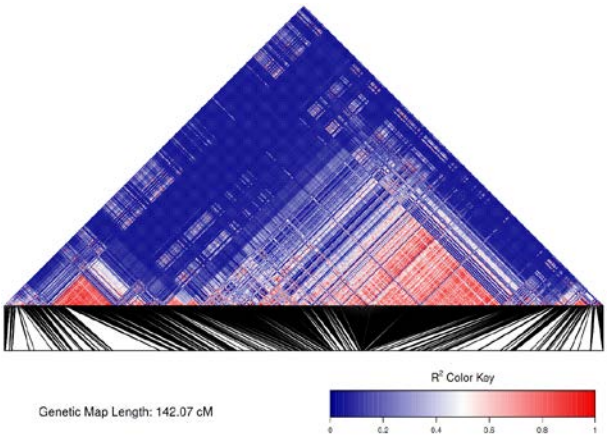

2A

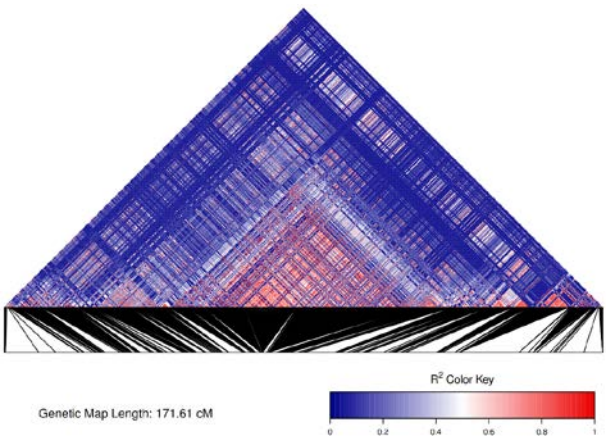

3A

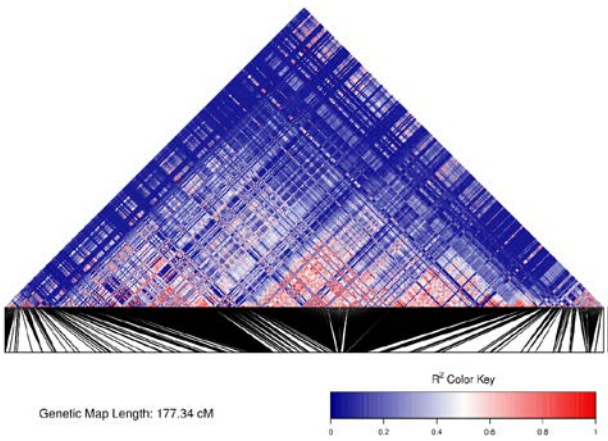

4A

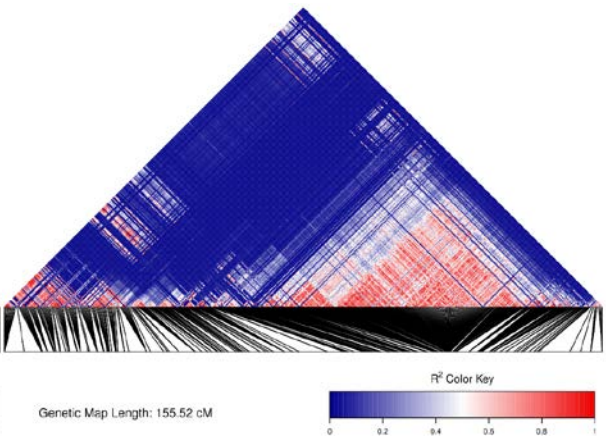

5A

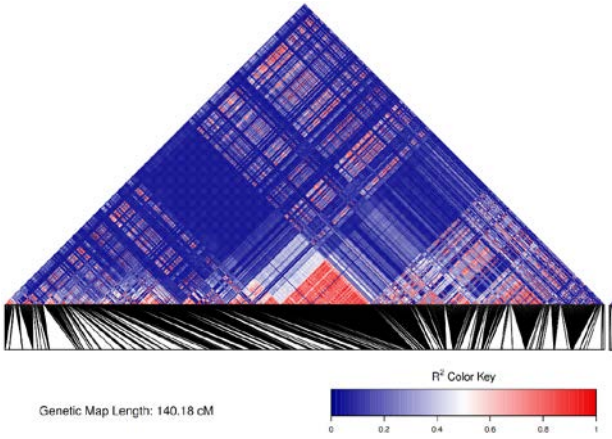

6A

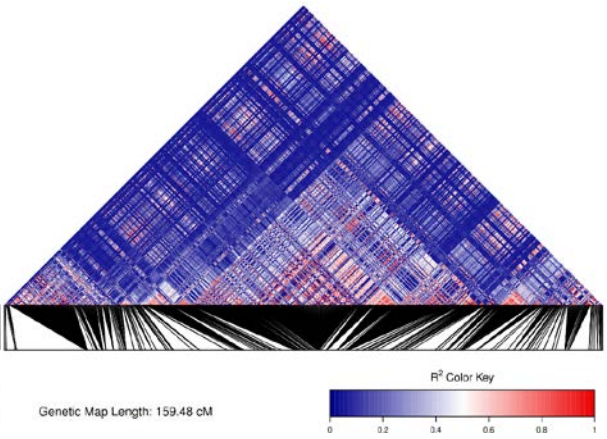

7A

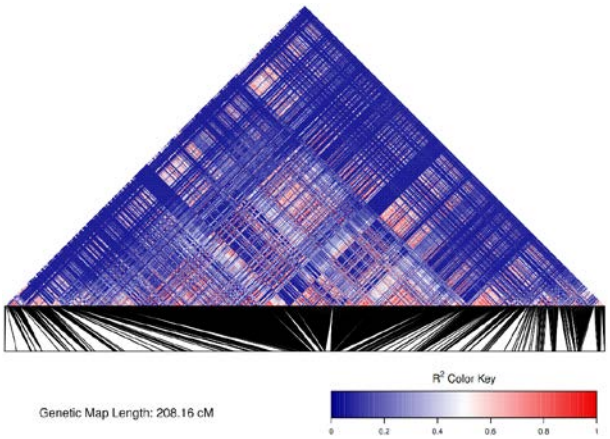

B-Genome

1B

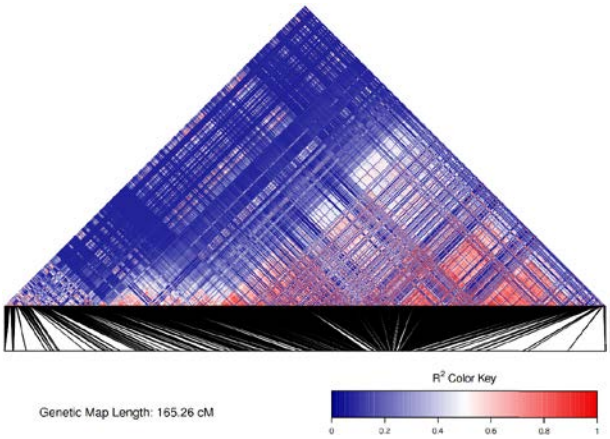

2B

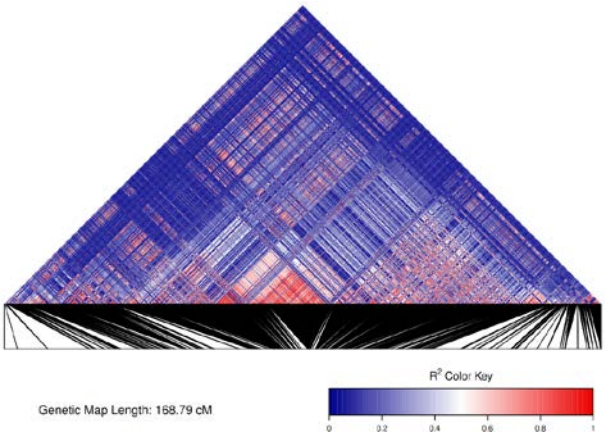

3B

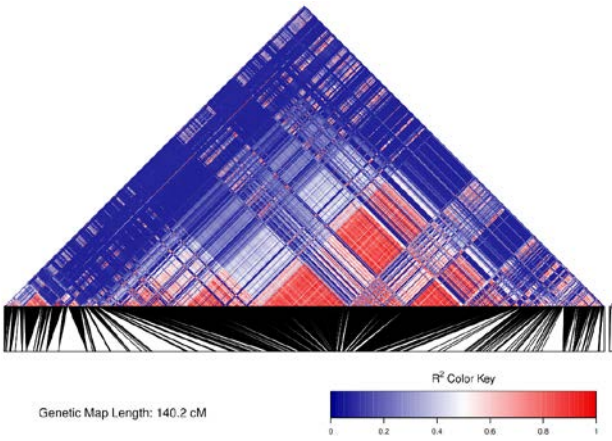
R² Color Key
Genetic Map Length: 140.2 cM

4B

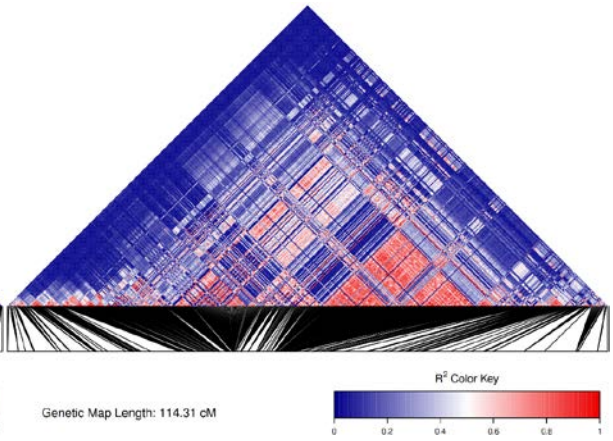
R² Color Key
Genetic Map Length: 114.31 cM

5B

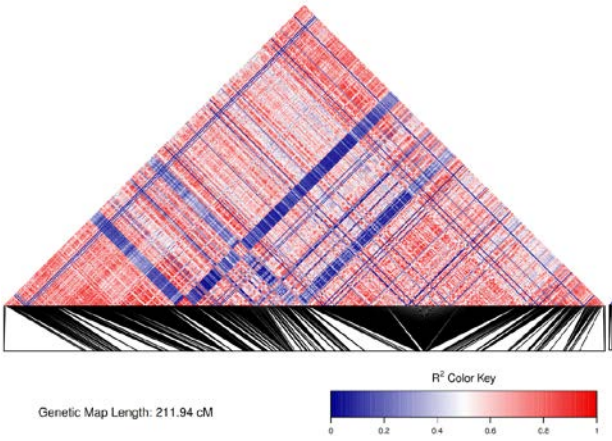
R² Color Key
Genetic Map Length: 211.94 cM

6B

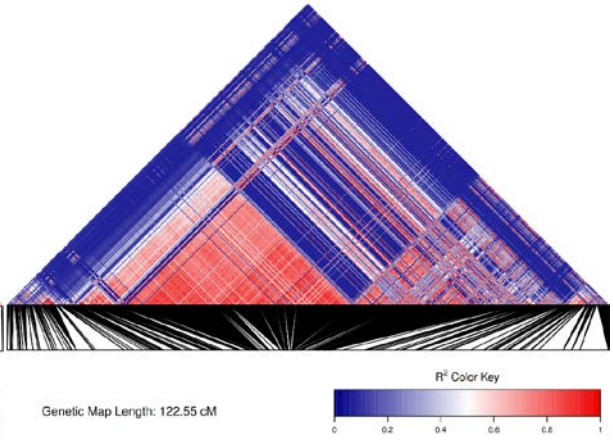
R² Color Key
Genetic Map Length: 122.55 cM

7B

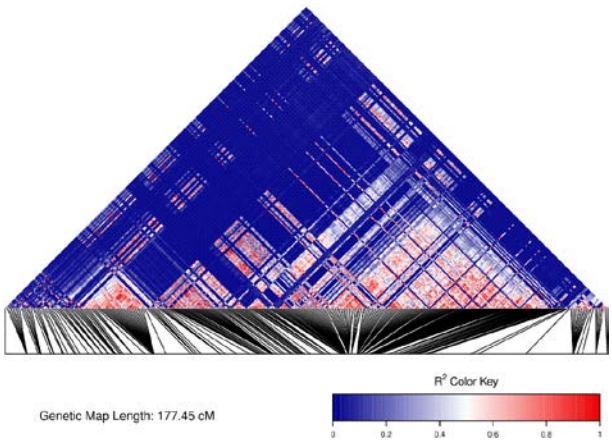
R² Color Key
Genetic Map Length: 177.45 cM

D-Genome

1D

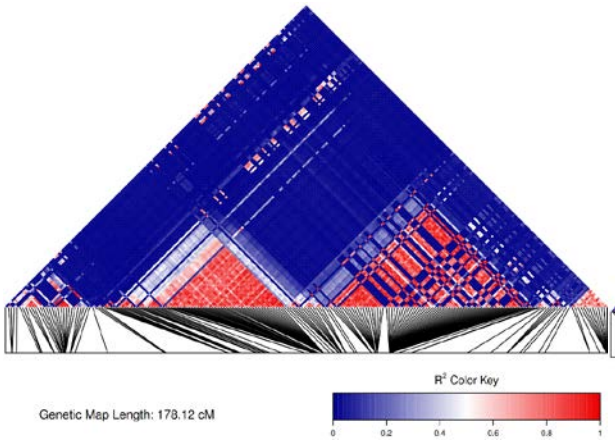

2D

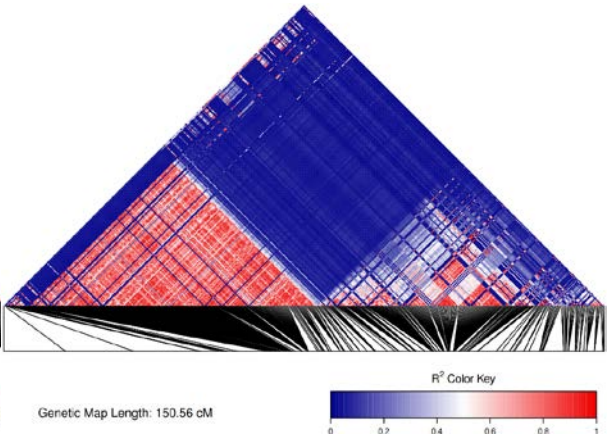

3D

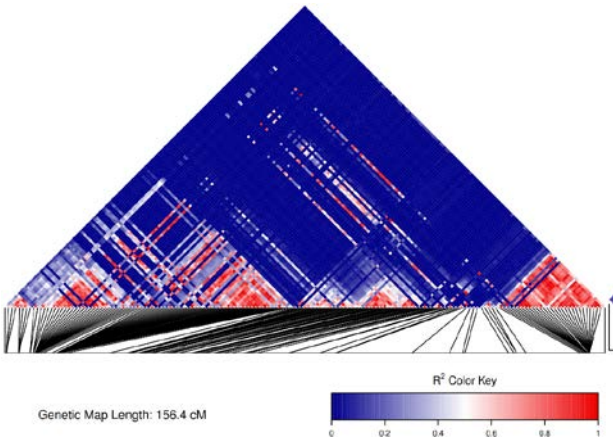

4D

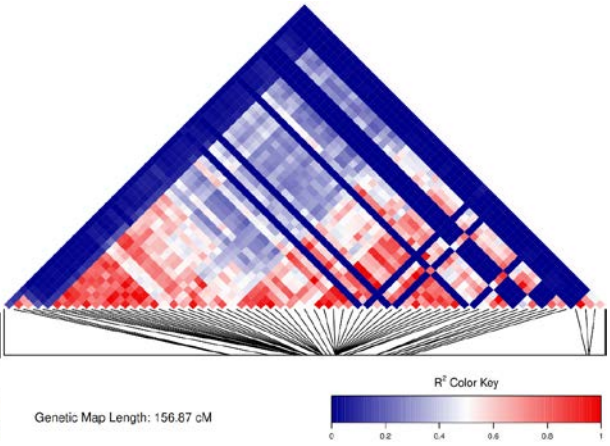

5D

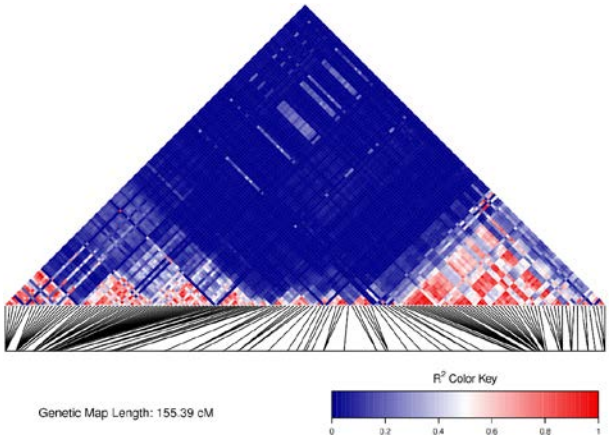

6D

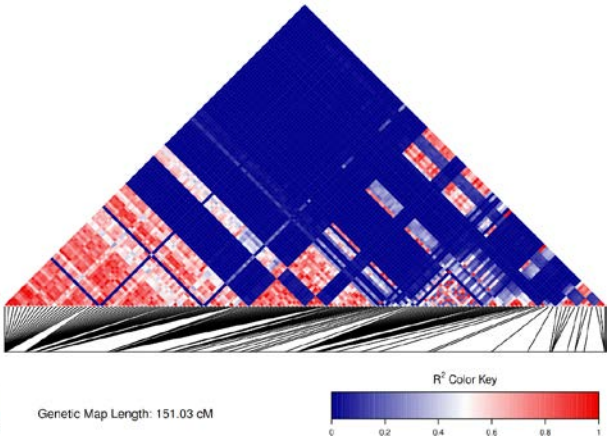

7D

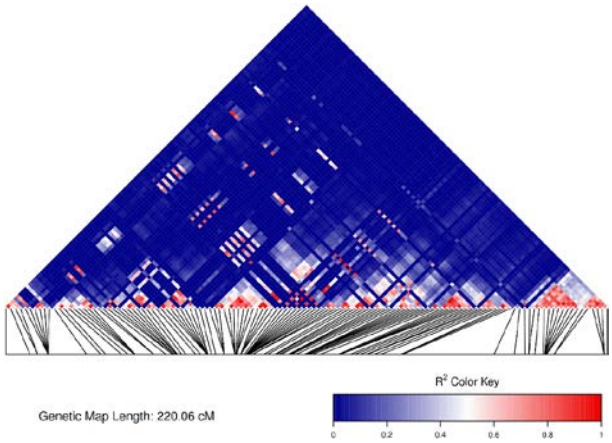

Appendix 3

Table 30. Summary of QTL for germination test with 50-250 mM NaCl

Treatment	Effect	Marker 1	Position		Flanking region	LOD	*F* value	FDR	R^2 [%]	H^2 (SE)	Marker 2	Position	
Control	M	Excalibur_c34167_128	1D	71.90	67.7-73.1	4.15	34.9	8.3E-02	9.8				
	M	Tdurum_contig11678_289	2A	126.38	126.3-126.4	3.70	15.2	1.3E-01	9.9				
	M	Excalibur_c41490_397	6A	84.11	84.1-81.1	4.60	24.5	5.6E-02	17.1				
	M	Excalibur_c64119_345	6B	24.64	23.3-24.6	3.80	21.9	1.1E-01	15.8				
	M	BobWhite_c8454_782	7D	29.97	26.2-30.0	6.64	41.4	1.9E-03	20.8				
	M	Σ							46.4	73.6 (0.10)			
	M_1*M_2	BobWhite_c8454_782	7D	29.97	26.2-30.0	12.5	49.6	4.3E-12	53.9	73.6 (0.10)	Excalibur_c34167_128	1D	71.90
50 mM NaCl	M*T	Kukri_c31964_109	1A	56.10	48.45- 65.4	5.1	21.3	1.1E-03	15.6				
	M*T	Kukri_c30847_551	2B	20.87	16.9-28.5	5.5	23.5	1.0E-03	15.4				
	M*T	wsnp_BE471213D_Ta_2_1	6D	153.08	150.4-160.5	5.0	21.2	1.1E-03	16.1				
	M*T	Σ							33.0	92 (0.01)			
	M_1*M_2*T	Excalibur_c7546_1286	6D	150.43	150.4-150.5	6.1	15.9	4.3E-03	21.4		Kukri_c28182_129	5D	196.08
	M_1*M_2*T	Excalibur_c7546_1286	6D	150.43	150.4-150.5	5.5	14.2	4.3E-03	29.3		TA003665_0980	4B	59.94
	M_1*M_2*T	Σ						4.3E-03	32.2	92 (0.01)			
100 mM NaCl	M*T	BobWhite_c11397_231	2B	16.88	16.9- 20.9	4.1	16.5	4.3E-03	8.8				
	M*T	KUKRI_C16034_113	7B	109.09	99.7- 118.8	4.6	19.1	4.3E-03	12.9				
	M*T	Σ							19.3	66.7 (0.12)			
	M_1*M_2*T	BobWhite_c11397_231	2B	16.88	16.9- 20.9	5.1	9.8	2.3E-03	22.4		Ex_c66324_1151	4A	66.0
	M_1*M_2*T	GENE_3006_113	5D	203.88	203.8-204.1	5.9	15.4	2.3E-03	21.1		Kukri_c16034_113	7B	109.1
	M_1*M_2*T	Σ							21.1	66.7 (0.12)			
150 mM NaCl	M*T	Excalibur_c35316_154	1A	16.7	13.7-26.6	4.83	20.2	3.2E-03	12.4				
	M*T	wsnp_Ex_c22202_31392780	2A	65.6	62.5-75.0	5.03	21.2	3.2E-03	12.0				
	M*T	wsnp_Ex_c5412_9564478	2A	76.9	67.5-82.8	5.36	22.9	2.3E-03	19.2				
	M*T	IAAV5635	3D	40.5	33.0-47.1	5.83	25.2	2.3E-03	15.0				
	M*T	wsnp_JD_c38619_27992279	4A	75.5	75.0-75.5	5.60	24.2	2.3E-03	15.5				
	M*T	Kukri_rep_c101620_1848	7B	171.1	170.1-172.0	3.37	13.1	8.0E-03	10.2				
	M*T	Σ							36.5	82.7 (0.08)			
	M_1*M_2*T	Ku_c766_2284	4A	37.05	7.41	19.	7.41	6.4E-04	27.9	82.7 (0.08)	Tdurum_contig42153_5454	2A	52.00

Note: LOD logarithm of the odds; FDR false discovery rate; R^2 explained genetic variance, H^2 broad-sense heritability; SE standard error

Table 30. Summary of QTL for germination test with 50-250 mM NaCl (cont.)

Treatment	Effect	Marker 1	Position		Flanking region	LOD	F value	FDR	R^2 [%]	H^2 (SE)	Marker 2	Position	
200 mM NaCl	M*T	Excalibur_c45326_479	3B	139.62	132.1-144.7	3.3	12.7	2.0E-02	7.6				
	M*T	BS00094095_51	5A	36.87	29.5- 46.7	5.2	21.8	2.0E-02	12.3				
	M*T	wsnp_Ku_c24391_34351602	6B	7.79	0.3-17.7	4.7	19.8	2.0E-02	16.9				
	M*T	BS00011523_51	6D	101.63	98.1-101.6	4.9	20.4	2.0E-02	14.9				
	M*T	Σ							48.8	96.9 (0.0)			
	M_1*M_2*T	wsnp_Ku_c24391_34351602	6B	7.79	0.3-17.7	6.42	28.8	2.4E-03	6.4	96.9 (0.0)	wsnp_Ra_rep_c106119_89961852	6D	17.01
250 mM NaCl	M*T	wsnp_Ex_c33778_42210283	4A	147.1	138.6-154.3	4.5	18.6	1.5E-02	10.4				
	M*T	BS00094095_51	5A	36.9	29.5-46.7	4.5	18.6	1.5E-02	13.8				
	M*T	Excalibur_c76347_77	5D	144.7	144.7-147.2	3.1	11.8	6.7E-02	9.9				
	M*T	RAC875_c37871_249	6B	0.4	0.4-9.6	3.4	13.3	4.5E-02	8.7				
	M*T	Σ							30.0	94.7 (0.02)			
	M_1*M_2*T	Excalibur_c76347_77	5D	144.69	144.7-147.2	6.1	11.8	2.1E-6	24.4	94.7 (0.02)	Tdurum_contig20299_142	1B	76.09

Table 31. Summary of QTL for germination test with 50-150 mM Na_2SO_4

Treatment	Effect	Marker 1	Position		Flanking region	*F* value	LOD	FDR	R^2 [%]	H^2 (SE)	Marker 2	Position	
50 mM Na_2SO_4	M*T	TA005883_0675	3D	23.67	22.9-25.1	26.58	6.1	7.2E-03	20.8				
	M*T	Tdurum_contig62213_423	7B	171.11	166.2-177.5	16.26	4.0	1.6E-01	9.0				
	M*T	**Σ**							25.3	92. (0.01)			
	M_1*M_2*T	Tdurum_contig12722_779	7A	76.28		13.80	5.80	3.9E-04	27.3	92.9 (0.01)	Tdurum_contig62213_156	7B	171.11
100 mM Na_2SO_4	M*T	Tdurum_contig59449_400	1B	71.85	62.4- 81.6	24.20	4.54	4.0E-03	12.2				
	M*T	BobWhite_c51109_415	5A	35.38	26.5- 40.0	18.56	3.49	4.7E-03	15.7				
	M*T	Σ							22.2	84.7 (0.09)			
	M_1*M_2*T	BS00104199_51	1D	133.99		10.37	4.31	3.1E-04	29.2	84.7 (0.09)	BobWhite_c8454_782	7D	29.97
150 mM Na_2SO_4	M*T	wsnp_Ra_c22775_32274079	4A	132.95	126.2-142.3	22.76	4.28	3.6E-02	13.2				
	M*T	Excalibur_rep_c68955_422	7A	74.19	65.4-89.2	21.90	4.11	3.6E-02	13.7				
	M*T	Σ							17.1	93.7 (0.01)			
	M_1*M_2*T	Excalibur_rep_c68955_422	7A	74.19		19.19	8.31	1.3E-06	24.0		Kukri_c57006_127	6D	107.40
	M_1*M_2*T	Excalibur_rep_c68955_422	7A	74.19		13.17	5.67	3.1E-05	19.9		Tdurum_contig43966_813	7B	81.76
	M_1*M_2*T	BS00067140_51	7D	26.92		10.03	4.15	2.0E-04	22.3		Excalibur_c41710_417	5A	92.87
	M_1*M_2*T	Σ							20.2	93.7 (0.01)			

Note: LOD logarithm of the odds; FDR false discovery rate; R^2 explained genetic variance, H^2 broad-sense heritability; SE standard error

Table 32. Summary of QTL detected for traits measured at seedling stage with 100 mM NaCl

Trait	Effect	Marker 1	Position		Flanking region	*F* value	LOD	FDR	R^2 [%]	H^2 (SE)	Marker 2	Position	
Shoot fresh weight	M	Excalibur_c7026_2635	1A	52.55	43.3-61.8	12.6	3.27	3.0E-02	9.9				
	M	BS00098868_51	3B	21.33	19.6-30.4	19.6	4.70	4.4E-03	17.5				
	M	Ra_c24707_827	5A	42.77	42.8-43.3	16.1	4.0	1.4E-02	11.7				
	M	wsnp_Ex_c20457_29526403	6A	123.48	122.3-125.2	14.5	3.67	1.9E-02	18.7				
	M	wsnp_JD_rep_c48797_33040150	6A	84.11	84.1-85.1	28.4	6.38	1.1E-03	25.1				
	M	BobWhite_c8454_782	7D	29.97	26.2-30.0	23.8	5.54	8.4E-03	14.3				
	M	Σ							63.0	99.1 (0.04)			
	M_1*M_2	Excalibur_c7026_2635	1A	52.55		13.6	5.34	3.3E-04	18.9		Ra_c24707_827	5A	42.77
	M_1*M_2	BS00098868_51	3B	21.33		19.6	9.61	8.0E-06	38.0		wsnp_JD_rep_c48797_33040150	6A	84.11
	M_1*M_2	Excalibur_rep_c68955_422	7A	74.19		12.2	4.79	5.9E-04	22.8		wsnp_Ex_c20457_29526403	6A	123.48
	M_1*M_2	Σ							65.3	99.1 (0.04)			
	M*T	RAC875_c25513_403	2B	152.59	147.5-152.6	13.6	3.48	1.9E-01	10.8				
	M*T	Ku_c1575_485	3B	81.8	75.1-83.5	11.6	3.05		10.9				
	M*T	Tdurum_contig61242_161	4B	78.96	76.7-79.5	19.5	4.69		9.7				
	M*T	TA004297_0876	6A	81.64	81.6-85.4	12.7	3.29		7.6				
	M*T	Kukri_c57006_127	6D	107.4	10000-107.4	13.5	3.46	1.9E-01	8.8				
	M*T	BobWhite_c8454_782	7D	29.97	26.2-30.0	14.2	3.61	1.9E-01	8.4				
	M*T	Σ							42.9	97.6 (0.0)			
	M_1*M_2*T	BS00045171_51	2A	48.44		8.6	4.5	4.7E-03	18.3		Kukri_rep_c72558_961	2D	42.59
	M_1*M_2*T	BS00105741_51	3B	14.10		16.2	6.3	4.4E-03	26.4		Kukri_rep_c72412_856	2A	79.33
	M_1*M_2*T	Σ							40.7	97.6 (0.0)			
Shoot dry weight	M	BS00098868_51	3B	21.33	21.1-21.4	16.5	4.1	1.2E-02	16.0				
	M	RAC875_s113853_61	3D	4.46	4.4-4.5	16.5	4.1	1.2E-02	19.7				
	M	wsnp_JD_rep_c48797_33040150	6A	84.11	74.2-85.4	30.4	6.8	4.0E-04	21.6				
	M	BobWhite_c8454_782	7D	29.97	26.2-30.0	21.47	5.09	1.6	15.0				
	M	Σ							46.1	94.5 (0.02)			
	M_1*M_2	BobWhite_c1082_134	6A	85.07		18.2	9.12	5.0E-08	31.0	94.5 (0.02)	BobWhite_c8454_782	7D	29.97
	M*T	Kukri_rep_c72412_856	2A	79.33	79,3-79,3	11.9	3.13	1.9E-01	13.6				
	M*T	RAC875_c25513_403	2B	152.59	147.5-152.6	13.6	3.48	1.9E-01	10.8				
	M*T	BS00098868_51	3B	21.33	21.1-21.4	15.5	3.87	1.9E-01	14.0				
	M*T	Kukri_c57006_127	6D	107.40	107.4-107.4	13.5	3.46	1.9E-01	8.8				
	M*T	BobWhite_c8454_782	7D	29.97	26.2-30.0	14.2	3.61	1.9E-01	8.4				
	M*T	Σ							42.9	96.5 (0.0)			
	M_1*M_2*T	BS00098868_51	3B	21.33			18.9	4.92	96 (0.0)	34.296.5 (0.0)	wsnp_JD_rep_c48797_33040150	6A	84.11
		Σ											

Table 32. Summary of QTL detected for traits measured at seedling stage with 100 mM NaCl (cont.)

Trait	Effect	Marker 1	Position		Flanking region	*F* value	LOD	FDR	R^2 [%]	H^2 (SE)	Marker 2	Position	
Shoot length	M	wsnp_Ex_c7271_12483592	1A	71.05	68.2-71.6	31.3	6.98	1.2E-04	10.8				
	M	wsnp_Ra_c22648_32132929	2D	82.82	72.9-86.0	15.5	3.89	4.4E-03	12.6				
	M	Kukri_c13830_556	3A	33.66	33.6-33.7	14.5	3.68	6.3E-03	12.1				
	M	RAC875_s113853_61	3D	4.46	4.4-4.5	14.0	3.58	7.4E-03	16.3				
	M	Tdurum_contig22511_355	4A	89.07	89.0-89.1	16.3	4.04	3.5E-03	13.6				
	M	BobWhite_c1082_134	6A	85.07	84.1-85.1	28.1	6.33	1.2E-04	18.5				
	M	**Σ**							62.2	77.5 (0.10)			
	M_1*M_2	GENE_1012_303	2B	114.09		11.6	5.99	1.6E-04	24.7		Kukri_c13830_556	3A	33.66
	M_1*M_2	BobWhite_c1082_134	6A	85.07		27.3	9.90	7.0E-06	31.3		wsnp_Ex_c7271_12483592	1A	71.05
	M_1*M_2	**Σ**							54.9	77.5 (0.10)			
	M*T	Excalibur_c7026_2635	1A	52.55	52.5-52.5	29.8	6.67	7.5E-04	21.3				
	M*T	Kukri_c13830_556	3A	33.66	33.6-33.7	11.8	3.11	2.1E-02	9.4				
	M*T	BS00098868_51	3B	21.33	21.3-21.3	14.5	3.66	8.3E-03	10.9				
	M*T	wsnp_Ra_c1022_2067517	4A	58.38	58.4-58.4	19.0	4.60	1.9E-03	13.6				
	M*T	BobWhite_c1082_134	6A	85.07	84.1-85.1	25.2	5.79	7.5E-04	19.8				
	M*T	**Σ**							54.5	96.6 (0.01)			
	M*M*T	BS00098868_51	3B	21.33		29.4	10.21	1.0E-06	32.2		Kukri_rep_c104386_273	1A	70.10
	M*M*T	BobWhite_c1082_134	6A	85.07		12.6	6.48	1.3E-04	29.3		Ku_c32426_324	7D	148.30
	M*M*T	BobWhite_c1082_134	6A	85.07		14.5	7.47	4.4E-05	28.5		Kukri_c13830_556	3A	33.66
	M*M*T	**Σ**							47.8	96.6 (0.01)			
Root fresh weight	M	GENE_1342_238	2A	101.97	101.9-103.6	15.3	3.85	7.2E-02	10.1				
	M	BS00023092_51	6A	80.09	80.0-80.1	17.2	4.24	7.2E-02	15.1				
	M	BobWhite_c8454_782	7D	29.97	26.2-30.0	18.2	4.44	7.2E-02	11.5				
	M	**Σ**							27.9	90.1 (0.05)			
	M*T	Kukri_c33374_1048	2A	20.14	18.0-20.1	15.8	3.92	8.9E-03	13.2				
	M*T	Excalibur_c34964_326	2A	113.30	113.3-113.3	24.3	5.63	2.6E-03	11.6				
	M*T	Tdurum_contig61242_161	4B	78.96	78.5-79.5	22.1	5.20	2.6E-03	9.2				
	M*T	**Σ**							30.9	90.1 (0.05)			
	M_1*M_2*T	Kukri_c33374_1048	2A	20.14		9.2	4.77	4.4E-04	19.7		tplb0040b02_681	7B	177.45
	M_1*M_2*T	BobWhite_c18852_91	2A	82.23		16.1	8.22	6.8E-05	20.2		Tdurum_contig61242_161	4B	78.96
	M_1*M_2*T	**Σ**							41.1	93.2 (0.03)			

Note: LOD logarithm of the odds; FDR false discovery rate; R^2 explained genetic variance, H^2 broad-sense heritability; SE standard error

Table 32. Summary of QTL detected for traits measured at seedling stage with 100 mM NaCl (cont.)

Trait	Effect	Marker 1	Position		Flanking region	*F* value	LOD	FDR	R^2 [%]	H^2 (SE)	Marker 2	Position	
Root dry weight	M	Excalibur_c49496_705	1B	122.52		15.6	3.91	1.7E-02	14.0				
	M	wsnp_Ex_c14953_23104041	2A	131.97		16.6	4.11	1.3E-02	13.4				
	M	Excalibur_c63409_73	2B	56.87		29.4	6.62	9.3E-04	15.8				
	M	Kukri_c11274_973	7B	72.74		27.2	6.20	9.3E-04	22.8				
	M	RAC875_rep_c70325_345	7D	143.68		22.0	5.19	3.3E-03	16.8				
	M	Σ							44.4	94.2 (0.03)			
Root dry weight	M_1*M_2	CAP11_c3464_68	1D	92.91		10.1	5.24	5.9E-05	19.9		Tdurum_contig64286_182	2D	103.33
	M_1*M_2	Excalibur_c63409_73	2B	56.87		34.2	15.84	6.0E-13	55.5		Kukri_c11274_973	7B	72.74
	M_1*M_2	Σ							29.4	94.2 (0.03)			
	M*T	Excalibur_c49496_705	1B	122.52	120.0-122.5	14.0	3.58	6.8E-02	13.7				
	M*T	wsnp_Ra_c4850_8698731	2A	101.97	101.9-104.1	15.8	3.93	6.6E-02	16.6				
	M*T	Tdurum_contig92931_882	4B	57.87	57.8-66.3	16.0	3.99	6.6E-02	10.0				
	M*T	RAC875_c25695_316	7D	32.16	32.1-37.4	16.2	4.03	6.6E-02	10.6				
	M*T	Σ							35.8	95.2 (0.02)			
	M_1*M_2*T	RAC875_c81076_317	3B	62.31	62.0-62.5	13.4	6.94	1.3E-03	21.0		Tdurum_contig46247_106	4B	78.57
	M_1*M_2*T	RAC875_c25695_316	7D	32.16	32.1-37.4	9.9	5.18	3.1E-03	27.9		tplb0060b03_432	7B	166.99
	M_1*M_2*T	Σ							40.0	95.2 (0.02)			
Root length	M	Tdurum_contig8382_300	1A	57.93	57.9-58.0	32.7	7.19	2.6E-04	20.3	92.5 (0.03)			
	M	IAAV1179	5A	69.34	69.3-69.4	28.8	6.50	2.6E-04	18.6				
	M	RAC875_c13785_2042	6A	84.11	84.1-84.1	22.1	5.20	1.1E-03	13.6				
	M	Excalibur_rep_c116920_300	7B	71.66	70.7-73.8	30.0	6.66	2.6E-04	25.4				
	M	BobWhite_c8454_782	7D	29.97	26.2-30.0	22.9	5.37	9.2E-04	11.0				
	M	Σ							46.5				
	M_1*M_2	D_F1BEJMU01A0OMY_356	2D	8.52		8.9	4.60	1.8E-04	20.5		IAAV1179	5A	69.34
	M_1*M_2	BS00022747_51	7A	135.81		29.2	10.24	2.6E-06	29.0		RFL_Contig1599_906	7B	69.39
	M_1*M_2	Σ							45.0	92.5 (0.03)			
	M*T	wsnp_JD_c38619_27992279	4A	75.50	75.0-75.5	38.5	8.22	5.4E-05	20.2				
	M*T	Tdurum_contig17500_876	5A	70.30	70.0-70.3	28.9	6.51	1.7E-04	18.1				
	M*T	Kukri_c57006_127	6D	107.40	107.0-107.4	18.0	4.39	1.2E-03	12.2				
	M*T	BS00066651_51	7A	127.75	127.1-129.0	31.4	6.92	1.7E-04	22.2				
	M*T	BobWhite_c8454_782	7D	29.97	26.2-30.0	20.8	4.95	7.2E-04	15.9				
	M*T	Σ							48.8	94.1 (0.02)			
	M_1*M_2*T	BS00066651_51	7A	127.75		13.8	7.03	5.2E-06	34.8		BS00072025_51	4A	66.28
	M_1*M_2*T	Excalibur_rep_c116920_300	7B	71.66	70.7-73.8	24.3	11.76	1.1E-07	38.1		Tdurum_contig17500_876	5A	70.30
	M_1*M_2*T	Σ							56.6	94.1 (0.02)			

Table 32. Summary of QTL detected for traits measured at seedling stage with 100 mM NaCl (cont.)

Trait	Effect	Marker 1	Position		Flanking region	*F* value	LOD	FDR	R^2 [%]	H^2 (SE)	Marker 2	Position	
Plant fresh weight	M	Excalibur_c7026_2635	1A	52.55	52.5-52.6	13.1	3.39	2.5E-02	9.0				
	M	BS00098868_51	3B	21.33	21.3-21.3	18.9	4.56	5.7E-03	15.8				
	M	RAC875_s113853_61	3D	4.46	4.4-4.5	18.7	4.53	5.7E-03	22.9				
	M	wsnp_JD_rep_c48797_33040150	6A	84.11	84.1-85.1	27.3	6.19	1.5E-03	25.9				
	M	IAAV1495	6A	136.70	136.7-136.8	11.8	3.10	3.8E-02	17.8				
	M	BobWhite_c8454_782	7D	29.97	26.2-30.0	28.1	6.36	1.5E-03	7.0	95.0 (0.02)			
	M	Σ							59.2				
	M_1*M_2	Excalibur_c7026_2635	1A	52.55		12.1	4.81	5.7E-04	29.8		RFL_Contig5037_560	6A	117.77
	M_1*M_2	IAAV1495	6A	136.70		10.5	4.19	1.3E-03	22.3		wsnp_CAP11_c3226_1588070	2B	147.47
	M_1*M_2	BobWhite_c8454_782	7D	29.97	26.2-30.0	18.3	9.18	1.2E-05	29.2		RAC875_s113853_61	3D	4.47
	M_1*M_2	Σ							64.1	95.0 (0.02)			
	M*T	RAC875_c25513_403	2B	152.59	149.9-152.6	11.4	3.02	9.9E-02	11.8				
	M*T	Ku_c1575_485	3B	81.80	75.1-83.5	11.6	3.05	9.9E-02	10.9				
	M*T	Tdurum_contig61242_161	4B	78.96	76.7-79.5	19.5	4.69	5.0E-02	9.7				
	M*T	TA004297_0876	6A	81.64	81.6-85.4	12.7	3.29	9.9E-02	7.6				
	M*T	Kukri_c57006_127	6D	107.40	102.1-110.4	14.7	3.72	9.9E-02	9.7				
	M*T	BobWhite_c8454_782	7D	29.97	26.2-30.0	15.6	3.91	9.9E-02	7.0				
	M*T	Σ							34.6	96.4 (0.01)			
	M_1*M_2*T	BS00068050_51	2A	48.44		7.79	4.06	2.9E-03	14.7		TA004297_0876	6A	81.64
	M_1*M_2*T	BS00105741_51	3B	14.10		17.26	6.65	1.3E-03	24.1		Kukri_rep_c72412_856	2A	79.33
	M_1*M_2*T	BS00065863_51	4A	29.86		11.26	5.90	1.3E-03	23.9		BobWhite_c8454_782	7D	29.97
	M_1*M_2*T	Σ							52.5	96.4 (0.01)			
Plant dry weight	M	BS00062869_51	2A	154.97	154.9-155.0	14.9	3.77	1.3E-02	17.0				
	M	BS00098868_51	3B	21.33	21.3-21.4	16.8	4.14	7.4E-03	14.6				
	M	RAC875_s113853_61	3D	4.46	4.4-4.5	20.5	4.89	2.2E-03	25.0				
	M	RAC875_c13785_2042	6A	84.11	84.1-81.2	29.6	6.61	5.7E-04	23.9				
	M	RFL_Contig5037_560	6A	117.77	117.7-117.8	12.6	3.28	2.8E-02	17.8				
	M	BobWhite_c8454_782	7D	29.97	26.2-30.0	30.1	6.72	5.7E-04	11.1				
	M	D_GA8KES401CTZ29_94	7D	161.13	161.1-161.8	13.3	3.42	2.3E-02	10.0				
	M	Σ							56.0	95.3 (0.02)			
	M_1*M_2	RAC875_c13785_2042	6A	84.11		22.2	8.28	1.9E-05	29.7		wsnp_Ex_c55051_57706127	3A	47.20
	M_1*M_2	CAP8_c665_242	7B	101.19		23.9	8.73	1.9E-05	29.6		RAC875_c13785_2042	6A	84.11
	M_1*M_2	BobWhite_c8454_782	7D	29.97	26.2-30.0	20.0	9.92	4.3E-06	32.5		RAC875_s113853_61	3D	4.46
	M_1*M_2	Σ							40.8	95.3 (0.02)			

Table 32. Summary of QTL detected for traits measured at seedling stage with 100 mM NaCl (cont.)

Trait	Effect	Marker 1	Position		Flanking region	*F* value	LOD	FDR	R^2 [%]	H^2 (SE)	Marker 2	Position	
Plant dry weight	M*T	Kukri_rep_c72412_856	2A	79.33	75.0-80.1	14.6	3.71	1.8E-01	12.9				
	M*T	Excalibur_c63409_73	2B	56.87	56.3-56.9	13.7	3.51	1.8E-01	10.9				
	M*T	BS00098868_51	3B	21.33	15.1-25.1	16.5	4.08	1.8E-01	11.8				
	M*T	Kukri_c17962_379	4A	114.46	114.5-118.7	12.2	3.19	1.8E-01	9.5				
	M*T	Kukri_c57006_127	6D	107.40	102.1-110.4	12.7	3.30	1.8E-01	8.5				
	M*T	BobWhite_c8454_782	7D	29.97	26.2-30.0	15.6	3.91	1.8E-01	11.0	97.0 (0.0)			
	M*T	Σ							44.1				
	M_1*M_2*T	BS00098868_51	3B	21.33		15.9	8.10	1.4E-04	28.6		RAC875_c63883_76	2D	6.75
	M_1*M_2*T	BobWhite_c8454_782	7D	29.97	26.2-30.0	10.6	5.58	2.0E-03	22.8		RFL_Contig3175_1271	6A	136.85
	M_1*M_2*T	Σ							44.1	97.0 (0.0)			

Table 33. Summary of QTL detected for traits measured at seedling stage with 100 mM Na_2SO_4

Trait	Effect	Marker 1	Position		Flanking region	*F* value	LOD	FDR	R^2 [%]	H^2 (SE)	Marker 2	Position	
Root length 0 DAS	M	Kukri_c28182_129	5D	196.08	196.1-199.8	12.6	6.77	2.7E-05	23.0	90.9 (0.04)			
	M	Excalibur_rep_c116920_300	7B	71.66	70.7-73.8	18.2	7.85	2.7E-05	22.9				
	M	BobWhite_c8454_782	7D	29.97	26.2-30.0	10.1	4.85	2.1E-04	15.2				
	M	Σ							40.8				
	M_1*M_2	RAC875_c8121_1997	3B	95.10		13.7	7.02	2.8E-06	34.6				
	M_1*M_2	BobWhite_c8454_782	7D	29.97		21.1	10.27	9.5E-07	37.1				
	M_1*M_2	Σ							54.3	90.9 (0.04)			
Root length 9 DAS	M	Kukri_c65146_460	4B	63.40	104.7-104.8	47.9	9.81	1.5E-07	22.8				
	M	wsnp_Ex_rep_c107564_91144523	4D	70.59	114.8-114.9	43.3	9.08	1.5E-07	22.8				
	M	wsnp_RFL_Contig2606_2264492	5D	60.61	55.2-56.0	22.5	5.27	5.5E-05	15.6				
	M	Excalibur_rep_c116920_300	7B	71.66	70.7-73.8	57.5	11.30	3.1E-08	33.5				
	M	BobWhite_c8454_782	7D	29.97	26.2-30.0	14.4	3.67	1.1E-03	14.2				
	M	Σ							57.0	94.9 (0.02)			
	M_1*M_2	wsnp_Ex_c11106_18003332	7B	55.23		33.0	13.7	7.5E-10	52.7	94.9 (0.02)	wsnp_Ex_c13337_21022658	7A	113.30
	M_1*M_2	BobWhite_c8454_782	7D	29.97		32.3	11.3	5.6E-09	42.7		Excalibur_rep_c116920_300	7B	71.66
	M_1*M_2	Σ											
	M*T	wsnp_Ku_c17161_26193994	7B	91.24	89.6-92.5	62.6	12.18	6.0E-09	34.5				
	M*T	BS00022449_51	7D	26.20	26.2-30.0	14.0	3.56	1.4E-03	9.9				
	M*T	Σ							41.0	98.9 (0.0)			
	M_1*M_2*T	Excalibur_c11093_519	7B	92.52		47.5	15.80	5.8E-12	39.8	98.9 (0.0)	wsnp_Ku_c46363_53116979	6B	113.67

Note: LOD logarithm of the odds; FDR false discovery rate; R^2 explained genetic variance, H^2 broad-sense heritability; SE standard error

Table 33. Summary of QTL detected for traits measured at seedling stage with 100 mM Na_2SO_4 (cont.)

Trait	Effect	Marker 1	Position		Flanking region	*F* value	LOD	FDR	R^2 [%]	H^2 (SE)	Marker 2	Position	
Root length 16 DAS	M	BS00022429_51	1B	30.34	29.0-33.9	18.9	4.56	1.5E-04	22				
	M	BS00022395_51	4A	121.67	115.5-123.1	12.7	3.29	2.0E-03	22				
	M	TA003708_0300	4B	61.84	55.1-63.0	62.1	12.09	4.0E-09	43.4				
	M	Kukri_rep_c101259_81	4B	104.79	104.1-109.8	22.8	5.37	3.4E-05	22				
	M	Excalibur_rep_c116920_300	7B	71.66	70.7-73.8	60.3	11.73	4.0E-09	47.6				
	M	BobWhite_c8454_782	7D	29.97	26.2-30.0	17.2	4.24	3.0E-04	11.9				
	M	Σ							69.2	95.2 (0.01)			
	M_1*M_2	Excalibur_rep_c116920_300	7B	71.66	70.7-73.8	57.0	16.77	1.0E-12	50.8		wsnp_Ex_c7002_12063380	6A	130.70
	M_1*M_2	CAP7_c9278_185	7D	123.51		11.7	4.57	4.2E-05	23.8		IAAV5564	4B	98.65
	M_1*M_2	Σ							63.5	95.2 (0.01)			
	M*T	wsnp_Ex_c4148_7495656	4B	104.79	104.7-104.8	25.8	5.85	5.9E-05	21.3				
	M*T	Kukri_c10913_480	5B	188.58	180.7-189.5	54.6	9.16	5.8E-06	32.7				
	M*T	Excalibur_c20931_669	7B	73.79	72.7-77.1	55.8	8.40	5.9E-06	36.3				
	M*T	BS00067140_51	7D	26.92	26.2-30.0	18.3	3.49	2.8E-03	8.0				
	M*T	Σ							54.0	76.8 (0.14)			
	M_1*M_2*T	Excalibur_rep_c116920_300	7B	71.66	70.7-73.8	36.9	15.98	1.5E-12	49.2	76.8 (0.14)	BS00068429_51	1B	41.21
Shoot length 0 DAS	M	RAC875_c2300_1021	2B	27.20	27.2-27.3	*21.5*	5.08	7.1E-02	13.7	86.4 (0.07)			
	M_1*M_2	RAC875_c2300_1021	2B	27.20	27.20	16.5	6.35	1.4E-03	17.1	86.4 (0.07)	Tdurum_contig82242_224	3B	36.82
	M_1*M_2	Tdurum_contig17500_876	5A		70.30	9.8	5.12	3.1E-03	19.1		Tdurum_contig48049_705	4A	41.02
	M_1*M_2	Σ							34.7				
Shoot length 9 DAS	M	TA001249_1083	2D	76.39	76.3-76.4	16.4	4.07	1.1E-01	6.4				
	M	RAC875_c81076_317	3B	62.31	62.0-62.5	14.4	3.65	1.2E-01	6.8				
	M	GENE_2778_24	4A	58.38	58.3-58.5	16.5	4.09	1.1E-01	10.7				
	M	BS00108573_51	7B	77.13	76.3-77.1	17.3	4.23	1.1E-01	10.1				
	M	Σ							24.0	88.4 (0.08)			
	M_1*M_2	GENE_2778_24	4A	58.4	58.3-58.5	17.0	6.58	7.0E-03	24.0	88.4 (0.08)	RAC875_c43295_135	7A	148.43
	M*T	Kukri_c40204_141	2A	19.60	19.6-26.0	15.6	3.87	1.5E-01	13.0				
	M*T	RAC875_c34767_147	2D	24.79	17.6-28.1	11.3	3.01	1.5E-01	13.1				
	M*T	wsnp_Ex_c24474_33721784	4A	69.96	59.9-75.5	13.5	3.48	1.5E-01	11.8				
	M*T	wsnp_Ku_c42416_50159402	5A	98.44	89.5-97.7	15.7	3.93	1.5E-01	14.2				
	M*T	Kukri_rep_c103186_134	6A	140.87	136.8-140.9	11.5	3.03	1.5E-01	12.9				
	M*T	Σ							34.6	90.4 (0.04)			
	M_1*M_2*T	Kukri_c40204_141	2A	19.60		12.8	6.49	1.7E-02	27.5		RAC875_c34767_147	2D	24.79
	M_1*M_2*T	BS00040933_51	5A	36.73		11.2	4.49	2.0E-02	15.7		TA001249_1083	2D	76.39
	M_1*M_2*T	Σ							44.5	90.4 (0.04)			

Table 33. Summary of QTL detected for traits measured at seedling stage with 100 mM Na_2SO_4 (cont.)

Trait	Effect	Marker 1	Position		Flanking region	*F* value	LOD	FDR	R^2 [%]	H^2 (SE)	Marker 2	Position	
Shoot length 16 DAS	M	TA001249_1083	2D	76.39	76.3-76.4	19.8	4.76	4.7E-02	8.3				
	M	GENE_2778_24	4A	58.38	58.3-58.5	16.6	4.68	4.8E-02	14.3				
	M	Kukri_c45876_61	6D	153.08	153.1-153.1	19.9	4.78	4.7E-02	10.8	88.5 (0.08)			
	M	Σ							29.3				
	M_1*M_2	D_wsnpbe497701_Contig1_2	6D	87.17		10.4	5.47	7.0E-04	22.7		Tdurum_contig10672_117	4A	139.97
	M_1*M_2	BS00063625_51	6D	116.85		18.9	7.21	6.0E-04	19.2		TA001249_1083	2D	76.39
	M_1*M_2	BS00077791_51	7A	136.43		10.8	5.69	6.3E-04	17.8		Kukri_c45876_61	6D	153.08
	M_1*M_2	Σ							44.4	88.5 (0.08)			
	M*T	Tdurum_contig67750_272	3B	70.68	70.6-72.2	17.3	4.24	1.1E-01	10.8				
	M*T	BS00077791_51	7A	136.43	136.0-136.5	15.3	3.84	1.1E-01	9.8				
	M*T	Σ							18.6	52.8 (0.19)			
	M_1*M_2*T	BS00009492_51	4A	59.99		16.9	6.55	3.0E-03	20.8	52.8 (0.19)	BS00077791_51	7A	136.43
Shoot fresh weight	M	TA001249_1083	2D	76.39	76.3-76.4	19.6	4.72	1.6E-01	11.8				
	M	wsnp_Ex_c10527_17198865	4A	48.52	48.5-49.0	12.5	3.25	1.6E-01	9.4				
	M	Σ							22.1	75.7 (0.08)			
	M_1*M_2	TA001249_1083	2D	76.39	76.3-76.4	14.7	7.59	1.2E-03	17.5		wsnp_JD_c2722_3653988	3A	35.55
	M_1*M_2	Kukri_c96249_58	5D	130.04		13.6	5.34	7.3E-03	24.8		Ra_c47493_933	5D	94.03
	M_1*M_2	Σ							42.0	75.7 (0.08)			
	M*T	RAC875_c11911_431	2D	34.15	34.1-34.2	20.3	4.85	4.9E-03	13.4				
	M*T	Kukri_rep_c72254_186	2D	49.59	49.3-50.8	20.7	4.92	4.7E-03	13.4				
	M*T	tplb0050o09_895	3D	4.46	4.0-5.6	25.7	5.90	4.1E-03	15.5				
	M*T	Σ							32.2	78.7 (0.06)			
	M_1*M_2*T	Kukri_rep_c72254_186	2D	49.59		12.7	6.60	5.1E-07	23.0	78.7 (0.06)	tplb0050o09_895	3D	4.46
Shoot dry weight	M	TA001249_1083	2D	76.39	76.3-76.4	20.5	4.91	1.1E-01	13.7				
	M	wsnp_Ex_c10527_17198865	4A	48.52	48.5-48.6	12.6	3.28	1.1E-01	9.8				
	M	RAC875_rep_c69766_246	7A	126.40	126.4-130.3	15.5	3.88	1.1E-01	11.7				
	M	Tdurum_contig61864_1352	7A	199.64	199.0-191.0	13.0	3.37	1.1E-01	9.9				
	M	Σ							30.4	81.3 (0.06)			
	M_1*M_2	TA001249_1083	2D	76.39	76.3-76.4	15.0	7.72	8.0E-04	26.0		wsnp_JD_c2722_3653988	3A	35.55
	M_1*M_2	RAC875_c9095_217	3B	62.67		10.1	5.29	6.7E-03	19.4		RAC875_rep_c69766_246	7A	126.40
	M_1*M_2	Σ							43.4	81.3 (0.06)			
	M*T	Excalibur_c20175_370	2D	40.05	40.0-41.0	12.8	3.32	1.5E-01	10.0				
	M*T	wsnp_JD_c10602_11238420	3B	74.26	74.2-74.3	11.4	3.03	2.4E-01	8.5				
	M*T	Excalibur_c19658_127	3D	4.56	4.0-5.6	21.9	5.16	1.5E-02	11.5				
	M*T	Σ							20.3	82.7 (0.06)			
	M_1*M_2*T	Kukri_rep_c72254_186	2D	49.59		12.4	6.4	7.3E-07	22.5	82.7 (0.06)	tplb0050o09_895	3D	4.46

Table 33. Summary of QTL detected for traits measured at seedling stage with 100 mM Na_2SO_4 (cont.)

Trait	Effect	Marker 1	Position		Flanking region	*F* value	LOD	FDR	R^2 [%]	H^2 (SE)	Marker 2	Position	
Root fresh weight	M	BS00050993_51	7B	52.91	52.0-53.9	20.8	4.95	2.3E-02	11.5				
	M_1*M_2	RAC875_c9095_217	3B	62.67		17.8	6.80	9.9E-04	24.1		TA001249_1083	2D	76.39
	M_1*M_2	BobWhite_c8027_421	7B	72.27		13.7	7.05	9.9E-04	20.3		Excalibur_c19658_127	3D	4.56
	M_1*M_2	Σ							43.2				
Root dry weight	M	RAC875_c9095_217	3B	62.67	57.9-69.7	20.0	4.80	2.1E-02	13.1				
	M	Excalibur_c19658_127	3D	4.56	4.0-4.6	12.7	3.29	2.3E-02	10.2				
	M	Σ							21.1				
	M_1*M_2	RAC875_c30315_692	5D	69.13		19.7	7.46	9.2E-04	19.8		Tdurum_contig62976_84	2A	101.97
	M_1*M_2	RAC875_c46980_148	7A	156.23		14.6	5.65	3.1E-03	20.8		wsnp_Ra_c24707_34262900	5A	43.27
	M_1*M_2	Σ							36.1				
Plant fresh weight	M	TA001249_1083	2D	76.39	76.3-76.4	17.4	4.29	4.4E-02	9.4	80.7 (0.07)			
	M	wsnp_Ex_c10527_17198865	4A	48.52	47.5-48.5	13.1	3.38	5.5E-02	12.7				
	M	Σ							23.1				
	M_1*M_2	TA001249_1083	2D	76.39		13.6	7.06	2.9E-03	24.6	80.7 (0.07)	wsnp_JD_c2722_3653988	3A	35.55
	M_1*M_2	RAC875_c9095_217	3B	62.67		9.4	4.93	1.1E-02	20.9		Ra_c47493_933	5D	94.03
	M_1*M_2	Σ							47.9				
	M*T	Kukri_rep_c72254_186	2D	49.59	49.3-50.8	20.37	4.86	4.8E-03	13.2				
	M*T	tplb0050o09_895	3D	4.46	4.0-4.6	27.04	6.17	3.0E-03	16.3				
	M*T	Σ							23.3	79.9 (0.10)			
	M_1*M_2*T	RAC875_c40298_394	2A	101.97		8.8	4.61	1.9E-03	20.3		wsnp_JD_c9902_10674725	3B	62.67
	M_1*M_2*T	Excalibur_rep_c77221_93	2B	109.53		18.9	9.54	1.1E-05	29.9		tplb0050o09_895	3D	4.47
	M_1*M_2*T	Kukri_rep_c100676_151	6B	58.26		8.6	4.51	2.1E-03	19.8		RAC875_c40298_394	2A	101.97
	M_1*M_2*T	CAP7_c3950_160	7B	155.42		8.1	4.21	2.9E-03	19.3		Excalibur_c130_3813	6B	117.66
	M_1*M_2*T	Σ							49.9	79.9 (0.10)			
Plant dry weight	M	TA001249_1083	2D	76.39	76.3-76.4	17.5	4.31	4.2E-02	10.4				
	M	wsnp_Ex_c10527_17198865	4A	48.52	47.5-48.5	13.6	3.48	4.2E-02	10.2				
	M	Ra_c47493_933	5D	94.03	94.0-95.0	12.5	3.25	4.0E-02	9.7				
	M	Σ							23.5	83.8 (0.08)			
	M_1*M_2	TA001249_1083	2D	76.39	76.3-76.4	13.86	7.17	3.3E-03	24.6		wsnp_JD_c2722_3653988	3A	35.55
	M_1*M_2	RAC875_c23775_406	5A	84.13		8.71	4.57	2.1E-02	20.0		Ra_c47493_933	5D	94.03
	M_1*M_2	Kukri_c96249_58	5D	130.04		12.11	4.81	1.9E-02	21.0		Ra_c47493_933	5D	94.03
	M_1*M_2	Σ							46.2	83.8 (0.08)			
	M*T	wsnp_JD_c10602_11238420	3B	74.26	74.2-77.2	12.3	3.21	1.8E-01	8.0				
	M*T	tplb0050o09_895	3D	4.46	4.0-4.6	21.7	5.13	1.4E-02	11.1				
	M*T	Σ							18.8	85.6 (0.06)			

Table 33. Summary of QTL detected for traits measured at seedling stage with 100 mM Na_2SO_4 (cont.)

Trait	Effect	Marker 1	Position	Flanking region	*F* value	LOD	FDR	R^2 [%]	H^2 (SE)	Marker 2	Position	
Plant dry weight	M_1*M_2*T	BS00022487_51	2A 64.06		7.7	4.05	7.4E-03	13.1		wsnp_JD_c10602_11238420	3B	74.26
	M_1*M_2*T	IAAV2585	2A 74.98		7.7	4.04	7.5E-03	16.6		Kukri_rep_c72254_186	2D	49.59
	M_1*M_2*T	tplb0050o09_895	3D 4.46		14.9	7.64	4.4E-04	26.2		wsnp_Ku_c46762_53407442	3A	173.15
	M_1*M_2*T	Σ						37.6	85.6 (0.06)			
Na^+ conc. in 3rd leaves	M	CAP8_c5108_139	2B 46.76	42.4-46.8	21.3	5.06	4.5E-03	14.7				
	M	Ex_c66324_1151	4A 65.95	65.0-66.0	16.4	4.08	1.3E-02	13.0				
	M	BS00064548_51	6A 82.79	82.7-83.7	28.5	6.47	1.6E-03	13.5				
	M	RAC875_c22233_83	7A 42.47	40.0-42.5	12.4	3.22	3.1E-02	9.0	97.2 (0.01)			
	M	RAC875_c25695_316	7D 32.16	32.1-37.4	22.6	5.31	3.3E-03	15.4				
	M	Σ						47.9				
	M*T	Excalibur_c9206_671	3B 30.33	30.3-30.7	26.1	6.00	8.7E-03	12.9	97.2 (0.01)			
	M*T	BS00021965_51	6A 119.64	119.0-119.7	14.7	3.71	1.2E-01	11.6				
	M*T	RAC875_c25695_316	7D 32.16	32.1-37.4	15.4	3.87	1.2E-01	12.0				
	M*T	Σ						33.1				
K conc. in 3rd leaves	M*T	wsnp_Ex_rep_c66545_64829026	2B 99.16	99.1-103.3	11.3	3.00	1.3E-01	10.7				
	M*T	Tdurum_contig4576_603	5A 82.66	82.5-82.7	16.6	4.08	1.3E-01	12.2				
	M*T	Σ						18.9	80.5 (0.10)			
	M*T	wsnp_Ra_c22648_32132929	2D 82.8	72.9-86.0	13.6	3.49	1.3E-01	15.0				
K^+/Na^+ conc. ration in 3rd	M*T	BS00024499_51	3B 110.2	110.0-110.3	13.5	3.45	1.3E-01	13.8				
	M*T	IAAV1179	5A 69.3	69.3-69.4	15.9	3.97	1.3E-01	10.4				
	M*T	RAC875_c93959_96	6A 117.9	117.8-118.0	12.6	3.29	1.3E-01	7.9				
	M*T	BS00029127_51	6A 130.4	130.3-130.4	14.8	3.74	1.3E-01	11.1				
	M*T	BobWhite_c8454_782	7D 30.0	26.2-30.0	18.0	4.40	1.3E-01	9.5				
	M*T	Σ						40.2	99.0 (0.0)			

Table 34. Summary of QTL detected for traits measured from field trials

Trait	Effect	Marker 1	Position		Flanking region	*F* value	LOD	FDR	R^2 [%]	H^2 (SE)	Marker 2	Position	
Grain yield [t/ha]	M	Kukri_c14889_1086	5A	70.3	60.6-76.3	33.2	7.2	5.0E-04	24.1	97.9 (0.01)			
	M_1*M_2	BobWhite_c28635_896	1B	70.7		8.9	4.5	3.5E-05	18.4		RAC875_c13490_1344	5A	100.90
	M_1*M_2	D_contig74612_253	2D	4.7		20.8	6.4	3.7E-07	23.9		Kukri_c14889_1086	5A	70.30
	M_1*M_2	Σ							34.3	97.9 (0.01)			
	M*T	RAC875_c2257_728	1B	57.60	57.6-60.3	34.6	7.3	4.4E-04	26.7	99.8 (0.0)			
	M_1*M_2*T	Kukri_c11141_203	7B	113.9		8.9	4.64	5.0E-04	37.5		Tdurum_contig50984_553	7B	72.74
	M_1*M_2*T	Kukri_c11141_203	7B	113.9		26.6	9.1	4.5E-06	36.9		RAC875_c2257_728	1B	57.60
	M_1*M_2*T	Σ							49.8	99.8 (0.0)			
TKW	M	Tdurum_contig76550_500	2B	143.0	142.9	22.3	5.3	3.4E-03	11.7				
	M	Tdurum_contig48049_705	4A	41.0	41.0	11.8	3.1	1.7E-02	7.8				
	M	D_GB5Y7FA02FHK0M_407	6D	53.1	53.8-54.3	19.0	4.6	3.4E-03	13.7				
	M	Σ							31.9	97.7 (0.01)			
	M_1*M_2	Kukri_rep_c83485_398	2A	98.4		14.6	7.5	6.8E-06	19.7	97.7 (0.01)	Tdurum_contig76550_500	2B	143.00
	M*T	BS00041707_51	2A	105.53	105.5-108.5	22.4	5.2	1.3E-02	12.5				
	M*T	Kukri_c24642_426	5A	38.72	38.7-38.7	17.1	4.2	1.3E-02	15.1				
	M*T	D_GB5Y7FA02FHK0M_407	6D	53.08	53.0-54.3	27.9	6.3	2.6E-03	18.4				
	M*T	Σ							34.7	99.4 (0.0)			
	M_1*M_2*T	D_GB5Y7FA02FHK0M_407	6D	53.08		18.4	9.0	5.2E-06	33.9	99.4 (0.0)	RAC875_c13942_2973	7D	111.21
Spikes length	M	RAC875_c43002_382	1A	142.31		36.9	7.9	9.7E-05	23.2				
	M	Tdurum_contig25641_409	1B	70.71		25.4	5.8	1.7E-03	15.7				
	M	wsnp_Ex_c361_707953	3A	177.24		14.0	3.6	1.7E-02	11.7				
	M	BobWhite_c48435_165	5B	90.35		32.2	7.1	2.1E-04	20.3				
	M	Σ							38.1	91.2 (0.04)			
	M_1*M_2	Excalibur_c39686_664	3D	129.25		29.1	13.9	2.0E-12	45.4	91.2(0.04)	Tdurum_contig25641_409	1B	70.71
	M*T	RAC875_c55872_149	5A	111.20	111.2-111.2	25.0	5.7	1.7E-02	25.0	97.6 (0.02)			
	M_1*M_2*T	D_contig24344_227	3D	123.83		15.5	7.7	3.6E-04	31.2	97.6 (0.02)	D_contig24344_227	3D	123.83
Spikelet per spike	M	Kukri_c31964_109	1A	56.1	56.1	11.5	3.0	5E-02	10.7				
	M	BobWhite_c82_578	6A	99.0	99.0	17.3	4.3	5E-02	12.4				
	M	Σ							20.3	94.3 (0.03)			
	M_1*M_2	BobWhite_c82_578	6A	99.0		16.6	6.4	9.4E-03	21.9	94.3 (0.03)	Excalibur_c7033_159	1A	77.78
	M*T	wsnp_JD_c825_1223506	1A	131.56	131.6	14.7	3.7	3.0E-01	11.7				
	M*T	Tdurum_contig13117_1316	1B	86.07	86.1	11.8	3.1	3.0E-01	8.5				
	M*T	BS00065105_51	2B	81.75	81.8	13.3	3.4	3.0E-01	11.3				
	M*T	Σ							28.3	99.5 (0.0)			
	M_1*M_2*T	Excalibur_c7033_159	1A	77.78		16.2	8.0	3.6E-04	32.8	99.5 (0.0)	Tdurum_contig13117_1316	1B	86.07

Table 34. Summary of QTL detected for traits measured from field trials (cont.)

Trait	Effect	Marker 1	Position		Flanking region	*F* value	LOD	FDR	R^2 [%]	H^2 (SE)	Marker 2	Position	
Peduncle length	M	BobWhite_c3146_128	2B	109.53	109.5	13.4	3.5	5.5E-02	9.1				
	M	Excalibur_c9166_913	7A	45.25	42.0- 45.3	11.4	3.0	6.1E-02	9.1	92.0 (0.05)			
	M	D_GBUVHFX01BEHL1_132	7D	95.68	95.6- 97.4	16.6	4.1	5.5E-02	11.7				
	M	Σ							19.5				
	M_1*M_2	BS00003866_51	4A	61.91		16.5	6.4	2.7E-05	20.1		D_GBUVHFX01BEHL1_132	7D	95.68
	M_1*M_2	BS00101071_51	5A	25.27		7.9	4.1	1.2E-04	14.0		wsnp_Ku_c19618_29134473	1B	70.08
	M_1*M_2							.	34.2	92.0 (0.05)			
	M*T	RAC875_c82888_83	1D	67.72	67.7- 73.2	18.6	4.5	4.7E-02	15.7	99.4 (0.0)			
	M_1*M_2*T	tplb0051d06_1385	5A	53.47		16.5	6.2	3.1E-03	26.3		BobWhite_c32313_688	4A	110.13
	M_1*M_2*T	BS00022550_51	7B	61.26		12.4	6.3	3.1E-03	25.0		wsnp_Ku_c53270_57959459	1D	81.93
	M_1*M_2*T	Σ						.	47.6	99.4 (0.0)			
Plant height	M	wsnp_CAP12_c1337_682282	1B	136.1	132.5 - 136.1	19.7	4.7	1.5E-02	12.6				
	M	D_GBB4FNX02ILZW2_114	7D	161.1	160.0-162.0	12.0	3.1	1.5E-02	10.0				
	M	Σ				14.0	7.2		25.2	98.3 (0.0)			
	M_1*M_2	D_GBB4FNX02ILZW2_114	7D	161.13		14.0	7.2	2.8E-03	25.3	98.3 (0.0)	wsnp_CAP12_c1337_682282	1B	136.11
	M*T	wsnp_Ex_c7266_12475249	5A	86.4	86.3-83.6	23.5	5.4	2.9E-02	18.3	99.0 (0.0)			
	M_1*M_2*T	Tdurum_contig8674_1236	3A	188.38		17.1	6.5	1.2E-03	22.8	99.0 (0.0)	wsnp_Ex_c7266_12475249	5A	86.36
Days to heading	M*T	IAAV2683	1B	85.57	85.1-86.0	14.9	3.7	1.7E-02	15.3				
	M*T	wsnp_BE590634B_Ta_2_5	1B	96.41	96.0-99.2	13.0	3.3	3.3E-02	16.9				
	M*T	wsnp_Ex_rep_c70756_69644826	2B	65.01	63.0-66.3	15.4	3.8	1.5E-02	16.7				
	M*T	Σ							26.0	98.5 (0.0)			
	M_1*M_2*T	BS00003568_51	6D	150.56		17.3	8.4	1.6E-07	35.2		IAAV2683	1B	85.6
	M_1*M_2*T	BS00065981_51	7B	95.71		49.1	20.0	1.1E-16	55.7		D_contig32283_420	1D	115.6
	M_1*M_2*T	Σ							39.2	98.5 (0.0)			
Protein content	M	BS00064570_51	2B	16.88	98.4	12.1	3.2	4.9E-02	7.6				
	M_1*M_2	BS00064570_51	2B	16.88		9.6	5.1	4.9E-02	17.2	83.5 (0.17)	RAC875_c21358_62	2B	141.32
	M*T	RAC875_c13490_1344	5A	100.90	100.9-104.9	19.6	4.7	5.0E-02	16.6	84.9 (0.15)			
	M_1*M_2*T	IACX8386	2B	138.78		11.9	6.1	1.0E-02	24.5		RAC875_c13490_1344	5A	100.90
	M_1*M_2*T	RAC875_c13490_1344	5A	100.90		13.3	5.2	1.3E-02	19.1		RAC875_c2253_238	6A	37.13
	M_1*M_2*T	BobWhite_c33778_146	5D	204.58		13.5	5.3	1.3E-02	18.9		RAC875_c13490_1344	5A	100.90
	M_1*M_2*T	IACX72	7A	126.80		10.0	5.1	1.3E-02	21.7		RAC875_c13490_1344	5A	100.90
	M_1*M_2*T	Excalibur_rep_c66918_307	7A	202.68		10.5	5.4	1.3E-02	21.3		RAC875_c13490_1344	5A	100.90
	M_1*M_2*T	D_GBQ4KXB01C5QDQ_113	7D	139.07		15.1	5.8	1.1E-02	21.0		RAC875_c13490_1344	5A	100.90
	M_1*M_2*T	Σ								84.9 (0.15)			

Table 34. Summary of QTL detected for traits measured from field trials (cont.)

Trait	Effect	Marker 1	Position		Flanking region	*F* value	LOD	FDR	R^2 [%]	H^2 (SE)	Marker 2	Position	
Starch content	M	wsnp_CAP11_c1506_840951	5A	98.44	98.4-99.1	13.1	3.4	2.5E-02	8.9	85.8 (0.12)			
	M_1*M_2	BS00022178_51	1D	133.99		5.8	3.0	3.2E-02	13.9		wsnp_Ex_rep_c70299_69243835	2A	140.94
	M_1*M_2	BS00012069_51	5D	204.58		11.8	4.7	3.2E-02	14.6		wsnp_CAP11_c1506_840951	5A	98.44
	M_1*M_2	Σ							28.4	85.8 (0.12)			
	M*T	BS00104432_51	5A	105.36	105.3-105.4	29.8	6.61	9.3E-04	20.1	95.3 (0.0)			
	M_1*M_2*T	BS00104432_51	5A	105.36		13.9	7.1	9.1E-04	26.9	95.3 (0.0)	Excalibur_rep_c66918_307	7A	202.68
Sedimentation value	M	BS00000020_51	5D	102.91	102.9	12.9	3.3	4.3E-02	7.9				
	M	RAC875_c23552_811	6A	33.31	32.2-42.1	14.9	3.8	4.3E-02	9.9				
	M	Σ							19.4	92.1 (0.05)			
	M_1*M_2	BS00000020_51	5D	102.91		11.0	5.7	4.6E-05	19.7	92.1 (0.05)	RAC875_c23552_811	6A	33.31
	M*T	wsnp_Ex_c1969_3705930	1D	21.80		16.1	4.0	2.3E-02	13.0	98.3 (0.0)			
	M_1*M_2*T	BobWhite_c18852_91	2A	82.23		17.7	6.7	6.0E-03	24.9	98.3 (0.0)	wsnp_Ex_c1969_3705930	1D	21.80
Fiber content	M	Excalibur_c28017_641	2A	109.20	105.5-109.2	37.7	8.02	5.6E-05	23.8	98.5 (0.0)			
	M_1*M_2	Excalibur_c28017_641	2A	109.20		20.7	10.11	4.5E-06	34.7	98.5 (0.0	Excalibur_c53864_331	4A	106.72
	M*T	RAC875_c39665_175	2D	54.58	53.6-54.6	38.6	8.1	6.5E-05	24.9				
	M*T	IAAV1383	4A	112.71	112.7	12.7	3.3	1.1E-02	10.0				
	M*T	RAC875_c58332_1099	5D	51.93	50.9- 51.9	16.2	4.0	8.0E-03	13.5				
	M*T	Σ							46.1	99.6 (0.0)			
	M_1*M_2*T	IAAV1383	4A	112.71		22.8	10.8	5.3E-07	38.8		RAC875_c39665_175	2D	54.58
	M_1*M_2*T	BS00000020_51	5D	102.91		15.7	7.9	7.1E-06	27.7		BS00021708_51	5A	37.79
	M_1*M_2*T	BS00000020_51	5D	102.91		20.6	7.6	7.7E-06	25.4		BS00004170_51	4A	41.02
	M_1*M_2*T	Σ							56.0	99.6 (0.0)			
NDF content	M	Tdurum_contig2945_75	2B	106.56	106.5	19.1	4.6	4.1E-03	13.9				
	M	TA004228_0191	3B	71.34	61.4-81.0	27.3	6.2	2.2E-03	22.4				
	M								34.0	99.5 (0.0)			
	M_1*M_2	TA004228_0191	3B	71.34		22.1	10.8	4.6E-09	34.1	99.5 (0.0)	Tdurum_contig2945_75	2B	106.56
	M*T	BS00110587_51	2A	113.30	104.1-115.4	22.2	5.2	2.7E-04	13.9				
	M*T	Tdurum_contig45661_684	2A	139.04	139.0-139.4	12.7	3.3	8.9E-03	5.2				
	M*T	BS00011869_51	3B	71.34	61.6-81.0	42.7	9.0	5.5E-06	22.5				
	M*T	Σ							39.8	99.0 (0.0)			
	M_1*M_2*T	BS00011869_51	3B	71.34		25.1	11.9	3.67E-10	36.9	99.0 (0.0)	Tdurum_contig2945_75	2B	106.56

Table 34. Summary of QTL detected for traits measured from field trials (cont.)

Trait	Effect	Marker 1	Position		Flanking region	*F* value	LOD	FDR	R^2 [%]	H^2 (SE)	Marker 2	Position	
Kernel hardness	M	wsnp_Ex_rep_c69799_68761171	2A	113.30	113.2-113.3	14.2	3.6	3.2E-02	10.6				
	M	RAC875_c58332_1099	5D	51.93	51.9	25.9	6.0	5.5E-03	19.4				
	M	Kukri_c3734_892	7B	3.27	3.2	16.6	4.1	8.2E-02	12.7				
	M	Σ							37.2	97.5 (0.0)			
	M_1*M_2	BS00035256_51	5A	82.72		11.9	6.2	2.5E-04	23.8		Excalibur_c11947_746	2A	97.51
	M_1*M_2	Kukri_c3734_892	7B	3.27		22.7	8.5	5.4E-05	29.3		RAC875_c58332_1099	5D	51.93
	M_1*M_2	Σ							44.4	97.5 (0.0)			
	M*T	wsnp_Ex_rep_c69799_68761171	2A	113.30		15.1	3.8	8.5E-02	13.4				
	M*T	Kukri_c37735_131	3B	80.13		13.6	3.5	9.5E-02	8.9				
	M*T	CAP11_c3209_76	5A	92.56		18.3	4.4	7.3E-02	19.6				
	M*T	RAC875_c58332_1099	5D	51.93		19.9	4.8	7.3E-02	8.4				
	M*T	Kukri_c96249_58	5D	130.03		18.9	4.5	7.3E-02	23.8				
	M*T	Σ							40.7	99.1 (0.0)			
	M_1*M_2*T	Kukri_c96249_58	5D	130.04		15.4	7.8	2.2E-04	28.6	99.1 (0.0)	RAC875_c58332_1099	5D	51.93

Appendix 4

Table 35. Ontology of the detected marker trait associations and the proposed functions

Marker	Chr	Pos	Annotation	Purpose	Species	Reference
Excalibur_c35316_154	1A	16.70	Prolamin gene locus/gamma gliadin gene	Storage protein	Aegilops tauschii	JX295577.2
Excalibur_c7026_2635	1A	52.55	E3 UFM1-protein ligase 1 homolog	Signaling pathway	Aegilops tauschii	XP_020187519.1
Tdurum_contig8382_300	1A	57.93	Uncharacterized protein	Unknown	Aegilops tauschii	LOC109744923
Kukri_rep_c104386_273	1A	70.10	rRNA biogenesis protein RRP5	Cellular function; Involved in the biogenesis of rRNA	Aegilops tauschii	LOC109742512
wsnp_Ex_c7271_12483592	1A	71.05	ADP-ribosylation factor GTPase-activating protein AGD8	Protein cycle	Aegilops tauschii	XP_020165334.1
Excalibur_c7033_159	1A	77.78	Membrane bound Peptidase, FtsH	Crucial role in housekeeping proteolysis of membrane proteins	Oryza sativa	IPR005936
wsnp_JD_c825_1223506	1A	131.56	Wall-associated receptor kinase, galacturonan-binding domain	Plasma membrane proteins potential signaling molecules.	Oryza sativa	IPR025287
Kukri_c65610_572	1A	139.93	Periodic tryptophan protein 1 homolog	May play an important role in cell growth	Aegilops tauschii	LOC109777212
BS00022429_51	1B	30.34	P-loop containing nucleoside triphosphate hydrolase	Involved in salt stress response by attenuation of oxidative stress and reactive oxygen species (ROS)	Arabidopsis thaliana	IPR027417
BS00068429_51	1B	41.21	P-loop containing nucleoside triphosphate hydrolase	Involved in salt stress response by attenuation of oxidative stress and reactive oxygen species (ROS)	Arabidopsis thaliana	IPR027417
RAC875_c2257_728	1B	57.60	Receptor-like serine/threonine-protein kinase SD1-7	Involved in the regulation of cellular expansion and differentiation	Aegilops tauschii	P_020197053.1
Ex_c2725_1442	1B	62.54	Leucine-rich repeat domain, L domain-like	Signaling and ABA biosynthesis as stress response	Aegilops tauschii	IPR032675
Tdurum_contig25641_409	1B	70.71	Mitochondrial fission 1 protein A-like	Plays a role in promoting the fission of mitochondria and peroxisomes	Aegilops tauschii	XP_020148187.1
Tdurum_contig59449_400	1B	71.85	F-box/FBD/LRR-repeat protein At5g22660-like	Regulation of biological process; involved in stress response	Oryza sativa	LOC107275296
Tdurum_contig20299_142	1B	76.09	Uncharacterized protein	Unknown	Aegilops tauschii	LOC109762342
IAAV2683	1B	85.57	Zinc-binding ribosomal protein	Ribosomal protein L33; Ribosomal biogenesis	Arabidopsis thaliana	IPR011332
Tdurum_contig13117_1316	1B	86.07	TRAM/LAG1/CLN8 homology domain	Involved in signaling mechanism and cell death regulation to cope with salt stress	Oryza sativa	IPR006634
wsnp_BE590634B_Ta_2_5	1B	96.41	Polyprenyl synthetase	Terpenoids biosynthesis involved in Cell wall/Wax+, Plant defense	Oryza sativa	IPR000092
Excalibur_c49496_705	1B	122.52	E3 ubiquitin-protein ligase MBR2-like isoform x3	Major role for protein degradation in control of plant life.	Arabidopsis thaliana	XP_020169213.1
wsnp_Ex_c41553_48351921	1B	132.13	P-loop containing nucleoside triphosphate hydrolase	Involved in salt stress response by attenuation of oxidative stress and reactive oxygen species (ROS)	Arabidopsis thaliana	IPR027417
wsnp_CAP12_c1337_682282	1B	136.11	Very-long-chain 3-ketoacyl-CoA synthase	Involved in fatty acid biosynthetic process	Oryza sativa	IPR012392
wsnp_Ex_c1969_3705930	1D	21.80	Protein kinase domain	Multiple cellular functions	Arabidopsis thaliana	IPR000719
RAC875_c82888_83	1D	67.72	Pyridoxal phosphate-dependent transferase	Involved in aminotransferases regulating salt and drought stress through ABA pathway	Oryza sativa	IPR015424
Excalibur_c34167_128	1D	71.90	Uncharacterized protein	Unknown	Aegilops tauschii	LOC109732878
wsnp_Ku_c53270_57959459	1D	81.93	Transcription factor IIS, N-terminal	Cellular process	Arabidopsis thaliana	IPR017923
CAP11_c3464_68	1D	92.91	GDSL esterase/lipase At5g45910-like	Involved in fatty acid metabolism	Aegilops tauschii	LOC109763450

Table 32. (cont.)

D_contig32283_420	1D	115.62	Alpha-glucan water dikinase	Key enzyme of starch metabolism; downregulation will lead to higher yield and biomass	Aegilops tauschii	XP_020163887.1
BS00104199_51	1D	133.99	Lecithin-cholesterol acyltransferase-like	lipid metabolic process of plasma membrane	Aegilops tauschii	LOC109752870
BS00022178_51	1D	133.99	Phospholipase D/Transphosphatidylase	Multiple functions including ABA pathway, signaling. Etc. regulating stress tolerance	Aegilops tauschii	XP_020167375.1
Kukri_c40204_141	2A	19.60	Golgin subfamily A member 6-like protein 22, transcript variant X2	Involved in membrane trafficking	Aegilops tauschii	LOC109783605
Kukri_c33374_1048	2A	20.14	Protein transport protein Sec24-like At3g07100	Protein transporter from the endoplasmic reticulum to the Golgi complex	Aegilops tauschii	XP_020159454.1
Ra_c510_171	2A	25.02	Naringenin-chalcone synthases (CHSs)	Involved in flavonoid synthesis	Oryza sativa	IPR001099
BS00045171_51	2A	48.44	Peptidase S8, subtilisin-IPR015500	Plant hormone activation	Hordeum vulgare	BAK04840.1
BS00068050_51	2A	48.44	Uncharacterized protein	Unknown	Aegilops tauschii	LOC109785320
Tdurum_contig42153_5454	2A	52.00	P-loop containing nucleoside triphosphate hydrolase	Involved in salt stress response by attenuation of oxidative stress and reactive oxygen species (ROS)	Arabidopsis thaliana	IPR027417
BS00022487_51	2A	64.06	FAD/NAD(P)-binding domain	Belonging to the family of pyridine nucleotide-disulphide oxidoreductases Related to GST; detoxification	Aegilops tauschii	IPR023753
wsnp_Ex_c22202_31392780	2A	65.60	Vps54-like protein	Probably involved in membrane trafficking system	Brachypodium distachyon	pfam07928
IAAV2585	2A	74.98	NETWORKED 2A-like	Membrane specific actin binding domain	Aegilops tauschii	LOC109761538
wsnp_Ex_c5412_9564478	2A	76.90	Importin-beta N-terminal domain; pfam03810	Nuclear import receptor for the ubiquitin-conjugating enzyme, UbcM2 which is involved in salt stress response	Aegilops tauschii	LOC109734977
Kukri_rep_c72412_856	2A	79.33	P-loop containing nucleoside triphosphate hydrolase	Cellular function/ involved in the ATP-dependent degradation of ubiquitinated proteins	Aegilops tauschii	XP_020182762.1
BobWhite_c18852_91	2A	82.23	Concanavalin A-like lectin/glucanase domain containing protein	Involved transcription factor activity for shoot Na+/K+ under in salt stress	Aegilops tauschii	IPR013320
Excalibur_c11947_746	2A	97.51	Uncharacterized protein	Unknown	Aegilops tauschii	XP_020201097.1
Kukri_rep_c83485_398	2A	98.43	Nucleolar protein 56-like	Involved in ribosome biogenesis	Aegilops tauschii	XP_020157820.1
GENE_1342_238	2A	101.97	Importin-beta, N-terminal domain	Involved in nuclear transport of ABA signal transduction regulating root growth or stomatal regulation	Arabidopsis thaliana	IPR016024
RAC875_c40298_394	2A	101.97	TVP38/TMEM64 family membrane protein slr0305	Multi-pass membrane protein	Aegilops tauschii	LOC109748324
wsnp_Ra_c4850_8698731	2A	101.97	Fatty acid desaturase-6 (Fad6)	Na+/K+ homeostasis	Arabidopsis thaliana	AT4G30950
BS00041707_51	2A	105.53	FATTY ACID EXPORT 1 (FAX1), chloroplastic-like	Export of fatty acids from plastids, required for biogenesis of the outer pollen cell wall	Aegilops tauschii	XP_020149029.1
Excalibur_c28017_641	2A	109.20	Leucine-rich repeat-containing N-terminal, plant-type	LRR-RLK, PXC1, is a regulator of secondary wall formation correlated with the TDIF-PXY/TDR-WOX4 signaling pathway	Arabidopsis thaliana	IPR013210
BS00110587_51	2A	113.30	FHY3/FAR1 family	Involved in chlorophyll biosynthesis and Integrate Light and Abscisic Acid Signaling	Arabidopsis thaliana	IPR031052
wsnp_Ex_rep_c69799_68761171	2A	113.30	PAZ domain	RNA binding module	Arabidopsis thaliana	IPR003100
Excalibur_c34964_326	2A	113.30	Short-chain dehydrogenase	Signaling and ABA biosynthesis as stress response	Arabidopsis thaliana	IPR002347
Tdurum_contig11678_289	2A	126.38	Kinesin-like protein KIN-14I	Involved in the regulation of cell division.	Arabidopsis thaliana	LOC109745638
wsnp_Ex_c14953_23104041	2A	131.97	FAD2; Fatty acid desaturase, type 2	Role in plant responses to abiotic stresses; membrane protein	Arabidopsis thaliana	IPR005067
Tdurum_contig45661_684	2A	139.04	Filament-like plant protein	Unknown	Arabidopsis thaliana	IPR008587

Table 32. (cont.)

wsnp_Ex_rep_c70299_69243835	2A	140.94	Tetratricopeptide repeat-containing domain	Tetratricopeptide Repeat-Containing Protein TTL1 Is Required for Osmotic Stress Responses and ABA sensitivity	Arabidopsis thaliana	IPR013026
BS00064570_51	2B	16.88	Yif1 family	Integral membrane protein required for membrane fusion of ER derived vesicles	Arabidopsis thaliana	IPR005578
BobWhite_c11397_231	2B	16.88	Autophagy-related genes; ATG8-interacting protein 1-like	Involved in salt stress response; autophagy-dependent degradation of plastid components	Brachypodium distachyon	XP_010239596.1
Kukri_c30847_551	2B	20.87	Golgin subfamily A member 6-like protein 22	Stress response protein; may have roles in membrane traffic and Golgi structure	Aegilops tauschii	LOC109783605
RAC875_c2300_1021	2B	27.20	Plant actin-related protein 9	Arp8 plays an important role in the functional organization of mitotic chromosomes.	Secale cereale	AKC03606.1
Excalibur_c63409_73	2B	56.87	Uncharacterized protein	Unknown	Aegilops tauschii	XR_002234656.1
wsnp_Ex_rep_c70756_69644826	2B	65.01	E3 ubiquitin-protein ligase UPL3-like	Involved in trichome development, might be related to salinity tolerance	Arabidopsis thaliana	IPR000569
Jagger_c1059_300	2B	96.99	Protein-tyrosine phosphatase-like	Involved in responses to stress signals and developmental processes	Arabidopsis thaliana	O82656
wsnp_Ex_rep_c66545_64829026	2B	99.16	Uncharacterized protein	Unknown	Aegilops tauschii	LOC109744219
Tdurum_contig2945_75	2B	106.56	Uncharacterized protein	Unknown	Aegilops tauschii	LOC109759768
BobWhite_c3146_128	2B	109.53	Gamma-soluble NSF attachment protein	Required for vesicular transport between the endoplasmic reticulum and the Golgi apparatus	Aegilops tauschii	XP_020170744.1
Excalibur_rep_c77221_93	2B	109.53	Uncharacterized protein	Unknown	Aegilops tauschii	LOC109747225
GENE_1012_303	2B	114.09	Lipocalin/cytosolic fatty-acid binding domain	Hormone reaction and oxidative stress response	Arabidopsis thaliana	A0A178VKZ0
IACX8386	2B	138.78	Uncharacterized protein	Unknown	Hordeum vulgare	BAK05132.1
RAC875_c21358_62	2B	141.32	Anamorsin homolog	Required for the maturation of extramitochondrial Fe-S proteins; Has anti-apoptotic effects in the cell	Aegilops tauschii	LOC109783541
Tdurum_contig76550_500	2B	142.99	Uncharacterized protein	Unknown	Aegilops tauschii	XR_002232570.1
wsnp_CAP11_c3226_1588070	2B	147.47	Na+/H+ antiporter (NHX2) mRNA	Antiporter Na+/K+ homeostasis	Triticum aestivum	AAK76738.2
RAC875_c25513_403	2B	152.59	Pcysteine protease ATG4B-like; Autophagy-related protein 4b	Cellular function/ Stress response	Aegilops tauschii	XP_020178856.1
RAC875_c63883_76	2D	6.75	NBS-LRR Vlr2	Disease resistance gene	Triticum ventricosum	AAF19148.1
D_F1BEJMU01A0OMY_356	2D	8.52	Amidase signature domain	Signaling pathway	Aegilops tauschii	XP_020192680.1
RAC875_c34767_147	2D	24.79	Uncharacterized protein	Unknown	Aegilops tauschii	LOC109756150
RAC875_c11911_431	2D	34.15	4-alpha-glucanotransferase DPE1, chloroplastic/amyloplastic	Chloroplastic alpha-glucanotransferase involved in maltotriose metabolism	Aegilops tauschii	LOC109760178
Excalibur_c20175_370	2D	40.05	Probable acyl-CoA dehydrogenase IBR3	Has a critical role in auxin activation through indole-3-butyric acid; May play a role in defense response to pathogenic bacteria	Aegilops tauschii	LOC109781256
Kukri_rep_c72558_961	2D	42.59	Condensin complex subunit 1	Cellular function	Aegilops tauschii	XP_020158867.1
Kukri_rep_c72254_186	2D	49.59	WEAK CHLOROPLAST MOVEMENT UNDER BLUE LIGHT 1-like	Chloroplast movement under light, drought and salinity stress	Aegilops tauschii	LOC109751252
RAC875_c39665_175	2D	54.58	P-loop containing nucleoside triphosphate hydrolase	Involved in salt stress response by attenuation of oxidative stress and reactive oxygen species (ROS)	Arabidopsis thaliana	IPR027417
TA011647_0807	2D	59.50	Cyclin-dependent kinase G-2	Regulates cell division; stress response	Aegilops tauschii	LOC109746450
TA001249_1083	2D	76.39	Plastid glutamine synthetase 2 (GS2) gene, GS2-B1c allele	Essential role in the metabolism of nitrogen by catalyzing the condensation of glutamate and ammonia to form glutamine	Triticum aestivum	ACT22497.1
wsnp_Ra_c22648_32132929	2D	82.82	P-type ATPase, transmembrane domain	Transmembrane proton pump	Triticum aestivum	CAA70944.1

Table 32. (cont.)

Tdurum_contig64286_182	2D	103.33	Uncharacterized protein	Unknown	Aegilops tauschii	LOC109763339
Kukri_c13830_556	3A	33.66	Delta(7)-sterol-C5(6)-desaturase-like	Involved in cholesterol biosynthesis and biosynthesis a plant cuticular wax	Aegilops tauschii	XP_020153224.1
wsnp_JD_c2722_3653988	3A	35.55	Ethylene-responsive transcription factor ERF118-like	Involved in the regulation of gene expression by stress factors and stress signal transduction	Arabidopsis thaliana	IPR001471
wsnp_Ex_c55051_57706127	3A	47.20	Ubiquitin-conjugating enzyme/RWD-like	C/N regulator; leaf senescence in response to the balance between atmospheric CO_2 and nitrogen availability	Aegilops tauschii	LOC109776715
wsnp_Ku_c14082_22272647	3A	123.01	Beta-glucosidase 5-like isoform X2	Involved in structure of cell wall	Arabidopsis thaliana	XP_020194022.1
wsnp_Ex_c361_707953	3A	177.24	E3 ubiquitin-protein ligase HERC2-like	Associated with KEEP ON GOING (KEG) as essential for growth and development	Aegilops tauschii	XP_020197642.1
Tdurum_contig8674_1236	3A	188.38	Malectin-like carbohydrate-binding domain	FERONIA is a malectin-like domain; FERONIA has a critical role in female fertility	Oryza sativa	IPR024788
BS00098868_51	3B	21.33	Protein-lysine N-methyltransferase mettl10-like Efm4	Intracellular transport	Aegilops tauschii	XP_020183415.1
Excalibur_c9206_671	3B	30.33	WD40 repeat; actin-interacting protein 1-2-like	Wide variety of functions including adaptor/regulatory modules in signal transduction; stress response protein	Aegilops tauschii	LOC109770953
Tdurum_contig82242_224	3B	36.82	Small heat shock protein HSP20	Protein folding etc; protecting plants against stress	Arabidopsis thaliana	AT1G76440
RAC875_c81076_317	3B	62.31	Glycoside hydrolase, family 28	Multiple functions	Arabidopsis thaliana	IPR000743
RAC875_c9095_217	3B	62.67	Arginine--tRNA ligase, cytoplasmic-like	Catalyzes specific amino acids to cognate tRNAs during protein synthesis	Aegilops tauschii	LOC109774020
wsnp_JD_c9902_10674725	3B	62.67	Arginine--tRNA ligase, cytoplasmic-like	Catalyzes specific amino acids to cognate tRNAs during protein synthesis	Aegilops tauschii	LOC109774020
JD_c13108_198	3B	67.45	Pentatricopeptide repeat	Role in organelle expression; involved in CMS	Oryza sativa	IPR002885
Tdurum_contig67750_272	3B	70.68	WD40/YVTN repeat-like-containing domain	Wide variety of functions including adaptor/regulatory modules in signal transduction; stress response protein	Oryza sativa	IPR015943
TA004228_0191	3B	71.34	ULTRAPETALA	Developmental regulator	Oryza sativa	IPR020533
wsnp_JD_c10602_11238420	3B	74.26	Vegetative cell wall protein gp1-like	Salt stress response cell wall protein	Aegilops tauschii	LOC109743334
RAC875_c8121_1997	3B	95.10	FAD/NAD(P)-binding domain	Belonging to the family of pyridine nucleotide-disulphide oxidoreductases Related to GST; detoxification	Aegilops tauschii	IPR023753
BS00024499_51	3B	110.15	Domain unknown function DUF295	Unknown	Arabidopsis thaliana	IPR005174
Tdurum_contig52980_116	3B	123.60	DNA mismatch repair protein MLH1-like	Salt stress response; repair function	Aegilops tauschii	LOC109756593
Excalibur_c45326_479	3B	139.62	Similar to Putative pentatricopeptide (PPR) repeat-containing protein	Regulation of plant responses to abiotic stresses	Sorghum bicolor	XM_002443946.1
RAC875_s113853_61	3D	4.46	Subtilisin-like protease SBT3.10; stomatal density	Surface formation of juvenile plants	Arabidopsis thaliana	XP_020201040.1
tplb0050o09_895	3D	4.46	Aquaporin NIP4-1-like	Involved pollen development and maintenance of osmotic potential by transmembrane channels for water	Aegilops tauschii	LOC109770355
Excalibur_c19658_127	3D	4.56	P-loop containing nucleoside triphosphate hydrolase	Involved in salt stress response by attenuation of oxidative stress and reactive oxygen species (ROS)	Arabidopsis thaliana	IPR027417
TA005883_0675	3D	23.67	Heat shock protein 16.9	Molecular chaperones in heat shock and salinity stress response	Triticum aestivum	AAA51390.1
IAAV5635	3D	40.50	Uncharacterized protein	Unknown	Aegilops tauschii	LOC109769753
Excalibur_c39686_664	3D	129.25	UV-stimulated scaffold protein A homolog	Involved in transcription-coupled nucleotide excision repair in response to UV damage	Aegilops tauschii	XP_020159730.1
BS00105800_51	3D	143.01	Soluble inorganic pyrophosphatase 4-like	K+ and Mg2+ depended hydrolysis of pyrophosphate to phosphate	Aegilops tauschii	XP_020185551.1
BS00065863_51	4A	29.86	Uncharacterized protein	Unknown	Aegilops tauschii	LOC109786737

Table 32. (cont.)

Ku_c766_2284	4A	37.05	Uncharacterized protein	Unknown	Hordeum vulgare	BAJ96927.1
Tdurum_contig48049_705	4A	41.02	Ribosomal RNA large subunit methyltransferase RlmN/Cfr	Metabolism; Radical SAM Enzymes Involved in Methylation of Ribosomal RNA	Triticum aestivum	IPR004383
BS00004170_51	4A	41.02	Chaperone tailless complex polypeptide 1 (TCP-1)	Involved in cell protection under biotic and abiotic stress	Oryza sativa	IPR017998
wsnp_Ex_c10527_17198865	4A	48.52	S-adenosyl-L-methionine-dependent methyltransferase	Abiotic stress response by regulation of polyamines metabolism (Betaine)	Arabidopsis thaliana	IPR029063
wsnp_Ra_c1022_2067517	4A	58.38	ARF guanine-nucleotide exchange factor GNOM-like	Regulating endosome–to–plasma membrane trafficking	Aegilops tauschii	LOC109785941
GENE_2778_24	4A	58.40	Switch-associated protein 70	Cellular signal transduction pathways	Aegilops tauschii	LOC109785940
BS00009492_51	4A	59.99	Zinc finger, RING/FYVE/PHD-type	Regulating Sodium and Potassium Homeostasis, Reactive Oxygen Species Scavenging and Osmotic Potential	Oryza sativa	IPR013083
BS00003866_51	4A	61.91	ABC-2 type transporter	Involved in the export or import of a wide variety of substrates	Oryza sativa	IPR013525
Ex_c66324_1151	4A	66.00	Leucine-rich repeat domain, L domain-like	Signaling and ABA biosynthesis as stress response	Aegilops tauschii	IPR032675
BS00072025_51	4A	66.28	Coactivator CBP, KIX domain	Transcription cofactor activity	Oryza sativa	IPR003101
wsnp_Ex_c24474_33721784	4A	69.96	Metallo-beta-lactamase	Plant resistance gene; Stress response	Arabidopsis thaliana	IPR001279
wsnp_JD_c38619_27992279	4A	75.50	hAT-like transposase,DAYSLEEPER protein, RNase-H fold	Essential for plant development and can also regulate global gene expression	Arabidopsis thaliana	IPR025525
Tdurum_contig22511_355	4A	89.07	GAF domain-like	Essential sensory domain of photosynthetic pathway	Arabidopsis thaliana	IPR029016
Excalibur_c53864_331	4A	106.72	Protein slr1919; uncharacterized	Protein of ABC1-transporter	Aegilops tauschii	LOC109775816
BobWhite_c32313_688	4A	110.13	DJ-1/PfpI	Activating glyoxalase which are involved in plant response to salt stress and oxidative stress	Arabidopsis thaliana	IPR002818
IAAV1383	4A	112.71	P-loop containing nucleoside triphosphate hydrolase	Involved in salt stress response by attenuation of oxidative stress and reactive oxygen species (ROS)	Arabidopsis thaliana	IPR027417
BS00022395_51	4A	121.67	GH3 family; Jasmonic acid-amido synthetase JAR1	Signaling	Glycine max	IPR004993
wsnp_Ra_c22775_32274079	4A	132.95	1-deoxy-D-xylulose 5-phosphate reductoisomerase (dxr gene)	Promotes biosynthesis of solanesol contributing to cell defense under biotic and abiotic stress	Hordeum vulgare	CAE47438.1
Tdurum_contig10672_117	4A	139.97	Uncharacterized protein	Unknown	Hordeum vulgare	BAK05944.1
wsnp_Ex_c33778_42210283	4A	147.10	1,3-beta-glucan synthase	Essential for uniform cell wall synthesis	Brachypodium distachyon	pfam14288
Tdurum_contig92931_882	4B	57.87	Signal transduction histidine kinase, dimerisation/phosphoacceptor domain	Signal transduction; Two-component signaling systems (TCSs)	Arabidopsis thaliana	IPR003661
TA003708_0300	4B	61.84	COBRA family proteins	Involved in determining the orientation of cell expansion, cellulose deposition. Cell wall related protein	Arabidopsis thaliana	XP_020199365.1
Kukri_c65146_460	4B	63.40	Rab GTPase-activating protein 1-like	Regulators of vesicles trafficking and plant responses to stresses	Aegilops tauschii	LOC109785673
Tdurum_contig46247_106	4B	78.57	Ubiquitin-related domain	Unknown	Arabidopsis thaliana	IPR029071
Tdurum_contig61242_161	4B	78.96	Serine acetyltransferase (SATase; EC 2.3.1.30)	Essential for amino acid metabolism	Aegilops tauschii	IPR010493
IAAV5564	4B	98.65	Myosin-10-like protein	Adaptation to blue light (movement of chloroplasts); Role in photosynthesis	Aegilops tauschii	LOC109763289
Kukri_rep_c101259_81	4B	104.79	Uncharacterized protein	Unknown	Aegilops tauschii	LOC109776472

Table 32. (cont.)

wsnp_Ex_c4148_7495656	4B	104.79	Concanavalin A-like lectin/glucanase domain containing protein	Involved transcription factor activity for shoot Na+/K+ under in salt stress	Aegilops tauschii	IPR013320
wsnp_Ex_rep_c107564_91144523	4D	70.59	UDP-glucose/GDP-mannose dehydrogenase, N-terminal	Cell wall construction	Arabidopsis thaliana	IPR001732
BobWhite_c51109_415	5A	35.38	Cobalamin-Independent Methionine Synthase	Associated with lignification of the cell wall under salt stress	Hordeum vulgare	cd03312
BS00040933_51	5A	36.73	Heavy metal-associated isoprenylated plant protein 35-like	Involved in stress responses and detoxification	Aegilops tauschii	XP_020195979.1
BS00094095_51	5A	36.87	Pyruvate dehydrogenase E1 component subunit beta-3	Photosynthesis	Brachypodium distachyon	XP_010237006.1
BS00021708_51	5A	37.79	Transcription initiation factor IIA, gamma subunit	Transcription factor complex along with RNA polymerase	Oryza sativa	IPR003194
Kukri_c24642_426	5A	38.72	Metallo-beta-lactamase	Unknown	Arabidopsis thaliana	IPR001279
Ra_c24707_827	5A	42.77	Uncharacterized protein	Unknown	Brachypodium distachyon	BRADI1G41700
tplb0051d06_1385	5A	53.47	FAD2; Fatty acid desaturase, type 2	Involved in Na+/H+ exchanger affecting salt tolerance	Arabidopsis thaliana	IPR016166
BobWhite_rep_c61813_322	5A	56.47	DNA-directed RNA polymerase, RBP11-like dimerization domain	Involved in response pathway to abiotic stress targeting chloroplasts	Arabidopsis thaliana	At5g06210
IAAV1179	5A	69.34	Uncharacterized protein	Unknown	Oryza sativa	IPR011676
Tdurum_contig17500_876	5A	70.30	SKP1-like protein 1B	Role in regulation of flowering and abiotic stress tolerance.	Aegilops tauschii	LOC109736331
Kukri_c14889_1086	5A	70.30	Malectin-like carbohydrate-binding domain	FERONIA is a malectin-like domain; FERONIA has a critical role in female fertility	Oryza sativa	IPR024788
Tdurum_contig4576_603	5A	82.66	Fatty acyl-CoA reductase 1-like	Involved in biosynthesis of the leaf blade cuticular wax	Aegilops tauschii	LOC109746696
BS00035256_51	5A	82.72	P-loop containing nucleoside triphosphate hydrolase	Involved in salt stress response by attenuation of oxidative stress and reactive oxygen species (ROS)	Arabidopsis thaliana	IPR027417
RAC875_c23775_406	5A	84.13	Uncharacterized protein	Unknown	Arabidopsis thaliana	IPR011141
wsnp_Ex_c7266_12475249	5A	86.36	Chaperone DnaJ, C-terminal	May be has a role in stress signaling	Oryza sativa	IPR002939
CAP11_c3209_76	5A	92.56	Cytochrome P450	CYP709B3, a cytochrome P450 monooxygenase gene involved in salt tolerance	Arabidopsis thaliana	IPR001128
Excalibur_c41710_417	5A	92.87	Myc-type, basic helix-loop-helix (bHLH) domain	Transcription factors in ABA-mediated gene expression under drought and salt stresses	Aegilops tauschii	IPR011598
wsnp_CAP11_c1506_840951	5A	98.44	Aldolase-type TIM barrel	Diverse responses to abiotic stresses	Oryza sativa	IPR013785
RAC875_c13490_1344	5A	100.90	MVD1 diphosphomevalonate decarboxylase;	Involved in sterol synthesis, is induced only in the absence of potassium	Arabidopsis thaliana	IPR005935
BS00104432_51	5A	105.36	Pheophorbide a oxygenase	Key regulator of chlorophyll catabolism	Arabidopsis thaliana	IPR013626
BobWhite_c48435_165	5B	90.35	Potassium transporter 18-like	High-affinity potassium transporters	Aegilops tauschii	LOC109773235
IAAV4395	5B	139.40	Multiple inositol polyphosphate phosphatase PhyIIc	Involved in phytase activity by hydrolyzing phytate into inorganic P	Triticum aestivum	DQ995974.1
Kukri_c10913_480	5B	188.58	P-loop containing nucleoside triphosphate hydrolase	Involved in salt stress response by attenuation of oxidative stress and reactive oxygen species (ROS)	Arabidopsis thaliana	IPR027417
RAC875_c58332_1099	5D	51.93	Protein LIN-9/Protein ALWAYS EARLY	Multiple functions; probably chromatin organization	Arabidopsis thaliana	IPR010561
wsnp_RFL_Contig2606_2264492	5D	60.61	Cationic amino acid transporter 2, vacuolar-like	Selective transporter of amino acids	Aegilops tauschii	LOC109780422

Table 32. (cont.)

Ra_c47493_933	5D	94.03	Acyl-coenzyme A thioesterase 9, mitochondrial	Participate in fatty acid and glycerolipid metabolism	Aegilops tauschii	LOC109774098
BS00000020_51	5D	102.91	Puroindoline b (PinB-D1)	Grain texture and flour quality	Triticum aestivum	KC585018.1
Kukri_c96249_58	5D	130.03	Copine	Ca2+-dependent phospholipid-binding proteins that are involved in membrane-trafficking, and in cell division and growth	Oryza sativa	IPR010734
Excalibur_c76347_77	5D	144.70	S-adenosyl-L-methionine-dependent methyltransferase	Abiotic stress response by regulation of polyamines metabolism (Betaine)	Arabidopsis thaliana	IPR029063
D_GB5Y7FA02JRQ1I_101	5D	187.21	Probable aldo-keto reductase 2	Oxidoreductase activity; involved in osmotic adaptation	Aegilops tauschii	LOC109745744
Kukri_c28182_129	5D	196.08	Actin-related protein 2/3 complex subunit 4	plays a critical role in the control of cell morphogenesis via the modulation of cell polarity development.	Aegilops tauschii	LOC109752408
TA013009_0365	5D	198.19	Uncharacterized protein	Unknown	Aegilops tauschii	LOC109732653
GENE_3006_113	5D	203.88	Arf GTPase activating protein (ADP-ribosylation factor (Arf) GTPases)	Arf GTPases regulate vesicle trafficking between plasma membrane (PM) and cytoplasm	Arabidopsis thaliana	IPR001164
BobWhite_c33778_146	5D	204.58	Uncharacterized protein	Unknown	Aegilops tauschii	XP_020158418.1
BS00012069_51	5D	204.58	Uncharacterized protein	Unknown	Aegilops tauschii	LOC109733656
Kukri_c39873_66	6A	12.91	SWEET14-like	Bidirectional sugar transporter	Aegilops tauschii	LOC109734706
Tdurum_contig12045_868	6A	13.45	Uncharacterized protein	Unknown	Aegilops tauschii	LOC109738627
RAC875_c23552_811	6A	33.31	High-affinity nitrate transporter (NRT2.3)	Putative substrate translocation pore	Triticum aestivum	AAL11016.1
RAC875_c2253_238	6A	37.13	BRAHMA (BRM) ATPase	Involved in repression of seed maturation genes in leaves	Arabidopsis thaliana	IPR031056
BS00023092_51	6A	80.09	Aconitase/3-isopropylmalate dehydratase, swivel	Cellular function	Arabidopsis thaliana	Q42560
TA004297_0876	6A	81.64	S-adenosyl-L-methionine-dependent methyltransferase (SAM MTases)	Salt stress response; Gly betaine regulation	Arabidopsis thaliana	IPR029063
Excalibur_c41490_397	6A	84.11	microRNA444.1a2 and microRNA444.1a gene	Plant antiviral depended signaling pathway	Hordeum vulgare	JX311436.1
RAC875_c13785_2042	6A	84.11	Mediator complex, subunit Med23	Importance of Mediator complex in the regulation and integration of diverse signaling pathways in plants	Arabidopsis thaliana	IPR021629
wsnp_JD_rep_c48797_33040150	6A	84.11	Aspartic peptidase A1 family	Cellular function/mobilization of storage proteins in seed at germination	Aegilops tauschii	IPR001461
BobWhite_c1082_134	6A	85.07	DExH-box ATP-dependent RNA helicase DExH15 chloroplastic	Cellular function/Modulates the determination of cell fate	Aegilops tauschii	XP_020187629.1
BobWhite_c82_578	6A	99.04	26S protease regulatory subunit 7A-like	Cellular metabolism	Aegilops tauschii	XP_020185865.1
Tdurum_contig61448_412	6A	99.04	Phosphoinositide phosphatase SAC2-like	Tonoplast associated enzyme influence vacuolar morphology	Aegilops tauschii	LOC109755546
RFL_Contig5037_560	6A	117.77	Probable monogalactosyldiacylglycerol synthase 3, chloroplastic	Involved in the synthesis of photosynthetic membranes of chloroplasts	Aegilops tauschii	LOC109769532
RAC875_c93959_96	6A	117.90	GDSL esterase/lipase	Plant resistance to wound stress and pathogenic stress	Arabidopsis thaliana	At4g10955
wsnp_Ex_c20457_29526403	6A	123.48	Chaperone DnaJ, C-terminal	Signaling/Hormone reaction. Associated with Heat shock protein Hsp70	Aegilops tauschii	IPR002939
BS00029127_51	6A	130.40	Metallo-beta-lactamase	Plant resistance gene; Stress response	Arabidopsis thaliana	IPR001279
wsnp_Ex_c7002_12063380	6A	130.70	SWEET13-like	bidirectional sugar transporter	Aegilops tauschii	LOC109757081
IAAV1495	6A	136.70	Uncharacterized protein	Unknown	Aegilops tauschii	LOC109748853
RFL_Contig3175_1271	6A	136.85	NADH dehydrogenase [ubiquinone] 1 alpha subcomplex subunit 9	Stress response/ROS detoxification/Photosynthesis; Involved in electron transport chain	Aegilops tauschii	LOC109748854

Table 32. (cont.)

Kukri_rep_c103186_134	6A	140.87	NAC domain-containing protein 78-like	Transcription activator regulating 20S and 26S proteasomes in response to high light stress	Aegilops tauschii	LOC109781707
RAC875_c37871_249	6B	0.38	E3 ubiquitin-protein ligase UPL3-like	Involved in cell morphogenesis in the trichomes	Arabidopsis thaliana	At4g38600
wsnp_Ku_c24391_34351602	6B	7.79	Oxidoreductase FAD/NAD(P)-binding	Involved in photosynthetic pathway. Energy transfer via ATP	Hordeum vulgare	IPR001433
Kukri_rep_c100676_151	6B	58.26	Uncharacterized protein	Unknown	Aegilops tauschii	LOC109785158
wsnp_Ex_c12433_19827016	6B	82.02	MCM2/3/5 family	Replication licensing factors	Aegilops tauschii	LOC109779496
wsnp_Ku_c46363_53116979	6B	113.67	plant intracellular Ras-group-related Leucine-rich repeat protein 6	Signal transduction; mediates protein interactions	Aegilops tauschii	LOC109770472
Excalibur_c130_3813	6B	117.66	Testis-expressed protein 2-like	Unknown	Aegilops tauschii	LOC109776167
wsnp_Ra_rep_c106119_89961852	6D	17.01	Protein FLX-like 1	Involved in vernalization and flowering process	Aegilops tauschii	LOC109759562
D_wsnpbe497701_Contig1_2	6D	87.17	Peptidase S1, PA clan	Cellular function	Arabidopsis thaliana	IPR009003
BS00011523_51	6D	101.63	Uncharacterized protein	Unknown	Aegilops tauschii	LOC109734951
Kukri_c57006_127	6D	107.40	Leucine-rich repeat domain, L domain-like	Signaling and ABA biosynthesis as stress response	Aegilops tauschii	IPR032675
BS00063625_51	6D	116.85	DUF4220 Domain of unknown function	Unknown	Triticum aestivum	IPR025315
Excalibur_c7546_1286	6D	150.43	Uncharacterized protein	Unknown	Aegilops tauschii	LOC109787311
BS00003568_51	6D	150.56	Plant antimicrobial peptide	Antifungal activity by receptor-mediated interaction with microbial membranes	Oryza sativa	IPR029227
Kukri_c45876_61	6D	153.08	Uncharacterized protein	Unknown	Aegilops tauschii	LOC109736775
wsnp_BE471213D_Ta_2_1	6D	153.08	Cation efflux protein transmembrane domain	cation transmembrane transporter activity; probable zinc ion transmembrane transporter activity	Oryza sativa	Q6K961
BS00084477_51	7A	33.24	Six-bladed beta-propeller, TolB-like	Unknown	Arabidopsis thaliana	IPR011042
Excalibur_c9166_913	7A	45.25	Cellulose synthase	Biosynthesis of cellulose	Oryza sativa	IPR005150
Excalibur_rep_c68955_422	7A	74.19	ABC-transporter extracellular N-terminal domain	Essential transporter for growth and development under abiotic stress	Oryza sativa	IPR029481
Tdurum_contig12722_779	7A	76.28	peptide methionine sulfoxide reductase A5	Plays a protective role against oxidative stress triggered by drought and salinity stress	Oryza sativa	Os06g0138100
wsnp_Ex_c13337_21022658	7A	113.30	E4 SUMO-protein ligase PIAL2-like	Stress response; proteolytic removal of sumoylation substrates	Aegilops tauschii	XM_020344828.1
RAC875_rep_c69766_246	7A	126.40	Putative transcription elongation factor SPT5 homolog 1	Has a critical role in auxin-related gene expression	Aegilops tauschii	LOC109754840
IACX72	7A	126.80	Tetratricopeptide repeat-containing domain	Tetratricopeptide Repeat-Containing Protein TTL1 Is Required for Osmotic Stress Responses and ABA sensitivity	Arabidopsis thaliana	IPR013026
BS00066651_51	7A	127.75	Pentatricopeptide repeat	Role in organelle expression; involved in fertility and CMS	Oryza sativa	IPR002885
Ra_c18741_604	7A	133.53	Leucine-rich repeat domain, L domain-like	Signaling and ABA biosynthesis as stress response	Aegilops tauschii	IPR032675
BS00022747_51	7A	135.81	UDP-sugar pyrophosphorylase	Salt stress response, Maintaining cellular osmotic equilibrium	Aegilops tauschii	XP_020166304.1
RAC875_c43295_135	7A	148.43	RPP13-like protein 3	Putative disease resistance	Aegilops tauschii	LOC109774305
Tdurum_contig61864_1352	7A	199.64	Transcription initiation factor TFIID subunit 1-like	Mediating regulation of RNA polymerase transcription	Aegilops tauschii	LOC109736908
Excalibur_rep_c66918_307	7A	202.68	Pyrophosphate-energised proton pump (H+-PPases)	Involved in K+ transport	Arabidopsis thaliana	IPR004131

Table 32. (cont.)						
Kukri_c3734_892	7B	3.27	Uncharacterized protein	Unknown	Hordeum vulgare	AK375736.1
wsnp_Ex_c11106_18003332	7B	55.23	Codeine O-demethylase-like	Morphine biosynthesis; Response to tissue damage, defense system	Aegilops tauschii	LOC109755792
BS00022550_51	7B	61.26	Spt5 transcription elongation factor, N-terminal	Involved in auxin-related gene expression and salt stress signaling	Arabidopsis thaliana	IPR017071
RFL_Contig1599_906	7B	69.39	S-adenosyl-L-methionine-dependent methyltransferase	Abiotic stress response by regulation of polyamines metabolism (Betaine)	Arabidopsis thaliana	IPR029063
Excalibur_rep_c116920_300	7B	71.66	Uncharacterized protein	Unknown	Aegilops tauschii	LOC109768540
Kukri_c11274_973	7B	72.74	Ribosomal protein L10P	Participate in development and translation under UV-B stress	Aegilops tauschii	IPR001790
Tdurum_contig50984_553	7B	72.74	P-loop containing nucleoside triphosphate hydrolase	Involved in salt stress response by attenuation of oxidative stress and reactive oxygen species (ROS)	Arabidopsis thaliana	IPR013083
Excalibur_c15029_350	7B	73.79	SPX and EXS domain-containing protein 5-like	Role in Phosphate homeostasis	Aegilops tauschii	IPR004342
Excalibur_c20931_669	7B	73.79	Serine/threonine protein phosphatase 2A 55 kDa regulatory subunit B alpha isoform	Key components of stress signal transduction pathways	Aegilops tauschii	LOC109753112
BS00108573_51	7B	77.13	Uncharacterized protein	Unknown	Aegilops tauschii	LOC109774749
Tdurum_contig43966_813	7B	81.76	Probable 2-oxoglutarate-dependent dioxygenase	Acting as a controller of stress-related responses towards oxidative stress	Aegilops tauschii	LOC109756343
wsnp_Ku_c17161_26193994	7B	91.24	Non-haem dioxygenase N-terminal domain	Dioxygenases catalyze the O-demethylation steps of morphine biosynthesis in opium poppy.	Arabidopsis thaliana	IPR026992
Excalibur_c11093_519	7B	92.52	Uncharacterized protein	Unknown	Aegilops tauschii	LOC109756041
BS00065981_51	7B	95.71	Uncharacterized protein	Unknown	Aegilops tauschii	LOC109737409
Kukri_c16034_113	7B	109.10	Disease resistance protein RPM1-like	Facilitates increase in cytosolic calcium that is necessary for the oxidative burst and hypersensitive cell death	Aegilops tauschii	LOC109754873
Kukri_c11141_203	7B	113.87	Disease resistance protein RPM1-like	Facilitates increase in cytosolic calcium that is necessary for the oxidative burst and hypersensitive cell death	Aegilops tauschii	XP_020163988.1
RAC875_c49954_1172	7B	147.02	EF-hand domain pair	Calcium-binding protein C800.10c-like	Aegilops tauschii	IPR011992
CAP7_c3950_160	7B	155.42	Probable transmembrane receptor protein serine/threonine-protein kinase PIX13	Involved in plant defense/ abiotic stress response?	Aegilops tauschii	LOC109751765
tplb0060b03_432	7B	166.99	Photosystem II stability/assembly factor HCF136, chloroplastic	Regulating photosynthesis under salinity stress	Aegilops tauschii	XP_020163505.1
Kukri_rep_c101620_1848	7B	171.10	Zinc finger, RING/FYVE/PHD-type	Regulating Sodium and Potassium Homeostasis, Reactive Oxygen Species Scavenging and Osmotic Potential	Oryza sativa	IPR013083
Tdurum_contig62213_156	7B	171.11	Signal peptide peptidase-like 5 SPP	Plays a critical role in the development and function of the reproductive tissues, especially in pollen development	Aegilops tauschii	LOC109782989
Tdurum_contig62213_423	7B	171.11	Uncharacterized protein	Unknown	Hordeum vulgare	BAJ97624.1
tplb0040b02_681	7B	177.45	Zinc finger, RING/FYVE/PHD-type Jas TPL-binding domain / Jas TPL-binding domain	Regulating Sodium and Potassium Homeostasis, Reactive Oxygen Species Scavenging and Osmotic Potential; probably involved in jasmonic acid signal transduction pathway	Oryza sativa	IPR013083/ IPR032308
BS00022449_51	7D	26.20	CYP709B3, a cytochrome P450 monooxygenase	Involved in salt stress response through alteration of metabolic process	Arabidopsis thaliana	IPR001128
BS00067140_51	7D	26.92	Fatty acyl-CoA reductase	Expression by wounding and salt stress	Hordeum vulgare	IPR026055
BobWhite_c8454_782	7D	29.97	Glutathione S-transferase, N-terminal	Plant protection against biotic and abiotic stresses; detoxification of reactive electrophilic compounds; regulator of cell elongation and plant development	Arabidopsis thaliana	At2g29470

Table 32. (cont.)

RAC875_c25695_316	7D	32.16	Succinate dehydrogenase subunit 8A, mitochondrial	Involved in Citric acid cycle	Oryza sativa	LOC109766931
D_GBUVHFX01BEHL1_132	7D	95.68	Protohaem IX farnesyltransferase	Heme biosynthesis; converting heme B to Heme O	Arabidopsis thaliana	IPR006369
RAC875_c13942_2973	7D	111.21	LIM-domain binding protein/SEUSS	Transcription regulator interacting with APETALA1 and SEPALLATA3 at flowering stage; also, down regulation of response to salt stress	Arabidopsis thaliana	IPR029005
wsnp_Ra_c2930_5550871	7D	114.05	Uncharacterized protein	Unknown	Aegilops tauschii	LOC109753329
CAP7_c9278_185	7D	123.51	BOBBER 1-like	Small heat shock protein; multifunctional; involved in the specification of the cotyledon primordia	Aegilops tauschii	LOC109766844
D_GBQ4KXB01C5QDQ_113	7D	139.07	Diphosphomevalonate/ phosphomevalonate decarboxylase	Involved in isoprene metabolism	Arabidopsis thaliana	IPR005935
RAC875_rep_c70325_345	7D	143.68	Leucine-rich repeat domain, L domain-like	Signaling and ABA biosynthesis as stress response	Aegilops tauschii	IPR032675
Ku_c32426_324	7D	148.30	Uncharacterized protein	Unknown	Aegilops tauschii	LOC109773107
D_GA8KES401CTZ29_94	7D	161.13	SEC12-like protein 2	Required for the formation or budding of transport vesicles from the ER	Aegilops tauschii	LOC109767845
D_GBB4FNX02ILZW2_114	7D	161.13	Uncharacterized protein	Unknown	Hordeum vulgare	BAJ98212.1
D_GBQ4KXB01EJHOJ_221	7D	161.88	Inorganic pyrophosphatase 2-like; H+ pump	Regulates salt and osmotic stress by involvement in antiporter activity and Na+ transport	Aegilops tauschii	LOC109747901

Appendix 5

Publication

Non-invasive assessment of leaf water status using a dual-mode microwave resonator

Said Dadshani[1]
Email: dadshani@uni-bonn.de

Andriy Kurakin[2]
Email: andriy.kurakin@safe-fail.net

Shukhrat Amanov[1]
Email: shukhratamanov@yahoo.com

Benedikt Hein[1]
Email: benedikt_hein@web.de

Heinz Rongen[2]
Email: h.rongen@fz-juelich.deSteve Cranstone[2]
Email: steve.cranstone@emisens.com

Ulrich Blievernicht[2]
Email: ulrich.blievernicht@emisens.com

Elmar Menzel[4]
Email: Elmar.Menzel@t-online.de

Jens Léon[1]
Email: j.leon@uni-bonn.de

Norbert Klein[2,3]
Email: n.klein@imperial.ac.uk

Agim Ballvora[1*]
[*] Corresponding author
Email: ballvora@uni-bonn.de

[1] INRES-Plant Breeding, University of Bonn, Katzenburgweg 5, 53115 Bonn, Germany

[2] EMISENS GmbH, Zur Rur 25, 52428 Juelich, Germany

[3] Department of Materials, Imperial College London, South Kensington Campus, London SW7 2AZ, UK

[4] Dr.- Ing. Elmar Menzel Ingenieurbüro, Birkenstr. 18, 63533 Mainhausen, Germany

Abstract

The water status in plant leaves is a good indicator for the water status in the whole plant revealing stress if the water supply is reduced. The analysis of dynamic aspects of water availability in plant tissues provides useful information for the understanding of the mechanistic basis of drought stress tolerance, which may lead to improved plant breeding and management practices. The determination of the water content in plant tissues during plant development has been a challenge and is currently feasible based on destructive analysis only. We present here the application of a non-invasive quantitative method to determine the volumetric water content of leaves and the ionic conductivity of the leaf juice from non-invasive microwave measurements at two different frequencies by one sensor device. A semi-open microwave cavity loaded with a ceramic dielectric resonator and a metallic lumped-element capacitor- and inductor structure was employed for non-invasive microwave measurements at 150 MHz and 2.4 Gigahertz on potato, maize, canola and wheat leaves. Three leaves detached from each plant were chosen, representing three developmental stages being representative for tissue of various age. Clear correlations between the leaf- induced resonance frequency shifts and changes of the inverse resonator quality factor at 2.4 GHz to the gravimetrically determined drying status of the leaves were found. Moreover, the ionic conductivity of Maize leaves, as determined from the ratio of the inverse quality factor and frequency shift at 150 MHz by use of cavity perturbation theory, was found to be in good agreement with direct measurements on plant juice. In conjunction with a compact battery- powered circuit board- microwave electronic module and a user-friendly software interface, this method enables rapid in-vivo water amount assessment of plants by a handheld device for potential use in the field.

Keywords

Water content, Microwave resonator, Non-invasive measurements

Background

Drought and salinity stress are undoubtedly important constraints limiting agricultural productivity which can even result in total yield loss [1,2]. To equilibrate the decrease of the uptake of the available water in soils, plants preserve the osmotic potential by reducing stomata conductance. This leads to a reduction of photosynthetic rate and finally reducing plant growth and yield [3,4]. Around 26% of arable land worldwide is suffering from water shortage constituting the most important abiotic stress [5]. In perspective to climate changes in the future an increase of drought stress and consequently problems with plant production [4,6-8] are expected. Understanding the mechanism of drought stress tolerance is in the focus of current plant research, in order to help breeders developing new cultivars that perform well, even under water scarcity.

The definition of the water status in plant tissue is of importance for the plant researcher to better understand the physiological processes and molecular mechanisms leading to tolerance with respect to water lack stress on the one hand. On the other hand it may help the producers to control the watering procedures. Systematic phenotyping of plants needs standardized and non-invasive methods to define and assess physiological parameters like water status in order to analyse the reactions of single plants or group of plants to environmental.

The water content in vegetative tissues is a parameter of high importance for the photosynthetic performance and an indicator of the plant's health. Currently it is measured by destructive methods such as comparing the fresh and dry weight of plant tissues [9]. Nevertheless, destructive methods do not allow the instantaneous and continuous monitoring of the water content in living tissue. Therefore, non-destructive techniques that require very weak interaction with the plant tissue in order to avoid altering its physiological activities are highly desired.

Non-destructive analysis by radiation in the microwave to terahertz range is most promising for the development of non-invasive methods to determine the water content because of the strong water absorption in this frequency range [10-12]. The selection of frequency is determined by the size of the assessed objects in comparison to the wavelength, if standard absorption or reflection methods are being used. In the case of plant leaves of centimetre dimension, frequencies above about 30 GHz (wavelength $\lambda = 1$ cm) are advantageous, in particular the THz range with λ below one millimetre.

Recently, THz measurements have been used to measure the water content in leaves [9,13]. However, THz technology is still quite expensive in comparison to the microwave bands below 20 GHz. Our work represents the first systematic study on individual plant leaves by a dielectric resonator based method, similar to the one described by Menzel, et al. [10], which was developed with direct involvement of one of the authors. Other than in the method described by Menzel, et al. [10], the additional use of a low frequency mode being excited in the same cavity at 150 MHz enables independent and simultaneous non-invasive determination of the ionic conductivity [14]. Different to microwave moisture sensors based on planar microwave transmission lines like the one reported by Rezaei, et al. [15] and planar antennae approaches by Sancho-Knapik, et al. [16] our method allows the determination of the real and imaginary components of the complex dielectric permittivity at two well separated frequencies. Moreover, our evanescent field approach overcomes the wavelength limitation and enables the use of much lower frequencies at 150 MHz and 2.4 GHz, with the advantage of cheap electronic components as being used in wireless communication. The potential commercial availability of an evanescent field dual mode microwave sensor system at moderate cost enables the implementation of non-invasive water and conductivity assessment in biological research laboratories.

Microwave properties of plant tissue

The microwave properties of plant tissue strongly correlate to the amount of stored water. The typical water content in healthy plant leaves is around 90% [17].

The interaction of microwaves with water, which is determined by a broad absorption peak due to Debye-type molecular relaxation, centered at around 20 GHz at room temperature, can be described by a strongly frequency dependent complex-valued dielectric permittivity,

$$\varepsilon^*(\omega) = \varepsilon'(\omega) + j\varepsilon''(\omega) = \varepsilon_\infty + \frac{\varepsilon_s - \varepsilon_\infty}{1+\omega^2\tau^2} + j\left[\frac{(\varepsilon_s - \varepsilon_\infty)\omega\tau}{1+\omega^2\tau^2} + \frac{\sigma}{\omega\varepsilon_0}\right], \quad (1)$$

with ε_s representing the static dielectric permittivity, ε_∞ the permittivity at $f \rightarrow \infty$, τ the dipole relaxation time of the water molecules and σ the ionic conductivity due to dissolved salts or other ions and metabolites [18]. In Eq. 1, the frequency f is expressed by the angular frequency $\omega = 2\pi f$, $\varepsilon_0 = 8.85 \cdot 10^{-12}$ F/m is the vacuum permittivity.

The dielectric properties of liquid water can be well described by Eq. 1 up to about 60 GHz, using temperature dependent values of ε_s, τ and σ [18,19]. At room temperature (T = 22°C), experimental data for distilled water can be well fitted using ε_s = 78.36, τ = 8.27 ps, ε_∞ = 5.16 and σ =0 [20]. At 2.4 GHz and 150 MHz, where the experiments are conducted, ε^*(2.4 GHz) = 77 + j 9.0 and ε^*(150 MHz.2) = 78 + j 0.57, respectively. In particular at 150 MHz, a large contribution of to the conductivity term (3rd term in Eq. 1) by dissolved ions to the imaginary part of ε^* can be expected: broadband microwave dielectric measurement on fluids extracted from wheat leaves revealed equivalent NaCl concentrations of around 1 % [21], which results in a conductivity of about 17,600 µS/cm, the corresponding imaginary part of ε^* at 2.4 GHz and 150 MHz are 13 and 211, respectively (3rd term in Eq. 1). Hence, the ratio Im (ε^*_{ions})/ Im (ε^*_{dipole}), which describes the ratio of ionic to dipole losses, comes out to be 1.47 at 2.4 GHz and 370 at 150 MHz for the given conductivity. Therefore, the mode at 150 MHz is ideally suited for non-invasive and contact-free conductivity measurements.

It is worth to note that the Debye relaxation parameters and the ionic conductivity are strongly temperature dependent, therefore it is important that the measurements are performed within well-defined temperature interval. The dielectric response of the leaf can be understood as an effective medium composed of water with ions and of dry bulk material. In contrast to water, the bulk material has a relatively low permittivity ε‘≤10, and the imaginary part is negligible, as demonstrated by measurements on totally dried leaves (see section about results and discussion) . Therefore, as long as the absolute water content is more than about 10% the contribution of the bulk plant material to the real part of the, dielectric permittivity can be neglected as well. However, as discussed in Ulaby, et al. [21], the calculation of complex permittivity of a representative effective medium would require detailed

information about the water distribution within the veins and as inter- and intracellular liquid, because of unequal amounts of water in different tissue compartments. Nevertheless, by assessing dielectric properties of two materials as reported by Sancho-Knapik, et al. [16], a very good correlation between RWC (relative water content) and reflectance at a frequency of 1730 MHz was found both for filter paper and leaves. Therefore, the integral complex permittivity, as determined by microwave dielectric measurement, represents a reasonable experimental quantity which is representative for the water content (or conductivity in case of the imaginary component at 150 MHz) of a leaf under investigation.

According to a comprehensive study within the framework of effective medium theories as described in Ulaby, et al. [21] the static permittivity for fresh wheat leaves is about 35, corresponding to a volumetric moisture of about 60%. This correlation depends on the density of the fresh leaf material, which may vary for different species, but was not analyzed within this study.

Results and Discussion

The dual mode cavity as leaf sensor

The patented dual mode cavity sensor, which is discussed in detail in Klein, et al. [14], enables simultaneous dielectric measurements at two distinct and far separated frequencies: For the sensor, which was employed in this study, one resonant frequency is at 150 MHz (Mode 0), the second one 2.4 GHz (Mode 1). For the study of the correlation between drying status and permittivity we employed Mode 1 only because of large signal-to-noise ratio, i.e. larger frequency shifts in comparison the resonant halfwidth. In spite of poor signal-to-noise ratio, preliminary data by Mode 0 on fresh wheat leaves are discussed. It is worth to note that Mode 0 is ideally suited for contact-free assessment of the ionic conductivity of bulky plant tissues such as potatoes and sugar beets, where the sample volume and hence the signal-to-noise ratio is much larger.

Mode 1 corresponds to the $TE_{01\delta}$-mode [22] of the cylindrically shaped dielectric resonator, embedded in the dual-mode cavity. The evanescent electric field is presented by concentric circles, the field magnitude increases from zero in the center of the aperture towards its maximum at about 2/3 of the radius of the dielectric resonator (light circle in Figure 1, C), and gradually decreases to zero towards the aperture. From the aperture plane (leaf measurement position), the evanescent field decreases exponentially in axial direction and reaches 50% of its value at the top edge of the aperture at a distance of about 20 mm above the aperture. The evanescent field of the lumped element mode (Mode 0) is strongly concentrated in close vicinity of the radial metallic rod, in particular near the centre of the cavity [14].

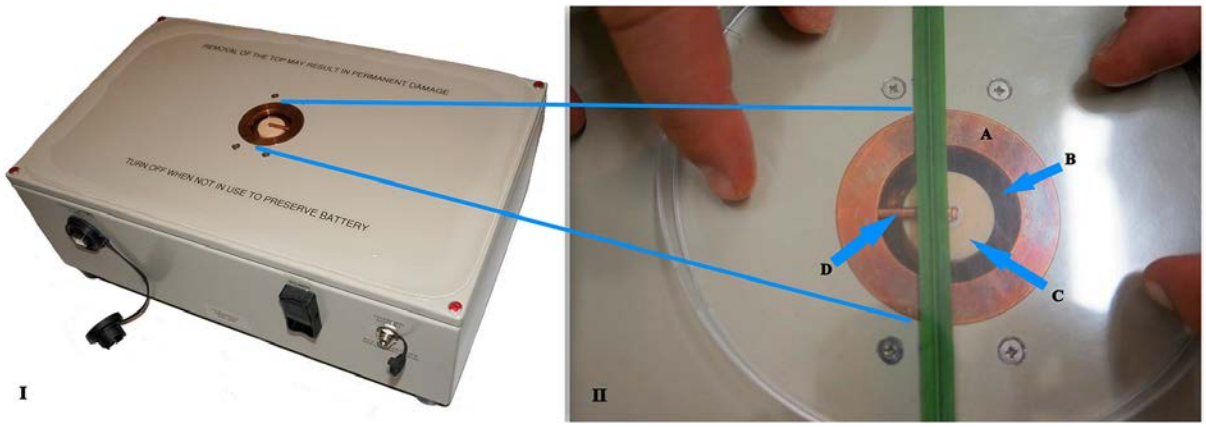

Figure 1 Microwave sensor. (I) – Photograph of the employed sensor system comprising a compact battery - powered circuit board - microwave electronic module, and (II) the zoomed measurement-window: dual mode cavity (copper, **A**) embedded in a housing with a wheat leaf in measurement position. The aperture in the copper cavity (dark circle, **B**) allows the evanescent field of the ceramic dielectric resonator (smaller light circle, **C**) to penetrate into the sample under test. The radial copper rod (**D**) which is partially covered by the leaf is a requirement for Mode 0 only.

As it will be discussed along with the experimental data, for Mode 1 the magnitude of the leaf induced alteration of the resonant properties depends on the degree of coverage of the aperture by the leaf under test. In case of a partial coverage, as indicated by the wheat leaf shown in Figure **1**(II), a strict protocol how to arrange the leaf on the sensor surface is required for each given type of leaf. A smaller aperture would be tempting for the assessment of smaller leaves, but would cause a strong reduction of the electric field amplitude at the leaf position, which leads to a significant reduction of sensitivity.

During the assessment of a leaf under test, the change of the inverse quality factor Q and the resonant frequency, f_r with respect to the empty resonator is recorded. Both Q and f_r are determined from a fit of a Lorentzian to the measured transmission curve using.

$$U(f) = \frac{U(f_r)}{\sqrt{1+4Q^2\left(\frac{f}{f_r}-1\right)^2}}. \qquad (2)$$

In Eq. 2 [24] $U(f)$ represents the frequency dependent detector voltage, which is proportional to the power transmitted through the resonator (square law detection) upon sweeping the generator frequency around the resonance frequency f_r. Both modes are excited by a different

pair of coaxial probes for each, the signals are generated and recorded by two independent electronic modules. Each of the two PCB (printed circuit-board) - based integrated electronic modules is composed of a digitally controlled synthesizer- PLL (phase locked loop) controlled microwave VCO (voltage controlled oscillator) and a detector unit.

Prior to each measurement with a leaf in place, f_r and Q are recorded for the empty resonator. For the analysis, the negative relative frequency shift due to the sample,

$$FRS \equiv -\frac{f_{r,sample} - f_{r,empty}}{f_{r,empty}}. \tag{3a}$$

and the sample induced change of the losses, i.e. change of the inverse Q factor, *IQS*,

$$IQS \equiv \frac{1}{Q_{sample}} - \frac{1}{Q_{empty}} \tag{3b}$$

are recorded. Since the frequency shift due to a dielectric object is usually negative, *FRS* is defined to be a positive number. It is important to note that IQS is independent of coupling losses, because coupling leads to a constant $1/Q$ contribution which does not change due the sample in measurement position.

For the case, that the field distribution of the evanescent field is not distorted by the sample, *FRS* and *IQS* can be directly related to the complex permittivity of the sample by extended cavity perturbation theory [23].

$$FRS = \frac{\kappa}{2}\left(\varepsilon' - 1\right) \qquad IQS = \kappa\varepsilon''$$
$$\kappa = \frac{\varepsilon_0 \int_V E_0^{\,2} dV}{2W} \tag{4}$$

In Eq. 4, the filling factor κ describes the electric resonant field energy within the sample of volume, the integral in the numerator extends over the volume fraction V of the sample which is exposed to the unperturbed resonator field E_0, normalized to the total electric field energy, W, of the cavity.

In order to test the applicability of the perturbation approach, electromagnetic field simulations of the cavity-leaf system have been performed with CST Microwave Studio [24] for a variety of configurations. The results indicate that the alteration of the magnitude of the electric field at the position of the leaf due to leaf itself is less than 10% in the worst case assuming a homogenous water distribution inside the leaf. Therefore, the analysis by Eq. 4 is justified within the experimental errors. However, we

cannot rule out that water being concentrated in veins may lead to some level redistribution of the local electromagnetic field, which is subject of an ongoing study.

The accurate calculation of the filling factor κ requires a detailed analysis of the shape of the leaf and its exact measurement position - along with the electric field distribution of the resonant mode. However, relative measurements of *FRS* and *IQS* for a given leaf in a reproducible measurement position allow the monitoring of relative changes of the complex permittivity. It is worth to mention that the ratio of *IQS* and *FRS* is independent of κ, and may represent a size and position independent figure of merit for a given leaf. For Mode 1, even in case of a complete coverage of the aperture, the leaf-induced alteration of resonance frequency and *Q* factor may depend on the exact measurement position of the leaf under test, because the water distribution in the leaves is inhomogeneous. This means, that a maximum of *FRS* and *IQS* is usually achieved if water filled veins are located around the position of maximum field. For the sake of a maximum signal-to-noise ratio, the position was optimized for maximum *FRS*. In case of elongated leaves like wheat the leaf axis was arranged at an offset of about 50–80 % of the radius of the dielectric resonator, corresponding to a field maximum of the TE_{01d} mode (Mode 1). The optimization of the position with regards to Mode 0 is subject to a separate analysis and will not be further addressed in this contribution.

However, as indicated in the section about results and discussion, the leaf-induced alterations can be used for a preliminary analysis.

Although the leaf under test is physically attached to the metallic aperture of the cavity in order to ensure a reproducible measurement position, the measurement is contact-less in nature. A thin plastic foil between aperture and sample would not have any significant effect on the results, because the electric field is coupled to the sample inductively, without any need of an electrical contact.

Measurement of water content in leaves of different plants

The four plant species being analyzed, wheat, maize, potato and canola were selected considering the size and morphology of their leaves. Wheat and maize leaves have similar shape, both are long but wheat leaves are thinner. On the other hand, the potato and canola have compound leaves with oval leaflets, the canola leaves are larger and thicker.

The three leaves detached from each plant were chosen from three developmental stages in order to characterize tissues of various ages. Shortly after removal from the plant, the leave under test was weighted and subsequently measured with the microwave sensor system. The leave was placed on the window such the measured frequency shift is maximized, as shown in Figure 1 for wheat. This first assessment was representative for the fresh leaf and which was considered as reference of 100% (w/w)

water content. In fact, the time interval between removal and measurement was less than 30 seconds in any case.

A significant change in the resonant frequency shift of Mode 1 (2.4 GHz) between fresh and dry leaves was demonstrated, which is far beyond the variation from leaf to leaf for a given plant (Figure 2). It is notable that the frequency shift of the dry leaf is zero within the measurement accuracy limits which indicates that water represents the dominant part of the response.

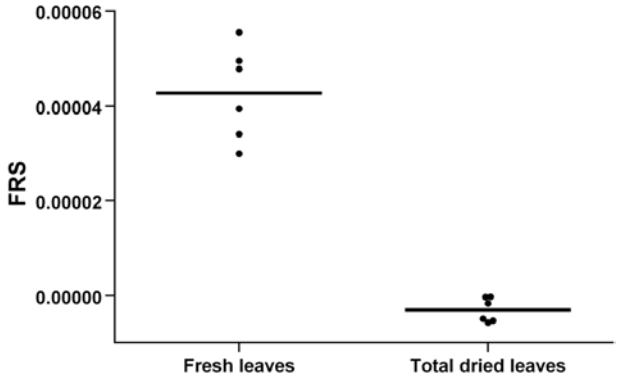

Figure 2 Comparative dielectric conductivity of fresh and totally dried wheat leaves. Six leaves in total were measured fresh and subsequently completely dried. The dots represent the average values of five measurements (technical replicates) and the lines the average values of six leaves

For Mode 0, only wheat leaves have been investigated till date. The measured values of *FRS* and *IQS* are of the same order of magnitiude as for Mode 1, but the signal-to-noise ratio is nearly ten times lower than for Mode 1. This is due to the smaller resonant halfwidth of the unloaded resonance, usually expressed by the quality factor Q_{empty} without sample, Q_{empty}(Mode 0) = 350, Q_{empty}(Mode 1) = 4200).

All measurements where performed at room temperature without any room temperatur conrol. Test measurements on canola and wheat leaves at 18°C, 22°C and 27°C showed no significant differences of the *FRS* or *IQS* values.

For Mode 1, the measured values of *FRS* and *IQS* as a function of percentage of fresh weight for four different types of plants were normalized to the average value of the fresh leave (Figure 3). Although the absolute values of *FRS* and *IQS* differ from leaf to leaf due to a different filling factor κ (Eq. 4) the normalized *FRS* and *IQS* values exhibit a systematic decrease with increasing weight loss, which indicates that water provides the most significant contribution to the dielectric permittivity of leaf tissue. The data points of individual leaves indicate this trend. The averaged values displayed in Figure 3 as horizontal lines are representative mean values for all leave stages. Based on t-test, significant differences between the mean values were revealed ($p < 0.05$). Measurement of three leaves and calculation of their mean values show stronger correlations to the water content than the single leaves measurement. Assuming that the mass density of the dry leave tissue is small in comparison to that of

water, the weight percentage represents the volumetric water concentration – multiplied by factor of about 0.5-0.7 (maximum water volume concentration in a fresh leaf) [21]. According to our data, the normalized *FRS* values drop to about 0.45-0.55 for wheat and maize, and to slightly higher values of about 0.65-0.75 for potato and canola - as result of weight reduction or water loss from 100% to 50%. It is remarkable, however, that the *FRS* – weight dependences exhibit a recognizable positive curvature and deviate from linearity, in contrast to the slight negative curvature being observed by broadband dielectric measurements on wheat leaves and stalks [21]. For potato leaves and in particular for canola leaves, where a considerable portion of water is stored in relatively thick veins, this effect is most pronounced. We presume that the drying process by evaporation works slower for large veins. As a result, the measured weight may not be representative for the real water concentration in the largest veins: if the largest veins are located close to a field maximum of the resonant field, the measured *FRS* values may overestimate the average water concentration in the leaf, which explains the observed curvature qualitatively.

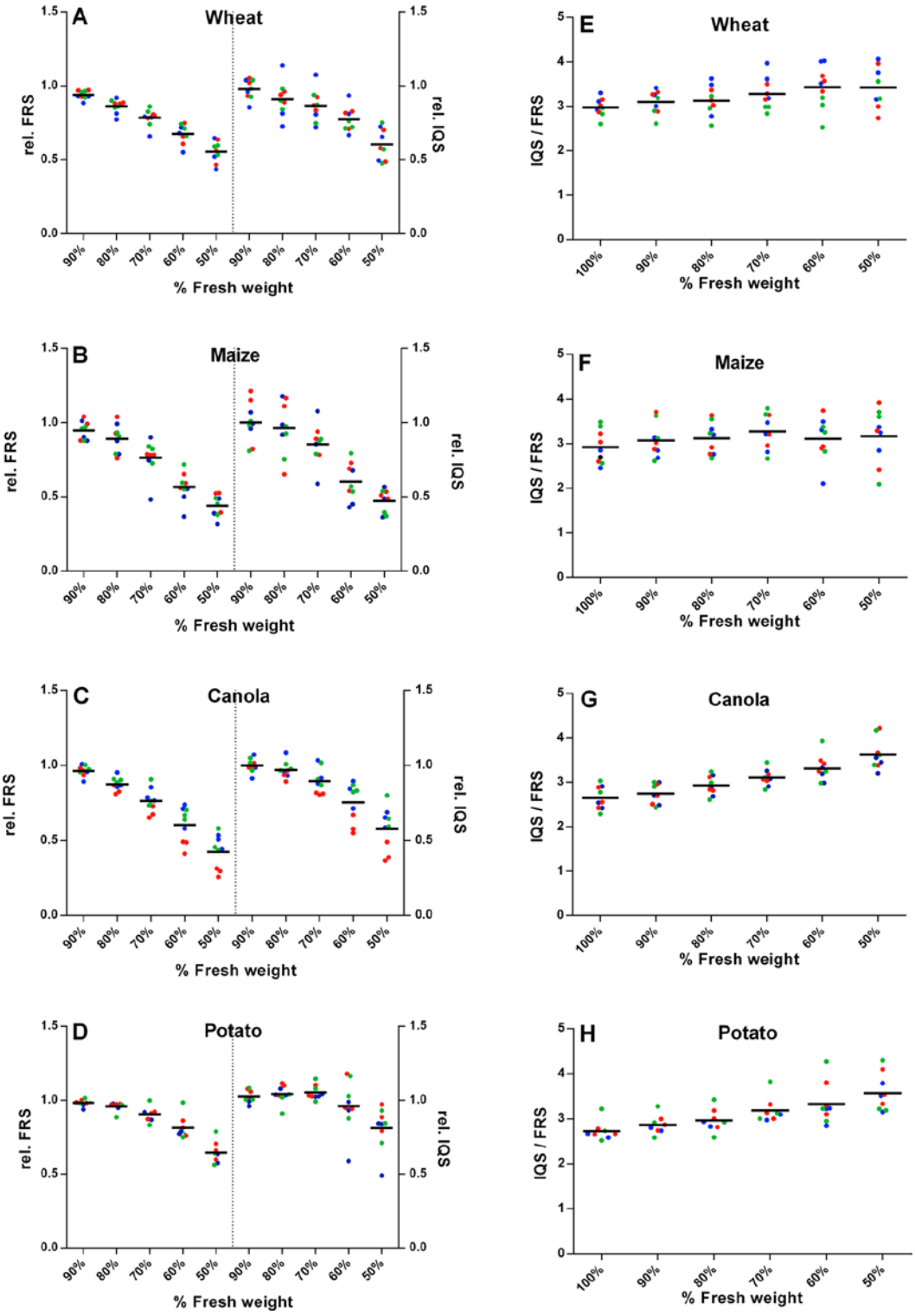

Figure 3 Experimental results of microwave measurements on leaves from four different crops. The analysis was performed at six time-points from initial fresh weight (100%) up to 50% of the initial weight by consecutive 10% drying in each step. (**A**) - Wheat, (**B**)-Maize, (**C**) - Canola, and (**D**) - Potato. Normalized FRS and IQS values based on values at 100% fresh weight for FRS and IQS, respectively are shown. E (Wheat), F (Maize), G (Canola) and H (Potato) display IQS values divided by FRS values for single leaves at different drying stages, and water contents, respectively. Bars indicate arithmetic means over three leaves. The absolute averaged FRS values at 100% fresh weight are $5.5 \cdot 10^{-5}$ for wheat, $1.25 \cdot 10^{-4}$ for maize, $1.41 \cdot 10^{-4}$ for canola and $1.24 \cdot 10^{-4}$ for potato. The colors of the dots indicate the developmental stage of the leaves: blue (first stage, young leaf), green (second stage, intermediate leaf) and red dots (third stage, older leaf).

For the fresh weight data, the average ratio IQS/FRS varies only slightly between 2.8 and 3 for the three different plants. Assuming the validity of the perturbation approach according to Eq. 4, *IQS*/*FRS* is equal to two times the loss tangent.

$$\frac{IQS}{FRS} = \frac{2\varepsilon''}{\varepsilon'-1} \approx \frac{2\varepsilon''}{\varepsilon'} = 2\tan\delta \tag{5}$$

As discussed in the section about microwave properties of plant tissues, the loss tangent of distilled water at 2.4 GHz is 0.12 and 0.3 for an assumed ionic conductivity of 14,000 µS/cm. In other words, within the framework of perturbation theory and the assumption that the losses are due to water and ions only, the analysis yields a nearly ten times higher conductvity than reported in the literature. In order to resolve this puzzle, we took a closer look at the *IQS* and *FRS* values of Mode 0, because the separation of ionic conductor losses from water dipole relaxation losses is much more pronounced at this low frequency (Table 1). In order to improve the measurement statistics, we measured *FRS* and *IQS* for 6 fresh leaves from one plant (indicated by the numbers in Table 1). Each of the listed *FRS* and *IQS* values corresponds to the average of five subsequent measurements performed on one leaf, the quoted error represents the standard deviation of these five subsequent measurements.

Table 1 Measured *FRS* and *IQS* (*f*=150MHz, Mode 0) **for 6 different fresh leaves of one wheat plant and calculated ionic conductivity.**

L. no	*FRS*	Δ_{FRS}/*FRS* [%]	*IQS*	Δ_{IQS}/*FRS* [%]	σ[µS/cm]	Δ_σ/σ [%]
1	$1.30\cdot10^{-5}$	40	$5.25\cdot10^{-5}$	27	$1.4\cdot10^{4}$	48
2	$1.47\cdot10^{-5}$	26	$6.11\cdot10^{-5}$	15	$1.4\cdot10^{4}$	30
3	$1.27\cdot10^{-5}$	46	$7.78\cdot10^{-5}$	27	$2.0\cdot10^{4}$	53
4	$1.86\cdot10^{-5}$	21	$6.84\cdot10^{-5}$	52	$1.2\cdot10^{4}$	56
5	$1.94\cdot10^{-5}$	7	$8.79\cdot10^{-5}$	20	$1.5\cdot10^{4}$	21
6	$1.96\cdot10^{-5}$	29	$9.52\cdot10^{-5}$	15	$1.6\cdot10^{4}$	14
AVE					$1.46\cdot10^{4}$	14

The conductivity is proportional to *IQS*/*FRS* (Eqs. 1 and 5)

$$\sigma = \omega\varepsilon_0\varepsilon_r \tan\delta = \frac{\omega\varepsilon_0\varepsilon_r}{2}\frac{IQS}{FRS} \tag{6}$$

with $\varepsilon_r \approx 78$ representing the real part of the permittivity of water at the measurement frequency of 150 MHz. The quoted value (1.46 ± 0.20) µS/cm corresponding to the weighted average of the six leaves is

in agreement with literature data [21]. To the best of our knowledge, this is the first non-invasive determination of the conductivity of the fluid inside a plant leaf.

As a possible explanation for the enhanced loss tanget measured at 2.4 GHz, it is likely that higher dielectric relaxation losses than assumed for free water may occur due to a high abundance of surface water, which has a significantly higher loss tangent than bulk water at 2.4 GHz [25,26]. The observed slight increase of *IQS*/*FRS* at 2.4 GHz with increasing weight loss is likely due to an increase of the ratio of surface to bulk water as result of faster evaporation of bulk water. In fact, the relatively small variation is far below the expectation of 50% water loss by evaporation, which is supportive for the hypothesis that surface water may contribute to the losses by a significant amount. Comparative measurements with Mode 0 at 150 MHz of sufficient accuracy and other frequencies may help to resolve this puzzle in the future.

Furthermore, in order to demonstrate the practical applicability of our microwave technique, wheat plants being challenged by salt stress were measured (at the moment only by Mode 1). The measured *FRS* values reveal a clear difference between the control leaves and the stressed ones (Figure 4). The decrease in the *FRS* value is likely to be linked to an increase of osmolarity induced by salt stress which is adversely affecting the uptake of water by the roots [27,28].

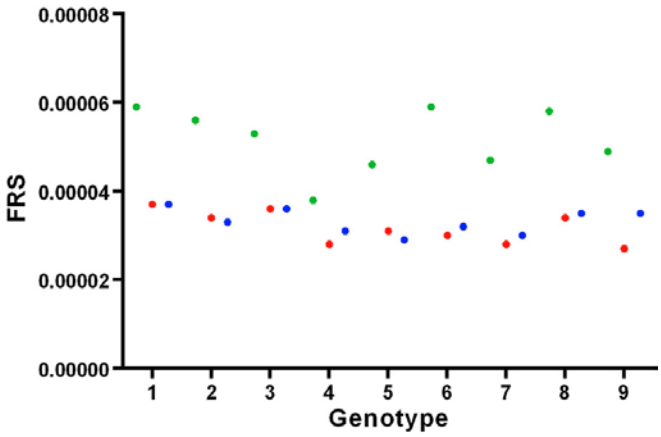

Figure 4 Analysis of wheat leaves from nine genotypes after 15 days of salt stress. Green dots represent control, red and blue dot leaves stressed with 100 mM NaCl and 50 mM Na_2SO_4, respectively. X-axes represent the genotypes analysed (numbered 1–9) and the y-axes the corresponding FRS values.

A reduction of the water content in the plant cell leads to an increase of osmolarity. Therefore, the osmotic potential of canola leaves at 6 time-points was determined. A strong negative correlation (r = − 0.97) between *IQS*/*FRS* values and the respective osmotic potential of the leaves at different steps of water reduction was found (Figure 5).

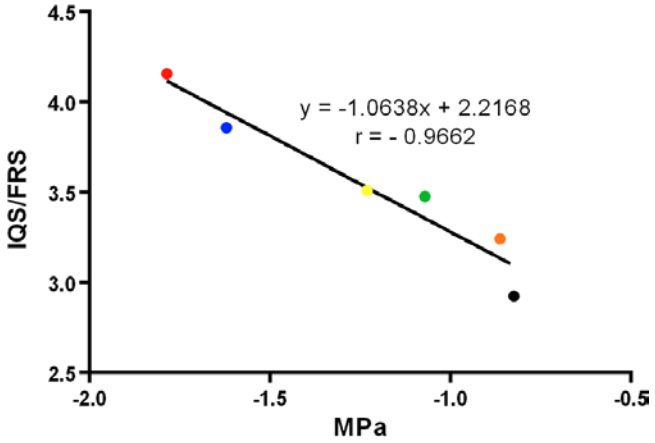

Figure 5 Correlation between osmotic potential and IQS/FRS values for canola leaves. Dot-colors indicate measurement of leaves with water content decreasing stepwise: black – 100% (initial fresh weight); brown – 90%, green – 80%; yellow – 70%; blue – 60% and red – 50% of the initial weight. Each dot represents the mean values from four leaves. For each leave, two measurements were performed to define osmotic potential and five for the *IQS*/*FRS* value.

Material and Methods

Plant material and growth conditions

Four species belonging to different classes of plant kingdom were selected: wheat (*Triticum aestivum* L.) cultivar Zentos, maize (*Zea mays* L.) cultivar Aurelia, potato (*Solanum tuberosum* L.) cultivar Linda and canola (*Brassica napus* L.), cultivar Expert. The plants were grown under greenhouse conditions in pots filled with soil (clay peat mix) and watered regularly.

For the salt stress experiment, nine wheat genotypes were grown in three replicates in aerated hydroponic system (unpublished data). The tested wheat genotypes were Zentos, Syn086 and 7 progenies of the cross between Zentos and Syn086 [29] which were selected based on their performance under salinity stress, representing salt tolerant and salt sensitive genotypes.

The stress was induced by adding to the nutritional solution either NaCl or Na_2SO_4, to end-concentration of 100 mM and 50 mM, respectively.

EC at control = 2.5 mS, NaCl = 11.5 mS, Na_2SO_4 = 9.5 mS), pH was checked every day and adjusted at 6.1 to 6.4. The stress was induced at three leave developmental stage (BBCH 13) and lasted for 15 days.

Measurements of salt stressed plants using the microwave cavity technique

The measurements were performed using a prototype of EMISENS's dual-mode sensor system, which was purpose-designed for this study. The quantities *IQS* and *FRS* were determined from the resonant frequency and *Q* factor, as determined by a fit of a Lorentzian to the measured resonant curves displayed in Figure 6. The leaves were pressed by a transparent plastic cover against the aperture of the dual-mode cavity. In case of small leaves which do not fully cover the aperture, the position was optimized for maximum *FRS*, which corresponds to the alignment of an elongated leaf (like the one depicted in in Figure 1) perpendicular to the radial metallic rod at a distance from the center corresponding to about half the radius of the dielectric resonator.

Figure 6 Screenshot of the user interface of the dual-mode sensor system. Blue and red curves

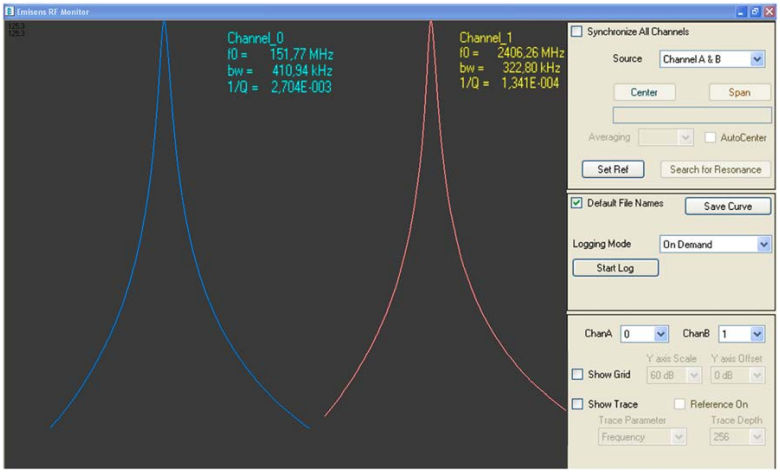

display the measured resonance of a measurement of modes 0 and 1, respectively. Shown are the values of resonance frequency (f0), inverse Q factor and 3 dB bandwidth bw = f_0/Q for both modes, as determined by a Lorentz fit (Eq. 2). The axis of these plots (horizontal = frequency), (vertical = detector voltage) are not depicted on the screenshot, the control panel on the right-hand side of the screen shot is not relevant for the presented analysis.

For measurements on different leaves of one plant species care was taken to ensure that nearly identical measurement positions were used. The plants were removed from the hydroponic boxes and one leaf of them was placed on the window of the sensor (Figure 1). Five measurements were performed for each leave without changing the position (technical replicates). Immediately after, the undamaged plants were returned into the hydroponic vessels.

Measurements of water content

In order to follow the kinetics of water content the measurements were performed on detached leaves from the corresponding plants.

The stepwise reduction of water content in leaves was achieved by incubating them at high temperatures. The gravimetric measurement of water loss in the leaves was done by weighting them before and after drying. Shortly, after removal from the plant the leaves were weighted and measured with the microwave sensor system. This first-time point was considered as reference for a leaf with 100% (w/w) water. After that, the leaves were placed in an incubator at 45°C until 10% of initial water content was lost and the microwave assessment was performed instantaneously. The drying procedure with 10% loss each step and subsequent microwave measurement was repeated 5 times until reduction to 50% of the initial weight.

Measurement of the osmotic potential

Leaves of canola plants were detached and after the microwave measurements they were analyzed with respect to their osmotic potential. This was repeated for each step of water reduction as described above. The sap of the leaves was extracted by squeezing them using a garlic presser. Fifteen µl sap-solution was employed to define the osmotic potential using an Osmomat (Osmomat 030-D, Gonotec GmbH, Berlin, Germany). The conversion of the osmolality values (osmol/kg) in osmotic potential (MPa) as described by Pariyar, et al. [30].

Conclusions

We have demonstrated non-invasive assessment of the water content by an evanescent field microwave sensor at 2.4 GHz for four different species of plant leaves due to a comparative study with gravimetric data. Our approach was proven to be highly reproducible and applicable for leaves of various size, shape and thickness. The frequency shift versus water content curves are slightly sub linear for the larger leaves, which may result from the inhomogeneous water distribution in the veins. For canola leaves, a strong correlation between the measured ratio of loss and frequency shift data to the osmotic potential was found, which indicates that the microwave method can be used for contact-free assessment of the osmolytes status of a plant. Due to the combination of a microwave (f = 2.5 GHz) and a sub-microwave frequency (f = 150 MHz) in one sensor device the method has a strong potential for simultaneous non-invasive assessment of water and salt status in a single leaf under test.

For the future, a down-scaled system operated at higher frequencies may be developed in order to achieve a higher reproducibility for the assessment of smaller leaves. The optimizition of the design of the dual mode sensor and a further refinement of the electronic modules and the employed algorithm for accurate measurements of small changes of the resonant parameters should enable the simultaneous study of water content and average mineral content.

We expect that our technique may advance to a standard tool for hydration monitoring in plants in the near future. A lightweight portable version for assessment of plants in the field is currently under

development. This may enable the realization of knowledge-based watering systems as integral procedure of precision agriculture in the future.

Competing interests

The authors declare that they have no competing interests.

Authors' contributions

SD, NK, JL and AB designed the study, analyzed and interpreted the data and drafted the manuscript. AK, HR, SC, EM, UB and NK developed and constructed the resonator, the electronic module and the software. SD, SA, BH performed the measurements with the plants using the microwave resonator. All authors read and approved the final manuscript.

Acknowledgements

The work has been done in laboratories of EMISENS Company and of INRES-Plant Breeding, University of Bonn. We thank EU for financial support in frame of network "CROP.SENSE.net" (EFRES grant Nr. z1011bc001 and BMZ for Project no.: 09.7860.1-001.00.

References

1. Khan MA, Ashraf MY, Mujtaba SM, Shirazi MU, Khan MA, Shereen A, et al. Evaluation of high yielding canola type brassica genotypes/mutants for drought tolerance using physiological indices as screening tool. Pak J Bot. 2010;42(6):3807–16.

2. Lugojan C, Ciulca S. Evaluation of relative water content in winter wheat. Journal of Horticulture, Forestry and Biotechnology. 2011;15(2):173–7.

3. Lawlor DW, Tezara W. Causes of decreased photosynthetic rate and metabolic capacity in water-deficient leaf cells: a critical evaluation of mechanisms and integration of processes. Annals of Botany. 2009.

4. Brestic M, Zivcak M. PSII fluorescence techniques for measurement of drought and high temperature stress signal in crop plants: protocols and applications. In: Molecular Stress Physiology of Plants. Springer; 2013. p. 87–131.

5. Sade B, Soylu S, Soylu E. Drought and oxidative stress. Afr J Biotechnol. 2013;10(54):11102–9.

6. Trnka M, Eitzinger J, Dubrovský M, Semerádová D, Štěpánek P, Hlavinka P, et al. Is rainfed crop production in central Europe at risk? Using a regional climate model to produce high resolution agroclimatic information for decision makers. J Agric Sci. 2010;148(06):639–56.

7. Entrup NL, Berendonk C, Demmel M, Dietzsch H, Dissemond A, Estler M, et al. Lehrbuch des Pflanzenbaues: Kulturpflanzen/Hrsg.: Norbert Lütke Entrup. AgroConcept: Bernhard Carl Schäfer; 2011.

8. Born N, Behringer D, Liepelt S, Beyer S, Schwerdtfeger M, Ziegenhagen B, et al. Monitoring plant drought stress response using terahertz time-domain spectroscopy. Plant Physiol. 2014;164(4):1571–7.

9. Jordens C, Scheller M, Breitenstein B, Selmar D, Koch M. Evaluation of leaf water status by means of permittivity at terahertz frequencies. J Biol Phys. 2009;35(3):255–64.

10. Menzel MI, Tittmann S, Buehler J, Preis S, Wolters N, Jahnke S, et al. Non-invasive determination of plant biomass with microwave resonators. Plant Cell Environ. 2009;32(4):368–79.

11. Ferrazzoli P, Paloscia S, Pampaloni P, Schiavon G, Solimini D, Coppo P. Sensitivity of microwave measurements to vegetation biomass and soil moisture content: A case study. Geoscience and Remote Sensing, IEEE Transactions on. 1992;30(4):750–6.

12. Castro-Camus E, Palomar M, Covarrubias A. Leaf water dynamics of Arabidopsis thaliana monitored in-vivo using terahertz time-domain spectroscopy. Scientific reports. 2013;3

13. Gente R, Born N, Voß N, Sannemann W, Léon J, Koch M, et al. Determination of leaf water content from terahertz time-domain spectroscopic data. Journal of Infrared, Millimeter, and Terahertz Waves. 2013;34(3–4):316–23.

14. Klein N, Vitusevich S, Danylyuk S. Resonator arrangement and method for analyzing a sample using the resonator arrangement. In.: US Patent No.: 8,410,792 B2; 2010.

15. Rezaei M, Ebrahimi E, Naseh S, Mohajerpour M. A new 1.4-GHz soil moisture sensor. Measurement. 2012;45(7):1723–8.

16. Sancho-Knapik D, Gismero J, Asensio A, Peguero-Pina JJ, Fernández V, Alvarez-Arenas TG, et al. Microwave l-band (1730MHz) accurately estimates the relative water content in poplar leaves. A comparison with a near infrared water index (R 1300 /R 1450). Agr Forest Meteorol. 2011;151(7):827–32.

17. Shry C, Reiley E. Introductory horticulture. Cengage Learning; 2010

18. Kaatze U. The dielectric properties of water in its different states of interaction. J Solut Chem. 1997;26(11):1049–112.

19. Stogryn A. Equations for calculating the dielectric constant of saline water (correspondence). Microwave Theory and Techniques, IEEE Transactions on. 1971;19(8):733–6.

20. Barthel J, Buchner R. High-frequency permittivity and its use in the investigation of solution properties. Pure Appl Chem. 1991;63(10):1473–82.

21. Ulaby FT, Jedlicka R. Microwave dielectric properties of plant materials. Geoscience and Remote Sensing, IEEE Transactions on. 1984(4):406–415.

22. Gillon P, Kajfez D. Dielectric resonators. Noble; 1998

23. Pozar DM. Microwave engineering, Ch. 8. New York: Wiley; 1998.

24. Studio CM. Computer simulation technology. Darmstadt, Germany: GmbH; 2009.

25. Nandi N, Bhattacharyya K, Bagchi B. Dielectric relaxation and solvation dynamics of water in complex chemical and biological systems. Chem Rev. 2000;100(6):2013–46.

26. Basey-Fisher TH, Guerra N, Triulzi C, Gregory A, Hanham SM, Stevens MM, et al. Microwaving blood as a non-destructive technique for haemoglobin measurements on microlitre samples. Advanced healthcare materials. 2014;3(4):536–42.

27. Gorham J, Jones RW, McDonnell E. Some mechanisms of salt tolerance in crop plants. In: *Biosalinity in Action: Bioproduction with Saline Water*. Springer; 1985: 15–40.

28. Munns R, Tester M. Mechanisms of salinity tolerance. Annu Rev Plant Biol. 2008;59:651–81.

29. Kunert A, Naz AA, Dedeck O, Pillen K, Léon J. AB-QTL analysis in winter wheat: I. Synthetic hexaploid wheat (T. turgidum ssp. dicoccoides× T. tauschii) as a source of favourable alleles for milling and baking quality traits. Theor Appl Genet. 2007;115(5):683–95.

30. Pariyar S, Eichert T, Goldbach HE, Hunsche M, Burkhardt J. The exclusion of ambient aerosols changes the water relations of sunflower (Helianthus annuus) and bean (Vicia faba) plants. Environ Exp Bot. 2013;88:43–52.

12. LIST OF PUBLICATIONS

Articles in peer reviewed journals

Dadshani, S., A. Kurakin, S. Amanov, B. Hein, H. Rongen, S. Cranstone, U. Blievernicht, E. Menzel, J. Léon and N. Klein (2015). "Non-invasive assessment of leaf water status using a dual-mode microwave resonator." Plant methods **11**(1): 8.

Muzammil, S. **S. Dadshani**, A. Shreshta, K. Pillen, S. Siddique, J. Léon, A. A. Naz, "A novel P5cs1 allele of wild origin confers drought adaptation in cultivated barley." Proceedings of the National Academy of Sciences. (Under Review)

Oral presentations:

Ballvora A, **Dadshani S**, Römer C, Wahabzada M, Rascher U, Thurau C, Bauckhage C, Kersting C, Plümer L, Kurakin A, Amanov S, Hein B, Rongen H, Cranstone S, Blievernicht U, Menzel E, Klein N, Léon J: "Non-invasive assessment of leaf water status using hyperspectral image camera and microwave resonator"; International Conference on Intelligent Agriculture (ICIA2017); Changchun, Jilin Province, China; 12.08-15.08.2017

Duarte-Delgado D, **Dadshani S**, Mathew B, Schoof H, Léon J, Ballvora A (2017): "Identification of novel candidate genes of bread wheat involved in early salt stress tolerance through the integration of genomics and transcriptomic resources"; 13th International Wheat Genetics Symposium; Tulln, Austria; 23.04-28.04.2017.

Poster presentations:

Duarte-Delgado D, **Dadshani S**, Vogt I, Schoof H, Léon J, Ballvora A (2017): "Identification of a calmoduline-like homologue from bread wheat involved in early salt stress response through the integration of genomics and transcriptomic resources"; Minisymposium, by GRK 2064 on Drought and Related Stresses in Plants; Bonn, Germany; 10.10.2017.

Benaouda S, **Dadshani S**, Léon J, Ballvora A (2016): Glutathione S-transferase shows differential expression pattern under salt stress in wheat. GPZ Congress on Genetic Variation in Plant Breeding; Bonn, Germany; 08.03-10.03.2016.

Dadshani S, Baum M, Sharma R, Ogbonnaya F, Léon J, Ballvora A (2014): Utilization of wild relatives of wheat in developing salinity tolerant cultivars. GPZ Congress on Genetic Variation in Plant Breeding; Kiel, Germany; 23.09-25.09.2014.

Dadshani S, Oyiga BC, Baum M, Sharma R, Ogbonnaya F, Léon J, Ballvora A (2013) Genetic and physiological analysis of traits related to salinity tolerance and improved end-use quality in wheat. Poster presentation at the 12th International Wheat Genetics Symposium; Yokohama, Japan; September 8th- 11th 2013.

13. ACKNOWLEDGEMENT

First and foremost, praises and thanks to **The Almighty**, for His blessings throughout my life and giving me the strength, ability and opportunity to undertake this research study.

I want to express my deepest appreciation, respect and love to my very first teacher, my late **Mother**. I would never forget her advice and encouraging words: “As long as you are young. As long as you can: Learn!” Peace be upon you. I love you, Mom.

I would like to express my deep and sincere gratitude to my research supervisor, **Professor Dr. Jens Léon**, Head of Professorship of plant breeding at the University of Bonn. I have great respect to his limitless prudence. He did not only give me guidance and support throughout this research, he was also there when I needed paternal advice.

My thanks go to **Professor Dr. Heiner Goldbach**, who did not hesitate to take over the role of co-referee in the examination committee and his willingness to critical review this manuscript. Furthermore, I want to thank **Professor Dr. Frank Hochholdinger** and **PD. Dr. Ulrike Steiner** who agreed to serve in my PhD thesis committee.

I am extremely grateful to **Dr. Agim Ballvora** for the guidance and support he was giving me throughout my research. He taught me genetics and opened my eyes for new and undiscovered horizons.

I especially want to express my greatest gratitude to my colleague and dear friend **Dr. Boby Mathew** for helping me with complex statistical analysis and teaching me R programming. My gratitude is also extended to **PD Dr. Ali Naz**, who always had the time to discuss scientific issues with me.

I am most grateful to the PhD candidate **Salma Benaouda** for her invaluable contribution to this project and for her precious friendship.

Many thanks go to **Dr. Henrik Schuman**, **Dr. Stephan Reinert**, **Dr. Benedict Oyiga**, **Tobias Kox**, **Shumaila Muzammil**, **Mirza Majid Baig**, **Marius Klaus**, **Andreas Honecker** for being

supportive colleagues and for their cheerful company during my PhD. And of course, mi mejor amiga **Diana Duarte-Delgado**. Muchas gracias!

I want to thank all the students for their help with the data collection, especially **Jost Weber**, who also became a good friend.

I am deeply honored and thankful to know **Karin Woitol**, who is one of the most generous and friendly person I have ever met. I'm thankful for her companionship during my research.

My thanks go to the technicians **Anne Reinders**, **Petra Rings**, **Josef Höckling** and **Josef Bauer**, **Martina Brodeßer** and **Alexa Brox**.

This research was funded by the "Bundesministerium fur wirtschaftliche Zusammenarbeit und Entwicklung (BMZ)" in conjunction with the German Agency for International Cooperation (GIZ), Germany, the International Centre for Research in Dryland Agriculture (ICARDA) and the Center for Development Research (ZEF), Friedrich-Wilhelms-University, Bonn, Germany.

The last words of acknowledgment I have saved for my dear wife **Diba Dadshani**, who was my greatest supporter for the past years. Her endless patience and her enduring encouragement made this thesis possible. With her indescribable generosity she was giving me the greatest present on earth, **Ariana**.